

# Table of contents

<b>CHAPTER 1. GENERAL INTRODUCTION .....</b>	<b>1</b>
1.1. Platinum-based anticancer drugs.....	1
1.1.1. Clinical applications and toxicities.....	1
1.1.2. Mechanism of action .....	5
1.2. Platinum drug-induced peripheral neurotoxicity.....	8
1.2.1. Clinical features.....	8
1.2.2. Mechanisms .....	11
1.3. Platinum drug-induced transcriptional inhibition .....	13
1.3.1. Evidence .....	13
1.3.2. Mechanisms .....	14
1.4. Summary and aims of thesis.....	17
<b>CHAPTER 2. MATERIALS AND METHODS.....</b>	<b>20</b>
2.1. Chemicals and reagents.....	20
2.2. Animals .....	20
2.3. Cell culture .....	21
2.4. Fluorescent immunocytochemistry .....	24
2.5. Experimental incubation .....	25
2.6. Assessment of nascent RNA synthesis by 5-ethynyl uridine incorporation .....	25
2.7. Assessment of nascent RNA synthesis by [ <sup>3</sup> H]uridine incorporation.....	26
2.8. Assessment of platinum binding to DNA .....	27
2.9. Measurement of total RNA content .....	27
2.10. Measurement of neuronal cell body size and number.....	28
2.11. Apoptosis assay .....	28
2.12. Statistical analysis .....	29

<b>CHAPTER 3. VISUALIZATION OF NASCENT RNA SYNTHESIS IN CULTURED RAT DRG NEURONS VIA A CLICK CHEMISTRY REACTION LABELLING TECHNIQUE .....</b>	<b>30</b>
3.1. Introduction .....	30
3.2. Results .....	33
3.2.1. Optimization of 5-ethynyl uridine exposure.....	33
3.2.2. Visualization of nascent RNA synthesis .....	36
3.2.3. Quantitation of nascent RNA synthesis, DNA content and cell body size.....	36
3.2.4. Correlation between the level of nascent RNA synthesis and cell body size.....	42
3.2.5. Effects of oxaliplatin .....	44
3.3. Discussion .....	56
<b>CHAPTER 4. TIME-COURSE STUDIES OF OXALIPLATIN EFFECTS IN CULTURED RAT DRG CELLS.....</b>	<b>61</b>
4.1. Introduction .....	61
4.2. Results .....	64
4.2.1. Platinum binding to DNA.....	64
4.2.2. Inhibition of nascent RNA synthesis.....	67
4.2.3. Depletion of total RNA content.....	67
4.2.4. Neuronal cell body atrophy .....	72
4.2.5. Temporal interrelationships between oxaliplatin effects.....	72
4.2.6. Number of neurons .....	77
4.2.7. Apoptosis assay .....	77
4.2.8. Effects of actinomycin D on neuronal cell body size.....	80
4.3. Discussion .....	87
<b>CHAPTER 5. EFFECTS OF INHIBITORS ON OXALIPLATIN TOXICITY IN CULTURED RAT DRG CELLS.....</b>	<b>91</b>
5.1. Introduction .....	91
5.2. Results .....	94

5.2.1. Sodium thiosulfate.....	94
5.2.2. Cimetidine .....	102
5.2.3. DNA-dependent protein kinase (DNA-PK) inhibition.....	110
5.2.4. Poly(ADP-ribose) polymerase 1 (PARP-1) inhibition.....	110
5.2.5. K <sup>+</sup> channel blockade.....	113
5.2.6. Cl <sup>-</sup> channel blockade.....	118
5.3. Discussion .....	118
<b>CHAPTER 6. COMPARATIVE EFFECTS OF DIFFERENT PLATINUM DRUGS ON CULTURED RAT DRG CELLS.....</b>	<b>125</b>
6.1. Introduction.....	125
6.2. Results .....	128
6.2.1. Platinum-based anticancer drugs.....	128
6.2.2. Enantiomers of diamminocyclohexane platinum-based compounds .....	136
6.3. Discussion .....	144
<b>CHAPTER 7. GENERAL DISCUSSION.....</b>	<b>148</b>
7.1. Platinum-DNA damage .....	149
7.2. Transcriptional inhibition.....	152
7.3. Neuronal cell body atrophy and peripheral neurotoxicity.....	156
7.4. Future directions.....	160
7.5. Conclusions .....	161
<b>LIST OF REFERENCES.....</b>	<b>162</b>
<b>APPENDIX.....</b>	<b>181</b>

# List of figures

Figure 1.1. The chemical structures of platinum-based anticancer drugs and compounds. ....	2
Figure 2.1. Primary culture of rat DRG cells.....	23
Figure 3.1. Optimization of 5-ethynyl uridine exposure conditions for detecting its incorporation into nascent RNA of cultured DRG neurons. ....	35
Figure 3.2. Visualization of nascent RNA synthesis in cultured DRG neurons.....	38
Figure 3.3. Quantitation of the level of nascent RNA synthesis in individual cultured DRG neurons compared with that of their DNA content and cell body size. ....	40
Figure 3.4. Neuronal cell body size correlated with the level of nascent RNA synthesis, but not with that of DNA content of cultured DRG neurons. ....	43
Figure 3.5. Effects of oxaliplatin treatment on nascent RNA synthesis and cell body size of cultured DRG neurons: representative photomicrographs.....	46
Figure 3.6. Effects of oxaliplatin treatment on nascent RNA synthesis and cell body size of cultured DRG neurons: quantitative data.....	48
Figure 3.7. Concentration-dependence of effects of oxaliplatin treatment on nascent RNA synthesis and cell body size of cultured DRG neurons: representative photomicrographs. ....	52
Figure 3.8. Concentration-dependence of effects of oxaliplatin treatment on nascent RNA synthesis and cell body size of cultured DRG neurons: quantitative data. ....	54
Figure 4.1. Time-course of binding of oxaliplatin-derived platinum to the DNA of cultured DRG cells.....	66
Figure 4.2. Time-course of oxaliplatin-induced inhibition of nascent RNA synthesis in cultured DRG cells.....	69
Figure 4.3. Time-course of oxaliplatin-induced depletion of total RNA content of cultured DRG cells.....	71
Figure 4.4. Time-course of oxaliplatin-induced cell body atrophy in cultured DRG neurons.	74
Figure 4.5. Temporal interrelationships between binding of oxaliplatin-derived platinum to DNA and oxaliplatin effects on nascent RNA synthesis, total RNA content and neuronal cell body size. ....	76
Figure 4.6. Lack of effect of oxaliplatin on the number of cultured DRG neurons.....	79

Figure 4.7. Lack of apoptotic effect of oxaliplatin on cultured DRG neurons. ....	82
Figure 4.8. Time-course of actinomycin D-induced inhibition of nascent RNA synthesis in cultured DRG cells.....	84
Figure 4.9. Time-course of actinomycin D-induced cell body atrophy in cultured DRG neurons.....	86
Figure 5.1. Sodium thiosulfate reduced platinum binding to the DNA of cultured DRG cells after exposure to oxaliplatin.....	97
Figure 5.2. Sodium thiosulfate protected cultured DRG cells from inhibition of nascent RNA synthesis induced by oxaliplatin. ....	99
Figure 5.3. Sodium thiosulfate protected cultured DRG neurons from cell body atrophy induced by oxaliplatin.....	101
Figure 5.4. Cimetidine reduced platinum binding to the DNA of cultured DRG cells after exposure to oxaliplatin.....	104
Figure 5.5. Cimetidine partially protected cultured DRG cells from inhibition of nascent RNA synthesis induced by oxaliplatin. ....	107
Figure 5.6. Cimetidine partially protected cultured DRG neurons from cell body atrophy induced by oxaliplatin.....	109
Figure 5.7. Lack of effect of DNA-PK inhibitors on oxaliplatin-induced inhibition of nascent RNA synthesis in cultured DRG cells. ....	112
Figure 5.8. Lack of effect of PARP-1 inhibitors on oxaliplatin-induced inhibition of nascent RNA synthesis in cultured DRG cells. ....	115
Figure 5.9. Lack of effect of K <sup>+</sup> channel blockers on oxaliplatin-induced cell body atrophy in cultured DRG neurons. ....	117
Figure 5.10. Lack of effect of Cl <sup>-</sup> channel blockers on oxaliplatin-induced cell body atrophy in cultured DRG neurons. ....	120
Figure 6.1. Platinum binding to the DNA of cultured DRG cells after exposure to different platinum-based anticancer drugs.....	130
Figure 6.2. Effects of different platinum-based anticancer drugs on nascent RNA synthesis in cultured DRG cells.....	133
Figure 6.3. Effects of different platinum-based anticancer drugs on cell body size of cultured DRG neurons. ....	135

Figure 6.4. Platinum binding to the DNA of cultured DRG cells after exposure to different enantiomers of diaminocyclohexane platinum-based compounds. ....	138
Figure 6.5. Effects of different enantiomers of diaminocyclohexane platinum-based compounds on nascent RNA synthesis in cultured DRG cells. ....	141
Figure 6.6. Effects of different enantiomers of diaminocyclohexane platinum-based compounds on cell body size of cultured DRG neurons. ....	143

## List of tables

Table 3.1. Quantitation of the level of nascent RNA synthesis in individual cultured DRG neurons compared with that of their DNA content and cell body size. ....	41
Table 3.2. Effects of oxaliplatin treatment on nascent RNA synthesis and cell body size of cultured DRG neurons: tabulated data. ....	49
Table 3.3. Concentration-dependence of effects of oxaliplatin treatment on nascent RNA synthesis and cell body size of cultured DRG neurons: tabulated data. ....	55

# Abbreviations

ANOVA	Analysis of variance
AU	Arbitrary unit
AVD	Apoptotic volume decrease
BrU	Bromouridine
BrUTP	Bromouridine triphosphate
CI	Confidence interval
Cl <sup>-</sup>	Chloride ion
CTR	Copper transporter
DACH	Diaminocyclohexane
DAPI	4',6-Diamidino-2-phenylindole
DIDS	4,4'-Diisothiocyanatostilbene-2,2'-disulfonic acid disodium salt hydrate
DNA	Deoxyribonucleic acid
DNA-PK	DNA-dependent protein kinase
DRG	Dorsal root ganglia
dUTP	2'-Deoxyuridine-5'-triphosphate
EC	5-Ethynyl cytidine
EU	5-Ethynyl uridine
FU	Fluorouridine
ICP-MS	Inductively coupled plasma mass spectrometry
IQR	Interquartile range
K <sup>+</sup>	Potassium ion



mRNA	Messenger RNA
NER	Nucleotide excision repair
NF-H	Neurofilament heavy subunit
NPPB	5-Nitro-2-(3-phenylpropylamino)benzoic acid
OCT	Organic cation transporter
PARP-1	Poly(ADP-ribose) polymerase 1
PBS	Phosphate buffered saline
RNA	Ribonucleic acid
rRNA	Ribosomal RNA
$r_s$	Spearman's rank correlation coefficient
TEA	Tetraethylammonium chloride
tRNA	Transfer RNA
TUNEL	Terminal deoxynucleotidyl transferase-mediated dUTP nick end labelling

# Co-Authorship Form

This form is to accompany the submission of any PhD that contains published or unpublished co-authored work. **Please include one copy of this form for each co-authored work.** Completed forms should be included in all copies of your thesis submitted for examination and library deposit (including digital deposit), following your thesis Acknowledgements. Co-authored works may be included in a thesis if the candidate has written all or the majority of the text and had their contribution confirmed by all co-authors as not less than 65%.

Please indicate the chapter/section/pages of this thesis that are extracted from a co-authored work and give the title and publication details or details of submission of the co-authored work.

Chapter 3 - 6 of this thesis were extracted from a co-authored work entitled "Role of platinum DNA damage-induced transcriptional inhibition in chemotherapy-induced neuronal atrophy and peripheral neurotoxicity" published in the Journal of Neurochemistry (2015), doi: 10.1111/jnc.13355.

Nature of contribution by PhD candidate	Conducting the experiments, research planning, data interpretation and preparation of the manuscript.
---	---

Extent of contribution by PhD candidate (%)	90
---	----





## CO-AUTHORS

Name	Nature of Contribution
Johnson J Liu	Research planning, data interpretation and preparation of the manuscript
Virginia Ip	Carrying out experiments, research planning, data interpretation and preparation of the manuscript
Stephen M F Jamieson	Carrying out experiments, research planning, data interpretation and preparation of the manuscript
Mark J McKeage	Research planning, data interpretation and preparation of the manuscript

## Certification by Co-Authors

The undersigned hereby certify that:

- ❖ the above statement correctly reflects the nature and extent of the PhD candidate's contribution to this work, and the nature of the contribution of each of the co-authors; and
- ❖ that the candidate wrote all or the majority of the text.

Name	Signature	Date
Johnson J Liu		7-12-2015
Virginia Ip		13/12/2015
Stephen M F Jamieson		7/12/15
Mark J McKeage		7/12/15

# Chapter 1. General Introduction

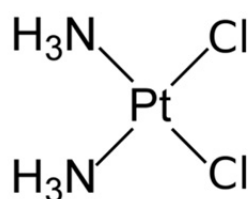
## 1.1. Platinum-based anticancer drugs

Since the cytotoxicity of platinum compounds was discovered fifty years ago, platinum-based anticancer drugs have been widely used in the clinic for the treatment of a variety of cancers. At present, three platinum-based anticancer drugs have been approved world-wide, including cisplatin (first generation), carboplatin (second generation) and oxaliplatin (third generation). Platinum-based anticancer drugs consist of a central platinum atom bonded to a hydrolysable leaving ligand and a non-hydrolysable carrier ligand. The cytotoxic activity of platinum-based anticancer drugs is primarily based on the formation of platinum-DNA damage.

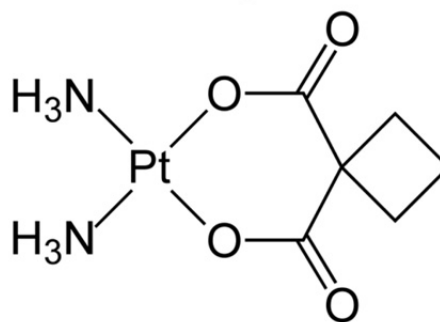
### 1.1.1. Clinical applications and toxicities

Cisplatin, or *cis*-diamminedichloroplatinum(II), is the first member of the family of platinum-based anticancer drugs (Figure 1.1). It was discovered in the nineteen-sixties, when Rosenberg and colleagues observed that electrolysis products formed around platinum electrodes inhibited growth of bacteria (Rosenberg et al., 1965, Rosenberg et al., 1969). Due to its convincing therapeutic efficacy in clinical trials, cisplatin was approved for clinical use in the nineteen-seventies (Higby et al., 1974). At present, cisplatin is employed to treat various malignancies, including testicular, ovarian, bladder and lung cancer (Wheate et al., 2010). Particularly, with cisplatin as the first-line treatment, testicular cancer has a more than 80% cure rate (Windebank and Grisold, 2008). However, the clinical application of cisplatin is limited by severe adverse effects, which include neurotoxicity, nephrotoxicity, ototoxicity,

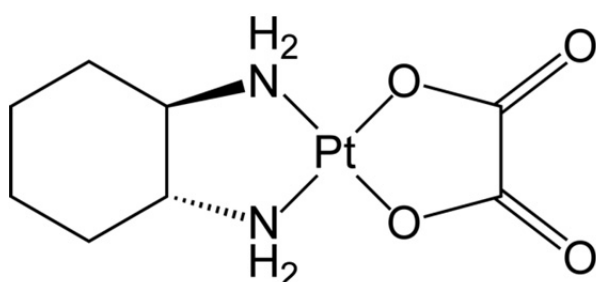
Cisplatin



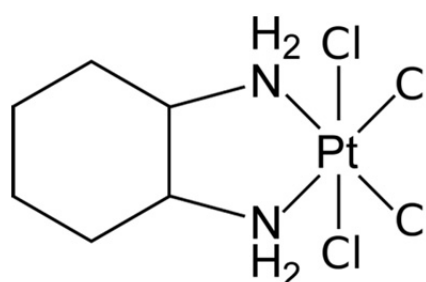
Carboplatin



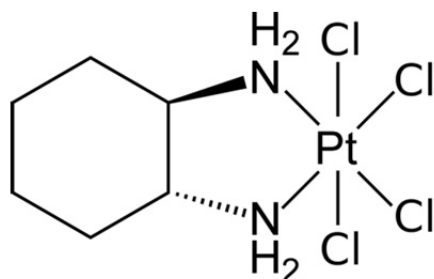
Oxaliplatin



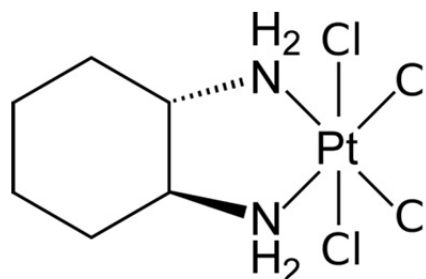
Ormaplatin



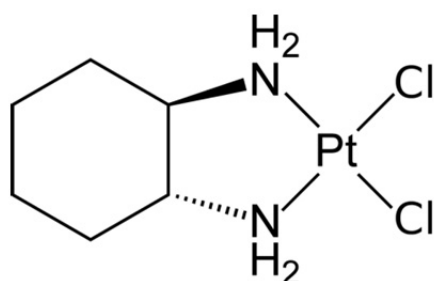
*R,R*-ormaplatin



*S,S*-ormaplatin



*R,R*-(DACH)PtCl<sub>2</sub>



*S,S*-(DACH)PtCl<sub>2</sub>

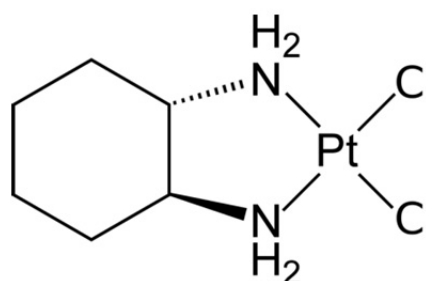


Figure 1.1. The chemical structures of platinum-based anticancer drugs and compounds.

myelosuppression and gastrointestinal disturbance (Di Francesco et al., 2002). Cisplatin-induced nephrotoxicity can be reduced by adequate hydration (Piccart et al., 2001). Also, the gastrointestinal adverse effects of cisplatin, such as vomiting and nausea, can be managed with administration of antiemetics (Kweekel et al., 2005). Cisplatin-induced neurotoxicity and ototoxicity are difficult to control, which may necessitate dose reduction or discontinuation of treatment (Kweekel et al., 2005). The clinical use of cisplatin is also restricted by inherent or acquired resistance of cancer cells (Kartalou and Essigmann, 2001, Di Francesco et al., 2002).

Since the success of cisplatin in cancer treatment, thousands of cisplatin analogues have been synthesized in an attempt to overcome its side effects and retain its antitumor activity. Among these cisplatin analogues, carboplatin, or *cis*-diammine(1,1-cyclobutanedicarboxylato-*O,O'*)platinum(II), showed a good compromise between antitumor efficacy and adverse effects. As a second-generation platinum-based anticancer drug, carboplatin has a bidentate cyclobutanedicarboxylate ligand, which replaced the dichloride ligands in cisplatin (Figure 1.1). Carboplatin is less cytotoxic (Micetich et al., 1985) and is administrated at higher doses compared to cisplatin (Wheate et al., 2010). Carboplatin has similar spectrum of antitumor activities as cisplatin, and has replaced cisplatin as the first-line treatment for ovarian cancer (Wheate et al., 2010). Carboplatin reduced the adverse effects, especially nephrotoxicity, associated with cisplatin treatment, but has myelotoxicity as its dose-limiting side effect (van Glabbeke et al., 1988). Furthermore, carboplatin usually shows cross-resistance with cisplatin (Di Francesco et al., 2002).

Further studies aiming to develop new platinum drugs demonstrated that platinum compounds with a diaminocyclohexane (DACH) ligand replacing the diammine groups in cisplatin showed a good antitumor efficacy and no cross-resistance with cisplatin (Di

Francesco et al., 2002). The DACH group has two chiral centres, so it can exist as three possible isomeric forms, *trans-R,R*-DACH, *trans-S,S*-DACH and *cis-R,S*-DACH. Interestingly, platinum compounds with different forms of DACH ligand showed different antitumor activities. *Trans*-DACH platinum compounds were shown to be more cytotoxic than their corresponding *cis*-isomers (Pendyala et al., 1995). Among *trans*-DACH platinum compounds, *R,R*-enantiomers showed more potent antitumor activity compared to their corresponding *S,S*-enantiomers (Pendyala et al., 1995).

Oxaliplatin, or (1*R*,2*R*-cyclohexanediamine-*N,N'*)(oxalato-*O,O'*)platinum(II), is a third-generation platinum-based anticancer drug. Oxaliplatin has a bidentate *R,R*-DACH ligand and an oxalate ligand replacing the diammine and dichloro groups in cisplatin, respectively (Figure 1.1). With the DACH ligand, oxaliplatin is able to overcome cisplatin resistance (Rixe et al., 1996). The oxalate ligand has improved the water solubility of oxaliplatin (Di Francesco et al., 2002), and also contributes to the difference in side effects between oxaliplatin and cisplatin (Boulikas and Vougiouka, 2003). Oxaliplatin in combination with 5-fluorouracil and leukovorin has been approved for the treatment of colorectal cancer, which is insensitive to cisplatin and carboplatin (Stein and Arnold, 2012). The toxicity profile of oxaliplatin is different compared to cisplatin, with less frequent nephrotoxicity and ototoxicity. However, peripheral sensory neurotoxicity is a dose-limiting side effect of oxaliplatin (Kweekel et al., 2005).

Ormaplatin, or tetrachloro(1,2-cyclohexanediamine-*N,N'*)platinum(IV), is another DACH platinum compound, although its DACH ligand is a racemic mixture of the *R,R*- and *S,S*-isomers (Figure 1.1). Ormaplatin was chosen for clinical development because of its capability of overcoming cisplatin resistance and its reduced nephrotoxicity (Luo et al., 1999). However, treatment with ormaplatin resulted in severe and poorly reversible neurotoxicity.

Therefore, the clinical development of ormaplatin was abandoned during phase I clinical trials (O'Rourke et al., 1994, Schilder et al., 1994).

### **1.1.2. Mechanism of action**

In general, the mechanism of action by which platinum-based anticancer drugs exerts their antitumor activity involves drug cellular uptake, activation of the platinum compound, formation of platinum-DNA adducts and cellular responses to the platinum-DNA damage (Jung and Lippard, 2007). First, platinum drugs and/or their active metabolites enter cancer cells through carrier-facilitated and active transport as well as passive diffusion. Several membrane transporters, such as copper transporters (CTR) and organic cation transporters (OCT), have been found to mediate the cellular uptake of platinum drugs (Liu et al., 2012). Then, platinum compounds are converted to their active forms through aquation reactions replacing their leaving ligands with water molecules. Next, the active forms of platinum compounds bind to DNA at the N-7 position of guanine (G) or adenine (A) to form primarily 1,2-GG, 1,2-AG and 1,3-GNG intrastrand cross-links, as well as a small portion of interstrand cross-links (Chaney et al., 2005, Kweekel et al., 2005, Todd and Lippard, 2009). These platinum-DNA adducts bend and unwind the DNA duplex (Jamieson and Lippard, 1999). The distortion of DNA structure inhibits DNA replication and transcription, resulting in cell cycle arrest (Jordan and Carmo-Fonseca, 2000, Kelland, 2007). Platinum-DNA damage can be removed by nucleotide excision repair (NER) and/or other DNA repair mechanisms (Reardon et al., 1999, Di Francesco et al., 2002, Wang and Lippard, 2005), or ultimately leads to the activation of apoptotic pathways and cancer cell death (Jordan and Carmo-Fonseca, 2000, Kelland, 2007).

Cisplatin undergoes aquation with the replacement of one or both of the chloride ligands with water molecules (Kelland, 2007). Aquated cisplatin binds to DNA at the N-7 position of guanine (G) or adenine (A), through covalent coordinate bonds. Subsequently, the platination process is completed by the formation of the second platinum-DNA bond (Kelland, 2007). Cisplatin forms platinum-DNA adducts containing diammine carrier ligands, with the presence of approximately 60-65% GG, 25-30% AG and 5-10% GNG intrastrand cross-links as well as a small portion of interstrand cross-links (Jung and Lippard, 2007). Interestingly, the platinum-DNA adducts formed by cisplatin are 30 times more toxic than that of its *trans*-isomer due to different repair effectivity (Mello et al., 1995).

Carboplatin shares the same *cis*-diammine carrier ligands with cisplatin, and thus forms the same platinum-DNA adducts, which could explain the similar spectrum of antitumor activities and cross-resistance between carboplatin and cisplatin (Chaney et al., 2005). However, the activation of carboplatin by aquation reactions is much slower than that for cisplatin (Alberts and Dorr, 1998, Go and Adjei, 1999). Therefore, compared to cisplatin, carboplatin forms platinum-DNA adducts more slowly, and is also less cytotoxic to cancer cell lines (Micetich et al., 1985). In the clinic, due to its lower cytotoxicity, carboplatin can be administered at much higher doses than cisplatin (Wheate et al., 2010).

Oxaliplatin is thought to be converted to its reactive forms through aquation reactions with the replacement of the oxalate leaving group with water molecules (Di Francesco et al., 2002). However, the aquation reactions takes more time for oxaliplatin than for cisplatin (Desoize and Madoulet, 2002). As with cisplatin, oxaliplatin forms platinum-DNA adducts through a two-step process, by which aquated platinum compounds sequentially form covalent coordinate bonds with two guanine (or adenine) in the DNA. However, this two-step process for oxaliplatin appears to be slower than that for cisplatin *in vitro* (Page et al., 1990, Saris et



al., 1996). The slow rate of reaction for oxaliplatin may be accounted for by the steric hindrance and hydrophobicity of the bulky DACH ligands. Oxaliplatin produces the same types of platinum-DNA adducts as cisplatin, at the same sites on the DNA (Jennerwein et al., 1989, Page et al., 1990, Woynarowski et al., 1998). Like cisplatin, oxaliplatin forms approximately 60–65% GG, 25–30% AG and 5–10% GNG intrastrand cross-links, as well as 1–3% GG interstrand cross-links (Levi et al., 2000, Chaney et al., 2005). Although oxaliplatin and cisplatin appear to form platinum-DNA adducts in a similar pattern, the level of platinum-DNA damage induced by oxaliplatin is two- to six-fold lower than that of cisplatin at equimolar concentration (Woynarowski et al., 1998). In addition, the chemical structure of the platinum adducts are different between oxaliplatin and cisplatin. The platinum-DNA adduct formed by oxaliplatin contains DACH carrier ligands, whereas that of cisplatin contains diammine carrier ligands. The DACH platinum-DNA adducts cause a greater distortion of the DNA because of its steric hindrance, which in turn may lead to more effective inhibition of DNA replication and transcription, as compared to the diammine platinum-DNA adducts formed by cisplatin (Desoize and Madoulet, 2002). Furthermore, the formation of the different adducts is thought to be the mechanism by which oxaliplatin bypasses cisplatin/carboplatin resistance (Boulikas and Vougiouka, 2003). The bulky hydrophobic DACH group pointing into the DNA major groove protects the platinum-DNA adducts from being recognized by some DNA repair mechanisms, such as mismatch repair (Kasparkova et al., 2008). Collectively, although producing lower amount of platinum-DNA adducts, oxaliplatin results in at least equal levels of cytotoxicity compared to cisplatin (Schmidt and Chaney, 1993, Rixe et al., 1996, Woynarowski et al., 2000, Desoize and Madoulet, 2002).

Ormaplatin containing a platinum(IV) is first reduced to Pt(DACH)Cl<sub>2</sub>, or dichloro(1,2-cyclohexanediamine-*N,N'*)platinum(II) (Figure 1.1) (Chaney et al., 1990). Pt(DACH)Cl<sub>2</sub> can be regarded as the DACH counterpart of cisplatin and subsequently undergoes similar biotransformation as cisplatin (Mauldin et al., 1988, Gibbons et al., 1989, Chaney et al., 1990). Eventually, ormaplatin forms similar DACH platinum-DNA adducts as oxaliplatin, with the difference being that the DACH carrier ligand of ormaplatin is a racemic mixture of *R,R*- and *S,S*-enantiomers (Wheate et al., 2010).

## **1.2. Platinum drug-induced peripheral neurotoxicity**

Nephrotoxic and gastrointestinal side effects of platinum-based anticancer drugs have been reduced in the clinic by the administration of intravenous hydration and antiemetics, respectively. At present, toxicity to the peripheral nervous system is a major dose-limiting side effect associated with at least some of the clinically used platinum drugs (Screnci and McKeage, 1999).

### **1.2.1. Clinical features**

Peripheral neurotoxicity is a major dose-limiting side effect of cisplatin and affects approximately 50% of patients treated with cisplatin chemotherapy (van der Hoop et al., 1990). Symptoms and signs of peripheral neurotoxicity, including tingling paresthesia, loss of tendon reflexes, loss of vibration sense and loss of position sense, predominantly involve the distal extremities and may progress proximally (Roelofs et al., 1984, Thompson et al., 1984). Sensory nerve conduction velocity and responses are reduced, whereas motor involvement is rare (Roelofs et al., 1984, Thompson et al., 1984). Sensory ataxia is observed in patients that

receive high-dose cisplatin therapy (Ozols and Young, 1985). The development of neurotoxicity is related to the cumulative dose of cisplatin that has been administered (Gregg et al., 1992, McKeage, 1995). The neurotoxicity becomes apparent in patients receiving 300 mg/m<sup>2</sup> of cisplatin, and becomes significant at a cumulative dose of 400–500 mg/m<sup>2</sup> or more (Walsh et al., 1982, Thompson et al., 1984, Ozols et al., 1985, Ozols and Young, 1985). The neurotoxicity continues or worsens for the first few months after cessation of treatment (Grunberg et al., 1989, Hovestadt et al., 1992). The recovery is slow and usually incomplete. Permanent peripheral nerve damage is often seen in cancer patients after cisplatin chemotherapy (van der Hoop et al., 1990).

Carboplatin is considered to have mild and infrequent peripheral neurotoxicity as compared to cisplatin (McKeage, 1995). Only approximate 6% of patients receiving carboplatin treatment develop peripheral neurotoxicity (Canetta et al., 1985). However, high-dose carboplatin may induce the similar type of neurotoxicity as cisplatin (Cavaletti et al., 1998). Also, patients who receive carboplatin in combination with other neurotoxic anticancer drugs, such as paclitaxel, have increased risk to develop neurotoxicity (International Collaborative Ovarian Neoplasm, 2002).

Oxaliplatin induces two different types of peripheral sensory neurotoxicity, an acute neuropathy that commonly appears during or shortly after the first few infusions and a chronic cumulative neuropathy that is similar to cisplatin-induced neurotoxicity (Grothey, 2003). The acute neurotoxicity affects approximately 85–95% of all patients receiving oxaliplatin-based chemotherapy (Gamelin et al., 2002). Symptoms of the acute neurotoxicity mainly include paresthesias and dysesthesias in the hands, feet and perioral region, and are often triggered or aggravated by cold exposure (Grothey, 2003). Approximate 1–2% of patients experience pharyngolaryngeal dysesthesia, a sensation of difficulties in breathing or

swallowing without any objective evidence of laryngeal obstruction (Grothey, 2003, Pasetto et al., 2006). Acute neurotoxic symptoms are transient in nature and can recover between cycles of treatment. The mechanism underlying the acute neurotoxicity may involve disorders of sodium ion channels located in the neural cell membrane and consequent hyperexcitability (Gamelin et al., 2002, Wilson et al., 2002), but other mechanisms are also possible.

The chronic neurotoxicity is the major dose-limiting side effect of oxaliplatin (Raymond et al., 1998, Gamelin et al., 2002) and is observed in about 50% of patients that receive oxaliplatin-based chemotherapy (Krishnan et al., 2005). The chronic neurotoxicity induced by oxaliplatin is similar to that of cisplatin. Symptoms and signs of this form of neurotoxicity include paresthesias and dysesthesias in the extremities and dysfunction of proprioception that may affect normal daily activities (Cersosimo, 2005). Sensory ataxia may develop, whereas motor involvement is rare (Grothey, 2003). The chronic neurotoxicity is cumulative in nature, which appears following a cumulative dose of 300 mg/m<sup>2</sup> and is most common in patients that receive a total dose of 540 mg/m<sup>2</sup> or more (Quasthoff and Hartung, 2002, Cersosimo, 2005). As with cisplatin, the chronic neurotoxic symptoms induced by oxaliplatin continue or progress for a few months after cessation of treatment (McWhinney et al., 2009). The recovery is slow and usually incomplete. Only about 40% of all patients experience complete recovery 6-8 months after oxaliplatin treatment has been stopped (Extra et al., 1998).

The clinical development of ormaplatin was discontinued during phase I clinical trials due to its severe and poorly revisable peripheral neurotoxicity (Screnci and McKeage, 1999). Several phase I clinical trials were carried out to examine different treatment schedule of ormaplatin (O'Rourke et al., 1994, Schilder et al., 1994, Tutsch et al., 1999). Neurotoxicity consisting of peripheral sensory neuropathy was shown to be the dosing-limiting side effect of ormaplatin. Patients that received cumulative doses greater than 165-200 mg/m<sup>2</sup> were at

higher risk to experience the neurotoxic side effect (O'Rourke et al., 1994, Schilder et al., 1994). In addition, the neurotoxic symptoms worsened after the completion of ormaplatin treatment (O'Rourke et al., 1994, Schilder et al., 1994). Ormaplatin shares some neurotoxic characteristics with cisplatin, such as cumulative toxicity, post-treatment deterioration and lack of motor involvement. However, ormaplatin causes sensory ataxia at lower cumulative doses and more frequently than cisplatin (Screnci and McKeage, 1999).

### **1.2.2. Mechanisms**

The mechanism by which platinum drugs induce peripheral neurotoxicity has not been fully elucidated so far, although dorsal root ganglia (DRG) have been shown to be the major site of damage. The DRG are part of the peripheral nervous system and are located bilaterally on the distal end of the dorsal roots in the intraforaminal space (Sghirlanzoni et al., 2005, Pope et al., 2013). The DRG contain primary sensory neurons that are surrounded by satellite cells (Sghirlanzoni et al., 2005). These primary sensory neurons are pseudounipolar, with a single axon that bifurcates into the peripheral and central branch, which transduce sensory information from the periphery to the central nervous system (Sapunar et al., 2012, Pope et al., 2013). DRG neurons can be classified by their morphology, neurotransmitters or receptors. All classifications distinguish two types of DRG neurons, large-light neurons and small-dark neurons. Large-light neurons are connected to A $\beta$  and A $\delta$  fibres, which transfer proprioceptive and tactile sensation, whereas small-dark neurons are connected to unmyelinated C fibres, which transfer thermal and nociceptive sensation (Sghirlanzoni et al., 2005).

At present, it has been generally accepted that the primary damage induced by platinum drugs to the peripheral nervous system happens in the cell bodies of DRG neurons, rather than their

axons (Tomiwa et al., 1986, Cavaletti et al., 1992b, Holmes et al., 1998, Krarup-Hansen et al., 1999, Cavaletti et al., 2001, McKeage et al., 2001, Jamieson et al., 2005, Liu et al., 2009, Renn et al., 2011, Ip et al., 2013). Histopathological studies have demonstrated that the decrease in cell body size of DRG neurons is one of the morphological hallmarks of platinum drug-induced peripheral neurotoxicity in patients (Krarup-Hansen et al., 1999) and animal models (Tomiwa et al., 1986, Cavaletti et al., 1992b, Holmes et al., 1998, Cavaletti et al., 2001, Jamieson et al., 2005, Renn et al., 2011). The decrease in DRG neuronal cell body size appears to indicate cell body atrophy given the lack of evidence of cell loss or death (Tomiwa et al., 1986, Barajon et al., 1996, Jamieson et al., 2005). These morphological changes may explain the reduction of sensory nerve conduction velocity observed in patients with platinum drug-induced peripheral neuropathy, because sensory nerve conduction velocity is related to cell body size of DRG neurons (Harper and Lawson, 1985).

High levels of platinum accumulation have been detected within the DRG, compared to spinal cord and brain, following exposure to platinum-based anticancer drugs in patients (Thompson et al., 1984, Gregg et al., 1992, Krarup-Hansen et al., 1999) and rodent models (Cavaletti et al., 1990, Screnci et al., 1997, Screnci et al., 2000, Cavaletti et al., 2001, Ip et al., 2013). As opposed to the central nervous system that protected by the blood-brain barrier, the DRG are supplied by fenestrated capillaries. This loose blood-nerve barrier exposes the DRG to circulating toxins, such as intravenously applied platinum-based anticancer drugs (Sghirlanzoni et al., 2005, Sapunar et al., 2012), which may at least partially explain the observed high-level platinum accumulation within the DRG. However, the tissue accumulation of platinum does not adequately explain the mechanism of platinum drug-induced peripheral neurotoxicity, because the neurotoxicity profiles of platinum-based

anticancer drugs appear not to correlate with the amount of platinum accumulating within the DRG tissue (Screnci et al., 1997, Holmes et al., 1998, Screnci et al., 2000).

More recently, a growing body of evidence has suggested that platinum-DNA damage within DRG neurons may play an important role in platinum drug-induced peripheral neurotoxicity. Cultured DRG neurons accumulated higher levels of platinum-DNA adducts after cisplatin treatment, as compared to a cancer cell line (McDonald et al., 2005). DRG tissue was also shown to accumulate platinum-DNA adducts more so than other tissues exposed to equivalent blood levels in cisplatin-treated rats (McDonald et al., 2005). Treatment with oxaliplatin and cisplatin resulted in different levels of platinum-DNA adducts in cultured DRG neurons, which was correlated with their neurotoxicity (Ta et al., 2006). Mice with dysfunctional nucleotide excision repair (NER) showed more severe peripheral neuropathy and higher levels of platinum-DNA adducts within the DRG after cisplatin treatment, as compared to those proficient for NER functions. In addition, independently from the specific NER phenotype, the severity of peripheral neuropathy was significantly correlated with the levels of platinum-DNA adducts in DRG neurons (Dzagnidze et al., 2007).

### **1.3. Platinum drug-induced transcriptional inhibition**

#### **1.3.1. Evidence**

In the late nineteen-eighties, Sorenson and colleagues reported that cell cycle arrest at G<sub>2</sub> phase was required for cisplatin-induced apoptosis in L1210 leukemia cells and that loss of DNA replication capability did not correlate with cisplatin-induced cell death (Sorenson and Eastman, 1988a, b, Sorenson et al., 1990). These findings suggested that cells arrested in G<sub>2</sub>

phase may be due to their inability to synthesize the mRNA required for passing into mitosis, implicating transcriptional inhibition as a key mechanism of cisplatin cytotoxicity.

To date, a growing body of evidence has demonstrated that platinum-based anticancer drugs induce transcriptional inhibition, and has suggested that the cytotoxicity of platinum drugs is directly correlated with their ability to block RNA synthesis (Todd and Lippard, 2009). Exposure of human fibrosarcoma cells to cisplatin and oxaliplatin inhibited rRNA synthesis at the level of the transcription of 47S/45S rRNA, and induced nucleolar disintegration (Burger et al., 2010b). In addition, treatment of HeLa cells with cisplatin caused a redistribution of the major components of the rRNA transcription machinery in the nucleolus, including upstream binding factor and RNA polymerase I (Jordan and Carmo-Fonseca, 1998). Inhibition of mRNA synthesis was also observed in human fibroblasts after cisplatin treatment, which was correlated with the induction of p53, p21 and apoptosis (Ljungman et al., 1999). Furthermore, as with these dividing cells, treatment of cultured cortical neurons with cisplatin induced transcriptional inhibition (Gozdz et al., 2008).

### **1.3.2. Mechanisms**

The mechanism by which platinum-based anticancer drugs inhibit transcription has not been fully elucidated, although platinum-DNA damage has been shown to play a central role in platinum drug-induced transcriptional inhibition. Several hypotheses have been proposed to link platinum-DNA damage to transcriptional inhibition.

Some studies have suggested that platinum-DNA damage may serve as a physical barrier to RNA polymerase progression and therefore inhibit transcription. Studies using reconstituted systems and cell extracts demonstrated that platinum-DNA damage blocked RNA polymerase



at the site of the platinum cross-link (Jung and Lippard, 2003, Tornaletti et al., 2003, Jung and Lippard, 2006, Laine and Egly, 2006), and that the stalled polymerase was able to resume transcription after chemical removal of the platinum-DNA adduct from the template (Jung and Lippard, 2003, 2006). Most recently, a study using live mammalian cells transfected with plasmid DNAs carrying platinum-DNA adducts further strengthened the hypothesis of platinum-DNA damage as a physical impediment to transcription (Ang et al., 2010). This study demonstrated that platinum-DNA damage derived from oxaliplatin and cisplatin inhibited transcription by impeding passage of RNA polymerase II and that NER can remove the blockage and restore transcription. In addition, the platinum-DNA adducts formed by oxaliplatin, which carries a bulky DACH ligand, caused greater inhibition of transcription, compared to that of cisplatin containing two ammine groups. A structure-function analysis using X-ray crystallography and RNA-extension assays demonstrated that RNA polymerase II stalled upstream of the platinum-DNA adducts due to a translocation barrier that prevented delivery of the lesion into the enzyme active site (Damsma et al., 2007).

Another possible mechanism by which platinum-DNA damage inhibit transcription could be disruption of nucleosome dynamics. Because accurate transcription requires proper nucleosome positioning and mobility (Luger, 2006, Workman, 2006), any disruption of nucleosome positioning and mobility resulted from platinum-DNA damage could potentially interfere with transcription. Previous studies using reconstituted nucleosome revealed that DNA strand containing a cisplatin cross-link significantly altered nucleosome positioning, whereby the platinum lesion faced inward towards the histone octamer core (Danford et al., 2005, Ober and Lippard, 2007, 2008). In addition, platinum-DNA adducts formed by oxaliplatin and cisplatin inhibited histone octamer-DNA sliding, altering nucleosome mobility (Wu and Davey, 2008, Zhu et al., 2013). Interestingly, platinum-protein adducts

were formed at specific histone methionine residues after treatment of nucleosome core particles with platinum drugs (Wu et al., 2008), which could also potentially alter nucleosome positioning and mobility. However, a recent study using single-round transcription assays with T7 RNA polymerase showed that cisplatin cross-links induced similar patterns of transcription inhibition in free and nucleosomal DNA samples, and that no transcripts corresponding to stalling of the polymerase at the nucleosome barrier were observed (Todd and Lippard, 2010). These findings suggested that T7 RNA polymerase can successfully navigate along cisplatin-damaged nucleosome templates, but stalls when physically contacting a platinum-DNA adduct. Therefore, these findings argued against disruption of nucleosome dynamics as a potential mechanism of platinum-DNA damage-induced transcriptional inhibition, but further supported the hypothesis that platinum-DNA adducts may physically block transcription, even in a nucleosome environment.

A model of transcription factor hijacking has also been proposed for platinum-DNA damage-induced transcriptional inhibition. According to this model, platinum-DNA adducts may serve as binding targets for transcription factors and lure these transcription factors away from their normal site of action, and therefore disrupt transcription. Transcription factors, such as TATA box-binding protein (TBP) and upstream binding factor (UBF), were shown to bind selectively to platinum-damaged DNA (Vichi et al., 1997, Zhai et al., 1998). In addition, transcription from an undamaged DNA template was inhibited by addition of a cisplatin-damaged exogenous DNA substrate in a concentration-dependent manner (Vichi et al., 1997, Zhai et al., 1998, Cullinane et al., 1999). This inhibition of transcription was reversed by adding transcription factors, such as TBP and UBF (Vichi et al., 1997, Zhai et al., 1998). Furthermore, structural analysis revealed a strong similarity between the structure of the

TATA box as found in TATA-TBP complex and that of platinated oligonucleotides (Vichi et al., 1997).

Some findings have also suggested that platinum-DNA damage may induce transcriptional inhibition through DNA damage signalling pathways, such as DNA-dependent protein kinase (DNA-PK)/poly(ADP-ribose) polymerase 1 (PARP-1) pathway. DNA-PK and PARP-1 are proteins that both play key roles in DNA damage repair (Meek et al., 2008, Luo and Kraus, 2012). DNA-PK has been shown to repress rRNA synthesis (Kuhn et al., 1995, Michaelidis and Grummt, 2002). PARP-1 has also been suggested to play a role in rRNA synthesis (Desnoyers et al., 1996, Boamah et al., 2012). Most recently, a study using 5-ethynyl uridine incorporation assay to monitor RNA synthesis demonstrated that inhibition of either DNA-PK or PARP-1 prevented cisplatin-induced block of rRNA synthesis, and that loss of DNA-PK function impeded activation of PARP-1 in damaged cells (Calkins et al., 2013). This finding suggested that a sequential activation of DNA-PK and PARP-1 by platinum-DNA damage may play an important role in cisplatin-induced inhibition of rRNA synthesis.

It should be noted that these hypotheses about how platinum-DNA damage induce transcriptional inhibition are not mutually exclusive. By one or more mechanisms, platinum-based anticancer drugs may inhibit transcription at both the initiation and elongation phase.

#### **1.4. Summary and aims of thesis**

The platinum-based anticancer drugs, including cisplatin, carboplatin and oxaliplatin, have been widely used for the treatment of a variety of cancer types in the clinic. Their anticancer activity is primarily based on the formation of platinum-DNA adducts at the N-7 position of

guanine or adenine, which inhibit DNA replication and transcription, and in turn trigger cell cycle arrest and apoptosis of cancer cells. Peripheral sensory neurotoxicity is a dose-limiting side effect of at least some of the platinum-based anticancer drugs. The mechanism by which platinum drugs induce peripheral neurotoxicity remains unclear, although the sensory neurons within the DRG have been shown to be the major site of damage. One of the morphological hallmarks of platinum drug-induced peripheral neurotoxicity is the cell body atrophy of DRG neurons. Recently, increasing evidence has suggested that platinum-DNA damage within DRG neurons may play an important role in platinum drug-induced peripheral neurotoxicity. As opposed to cancer cells, DRG neurons are post-mitotic cells that do not undergo DNA replication or progress through the cell cycle. Therefore, although both cancer cells and DRG neurons accumulate platinum-DNA damage after exposure to platinum drugs, the mechanism linking the formation of platinum-DNA damage to the development of peripheral neurotoxicity must differ from that of their antitumor action. Platinum-DNA damage has been shown to inhibit transcription in some cell types, but this mechanism has not been well investigated in DRG neurons. These considerations led us to hypothesize that platinum-DNA damage may be critically involved in the DRG neuronal cell body atrophy and platinum drug-induced peripheral neurotoxicity through its induction of transcriptional inhibition.

Therefore, the overall aims of this thesis were:

- To characterize the transcriptional activity of DRG neurons;
- To investigate the potential role of platinum-DNA damage-induced transcriptional inhibition in DRG neuronal cell body atrophy and peripheral neurotoxicity induced by oxaliplatin;

- To further explore the potential role of platinum-DNA damage-induced transcriptional inhibition in DRG neuronal cell body atrophy and peripheral neurotoxicity induced by other platinum-based anticancer drugs.

In order to achieve these overall aims, experiments were carried out to:

- Establish an *in vitro* method for visualization and quantitation of nascent RNA synthesis in individual cultured DRG neurons;
- Determine the temporal interrelationship between platinum-DNA damage, transcriptional inhibition and neuronal cell body atrophy induced by oxaliplatin in cultured DRG cells;
- Determine the effects of different pharmacological inhibitors on oxaliplatin toxicity in cultured DRG cells;
- Compare the effects of different platinum drugs and compounds on cultured DRG cells.
- Compare the effects of platinum drugs with those of a model transcriptional inhibitor.

## Chapter 2. Materials and methods

### 2.1. Chemicals and reagents

Oxaliplatin was obtained from Sanofi (Paris, France) and Sigma-Aldrich (St Louis, MO, USA). Cisplatin and carboplatin were obtained from Sigma-Aldrich. The racemic mixture of ormaplatin was kindly provided by the National Cancer Institute (Bethesda, MD, USA). *R,R*-ormaplatin, *S,S*-ormaplatin, *R,R*-Pt(DACH)Cl<sub>2</sub> and *S,S*-Pt(DACH)Cl<sub>2</sub> were synthesized as outlined previously (Screnci et al., 1997). Sodium thiosulfate pentahydrate was purchased from Scharlau (Barcelona, Spain). Cimetidine, actinomycin D, tetraethylammonium chloride (TEA), potassium chloride, 4,4'-diisothiocyanatostilbene-2,2'-disulfonic acid disodium salt hydrate (DIDS), 5-nitro-2-(3-phenylpropylamino)benzoic acid (NPPB) and benzamide were purchased from Sigma-Aldrich. Wortmannin, NU 7026 and olaparib were purchased from Cayman Chemical (Ann Arbor, MI, USA). Both 5% glucose and 0.9% sodium chloride were obtained from Baxter (Deerfield, IL, USA).

### 2.2. Animals

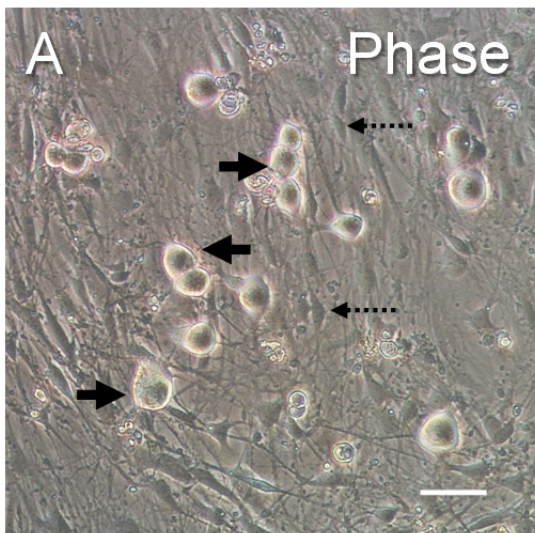
Animals were housed by the Vernon Jansen Unit at the University of Auckland, and were maintained in a temperature-controlled environment on a 12-hour light-dark cycle with access to food and water *ad libitum*. All animal procedures were approved by and performed in compliance with ethical guidelines of the Animal Ethics Committee of the University of Auckland.

### 2.3. Cell culture

Primary culture of rat dorsal root ganglion (DRG) cells was established as described previously with slight modifications (Jong et al., 2011, Liu et al., 2013). In brief, DRGs from all spinal levels were dissected from 20-day-old Wistar rats euthanized with pentobarbitone (Chemstock Animal Health, Christchurch, New Zealand). Then, DRGs were digested with 2.5 mg/ml collagenase and 1 mg/ml dispase (Life Technologies, Carlsbad, CA, USA) for 50 min at 37°C, followed by trypsinization using 0.25% trypsin (Life Technologies) for 40 min at 37°C. Subsequently, DRGs were mechanically triturated using fine-bore glass Pasteur pipettes to dissociate and release cells, and the resulting cell suspension was filtered through a 100- $\mu$ m cell strainer (Becton Dickinson, Franklin Lakes, NJ, USA) to remove tissue debris. DRG cells were isolated by centrifugation at  $800 \times g$  in Percoll solution (density: 1.040 g/ml) (Sigma-Aldrich) for 20 min at room temperature. Then, DRG cells were re-suspended and cultured in Neurobasal-A medium supplemented with 5% horse serum, 100 U/ml penicillin, 0.1 mg/ml streptomycin, 2 mM glutamine and 1% N-2 supplement (Life Technologies) at 37°C in a humid atmosphere of 5% CO<sub>2</sub>-95% air. For the first two days of culture, 40  $\mu$ M 5-fluoro-2'-deoxyuridine and 120  $\mu$ M uridine (Sigma-Aldrich) were added to remove non-neuronal cells. Then, DRG cells were cultured in the normal culture medium for a further one day before any experimental manipulation.

Cultured DRG cells consisted of sensory neurons and non-neuronal cells that were easily distinguishable by their morphology under phase-contrast microscopy (Figure 2.1). Typically, DRG neurons were characterized by their large and round cell bodies with a sharp halo, whereas non-neuronal cells showed small and spindle-shaped morphology. This observation

Living cells



Fixed cells

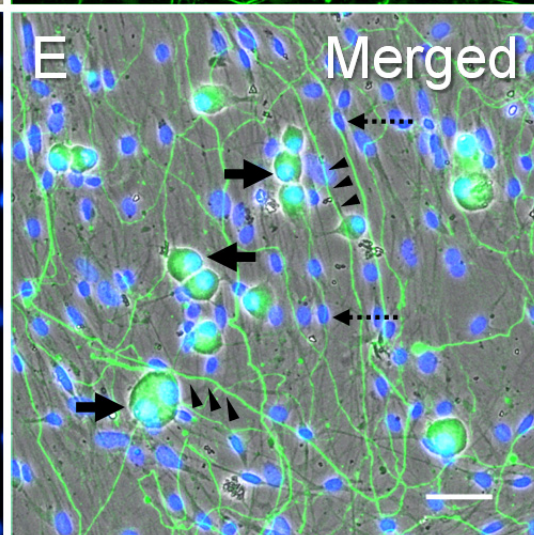
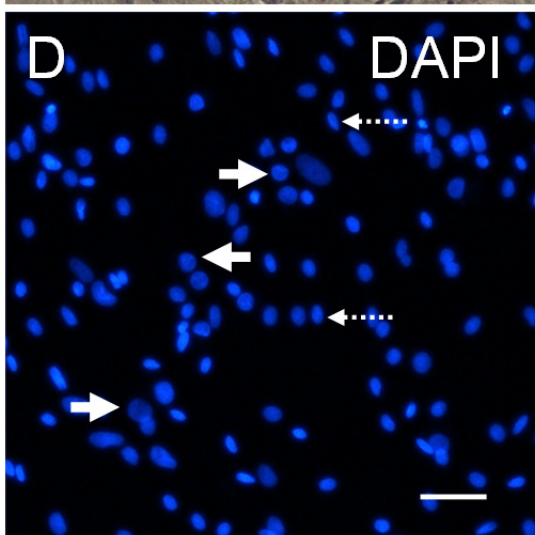
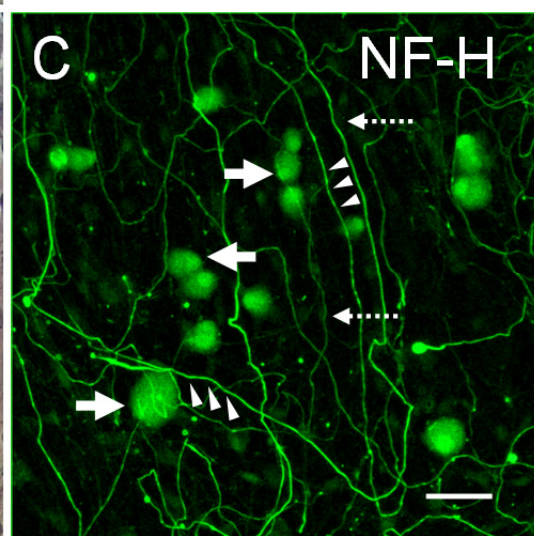
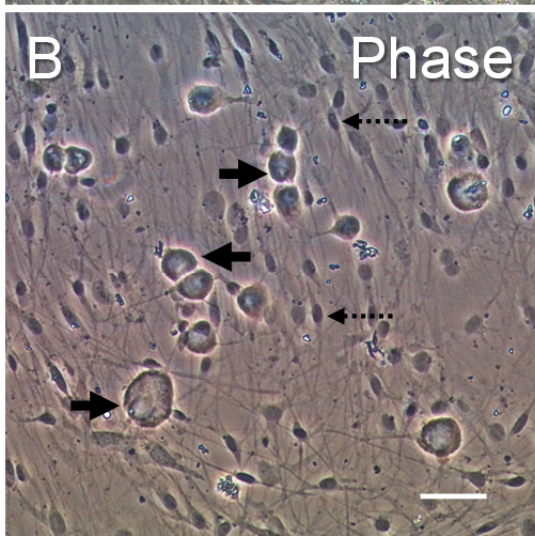




## Figure 2.1. Primary culture of rat DRG cells.

Rat DRG cells grown in culture for three days were photographed from the same field of view before (A) and after neurofilament heavy subunit (NF-H, green) fluorescence immunocytochemistry (B-E). Nuclear DNA was counterstained with DAPI (blue). Images were acquired using a 10x objective.

Images show that cultured rat DRG cells consisted of sensory neurons and non-neuronal cells that were easily distinguishable by their morphology under phase-contrast microscopy and by immunocytochemistry using a neuronal marker, NF-H.

(A) Phase contrast image of living DRG cells. DRG neurons (➡) were characterized by their large and round cell bodies with a sharp halo. Non-neuronal cells (↔) showed small and spindle-shaped morphology similar to Schwann cells.

(B) Phase contrast image of fixed DRG cells. DRG neurons (➡) and non-neuronal cells (↔) were easily identified by their morphology as mentioned in (A).

(C) NF-H staining (green) showing DRG neurons (➡) and their neurites (▶), but not non-neuronal cells (↔). Neurites of DRG neurons grew well in the culture.

(D) DAPI staining (blue) showing nuclei of DRG neurons (➡) and non-neuronal cells (↔).

(E) Merged image of (B-D) showing DRG neurons (➡), neurites (▶) and non-neuronal cells (↔).

Bar= 50  $\mu$ m.

was confirmed by immunocytochemistry using a neuronal marker, neurofilament heavy subunit.

## **2.4. Fluorescent immunocytochemistry**

Rat DRG cells grown on chamber slides were washed with pre-warmed phosphate buffered saline (PBS), fixed with 4% paraformaldehyde for 15 min at room temperature, and then permeabilized using 0.2% Triton X-100 in PBS for 15 min at room temperature. Next, cells were incubated with blocking solution (PBS containing 0.2% Triton X-100, 3% goat serum and 2% bovine serum albumin) for 60 min at room temperature. After rinsing with 0.2% Triton X-100 in PBS, cells were incubated with Anti-Neurofilament 200 (NF-H) primary antibody (1:800, Sigma-Aldrich) diluted in immunobuffer (PBS containing 0.2% Triton X-100 and 1% goat serum) for overnight at 4°C in darkness. Subsequently, cells were rinsed with 0.2% Triton X-100 in PBS, and were incubated with Alexa Fluor 488-labelled anti-rabbit IgG secondary antibody (1:500, Life Technologies) diluted in immunobuffer for 3 h at 4°C, protected from light. After incubation, cells were washed with PBS and then counterstained and coverslipped with VECTASHIELD mounting medium containing 4',6-diamidino-2-phenylindole (DAPI) (Vector Laboratories, Burlingame, CA, USA). Fluorescence images were acquired using a Nikon Eclipse Ti-U inverted microscope equipped with a Nikon DS-Fi1c digital camera (Nikon, Tokyo, Japan), at 465-495 nm excitation and 515-555 nm emission for NF-H staining and at 330-380 nm excitation and >420 nm emission for DAPI staining.

## **2.5. Experimental incubation**

In most experiments, rat DRG cells grown on plates or chamber slides were exposed to experimental conditions either for 3 h followed by culture in drug-free medium until up to 48 h after the start of treatment, or continuously for up to 48 h, as indicated in each chapter.

To investigate the effects of DNA-PK and PARP-1 inhibitors on oxaliplatin toxicity in Chapter 5, rat DRG cells were pre-treated with these inhibitors for 1 h before exposure to oxaliplatin for 3 h, followed by culture in drug-free medium until 24 h.

## **2.6. Assessment of nascent RNA synthesis by 5-ethynyl uridine incorporation**

A Click-iT RNA Imaging Kit (Life Technologies) was used according to manufacturer's instructions with slight modifications. In brief, 20 h before the end of the experiment, 1 mM 5-ethynyl uridine (EU) was added to the cells grown on chamber slides. At the end of the experiment, cells were washed with pre-warmed PBS, fixed with 4% paraformaldehyde for 15 min at room temperature, and then permeabilized using 0.2% Triton X-100 in PBS for 15 min at room temperature. To detect RNA-incorporated EU using a click chemistry reaction with Alexa Fluor 594-labelled azide, cells were then incubated with Click-iT reaction cocktail for 30 min at room temperature, protected from light. After incubation, cells were washed with Click-iT reaction rinse buffer and PBS, and then counterstained and coverslipped with VECTASHIELD mounting medium containing DAPI (Vector Laboratories).

Fluorescence images were acquired using a Nikon Eclipse Ti-U inverted microscope equipped with a Nikon DS-Fi1c digital camera (Nikon), at 540-580 nm excitation and 600-660 nm emission for Alexa594 labelling of RNA-incorporated EU and at 330-380 nm excitation and >420 nm emission for DAPI staining of nuclear DNA. After background correction, the fluorescence pixel intensities of EU-Alexa594 staining within cell bodies and DAPI staining within nuclei were measured for individual neurons using Nikon NIS-Elements software (Nikon). The same individual neurons were also measured for cell body areas as described in section 2.10.

## **2.7. Assessment of nascent RNA synthesis by [<sup>3</sup>H]uridine incorporation**

One hour before the end of the experiment, 5  $\mu$ Ci/ml [<sup>3</sup>H]uridine (sp. act. >20 Ci/mmol, PerkinElmer, Waltham, MA, USA) was added to the culture. At the end of the experiment, labelling medium was removed and cells were re-suspended using 0.25% trypsin (Life Technologies). The cell suspension was thoroughly mixed with ice-cold 10% (w/v) trichloroacetic acid (Sigma-Aldrich) and placed on ice for 30 min. The acid-precipitable material was collected on a GF/C glass-fibre filtermat (Filtermat A, PerkinElmer) by a plate harvester (Harvester 96, Tomtec, Hamden, CT, USA). The filtermats were dried at room temperature overnight and their radioactivity was measured in a scintillation cocktail (Betaplate Scint, PerkinElmer) by a liquid scintillation counter (Wallac 1450 MicroBeta JET, PerkinElmer).

## **2.8. Assessment of platinum binding to DNA**

Following experimental incubations, DRG cells were harvested and their genomic DNA was extracted using a Wizard Genomic DNA Purification Kit (Promega, Madison, WI, USA) according to the manufacturer's instructions, with the modification that isopropanol precipitation was performed at 4°C overnight. The DNA content was determined by measuring the absorbance at 260 nm with a NanoDrop ND-1000 spectrophotometer (Thermo Fisher Scientific, Waltham, MA, USA). Subsequently, DNA samples were digested with an equal volume of 70% nitric acid at room temperature overnight and then at 95°C for 2 h. The resulting digests were diluted in Milli-Q water spiked with 50 ppb thallium (SPEX CertiPrep, Metuchen, NJ, USA) as internal standard. The platinum content was quantitated by inductively coupled plasma mass spectrometry (ICP-MS) on a Varian 820-MS (Varian, Palo Alto, CA, USA) using a standard calibration method. The final platinum content was normalized to the DNA content.

## **2.9. Measurement of total RNA content**

Total RNA from cultured DRG cells was extracted using an RNeasy Mini Kit (QIAGEN, Venlo, Netherlands) according to the manufacturer's instructions. Total RNA content was determined by measuring the absorbance at 260 nm with a NanoDrop ND-1000 spectrophotometer (Thermo Fisher Scientific).

## **2.10. Measurement of neuronal cell body size and number**

Cultured DRG cells were photographed by phase-contrast microscopy on a Nikon Eclipse Ti-U inverted microscope equipped with a Nikon DS-Fi1c digital camera (Nikon). Cross-sectional areas of neuronal cell bodies were measured using Nikon NIS-Elements software (Nikon). The number of neurons in each photomicrograph was determined using ImageJ software (National Institutes of Health, Bethesda, MD, USA).

## **2.11. Apoptosis assay**

Apoptosis assay was performed using an *In Situ* Cell Death Detection Kit (Roche, Basel, Switzerland) based on terminal deoxynucleotidyl transferase-mediated dUTP nick end labelling (TUNEL) technique, according to manufacturer's instructions with slight modifications. After the experimental manipulations, rat DRG cells grown on chamber slides were washed with pre-warmed PBS, fixed with 4% paraformaldehyde for 15 min at room temperature, and then permeabilized using 0.2% Triton X-100 in PBS for 15 min at room temperature. Cells were then incubated with TUNEL reaction mixture in a humidified atmosphere for 60 min at 37°C in the dark. After incubation, cells were washed with PBS, and then coverslipped with VECTASHIELD mounting medium containing DAPI (Vector Laboratories). Fluorescence images were acquired using a Nikon Eclipse Ti-U inverted microscope equipped with a Nikon DS-Fi1c digital camera (Nikon) at 465-495 nm excitation and 515-555 nm emission.

## 2.12. Statistical analysis

Data were analyzed using GraphPad Prism 6 software (GraphPad Software, La Jolla, CA, USA). The statistical significance of differences between means was assessed by unpaired  $t$ -test and one-way analysis of variance (ANOVA) with Tukey's post-test. The statistical significance of differences between medians was assessed by Kruskal-Wallis test with Dunn's post-test. The statistical significance of correlations between experimental parameters was assessed by Spearman's rank correlation analysis. In all statistical tests, a  $P$  value less than 0.05 was considered statistically significant.

# **Chapter 3. Visualization of nascent RNA synthesis in cultured rat DRG neurons via a click chemistry reaction labelling technique**

## **3.1. Introduction**

Dorsal root ganglion (DRG) neurons may require significant capacity for RNA synthesis in order to support their extraordinarily large cell bodies and long axonal projections, and their physiological sensory functions. Interference with their capacity for RNA synthesis could potentially alter their structure and function leading to diseases. Eukaryotic RNA synthesis is mainly catalyzed by three RNA polymerases. RNA polymerase I synthesizes 45S rRNA in the nucleolus, which is then processed to mature forms of 5.8-, 18-, and 28S rRNA. RNA polymerase II is responsible for transcribing pre-mRNAs of protein-coding genes as well as some of small RNAs in the nucleoplasm. RNA polymerase III is also localized in the nucleoplasm that transcribes tRNAs, 5S rRNA and some of small RNAs (Hetman et al., 2010). To date, there have been few reports of studies of global RNA synthesis in DRG neurons. The major site of RNA synthesis in DRG neurons has been shown to be the nucleus, with relatively higher transcriptional activity in the nucleolus compared to the nucleoplasm (Carmichael and Cavanagh, 1976, Casafont et al., 2010, Palanca et al., 2014). The level of RNA synthesis in DRG neurons has been demonstrated to be affected by various factors. Both mercury poisoning (Chang et al., 1972, Carmichael and Cavanagh, 1976) and treatment with bortezomib, an anticancer drug causing peripheral neuropathy (Casafont et al., 2010, Palanca et al., 2014), reduced levels of RNA synthesis in DRG neurons *in vivo*. In contrast,



the presence of nerve growth factor stimulated the transcriptional activity in cultured DRG neurons (Sensenbrenner et al., 1970). In addition, a significant biphasic increase in both nucleolar and non-nucleolar RNA transcription was reported in axotomized DRG neurons after crush injuries of the sciatic nerve (Wells and Vaidya, 1994). Furthermore, the competence of DRG neurons for distinct types of axon regrowth depends on different patterns of total mRNA transcription (Smith and Skene, 1997). Taken together, although RNA synthesis may play an important role in physiological and pathological processes of DRG neurons, this area has not been previously studied in depth.

Traditionally, two techniques have been used to detect nascent RNA synthesis in cells. The first technique relies on labelling newly synthesized RNA with radiolabeled nucleosides, such as [<sup>3</sup>H]uridine, which can be visualized by autoradiography (Uddin et al., 1984, Wassermann et al., 1988, Wells and Vaidya, 1994). However, autoradiography is time-consuming, requiring exposure times of weeks to months, and the resolution of photomicrographs obtained is poor. Also, working with radioactive materials requires a high level of caution and a special laboratory setting. The second technique is based on RNA-incorporation of halogenated nucleosides or nucleotides, such as bromouridine (BrU) (Halicka et al., 2000), fluorouridine (FU) (Boisvert et al., 2000, Casafont et al., 2006, Kalita et al., 2008) and bromouridine triphosphate (BrUTP) (Cmarko et al., 1999, Wei et al., 1999, Sadoni and Zink, 2004), which can be detected by immunostaining. Although the use of halogenated nucleosides (or nucleotides) is safer and more convenient than that of their radioactive analogues, it has some limitations. Firstly, because cells are impermeable to BrUTP, extra work has to be performed to deliver BrUTP into cells (Cmarko et al., 1999, Wei et al., 1999, Sadoni and Zink, 2004). The techniques used for delivery of BrUTP may not be applicable to all cell types. Secondly, as an antibody-based technique, immunostaining may require harsh

permeabilization conditions for access of antibodies to the RNAs, and detection of RNA synthesis in whole-mount tissues may be practically limited. Furthermore, in most studies, the primary antibody used to detect RNA-incorporated halogenated uridine (or its triphosphate) is raised against bromodeoxyuridine (BrdU), but not all commercially available anti-BrdU antibodies cross-react with these uridine analogues (Halicka et al., 2000).

Most recently, a new technique for detection of RNA synthesis has been developed, which is based on RNA-incorporation of alkyne-modified nucleosides, such as 5-ethynyl uridine (EU) (Jao and Salic, 2008) and 5-ethynyl cytidine (EC) (Qu et al., 2013). RNA-incorporated EU or EC can be detected by using a Sharpless-Meldal copper(I)-catalyzed Huisgen cycloaddition reaction (often referred to as click chemistry reaction) with azide-containing fluorophores, followed by fluorescence microscopy. This click chemistry reaction labelling technique has several advantages (Rostovtsev et al., 2002, Tornøe et al., 2002, Breinbauer and Kohn, 2003, Wang et al., 2003, Jao and Salic, 2008, Kalveram et al., 2013, Qu et al., 2013). Firstly, the click chemistry reaction is highly selective, which makes it possible to detect newly synthesized RNA with great sensitivity in complex biological samples due to low background. Secondly, the click chemistry reaction is efficient, which is complete within ~30 minutes without requiring any extreme temperature or solvent. Moreover, both components of the reaction are bioinert, and the detection molecule, azide-containing fluorophore, can easily penetrate complex samples due to its much smaller size than antibodies. Lastly, researchers are not limited in their choice of antibodies when combining the detection of RNA synthesis with classical immunostaining for other biomolecules. Taken together, the click chemistry reaction labelling technique provides a sensitive and efficient way to detect nascent RNA synthesis in cells and tissues.

With this background, the aims of the work presented in this chapter were to establish an *in vitro* method for visualization and quantitation of nascent RNA synthesis in individual cultured rat DRG neurons, using recently developed click chemistry reaction labelling techniques, and to demonstrate the experimental utility of this click chemistry-based method for investigation of DRG neuronal RNA synthesis.

## **3.2. Results**

### **3.2.1. Optimization of 5-ethynyl uridine exposure**

To optimize the *in vitro* exposure conditions of 5-ethynyl uridine (EU) for detecting nascent RNA synthesis in cultured DRG neurons, cultured cells were exposed to different concentrations of EU for different time periods. Cultured cells were then fixed with 4% paraformaldehyde before labelling of RNA-incorporated EU with Alexa Fluor 594 (Alexa594) via a click chemistry reaction. Alexa594-labelled RNA-incorporated EU was then visualized by fluorescence microscopy at 540-580 nm excitation and 600-660 nm emission.

Representative images showed that the Alexa594 fluorescence labelling of RNA-incorporated EU in cultured DRG cells appeared to increase with increasing EU exposure concentration and duration (Figure 3.1). Little or no fluorescence signals were observed when cells were exposed to 200  $\mu$ M EU for 1 h (Figure 3.1 C and D). However, the number and intensity of fluorescence signals was increased by increasing EU exposure concentration to 1 mM and the exposure time period to 20 h. Exposure of cells to 1 mM EU for 20 h resulted in the clearest fluorescence signals without any apparent background staining (Figure 3.1 I and J). These exposure conditions were then selected for use in subsequent experiments.

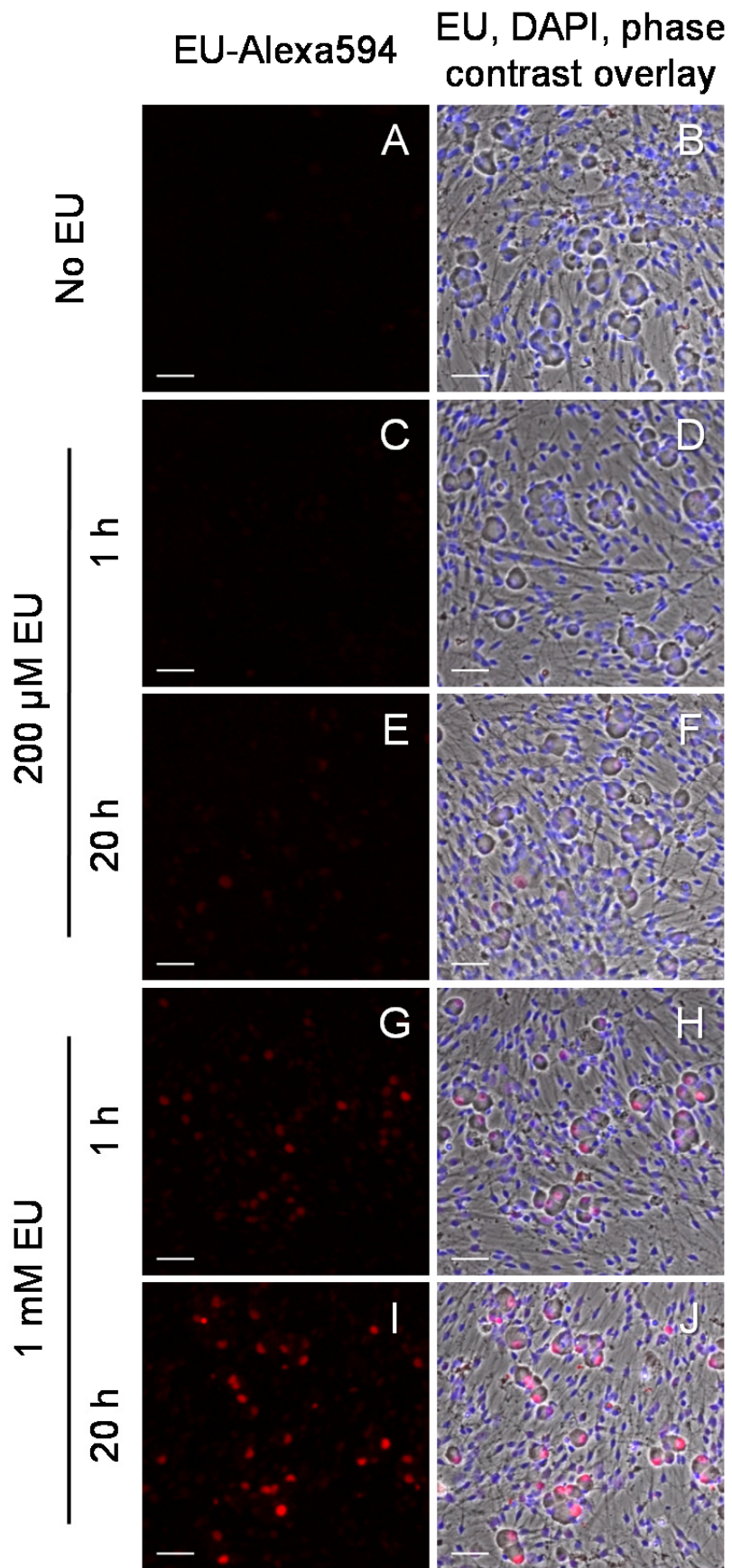


**Figure 3.1. Optimization of 5-ethynyl uridine exposure conditions for detecting its incorporation into nascent RNA of cultured DRG neurons.**

DRG cells were harvested from two rats and cultured for three days before labelling with 200  $\mu$ M 5-ethynyl uridine (EU) for 1 (C and D) or 20 h (E and F), with 1 mM EU for 1 (G and H) or 20 h (I and J) or without EU (A and B). After fixation, RNA-incorporated EU was visualized using a click chemistry reaction with Alexa594-labelled azide (red). Nuclear DNA was counterstained with DAPI (blue). Images were captured using a 10x objective.

Images show that the Alexa594 fluorescence staining of RNA-incorporated EU in cultured DRG cells appeared to increase with increasing EU exposure concentration and duration.

(A, C, E, G and I) Alexa594 staining of RNA-incorporated EU (red).

(B, D, F, H and J) Phase contrast images overlaid with EU-Alexa594 (red) and DAPI (blue) staining.

Scale bar=50  $\mu$ m.

### **3.2.2. Visualization of nascent RNA synthesis**

To visualize nascent RNA synthesis in cultured DRG cells, cells were labelled with 1 mM EU for 20 h, then fixed before RNA-incorporated EU was detected using a click chemistry reaction with Alexa594-labelled azide. Representative images showed that nascent RNA synthesis was localized to the nuclei of cultured DRG neurons (Figure 3.2). DRG neurons were distinguished from non-neuronal cells by their unique large and round cell bodies with a sharp pericellular halo (Figure 3.2 E and F). Nuclei were identified by DAPI staining (Figure 3.2 C and D). Strong EU-Alexa594 staining, indicative of nascent RNA synthesis, was observed collocated with the nuclei of DRG neurons, with little or no staining of their neuronal cytoplasm or of non-neuronal cells (Figure 3.2 A, B, E and F).

### **3.2.3. Quantitation of nascent RNA synthesis, DNA content and cell body size**

To quantitate nascent RNA synthesis, DNA content and cell body size of individual cultured DRG neurons, fluorescence pixel intensities of EU-Alexa594 and DAPI staining, and planimetric areas of neuronal cell bodies, were measured. Data were presented as frequency histograms and box-and-whiskers plots, and analysed using descriptive statistics. Fluorescence pixel intensity was measured in arbitrary units without calibration. As these measurements were not comparable from experiment to experiment, data from two independent experiments were presented separately.

The level of nascent RNA synthesis varied widely between individual cultured DRG neurons, more so than their DNA content and cell body size (Figure 3.3, Table 3.1). The fluorescence pixel intensity of EU-Alexa594 staining in individual DRG neurons was non-normally distributed ( $P < 0.0001$ , D'Agostino-Pearson omnibus test). EU-Alexa594 staining intensity

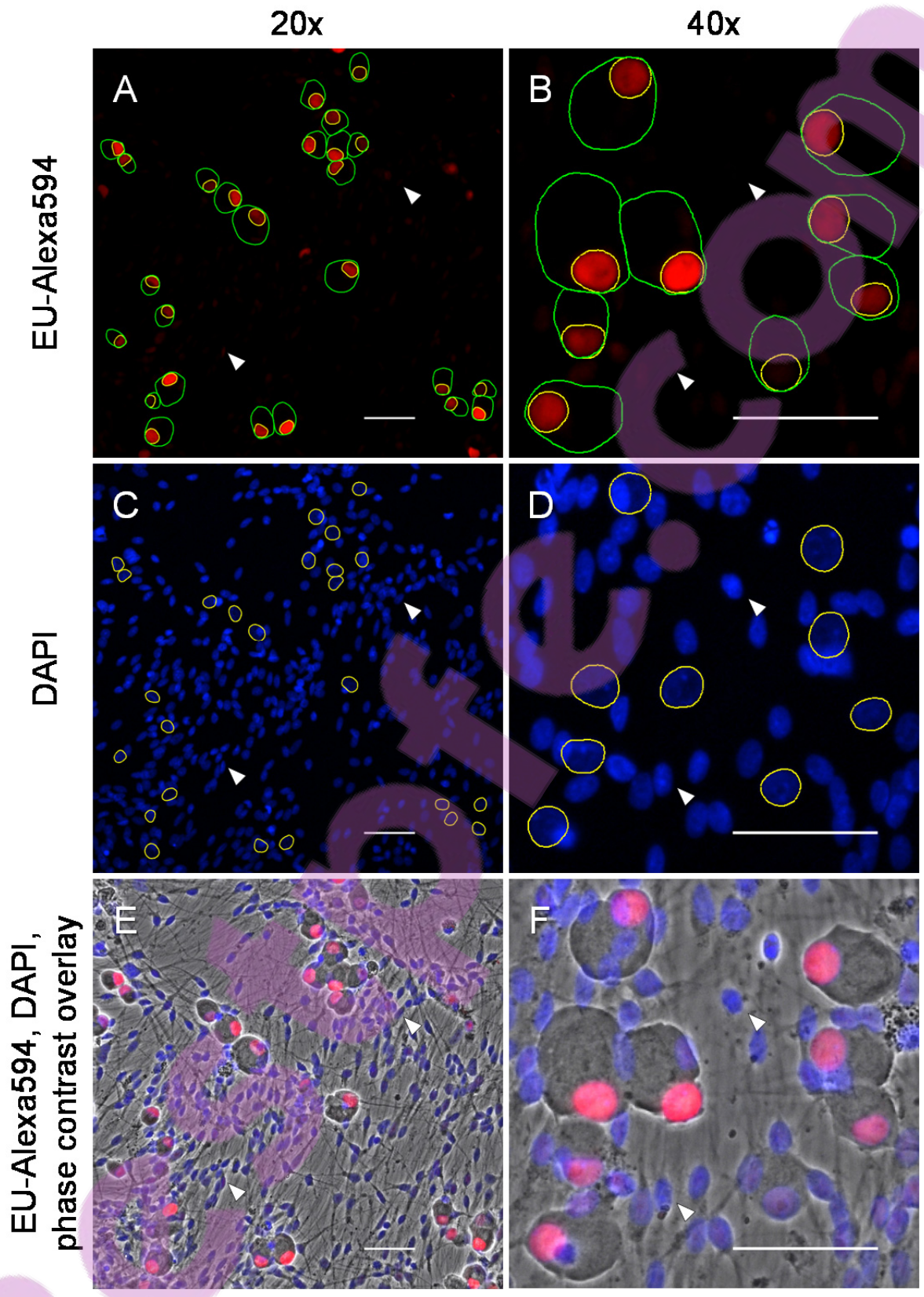


**Figure 3.2. Visualization of nascent RNA synthesis in cultured DRG neurons.**

DRG cells were harvested from one to three rats and cultured for three days before labelling with 1 mM 5-ethynyl uridine (EU) for 20 h. After fixation, RNA-incorporated EU was visualized using a click chemistry reaction with Alexa594-labelled azide (red). Nuclear DNA was counterstained with DAPI (blue). Images were captured using a 20x (A, C and E) or 40x (B, D and F) objective.

Images show that nascent RNA synthesis was localized to the nuclei of cultured DRG neurons (yellow circles), with little or no EU-Alexa594 staining of their neuronal cytoplasm (between green and yellow circles) or of non-neuronal cells (arrowheads).

(A and B) Alexa594 staining of RNA-incorporated EU (red). Green circles indicate outlines of neuronal cell bodies. Yellow circles indicate outlines of neuronal nuclei. Arrowheads indicate non-neuronal cells.

(C and D) DAPI staining showing nuclei (blue). Yellow circles indicate outlines of neuronal nuclei. Arrowheads indicate non-neuronal cells.

(E and F) Phase contrast images overlaid with EU-Alexa594 (red) and DAPI (blue) staining. Arrowheads indicate non-neuronal cells.

Scale bar=50  $\mu$ m.



Exp. 1

Exp. 2

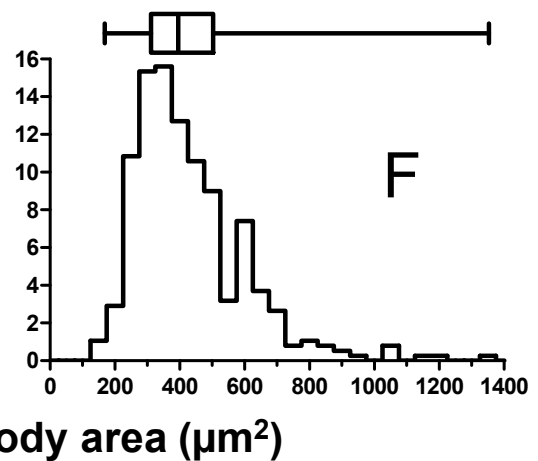
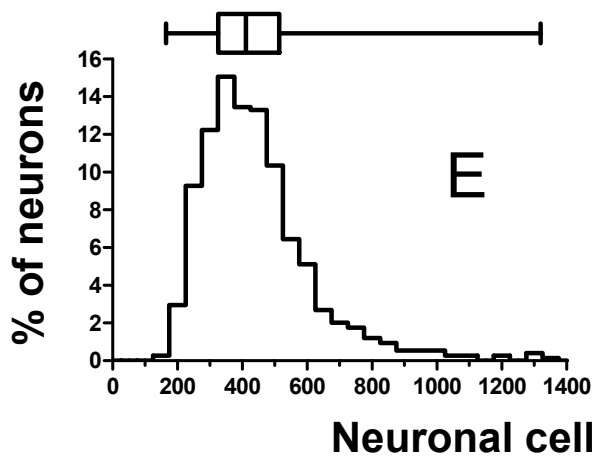
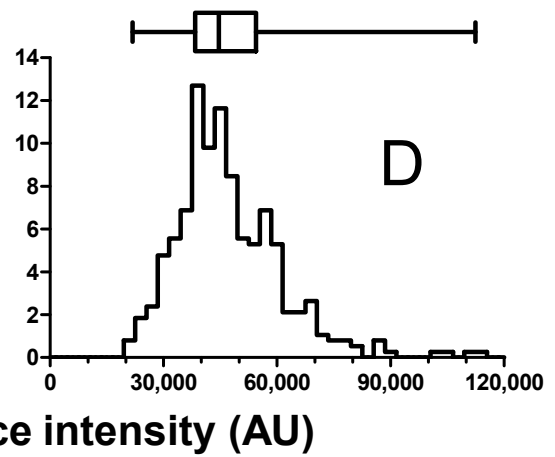
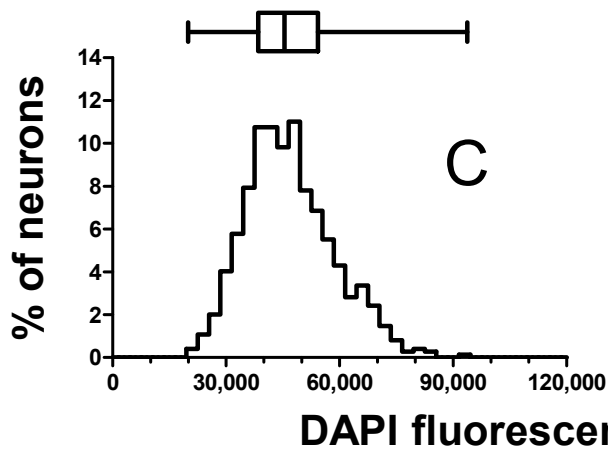
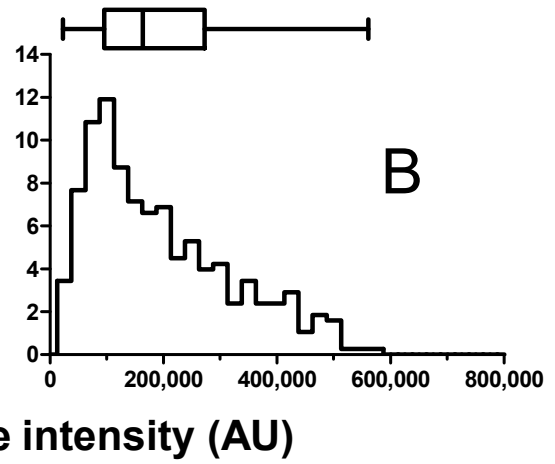
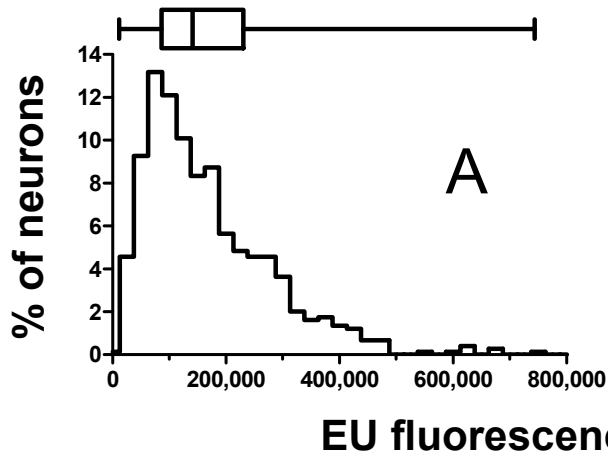


**Figure 3.3. Quantitation of the level of nascent RNA synthesis in individual cultured DRG neurons compared with that of their DNA content and cell body size.**

DRG cells were harvested from one to three rats for each experiment and cultured for three days before labelling with 1 mM 5-ethynyl uridine (EU) for 20 h. After fixation, RNA-incorporated EU was visualized using a click chemistry reaction with Alexa594-labelled azide. Nuclear DNA was counterstained with DAPI. Images for quantitation were captured using a 40x objective. In two independent experiments, a total of 744 (experiment 1: A, C and E) and 378 (experiment 2: B, D and F) neurons from three culture wells were measured to quantitate the fluorescence pixel intensity of EU-Alexa594 (A and B) and DAPI staining (C and D) and neuronal cell body area (E and F).

Data show that the level of nascent RNA synthesis varied widely between individual cultured DRG neurons, more so than their DNA content and cell body size.

(A and B) Distribution of individual neuron levels of RNA-incorporation of EU showing a non-normal distribution and more than 25-fold difference between the minimum and maximum values.

(C and D) Distribution of individual neuron levels of DAPI staining showing a non-normal distribution and five-fold difference between the minimum and maximum values.

(E and F) Distribution of individual neuronal cell body areas showing a non-normal distribution and eight-fold difference between the minimum and maximum values.

Data are shown as frequency histograms and box-and-whiskers plots indicating the median value (vertical line across the box), interquartile range (box) and range (whiskers).

**Table 3.1. Quantitation of the level of nascent RNA synthesis in individual cultured DRG neurons compared with that of their DNA content and cell body size.**

		EU fluorescence intensity (AU)		DAPI fluorescence intensity (AU)		Neuronal cell body area ( $\mu\text{m}^2$ )	
Experiment		1	2	1	2	1	2
<b>Descriptive statistics</b>	Median	138,938	163,101	45,428	44,744	412	394
	25% percentile	83,565	94,470	38,501	38,483	326	309
	75% percentile	228,558	272,115	54,282	54,570	516	502
	Relative IQR (%) <sup>a</sup>	104.4	108.9	34.7	36.0	46.1	49.0
	Minimum	8,551	21,411	19,870	21,883	164	165
	Maximum	744,705	562,610	93,844	112,733	1,326	1,359
	Fold variation <sup>b</sup>	87.1	26.3	4.7	5.2	8.1	8.2
	Number	744	378	744	378	744	378
	Normality ( <i>P</i> value) <sup>c</sup>	< 0.0001	< 0.0001	< 0.0001	< 0.0001	< 0.0001	< 0.0001
<b>Correlation with cell body area</b>	Spearman <i>r</i>	0.5913	0.4802	-0.0252	0.0749	N/A	N/A
	<i>P</i> value	< 0.0001	< 0.0001	0.4922	0.1464	N/A	N/A

<sup>a</sup> Relative IQR: interquartile range expressed as the percentage of the median value, i.e. (75%-25% percentile)/median $\times$ 100%.

<sup>b</sup> Fold variation: fold difference between minimum and maximum values, i.e. maximum/minimum.

<sup>c</sup> Normality of data was assessed by D'Agostino-Pearson omnibus normality test. Data with  $P < 0.05$  was considered non-normally distributed.

varied by 87.1-fold from minimum to maximum values in experiment 1 and by 26.3-fold in experiment 2. Relative interquartile ranges (interquartile range/median×100%) of EU-Alexa594 fluorescence pixel intensity were 104.4% in experiment 1 and 108.9% in experiment 2 (Figure 3.3 A and B, Table 3.1). In contrast, the fluorescence pixel intensity of DAPI staining in individual DRG neurons varied from minimum to maximum values by only 4.7-fold in experiment 1 and 5.2-fold in experiment 2, and had relative interquartile ranges of only 34.7% in experiment 1 and 36.0% in experiment 2 (Figure 3.3 C and D, Table 3.1). In addition, the cell body areas of individual DRG neurons varied from minimum to maximum values by only 8.1-fold in experiment 1 and 8.2-fold in experiment 2, and had relative interquartile ranges of only 46.1% in experiment 1 and 49.0% in experiment 2 (Figure 3.3 E and F, Table 3.1). Like EU-Alexa594 staining, both fluorescence pixel intensity of DAPI staining and cell body areas of individual DRG neurons were non-normally distributed ( $P<0.0001$ , D'Agostino-Pearson omnibus test). Taken together, these results showed that the level of nascent RNA synthesis varied widely between individual cultured DRG neurons, more so than their DNA content and cell body size.

#### **3.2.4. Correlation between the level of nascent RNA synthesis and cell body size**

To evaluate interrelationships between levels of nascent RNA synthesis, DNA content and neuronal cell body size, data were analysed by Spearman's correlation analyses. Neuronal cell body size correlated positively with the level of nascent RNA synthesis, with higher levels of nascent RNA synthesis being present in neurons with larger cell bodies and lower levels of nascent RNA synthesis being present in neurons with smaller cell bodies (Figure 3.4). Significantly positive correlations between EU-Alexa594 fluorescence pixel intensity and cell body area of DRG neurons were observed in both independent experiments, with Spearman's rank correlation coefficients of 0.5913 ( $P<0.0001$ ) and 0.4802 ( $P<0.0001$ ) in experiment 1

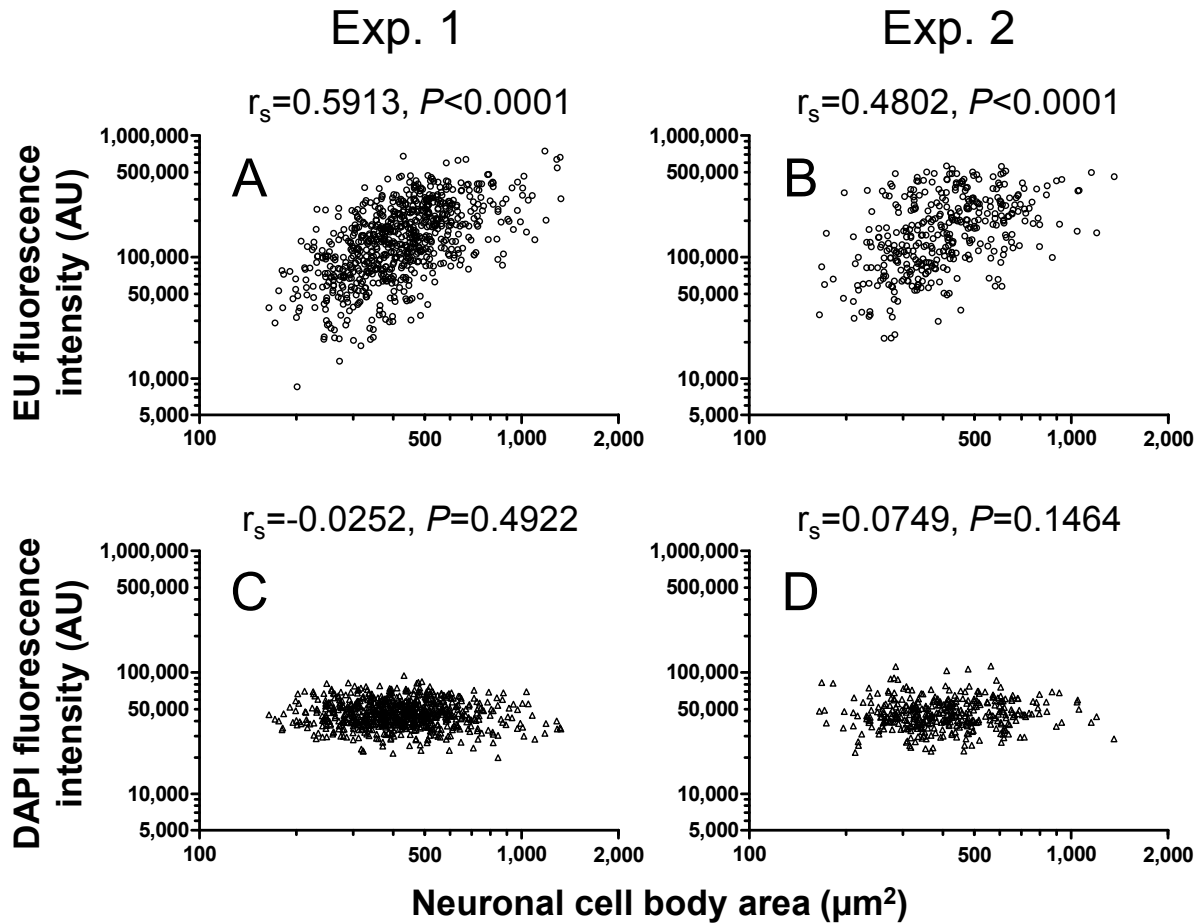


**Figure 3.4. Neuronal cell body size correlated with the level of nascent RNA synthesis, but not with that of DNA content of cultured DRG neurons.**

Data from the two independent experiments shown in Figure 3.3 were plotted for correlation analysis (experiment 1: A and C, experiment 2: B and D).

Data show that the cell body size of cultured DRG neurons correlated positively with the level of nascent RNA synthesis (A and B), but not with that of DNA content (C and D).

Each symbol represents values for an individual DRG neuron. The Spearman's rank correlation coefficients ( $r_s$ ) and the corresponding  $P$  values are shown.

and 2, respectively (Figure 3.4 A and B, Table 3.1). In contrast, no correlation was found between DAPI fluorescence pixel intensity and cell body area of DRG neurons in neither of the two experiments ( $P>0.05$ ) (Figure 3.4 C and D, Table 3.1). In addition, EU-Alexa594 and DAPI fluorescence pixel intensity were only weakly correlated.

### 3.2.5. Effects of oxaliplatin

To investigate effects of oxaliplatin treatment on nascent RNA synthesis and cell body size of cultured DRG neurons, EU-Alexa594 staining and cell body areas were measured before and after a 3-h exposure to oxaliplatin of 100  $\mu\text{M}$ . Representative images showed reduced levels of nascent RNA synthesis and decreased cell body size of cultured DRG neurons one and two days after a 3-h exposure to 100  $\mu\text{M}$  oxaliplatin, without any obvious change in their DAPI signals (Figure 3.5). Distribution profiles of EU-Alexa594 fluorescence pixel intensity of DRG neurons were shifted to lower values at one and two days after a 3-h exposure to 100  $\mu\text{M}$  oxaliplatin (Figure 3.6 A). Relative to baseline values (0 h; median: 64450 AU, interquartile range: 46035-89070 AU), EU-Alexa594 fluorescence pixel intensity of DRG neurons was decreased to 57.7% (median: 37177 AU, interquartile range: 24778-55279 AU,  $P<0.001$ ) and to 36.3% (median: 23393 AU, interquartile range: 15293-37811 AU,  $P<0.001$ ) one and two days after oxaliplatin treatment, respectively. In addition, EU-Alexa594 fluorescence pixel intensity was significantly reduced two days compared to one day after treatment ( $P<0.001$ ) (Figure 3.6 A, Table 3.2). Distribution profiles of neuronal cell body areas were also shifted to lower values one and two days after a 3-h exposure to 100  $\mu\text{M}$  oxaliplatin (Figure 3.6 B). Relative to baseline values (0 h; median: 421  $\mu\text{m}^2$ , interquartile range: 339-515  $\mu\text{m}^2$ ), neuronal cell body areas were decreased to 74.3% (median: 313  $\mu\text{m}^2$ , interquartile range: 255-383  $\mu\text{m}^2$ ,  $P<0.001$ ) and to 71.1% (median: 299  $\mu\text{m}^2$ , interquartile

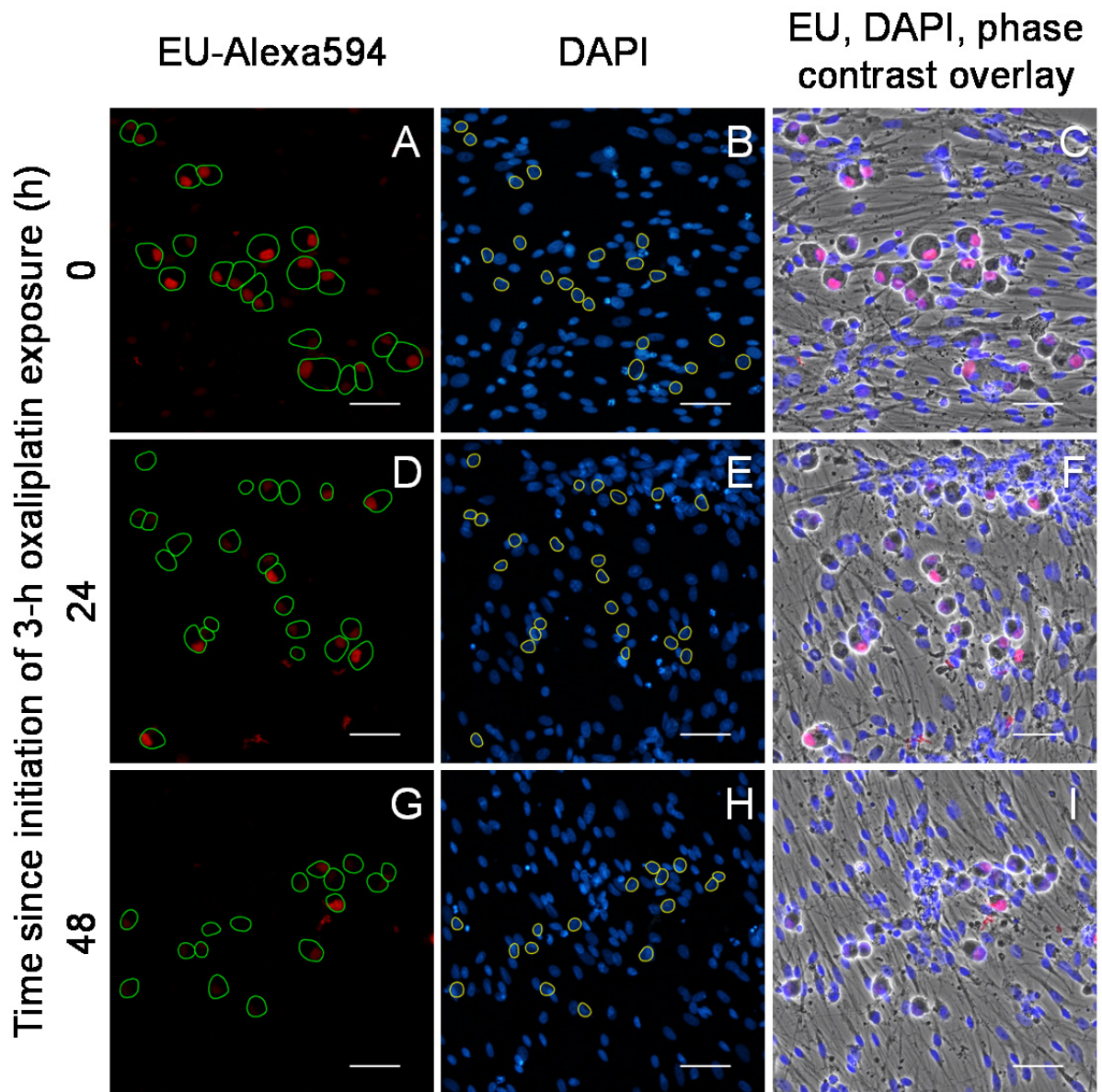


**Figure 3.5. Effects of oxaliplatin treatment on nascent RNA synthesis and cell body size of cultured DRG neurons: representative photomicrographs.**

DRG cells were harvested from one rat and cultured for three days before experiments. Then cells were studied before (A-C) and after exposure to 100  $\mu$ M oxaliplatin for 3 h, followed by culture in drug-free medium for a further one (D-F) and two days (G-I). 5-ethynyl uridine (EU, 1 mM) was added to the cultures one day before each designated time-point. At the end of the experiment, cells were fixed and then RNA-incorporated EU was visualized using a click chemistry reaction with Alexa594-labelled azide (red). Nuclear DNA was counterstained with DAPI (blue). Images were captured using a 20x objective.

Images show that oxaliplatin treatment reduced both the level of nascent RNA synthesis and cell body size of cultured DRG neurons when visualized one and two days after a three hour treatment.

(A, D and G) Alexa594 staining of RNA-incorporated EU (red). Green circles indicate outlines of neuronal cell bodies.

(B, E and H) DAPI staining showing nuclei (blue). Yellow circles indicate outlines of neuronal nuclei.

(C, F and I) Phase contrast images overlaid with EU-Alexa594 (red) and DAPI (blue) staining.

Scale bar=50  $\mu$ m.



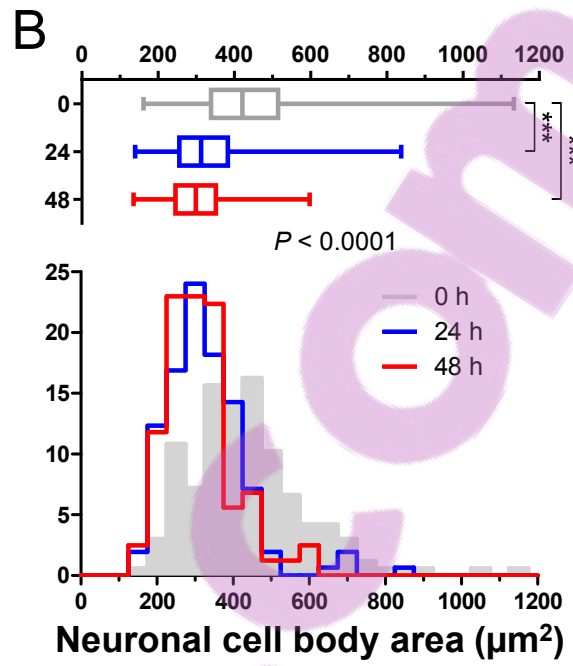
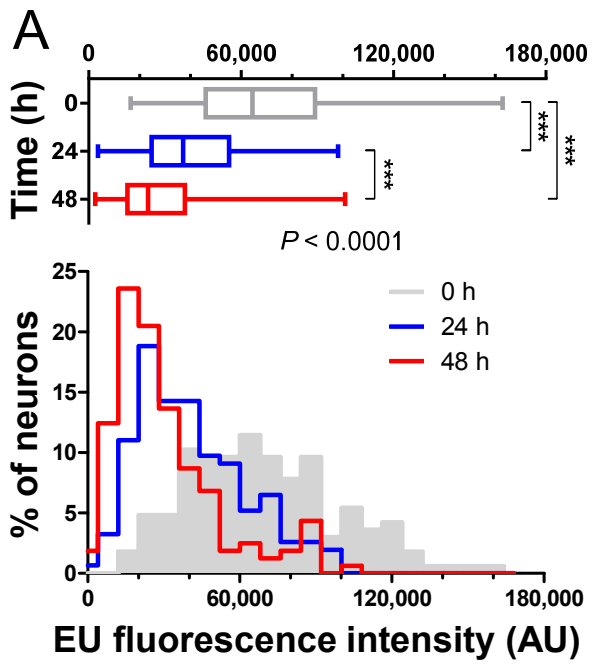


**Figure 3.6. Effects of oxaliplatin treatment on nascent RNA synthesis and cell body size of cultured DRG neurons: quantitative data.**

DRG cells were harvested from one rat and cultured for three days before experiments. Then cells were studied before and after exposure to 100  $\mu$ M oxaliplatin for 3 h, followed by culture in drug-free medium for a further one and two days. 5-ethynyl uridine (EU, 1 mM) was added to the cultures one day before each designated time-point. At the end of the experiment, cells were fixed and then RNA-incorporated EU was visualized using a click chemistry reaction with Alexa594-labelled azide. Images for quantitation were captured using a 20x objective. A total of between 154 to 166 neurons from three culture wells for each time-point were measured to quantitate fluorescence pixel intensity of EU-Alexa594 staining (A) and neuronal cell body area (B).

Data show that oxaliplatin treatment reduced both the level of nascent RNA synthesis and cell body size of cultured DRG neurons within one to two days after a three hour treatment.

Data are shown as frequency histograms and box-and-whiskers plots indicating the median value (vertical line across the box), interquartile range (box) and range (whiskers). *P* values shown in the figures are for overall differences between groups by Kruskal-Wallis test. \*\*\*  $P < 0.001$  indicate the statistical significance of differences between groups assessed by Dunn's multiple comparison post-test.

**Table 3.2. Effects of oxaliplatin treatment on nascent RNA synthesis and cell body size of cultured DRG neurons: tabulated data.**

		EU fluorescence intensity (AU)			Neuronal cell body area ( $\mu\text{m}^2$ )		
		0	24	48	0	24	48
<b>Descriptive statistics</b>	Median	64,450	37,177	23,393	421	313	299
	(% of 0 h)	(100%)	(57.7%)	(36.3%)	(100%)	(74.3%)	(71.1%)
	25% Percentile	46,035	24,778	15,293	339	255	246
	75% Percentile	89,070	55,279	37,811	515	383	352
	Minimum	16,419	3,685	2,554	162	140	136
	Maximum	162,908	98,115	100,912	1,134	838	598
	Number	166	154	161	166	154	161
<b>P value <sup>a</sup></b>	Overall difference		< 0.0001			< 0.0001	
	vs 0 h	N/A	< 0.001	< 0.001	N/A	< 0.001	< 0.001
	vs 24 h	N/A	N/A	< 0.001	N/A	N/A	> 0.05

<sup>a</sup> The statistical significance of differences between groups was assessed by Kruskal-Wallis test and Dunn's multiple comparison post-test.

range: 246-352  $\mu\text{m}^2$ ,  $P<0.001$ ) one and two days after oxaliplatin treatment, respectively (Figure 3.6 B, Table 3.2).

To investigate the concentration-dependence of effects of oxaliplatin on nascent RNA synthesis and cell body size of cultured DRG neurons, EU-Alexa594 staining and cell body areas were measured two days after a 3-h exposure to oxaliplatin of 10, 30 and 100  $\mu\text{M}$ . Representative images showed that oxaliplatin treatment reduced both the level of nascent RNA synthesis and cell body size of cultured DRG neurons in a concentration-dependent manner, without any obvious change in their DAPI signals (Figure 3.7). Distribution profiles of EU-Alexa594 fluorescence pixel intensity of DRG neurons were shifted to lower values in a concentration-dependent manner two days after a 3-h exposure to 10, 30 and 100  $\mu\text{M}$  oxaliplatin (Figure 3.8 A). Relative to control values (0  $\mu\text{M}$ ; median: 77030 AU, interquartile range: 49046-105564 AU), EU-Alexa594 fluorescence pixel intensity of DRG neurons were decreased to 63.9% (median: 49258 AU, interquartile range: 28872-76538 AU,  $P<0.001$ ), 48.5% (median: 37381 AU, interquartile range: 23948-54262 AU,  $P<0.001$ ) and 37.3% (median: 28715 AU, interquartile range: 16672-40531 AU,  $P<0.001$ ) two days after a 3-h exposure to 10, 30 and 100  $\mu\text{M}$  oxaliplatin, respectively. In addition, EU-Alexa594 fluorescence pixel intensity were significantly altered at 10 versus 30  $\mu\text{M}$  ( $P<0.01$ ), 10 versus 100  $\mu\text{M}$  ( $P<0.001$ ) and 30 versus 100  $\mu\text{M}$  treatment groups ( $P<0.01$ ) (Figure 3.8 A, Table 3.3). Distribution profiles of neuronal cell body areas were also shifted to lower values in a concentration-dependent manner two days after a 3-h exposure to 10, 30 and 100  $\mu\text{M}$  oxaliplatin (Figure 3.8 B). Relative to control values (0  $\mu\text{M}$ ; median: 405  $\mu\text{m}^2$ , interquartile range: 343-519  $\mu\text{m}^2$ ), neuronal cell body areas were decreased to 80.7% (median: 327  $\mu\text{m}^2$ , interquartile range: 253-414  $\mu\text{m}^2$ ,  $P<0.001$ ), 76.5% (median: 310  $\mu\text{m}^2$ , interquartile range: 243-376  $\mu\text{m}^2$ ,  $P<0.001$ ) and 73.0% (median: 296  $\mu\text{m}^2$ , interquartile range: 244-364  $\mu\text{m}^2$ ,

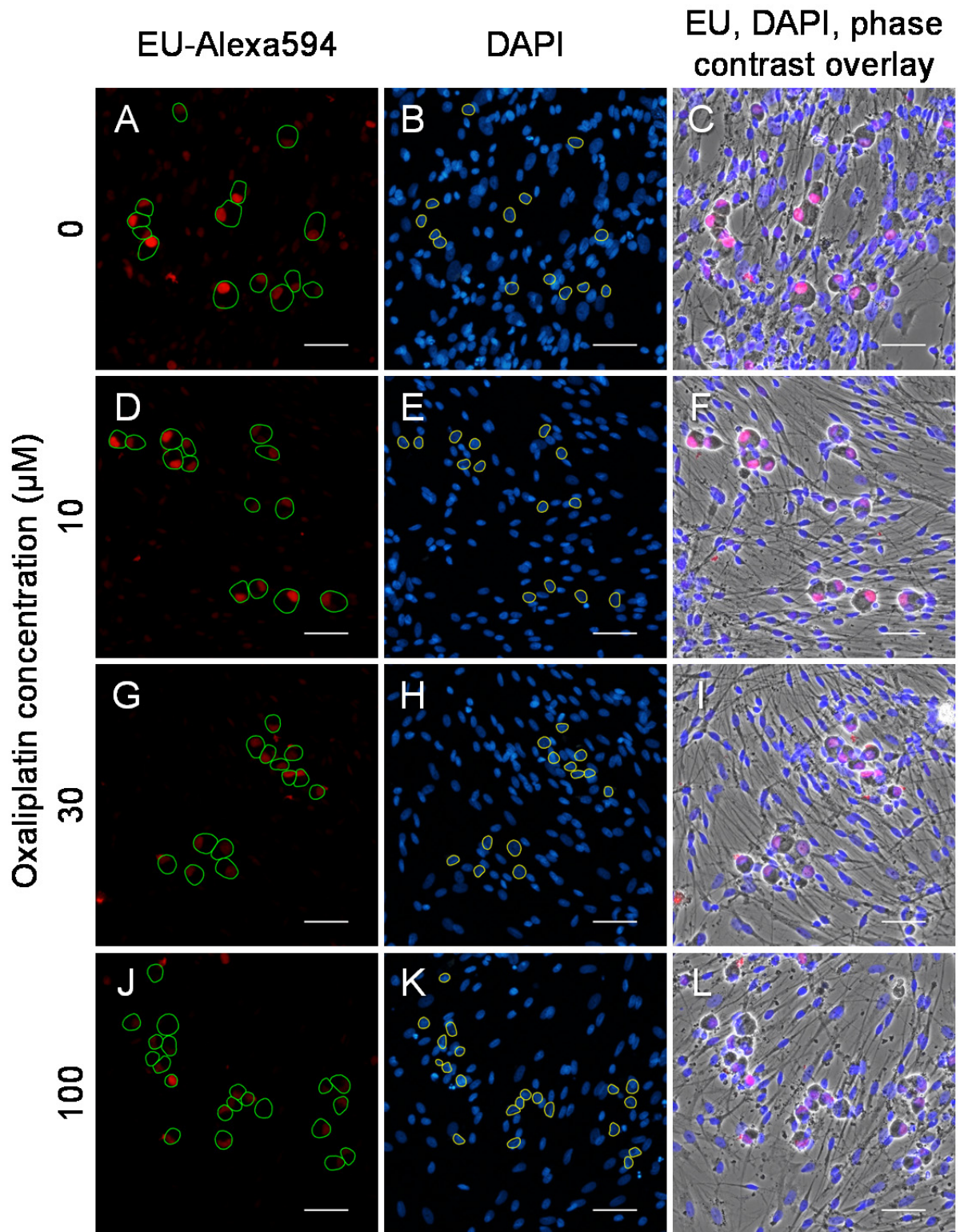


**Figure 3.7. Concentration-dependence of effects of oxaliplatin treatment on nascent RNA synthesis and cell body size of cultured DRG neurons: representative photomicrographs.**

DRG cells were harvested from one rat and cultured for three days before experiments. Then cells were exposed to drug vehicle (0  $\mu$ M, A-C) or oxaliplatin at concentrations of 10 (D-F), 30 (G-I) or 100  $\mu$ M (J-L) for 3 h, followed by culture in drug-free medium for a further two days. 5-ethynyl uridine (EU, 1 mM) was added to the cultures one day before the end of the experiment. At the end of the experiment, cells were fixed and then RNA-incorporated EU was visualized using a click chemistry reaction with Alexa594-labelled azide (red). Nuclear DNA was counterstained with DAPI (blue). Images were captured using a 20x objective.

Images show that oxaliplatin treatment reduced both the level of nascent RNA synthesis and cell body size of cultured DRG neurons in a concentration-dependent manner.

(A, D, G and J) Alexa594 staining of RNA-incorporated EU (red). Green circles indicate outlines of neuronal cell bodies.

(B, E, H and K) DAPI staining showing nuclear DNA (blue). Yellow circles indicate outlines of neuronal nuclei.

(C, F, I and L) Phase contrast images overlaid with EU-Alexa594 (red) and DAPI (blue) staining.

Scale bar=50  $\mu$ m.

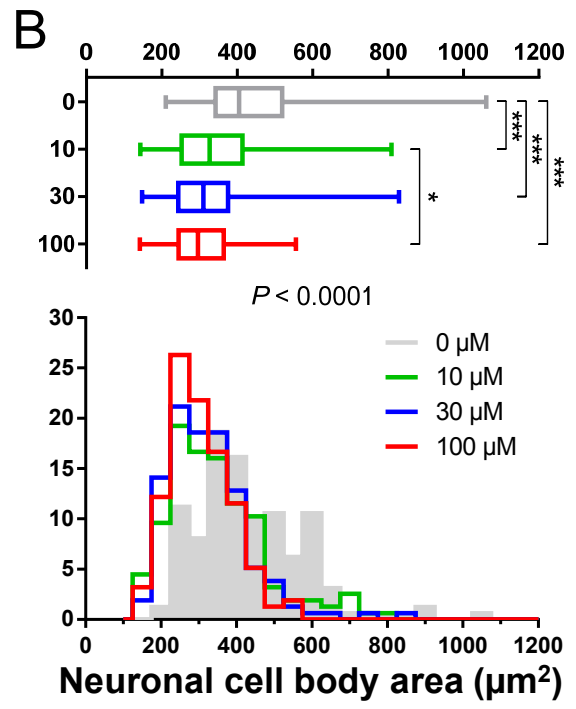
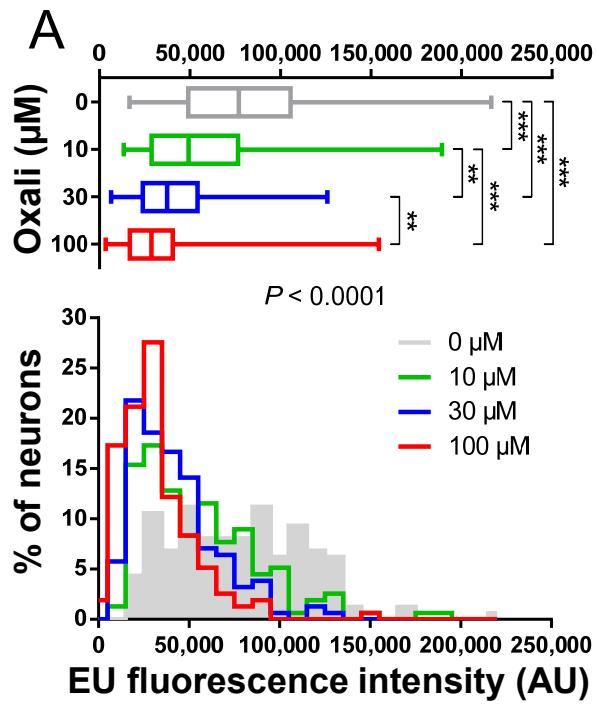


**Figure 3.8. Concentration-dependence of effects of oxaliplatin treatment on nascent RNA synthesis and cell body size of cultured DRG neurons: quantitative data.**

DRG cells were harvested from one rat and cultured for three days before experiments. Then cells were exposed to drug vehicle (0  $\mu\text{M}$ ) or oxaliplatin at concentrations of 10, 30 or 100  $\mu\text{M}$  for 3 h, followed by culture in drug-free medium for a further two days. 5-ethynyl uridine (EU, 1 mM) was added to the cultures one day before the end of the experiment. At the end of the experiment, cells were fixed and then RNA-incorporated EU was visualized using a click chemistry reaction with Alexa594-labelled azide. Images for quantitation were captured using a 20x objective. A total of between 156 to 161 neurons from three culture wells for each treatment condition were measured to quantitate fluorescence pixel intensity of EU-Alexa594 staining (A) and neuronal cell body area (B).

Data show that oxaliplatin treatment reduced both the level of nascent RNA synthesis and cell body size of cultured DRG neurons in a concentration-dependent manner.

Data are shown as frequency histograms and box-and-whiskers plots indicating the median value (vertical line across the box), interquartile range (box) and range (whiskers). *P* values shown in the figures are for overall differences between groups by Kruskal-Wallis test. \*  $P < 0.05$ , \*\*  $P < 0.01$ , \*\*\*  $P < 0.001$  indicate the statistical significance of differences between indicated groups assessed by Dunn's multiple comparison post-test.



**Table 3.3. Concentration-dependence of effects of oxaliplatin treatment on nascent RNA synthesis and cell body size of cultured DRG neurons: tabulated data.**

		EU fluorescence intensity (AU)				Neuronal cell body area ( $\mu\text{m}^2$ )			
		0	10	30	100	0	10	30	100
<b>Descriptive statistics</b>	Median	77,030	49,258	37,381	28,715	405	327	310	296
	(% of 0 h)	(100%)	(63.9%)	(48.5%)	(37.3%)	(100%)	(80.7%)	(76.5%)	(73.0%)
	25% Percentile	49,046	28,872	23,948	16,672	343	253	243	244
	75% Percentile	105,564	76,538	54,262	40,531	519	414	376	364
	Minimum	16,647	13,399	6,422	3,336	210	143	148	142
	Maximum	216,449	189,223	125,914	154,334	1,060	809	829	556
	Number	161	156	156	156	161	156	156	156
<b>P value</b> <sup>a</sup>	Overall difference		< 0.0001				< 0.0001		
	vs 0 $\mu\text{M}$	N/A	< 0.001	< 0.001	< 0.001	N/A	< 0.001	< 0.001	< 0.001
	vs 10 $\mu\text{M}$	N/A	N/A	< 0.01	< 0.001	N/A	N/A	> 0.05	< 0.05
	vs 30 $\mu\text{M}$	N/A	N/A	N/A	< 0.01	N/A	N/A	N/A	> 0.05

<sup>a</sup> The statistical significance of differences between groups were assessed by Kruskal-Wallis test and Dunn's multiple comparison post-test.

$P < 0.001$ ) two days after a 3-h exposure to 10, 30 and 100  $\mu\text{M}$  oxaliplatin, respectively. In addition, neuronal cell body areas were significantly altered for 10 versus 100  $\mu\text{M}$  ( $P < 0.05$ ) (Figure 3.8 B, Table 3.3).

### **3.3. Discussion**

In the current study, an *in vitro* method was established to visualize and quantitate nascent RNA synthesis in individual cultured DRG neurons. This method was based on the biosynthetic incorporation of 5-ethynyl uridine (EU) into newly synthesized RNA and the use of a subsequent click chemistry reaction to attach a fluorophore label, Alexa Fluor 594, to the RNA-incorporated EU. Following the exposure of live DRG cells to EU, their fixation with 4% paraformaldehyde and Alexa594 click chemistry labelling, fluorescently-labelled RNA-incorporated EU was visualized and quantitated by fluorescence microscopy. Optimized EU exposure conditions were determined experimentally that resulted in clear and reproducible observations of nascent RNA synthesis in cultured DRG cells. Among the different conditions tested, exposure of DRG cells to 1 mM EU for 20 h resulted in the clearest Alexa594 fluorescence labelling of RNA-incorporated EU without any apparent background staining. Previously, several nucleoside incorporation techniques have been used for visualization of nascent RNA synthesis in cells, such as radioautography of RNA-incorporated radiolabeled uridine (Uddin et al., 1984, Wassermann et al., 1988, Wells and Vaidya, 1994) and immunostaining of RNA-incorporated halogenated uridine (Boisvert et al., 2000, Halicka et al., 2000, Casafont et al., 2006, Kalita et al., 2008). Compared to those techniques, the click chemistry reaction labelling technique employed in this study requires less time and less expensive equipment, yet provides high selectivity and specificity (Jao and Salic, 2008). In addition, the method established in this study for investigation of nascent

RNA synthesis in cultured DRG neurons is generalizable to other studies and projects conducted in different laboratory settings, as the required reagents are available in a commercial kit and fluorescence microscopes are accessible in most research facilities.

This study also demonstrated the experimental utility of this newly established *in vitro* method for visualizing and quantitating nascent RNA synthesis in individual cultured DRG neurons. With this method, it was possible to measure the level of nascent RNA synthesis in an individual neuron and relate that measurement to other characteristics of that particular cell, such as its type, size and DNA content, *etc.* Several new findings were made from the work described in this chapter that demonstrated the usefulness of this method. For example, by using this method, this study showed that DRG neurons had relatively higher levels of nascent RNA synthesis than non-neuronal cells present in DRG cell primary cultures. Strong EU-Alexa594 staining, indicative of nascent RNA synthesis, was observed in DRG neurons, with little or no staining of non-neuronal cells. Similar differences in global RNA synthesis between neurons and non-neuronal supporting cells have been reported in central nervous system (Sato et al., 1994) but not previously in DRG as far as we are aware. The current study also showed nuclear localization of newly synthesized RNA transcripts that had incorporated EU and were visualized by fluorescence labelling in cultured DRG neurons. Strong EU-Alexa594 staining was observed collocated with the nuclei of DRG neurons, with little or no staining of their neuronal cytoplasm. Another finding of potential importance was the demonstration of widely varying levels of nascent RNA synthesis between individual DRG neurons. To quantitate nascent RNA synthesis of individual cultured DRG neurons, fluorescence pixel intensities of EU-Alexa594 staining of whole cell bodies were measured. EU-Alexa594 staining intensity varied by more than 26-fold from minimum to maximum values, and its relative interquartile ranges ( $\text{interquartile range}/\text{median} \times 100\%$ ) were more

than 104%, in two independent experiments. Taken together, these data show that the method established in this chapter could be used as a useful tool for investigating nascent RNA synthesis, and determining the influence of drug treatments and other factors on global transcriptional activity, in individual cultured DRG neurons.

The findings described in this chapter of this thesis have suggested that levels of nascent RNA synthesis and cell body size of individual cultured DRG neurons may be closely interrelated. Cultured DRG neurons were shown to have large but variable cell body size. The neuronal cell body areas varied by more than 8-fold from minimum ( $\sim 160 \mu\text{m}^2$ ) to maximum values ( $\sim 1300 \mu\text{m}^2$ ), with median values of  $\sim 400 \mu\text{m}^2$ , in two independent experiments. This finding is in keeping with previous studies of cultured DRG neurons (Harper and Lawson, 1985, Windebank and Blexrud, 1989, Scroggs and Fox, 1992, Haller et al., 2006). Also, cultured DRG neurons were shown to have highly variable levels of nascent RNA synthesis, as discussed above. The cell body size of DRG neurons correlated positively with the level of nascent RNA synthesis, with highly statistically significant Spearman's rank correlations demonstrated in two independent experiments. Higher levels of nascent RNA synthesis were present in neurons with larger cell bodies and lower levels of nascent RNA synthesis were present in those with smaller cell bodies. Further strengthening possible interrelationships found between nascent RNA synthesis and neuronal cell body size was the finding of oxaliplatin treatment having reduced both the level of nascent RNA synthesis and cell body size of cultured DRG neurons in a concentration-dependent manner, in an exploratory study. Similar relationships between cell size and levels of global RNA synthesis have been reported in other cell types but not previously in DRG neurons as far as we are aware. For example, a previous study comparing liver, spleen and thymus cells showed that cell types with large cell size synthesized more RNA than cell types with small cell size (Schmidt and

Schibler, 1995). Similar findings were also made in another study of frog spinal motoneurons (Sato et al., 1994). Taken together, these findings suggested tight interrelationships between levels of nascent RNA synthesis and neuronal cell body size in cultured DRG neurons.

The mechanism remains unclear by which the levels of nascent RNA synthesis in DRG neurons are positively associated with neuronal cell body size. It may be reasonable to assume that larger DRG neurons need higher RNA synthesis than smaller DRG neurons to maintain their large size, increased protein mass, greater metabolic activity and higher number of synaptic contacts (Goldschmidt and Steward, 1992, Berciano et al., 2007, Marguerat and Bahler, 2012). Cell size-related variations of nascent RNA synthesis in DRG neurons may be accounted for by differences in RNA polymerase activities. For instance, RNA polymerase II activities has been shown to contribute to cell size-related RNA synthesis in other cell types (Schmidt and Schibler, 1995, Zhurinsky et al., 2010), by means of changing of RNA polymerase II gene occupancy (Zhurinsky et al., 2010). Similarly, RNA polymerase I-driven transcription has also been associated with cell body size of neurons from central nervous system (Gomes et al., 2011). Therefore, it is possible that size-related high levels of nascent RNA synthesis could make large DRG neurons more vulnerable than small DRG neurons to transcriptional inhibition induced by toxins or other agents, such as oxaliplatin, which could explain why large neurons appear to be targeted in oxaliplatin damage in rat DRG tissues (Jamieson et al., 2005). The current study also demonstrated that oxaliplatin reduced both the level of nascent RNA synthesis and neuronal cell body size, which could explain the nucleolar shrinkage observed in oxaliplatin-damaged DRG neurons (McKeage et al., 2001). A more comprehensive and in-depth study on oxaliplatin effects will be conducted in the next chapter.

In conclusion, an *in vitro* method has been established to visualize and quantitate nascent RNA synthesis in individual cultured DRG neurons, based on recently developed click chemistry reaction labelling techniques. Several new findings, such as the close interrelationship between the level of nascent RNA synthesis and cell body size of individual cultured DRG neurons, have been made that demonstrated the experimental utility of this newly established method.

# **Chapter 4. Time-course studies of oxaliplatin effects in cultured rat DRG cells**

## **4.1. Introduction**

Oxaliplatin is a third-generation platinum-based anticancer drug, which has been regarded as one of the most important chemotherapeutic drugs used for the clinical treatment of colorectal cancer (Stein and Arnold, 2012). Like other platinum-based anticancer drugs, oxaliplatin targets DNA with the formation of platinum-DNA adducts, which exert cytotoxicity by inhibiting DNA replication, resulting in cell cycle arrest and inducing apoptosis in dividing cells (Di Francesco et al., 2002). The platinum-DNA adducts are formed at the N-7 positions of guanine (G) or adenine (A), with the presence of approximately 60-65% GG, 25-30% AG and 5-10% GNG intrastrand cross-links. Interstrand cross-links and DNA-protein cross-links represent only a small portion of the total adducts (Chaney et al., 2005, Kweekel et al., 2005). Nucleotide excision repair (NER) has been suggested to be the major cellular defence mechanism repairing platinum-DNA intrastrand cross-links, and enhancement in the NER pathway appears to associate with drug resistance (Reardon et al., 1999, Di Francesco et al., 2002, Dzagnidze et al., 2007).

Peripheral sensory neurotoxicity is a dose-limiting side effect of oxaliplatin and some of other platinum-based anticancer drugs, such as cisplatin and ormaplatin (Screnci and McKeage, 1999, McKeage et al., 2001, Amptoulach and Tsavaris, 2011). At present, the mechanisms of platinum drug-induced peripheral neurotoxicity remains unclear, although it has been generally accepted that the primary damage happens at the level of cell bodies of

sensory neurons within dorsal root ganglia (DRG) (Tomiwa et al., 1986, Cavaletti et al., 1992b, Holmes et al., 1998, Krarup-Hansen et al., 1999, Cavaletti et al., 2001, McKeage et al., 2001, Jamieson et al., 2005, Liu et al., 2009, Renn et al., 2011, Ip et al., 2013). Histopathological studies have shown decreased cell body size of DRG neurons as one of the morphological hallmarks of platinum drug-induced peripheral neuropathy in patients (Krarup-Hansen et al., 1999) and animal models (Tomiwa et al., 1986, Cavaletti et al., 1992b, Holmes et al., 1998, Cavaletti et al., 2001, Jamieson et al., 2005, Renn et al., 2011). The change in DRG neuronal cell body size appears to indicate neuronal atrophy because of the lack of evidence of cell loss or death (Tomiwa et al., 1986, Barajon et al., 1996, Jamieson et al., 2005).

High levels of platinum accumulation have been detected in the DRG that are not protected by blood-brain barrier, compared to tissues such as spinal cord and brain that have the barrier, following exposure to oxaliplatin and other platinum-based anticancer drugs in patients (Thompson et al., 1984, Gregg et al., 1992, Krarup-Hansen et al., 1999) and rodent models (Cavaletti et al., 1990, Screnci et al., 1997, Screnci et al., 2000, Cavaletti et al., 2001, Ip et al., 2013). However, the differential neurotoxicity profiles of platinum-based anticancer drugs are not readily accounted for by differences in the amount of platinum accumulating within the DRG tissue (Screnci et al., 1997, Holmes et al., 1998, Screnci et al., 2000). Recently, an increasing number of studies have demonstrated platinum-DNA adducts within DRG neurons (Meijer et al., 1999, McDonald et al., 2005) and that the level of platinum-DNA adducts correlates with severity of platinum drug-induced peripheral neurotoxicity (Ta et al., 2006). Indeed, mice with dysfunctional NER show more severe peripheral neuropathy after cisplatin treatment compared to those proficient for NER functions (Dzagnidze et al., 2007). However, in contrast to cancer cells, DRG neurons are post-mitotic cells that do not undergo DNA



replication or progress through the cell cycle. Therefore, although both cancer cells and DRG neurons accumulate platinum-DNA adducts after treatment with oxaliplatin and other platinum drugs, the mechanism linking formation of platinum-DNA damage to development of peripheral neurotoxicity must differ from that of their antitumor action discussed above.

A possible mechanism that could explain peripheral neurotoxicity induced by oxaliplatin and other platinum-based anticancer drugs may be transcriptional inhibition. The evidence to date has shown that platinum-DNA damage formed after treatment with platinum-based anticancer drugs inhibits eukaryotic transcription and strongly suggests that platinum-DNA damage-induced transcriptional inhibition is directly correlated to their cytotoxicity (Todd and Lippard, 2009). Treatment of human fibroblasts with cisplatin induced a dose-dependent decrease in levels of mRNA synthesis, which correlated with the induction of p53, p21 and apoptosis (Ljungman et al., 1999). Blocking synthesis of rRNA has also been suggested to play an important role in cisplatin cytotoxicity (Jordan and Carmo-Fonseca, 1998). More recently, using live mammalian cells with transfected plasmid DNAs that carry specific platinum-DNA adducts derived from oxaliplatin or cisplatin, Ang *et al.* have shown that platinum-DNA adducts inhibit transcription by impeding passage of RNA polymerase II and that NER can remove the blockage and restore transcription (Ang et al., 2010). Similar to dividing cells, post-mitotic neurons have also shown transcriptional inhibition after treatment with platinum-based anticancer drugs (Gozdz et al., 2008). Although nucleolar dysfunction/disorganization indicative of disrupted rRNA synthesis has been observed in DRG neurons from animals treated with platinum-based anticancer drugs (Tomiwa et al., 1986, Turecek et al., 1996, McKeage et al., 2001, Ip et al., 2013), there are relatively few studies that have directly investigated transcriptional inhibition induced by oxaliplatin and

other platinum drugs in DRG neurons, especially its interrelationships with platinum-DNA damage, neuronal cell body atrophy and peripheral neurotoxicity.

With this background, the studies presented in this chapter aimed to determine the temporal interrelationships between platinum-DNA damage, transcriptional inhibition and neuronal cell body atrophy induced by oxaliplatin in DRG cells, in an attempt to investigate the potential mechanism underlying platinum drug-induced peripheral neurotoxicity.

## **4.2. Results**

### **4.2.1. Platinum binding to DNA**

To characterize the time-course of binding of oxaliplatin-derived platinum to the DNA of cultured DRG cells, the platinum content of DNA extracted from DRG cells was measured before and at 1, 2, 4, 8, 24 and 48 h after the start of a 3-h exposure to 100  $\mu$ M oxaliplatin. Platinum binding to the DNA of cultured DRG cells was detectable at all time-points after the start of a 3-h exposure to 100  $\mu$ M oxaliplatin (Figure 4.1). DNA-bound platinum was first detected at one hour after the start of oxaliplatin treatment ( $0.0148 \pm 0.0009$  ng/ $\mu$ g DNA,  $P < 0.001$ ). Platinum-DNA levels then peaked at between four ( $0.0489 \pm 0.0049$  ng/ $\mu$ g DNA,  $P < 0.001$ ) and eight hours ( $0.0435 \pm 0.0052$  ng/ $\mu$ g DNA,  $P < 0.001$ ) after the start of oxaliplatin treatment. Thereafter, the level of DNA-bound platinum declined slowly but remained at 48.2% of its peak level (4 h) two days after oxaliplatin treatment ( $0.0235 \pm 0.0018$  ng/ $\mu$ g DNA,  $P < 0.001$ ).

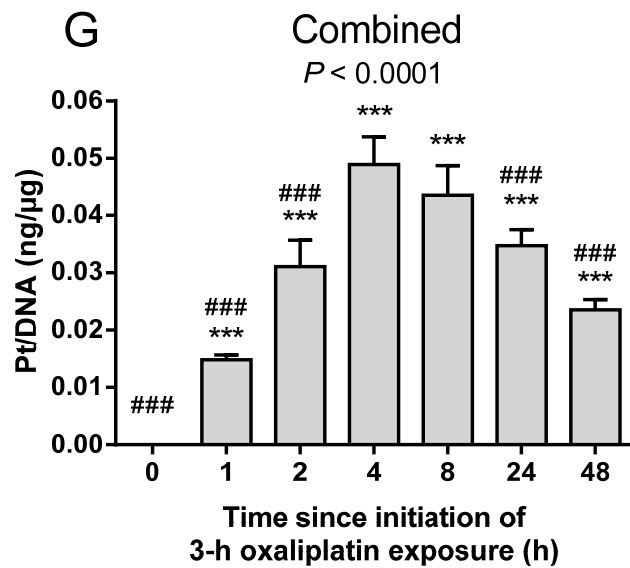
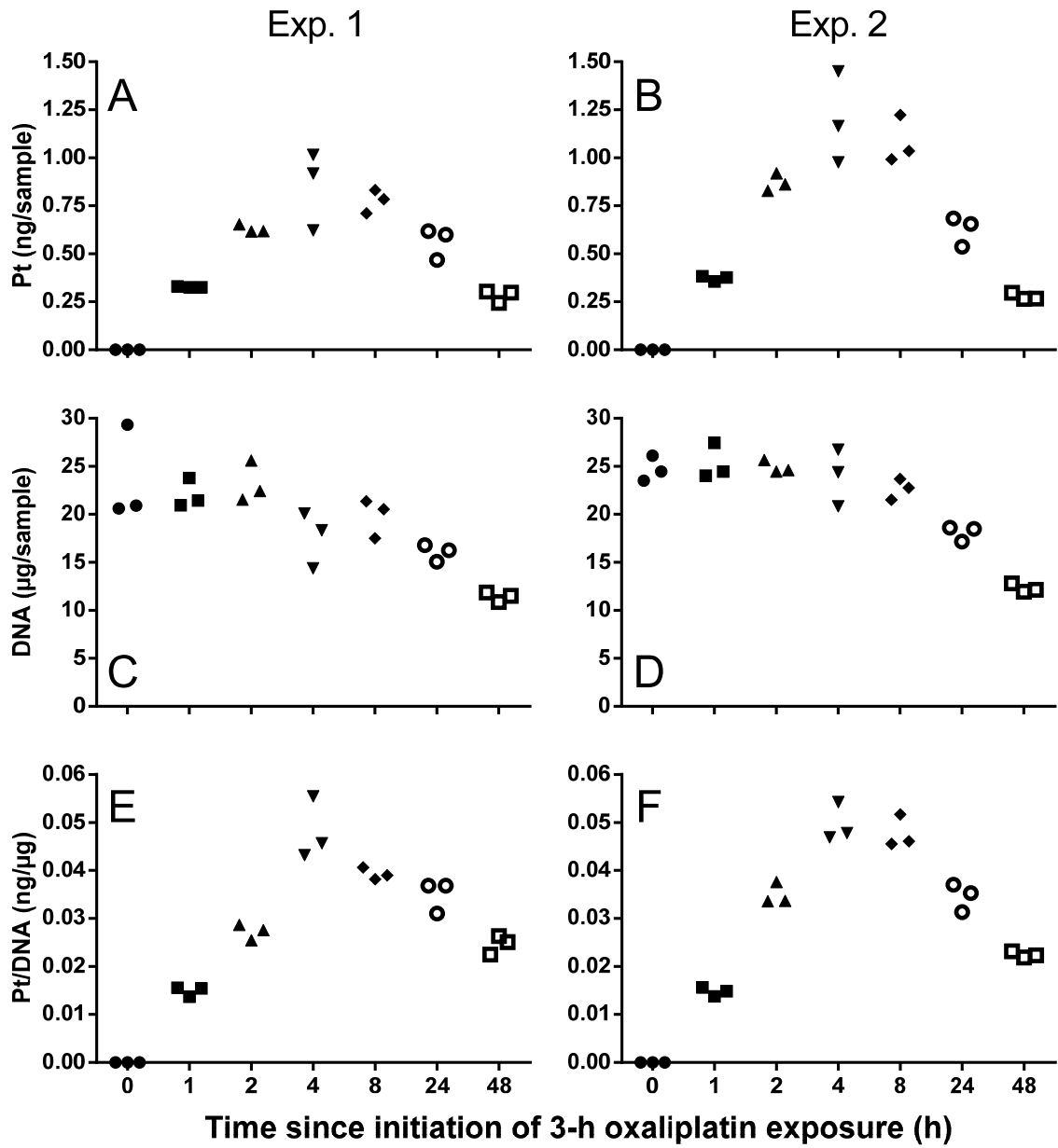


**Figure 4.1. Time-course of binding of oxaliplatin-derived platinum to the DNA of cultured DRG cells.**

DRG cells were harvested from 5 to 12 rats for each experiment and cultured for three days before experiments. Then they were exposed to 100  $\mu$ M oxaliplatin for up to 3 h, followed by culture in drug-free medium for up to a further two days. Two independent experiments were conducted (experiment 1: A, C and E; experiment 2: B, D and F). In each experiment, three culture wells for each time-point were independently assayed for platinum (A and B) and DNA content (C and D), followed by calculation of platinum content per DNA content (E and F). Then the data from individual experiments for platinum content per DNA content (E and F) were combined (G).

Data show that levels of platinum binding to the DNA of cultured DRG cells increased during and shortly after oxaliplatin treatment, followed by a slow decline thereafter.

(A-F) (●) 0 h, (■) 1 h, (▲) 2 h, (▼) 4 h, (◆) 8 h, (○) 24 h, (□) 48 h.

(G) Combined data are presented as mean  $\pm$  standard deviation (n=6). The *P* value in the figure is for overall difference between groups by one-way ANOVA test. \*\*\* *P*<0.001 indicate the statistical significance of differences compared to 0 h, ### *P*<0.001 indicate the statistical significance of differences compared to 4 h, assessed by Tukey's multiple comparison post-test.

#### 4.2.2. Inhibition of nascent RNA synthesis

To determine the time-course of oxaliplatin-induced inhibition of nascent RNA synthesis in cultured DRG cells, levels of RNA-incorporated [<sup>3</sup>H]uridine were measured before and at 4, 8, 24 and 48 h after the start of a 3-h exposure to 100 μM oxaliplatin. Nascent RNA synthesis in cultured DRG cells decreased over time after a three-hour exposure to oxaliplatin (Figure 4.2). Compared to baseline levels (0 h; 100 ± 43.9%), levels of RNA-incorporated [<sup>3</sup>H]uridine were first reduced at four hours (48.7 ± 14.4%, *P*<0.001) after the start of a 3-h exposure to 100 μM oxaliplatin. Levels of RNA-incorporated [<sup>3</sup>H]uridine then decreased further at eight (26.1 ± 9.0%, *P*<0.001) and twenty-four hours (13.4 ± 3.4%, *P*<0.001) after the start of oxaliplatin treatment. Two days after oxaliplatin treatment, nascent RNA synthesis remained suppressed at 16.8 ± 5.5% of baseline levels (*P*<0.001).

#### 4.2.3. Depletion of total RNA content

To investigate the time-course of oxaliplatin-induced depletion of total RNA content of cultured DRG cells, total RNA was isolated and measured before and at 4, 8, 24 and 48 h after the start of a 3-h exposure to 100 μM oxaliplatin. Total RNA content of cultured DRG cells gradually decreased throughout the duration of the experiment (Figure 4.3). Compared to baseline levels (0 h; 7.17 ± 0.79 μg), total RNA content was first reduced at four hours after the start of a three-hour exposure to oxaliplatin (6.22 ± 0.45 μg, *P*<0.01). Total RNA content then decreased further at eight (5.70 ± 0.17 μg, *P*<0.001) and twenty-four hours (4.03 ± 0.15 μg, *P*<0.001) after the start of oxaliplatin treatment. Thereafter, total RNA content reached its maximal levels of reduction at two days after oxaliplatin treatment (2.58 ± 0.33 μg, *P*<0.001).

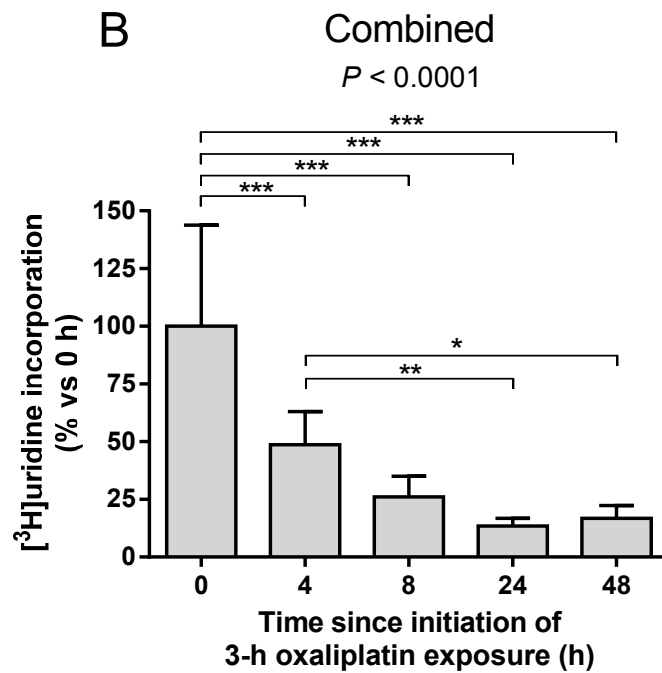
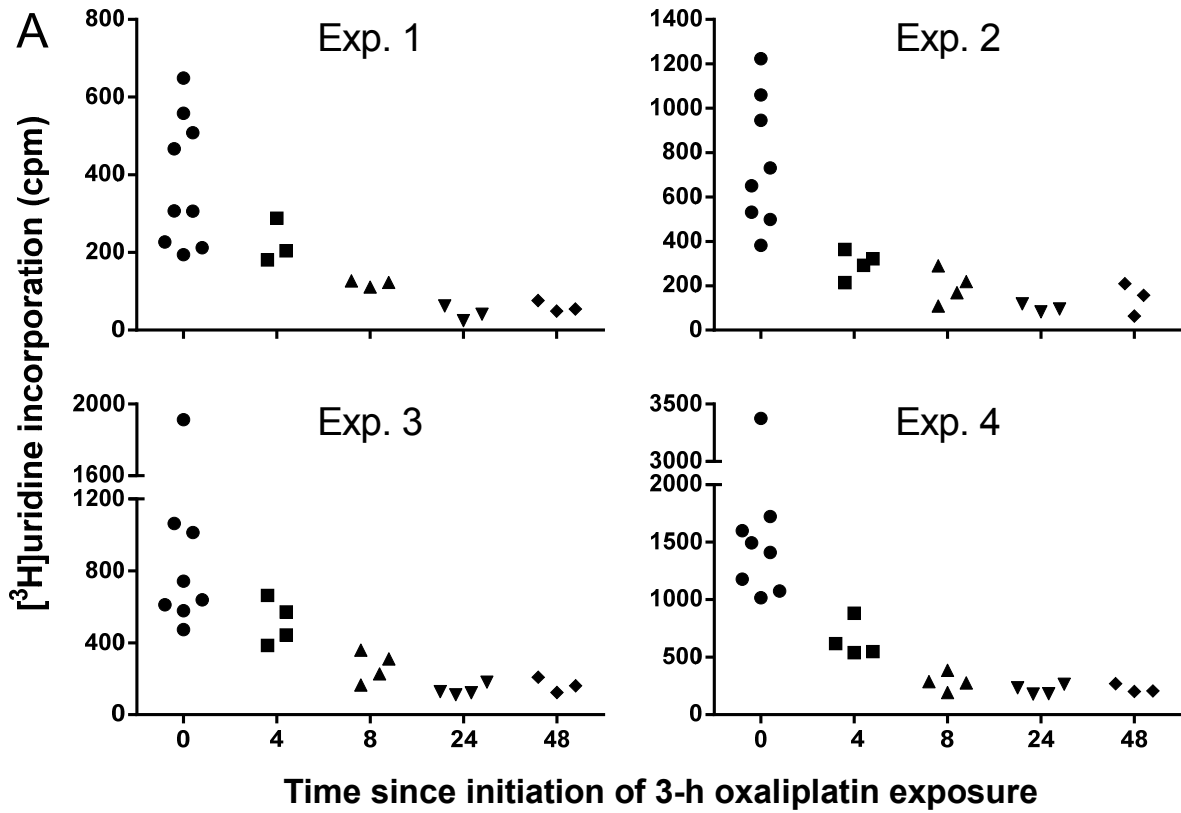


**Figure 4.2. Time-course of oxaliplatin-induced inhibition of nascent RNA synthesis in cultured DRG cells.**

DRG cells were harvested from one to three rats for each experiment and cultured for three days before experiments. Then they were exposed to 100  $\mu\text{M}$  oxaliplatin for 3 h, followed by culture in drug-free medium for up to a further two days. Four independent experiments were conducted (A). In each experiment, between three to nine culture wells for each time-point were independently studied for levels of RNA-incorporated [ $^3\text{H}$ ]uridine. Then the data from individual experiments were combined after normalization to the mean value of their respective 0 h (B).

Data show that nascent RNA synthesis in cultured DRG cells decreased over time after oxaliplatin treatment.

(A) (●) 0 h, (■) 4 h, (▲) 8 h, (▼) 24 h, (◆) 48 h.

(B) The combined data are presented as mean  $\pm$  standard deviation (n=12-33). The *P* value in the figure is for overall difference between groups by one-way ANOVA test. \*  $P < 0.05$ , \*\*  $P < 0.01$ , \*\*\*  $P < 0.001$  indicate the statistical significance of differences between indicated groups assessed by Tukey's multiple comparison post-test.

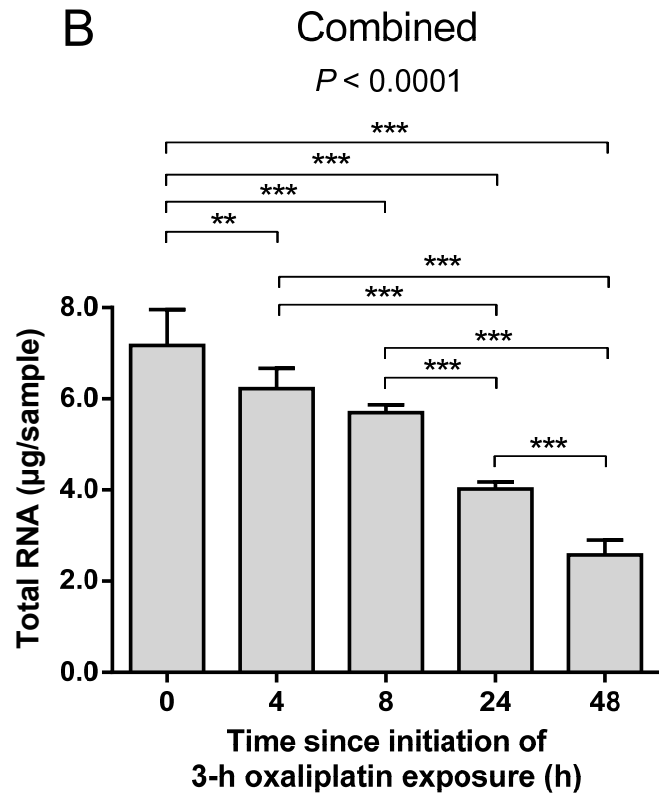
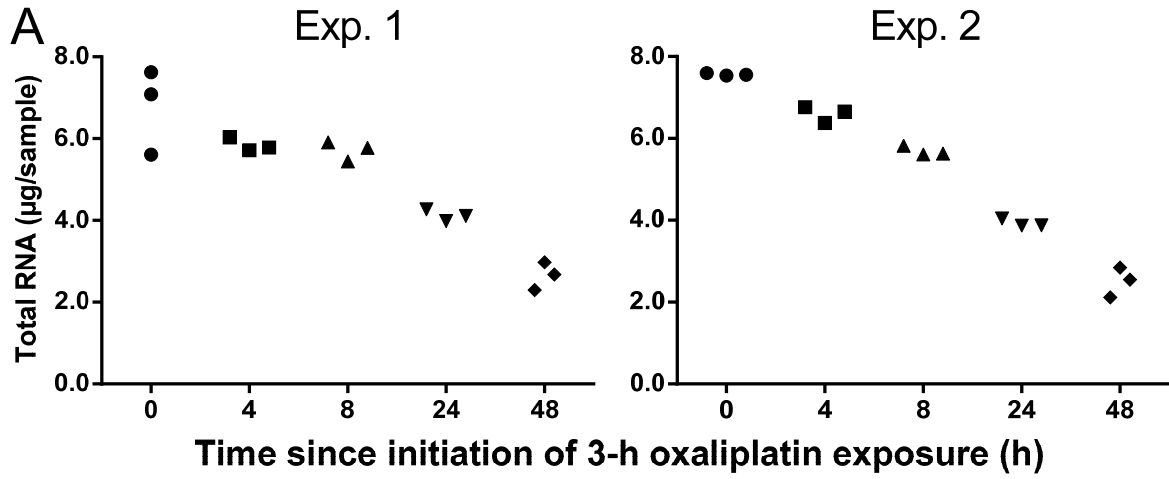




**Figure 4.3. Time-course of oxaliplatin-induced depletion of total RNA content of cultured DRG cells.**

DRG cells were harvested from four to five rats for each experiment and cultured for three days before experiments. Then they were exposed to 100  $\mu$ M oxaliplatin for 3 h, followed by culture in drug-free medium for up to a further two days. Two independent experiments were conducted (A). In each experiment, three culture wells for each time-point were independently assayed for total RNA content. Then the data from individual experiments were combined (B).

Data show that total RNA content of cultured DRG cells declined over time after oxaliplatin treatment.

(A) (●) 0 h, (■) 4 h, (▲) 8 h, (▼) 24 h, (◆) 48 h.

(B) The combined data are presented as mean  $\pm$  standard deviation (n=6). The *P* value in the figure is for overall difference between groups by one-way ANOVA test. \*\*  $P < 0.01$ , \*\*\*  $P < 0.001$  indicate the statistical significance of differences between indicated groups assessed by Tukey's multiple comparison post-test.

#### **4.2.4. Neuronal cell body atrophy**

To characterize the time-course of oxaliplatin-induced cell body atrophy in cultured DRG neurons, cell body areas of DRG neurons were measured before and at 4, 8, 24 and 48 h after the start of a 3-h exposure to 100  $\mu\text{M}$  oxaliplatin. The cell body size of cultured DRG neurons became reduced over time after a three-hour exposure to oxaliplatin (Figure 4.4). Distribution profiles of neuronal cell body area were shifted to lower values over time by oxaliplatin treatment. Compared to baseline levels (0 h; median: 337  $\mu\text{m}^2$ , interquartile range: 263-414  $\mu\text{m}^2$ ), neuronal cell body areas became significantly reduced first at eight hours after the start of a three-hour exposure to oxaliplatin (median: 289  $\mu\text{m}^2$ , interquartile range: 241-352  $\mu\text{m}^2$ ,  $P < 0.001$ ). Neuronal cell body areas then reduced further to the maximal levels of reduction at between one (median: 245  $\mu\text{m}^2$ , interquartile range: 205-293  $\mu\text{m}^2$ ,  $P < 0.001$ ) and two days (median: 248  $\mu\text{m}^2$ , interquartile range: 197-301  $\mu\text{m}^2$ ,  $P < 0.001$ ) after the start of oxaliplatin treatment.

#### **4.2.5. Temporal interrelationships between oxaliplatin effects**

Next, the temporal interrelationships between oxaliplatin-induced platinum binding to DNA, transcriptional inhibition and neuronal cell body atrophy in cultured DRG neurons were examined. Time-dependent changes in levels of platinum binding to DNA (Figure 4.1), RNA-incorporation of [ $^3\text{H}$ ]uridine (Figure 4.2), total RNA content (Figure 4.3) and cell body areas (Figure 4.4) were summarized and compared in Figure 4.5. For the sake of easy comparison, the data of total RNA content and cell body area were expressed as percentage of their respective baseline values. Binding of oxaliplatin-derived platinum to the DNA of cultured DRG cells appeared to have occurred before the induction of inhibition of nascent RNA synthesis and depletion of total RNA content. Oxaliplatin-induced neuronal cell body

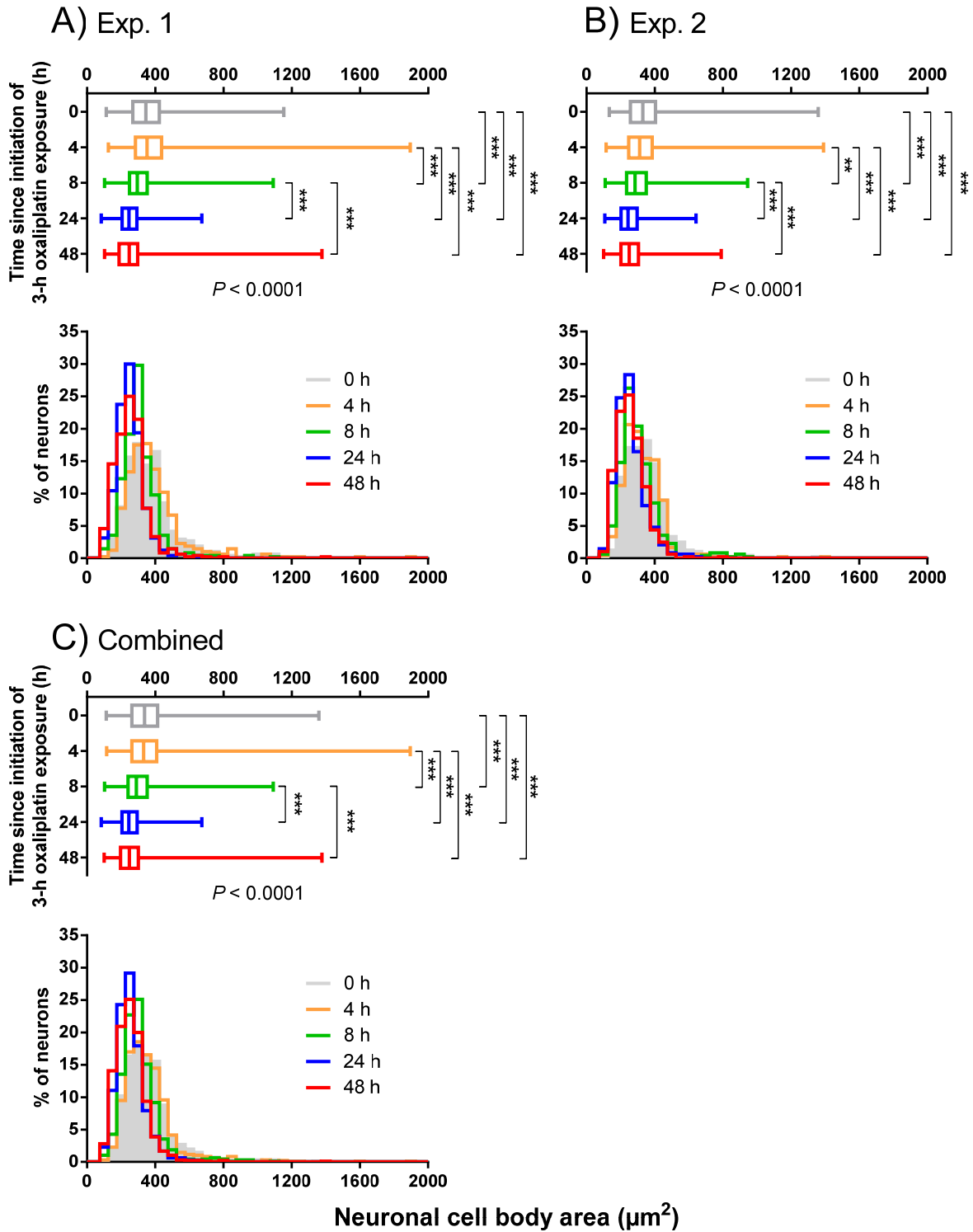


**Figure 4.4. Time-course of oxaliplatin-induced cell body atrophy in cultured DRG neurons.**

DRG cells were harvested from two to three rats for each experiment and cultured for three days before experiments. Then they were exposed to 100  $\mu\text{M}$  oxaliplatin for 3 h, followed by culture in drug-free medium for up to a further two days. Two independent experiments were conducted (A and B). In each experiment, a total of 480 neurons from three culture wells for each time-point were measured for cell body areas. Then the data from individual experiments were combined to achieve a group size of  $n=960$  (C).

Data show that the cell body size of cultured DRG neurons decreased over time after oxaliplatin treatment.

Data are presented as frequency histograms with bin width of  $50 \mu\text{m}^2$  and box-and-whiskers plots indicating the median value (vertical line across the box), interquartile range (box) and range (whiskers).  $P$  values in the figure are for overall difference between groups by Kruskal-Wallis test. \*\*  $P<0.01$ , \*\*\*  $P<0.001$  indicate the statistical significance of differences between indicated groups assessed by Dunn's multiple comparison post-test.

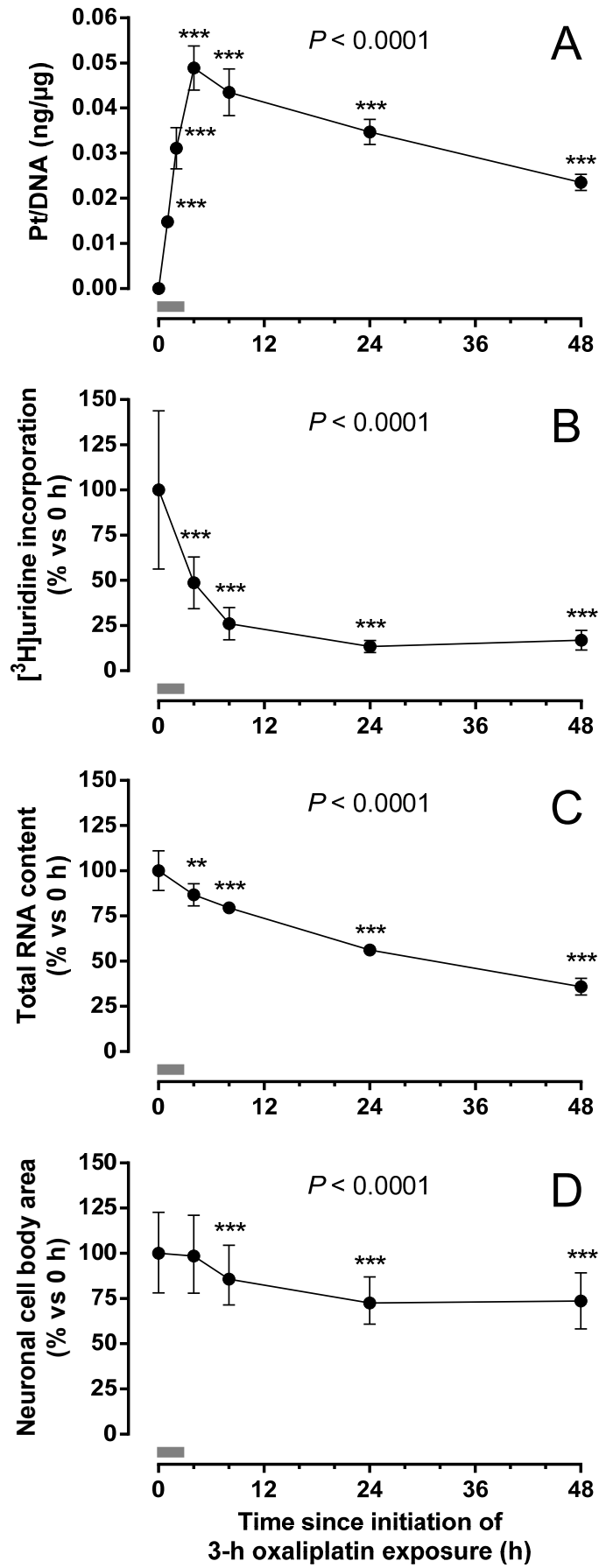


**Figure 4.5. Temporal interrelationships between binding of oxaliplatin-derived platinum to DNA and oxaliplatin effects on nascent RNA synthesis, total RNA content and neuronal cell body size.**

Data from Figure 4.1 G, 4.2 B, 4.3 B, and 4.4 C are shown as line graphs in the same figure for the sake of easy comparison.

Data show that platinum binding to the DNA of cultured DRG cells occurred before the oxaliplatin-induced inhibition of nascent RNA synthesis and depletion of total RNA content, which were all followed by the development of neuronal cell body shrinkage.

(A) Data are presented as mean  $\pm$  standard deviation.

(B and C) Data are normalized to percentage of the mean value of 0 h and presented as mean  $\pm$  standard deviation.

(D) Data are normalized to percentage of the median value of 0 h and presented as median  $\pm$  interquartile range.

*P* values in the figure are for overall difference between groups by one-way ANOVA (A-C) or Kruskal-Wallis test (D). \*\* *P*<0.01, \*\*\* *P*<0.001 indicate the statistical significance of difference compared to 0 h assessed by Tukey's (A-C) or Dunn's multiple comparison post-test (D). Grey bars indicate the duration of oxaliplatin treatment (i.e. 0-3 h).

shrinkage appeared delayed until after the occurrence of binding of platinum to DNA and inhibition of transcription (Figure 4.5). Platinum binding to DNA, inhibition of RNA-incorporation of [<sup>3</sup>H]uridine and depletion of total RNA content of DRG cells were all first detected within the first four hours of the experiment, whereas the reduction of neuronal cell body area was not first detected until eight hours. Maximum levels of platinum binding to the DNA of DRG cells were achieved at four hours, whereas the maximal decreases in levels of RNA-incorporation of [<sup>3</sup>H]uridine, total RNA content and neuronal cell body areas were not observed until at least one day after oxaliplatin treatment. Taken together, these data suggested that platinum binding to DNA preceded oxaliplatin-induced transcriptional inhibition in cultured DRG cells, which was then followed by the development of neuronal cell body shrinkage.

#### **4.2.6. Number of neurons**

To evaluate the effect of oxaliplatin on the number of cultured DRG neurons, the total number of DRG neurons per microscopic field was counted before and at 4, 8, 24 and 48 h after the start of a 3-h exposure to 100  $\mu$ M oxaliplatin. The number of cultured DRG neurons was unaffected by oxaliplatin treatment throughout the duration of the experiment (Figure 4.6). Compared to baseline levels, no significant differences were observed in the number of neurons at different time-points ( $P>0.05$ ).

#### **4.2.7. Apoptosis assay**

To investigate the apoptotic effect of oxaliplatin on cultured DRG neurons, apoptosis assay was conducted at two days after continuous exposure to oxaliplatin (10 or 30  $\mu$ M), using terminal deoxynucleotidyl transferase-mediated dUTP nick end labelling (TUNEL) technique.

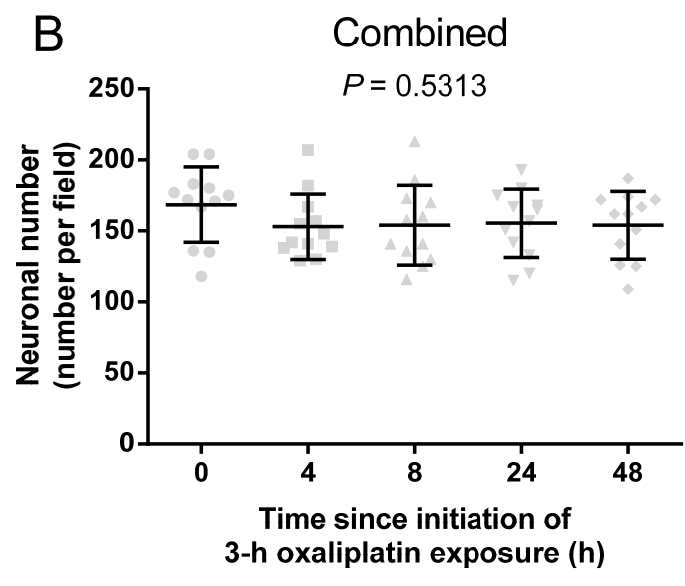
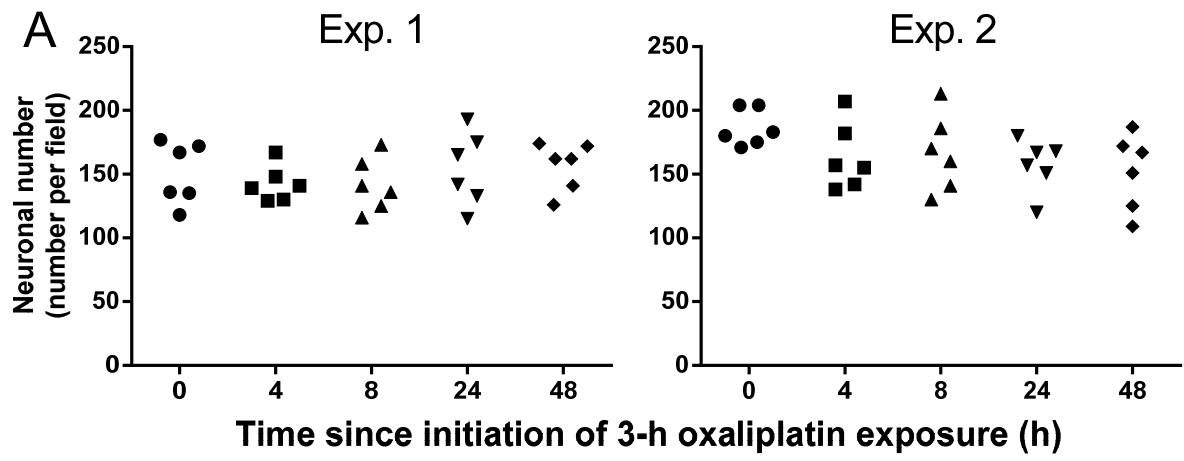




**Figure 4.6. Lack of effect of oxaliplatin on the number of cultured DRG neurons.**

DRG cells were harvested from two to three rats for each experiment and cultured for three days before experiments. Then they were exposed to 100  $\mu$ M oxaliplatin for 3 h, followed by culture in drug-free medium for up to a further two days. Two independent experiments were conducted (A). In each experiment, six microscopic fields from three culture wells (two fields per well) for each time-point were measured for the number of DRG neurons. Then the data from individual experiments were combined (B).

Data show that the number of cultured DRG neurons was unaffected by oxaliplatin treatment throughout the duration of the experiment.

(●) 0 h, (■) 4 h, (▲) 8 h, (▼) 24 h, (◆) 48 h. The horizontal lines represent mean  $\pm$  standard deviation. The *P* value in the figure is for overall difference between groups by one-way ANOVA test.

Representative images showed that oxaliplatin treatment appeared not to induce apoptosis in cultured DRG neurons, but in non-neuronal cells (Figure 4.7). Following a two-day continuous exposure to 30  $\mu\text{M}$  oxaliplatin, TUNEL staining was observed in the culture, which appeared to collocate with non-neuronal cells but not with DRG neurons.

#### **4.2.8. Effects of actinomycin D on neuronal cell body size**

To further explore the association between transcriptional inhibition and cell body shrinkage in cultured DRG neurons, effects of a model transcriptional inhibitor, actinomycin D, were studied. Levels of RNA-incorporated [ $^3\text{H}$ ]uridine and neuronal cell body areas were measured in cultured DRG cells before and after 1, 2, 4, 8 and 24 h of continuous exposure to 3  $\mu\text{M}$  actinomycin D. Actinomycin D treatment caused neuronal cell body atrophy following its inhibition of nascent RNA synthesis in cultured DRG cells (Figure 4.8 and 4.9). Compared to baseline levels (0 h;  $100 \pm 27.9\%$ ), levels of RNA-incorporated [ $^3\text{H}$ ]uridine were reduced by actinomycin D treatment at 1 h ( $4.2 \pm 2.1\%$ ,  $P < 0.001$ ) and throughout the rest of the experiment until 24 h ( $2.1 \pm 1.1\%$ ,  $P < 0.001$ ) (Figure 4.8). Distribution profiles of neuronal cell body area were shifted to lower values by actinomycin D treatment over time. Compared to baseline levels (0 h; median:  $328 \mu\text{m}^2$ , interquartile range:  $267\text{-}404 \mu\text{m}^2$ ), reduction of neuronal cell body area induced by actinomycin D was first detected at 4 h (median:  $309 \mu\text{m}^2$ , interquartile range:  $247\text{-}394 \mu\text{m}^2$ ,  $P < 0.01$ ), persisted at 8 h (median:  $305 \mu\text{m}^2$ , interquartile range:  $240\text{-}385 \mu\text{m}^2$ ,  $P < 0.001$ ) and decreased further at 24 h (median:  $251 \mu\text{m}^2$ , interquartile range:  $193\text{-}314 \mu\text{m}^2$ ,  $P < 0.001$ ) (Figure 4.9). Taken together, these data suggested that actinomycin D treatment caused neuronal cell body atrophy following its inhibition of nascent RNA synthesis.

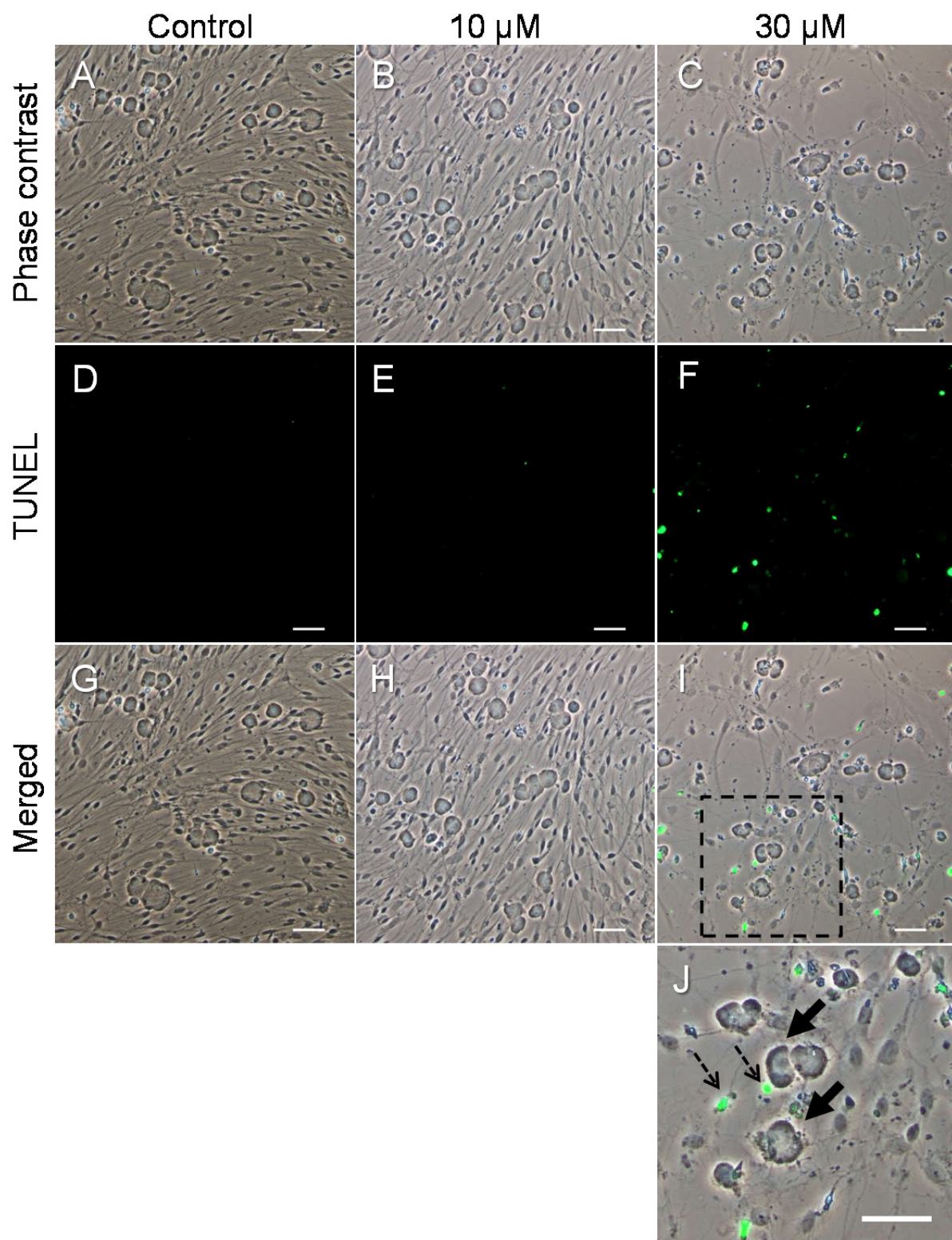


**Figure 4.7. Lack of apoptotic effect of oxaliplatin on cultured DRG neurons.**

DRG cells were harvested from three rats and cultured for three days before experiments. Then cells were continuously exposed to vehicle control (A, D, G) or oxaliplatin at concentrations of 10 (B, E, H) or 30  $\mu$ M (C, F, I, J) for two days. At the end of the experiment, cells were fixed and then stained using terminal deoxynucleotidyl transferase-mediated dUTP nick end labelling technique (TUNEL, green) to detect apoptosis. Images were acquired with a 10x objective.

Images show that oxaliplatin treatment appeared not to induce apoptosis in cultured DRG neurons (block arrows), but in non-neuronal cells (dotted arrows).

(A-C) Phase contrast images.

(D-F) TUNEL staining indicating apoptosis (green).

(G-I) Phase contrast images overlaid with TUNEL staining (green).

(J) Enlarged frame in (I). Block arrows indicate DRG neurons. Dotted arrows indicate non-neuronal cells.

Scale bar=50  $\mu$ m.

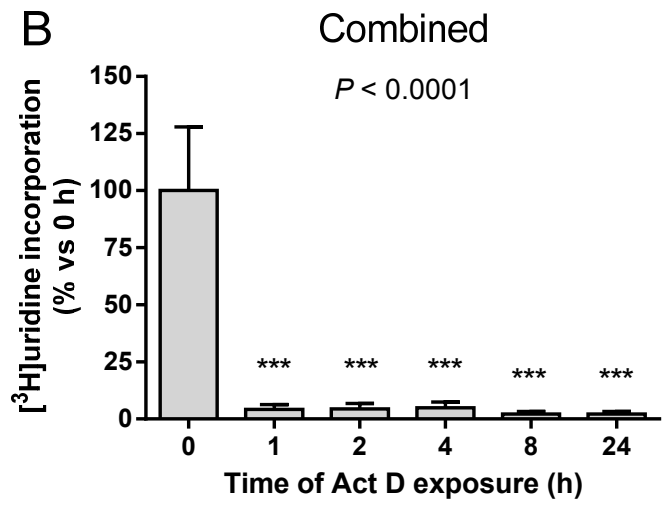
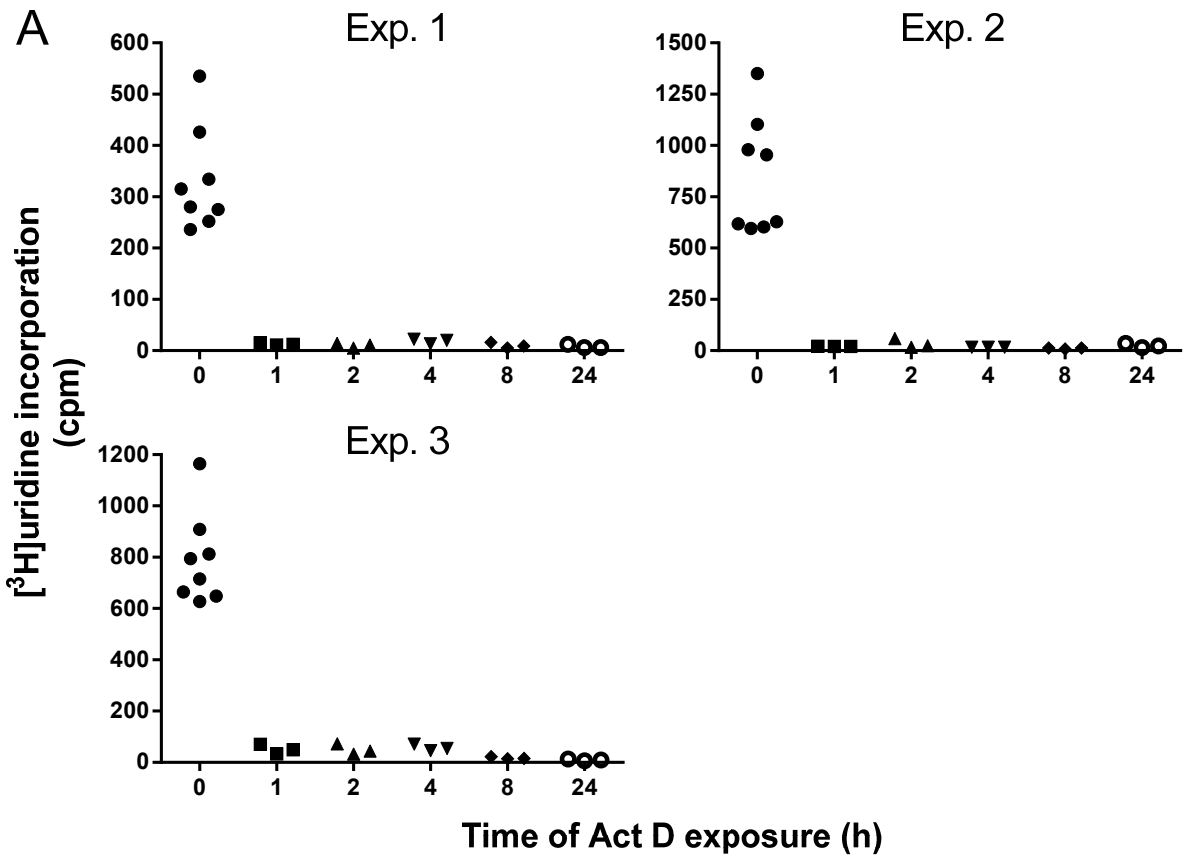


**Figure 4.8. Time-course of actinomycin D-induced inhibition of nascent RNA synthesis in cultured DRG cells.**

DRG cells were harvested from two to three rats for each experiment and cultured for three days before experiments. Then they were continuously exposed to 3  $\mu$ M actinomycin D (Act D) for up to one day. Three independent experiments were conducted (A). In each experiment, between three to eight culture wells for each time-point were independently studied for levels of RNA-incorporated [ $^3$ H]uridine. Then the data from individual experiments were combined after normalization to the mean value of their respective 0 h (B).

Data show that nascent RNA synthesis in cultured DRG cells was decreased over time by actinomycin D treatment.

(A) (●) 0 h, (■) 1 h, (▲) 2 h, (▼) 4 h, (◆) 8 h, (○) 24 h.

(B) The combined data are presented as mean  $\pm$  standard deviation (n=9-24). The *P* value in the figure is for overall difference between groups by one-way ANOVA test. \*\*\* *P*<0.001 indicate the statistical significance of differences compared to 0 h assessed by Tukey's multiple comparison post-test.

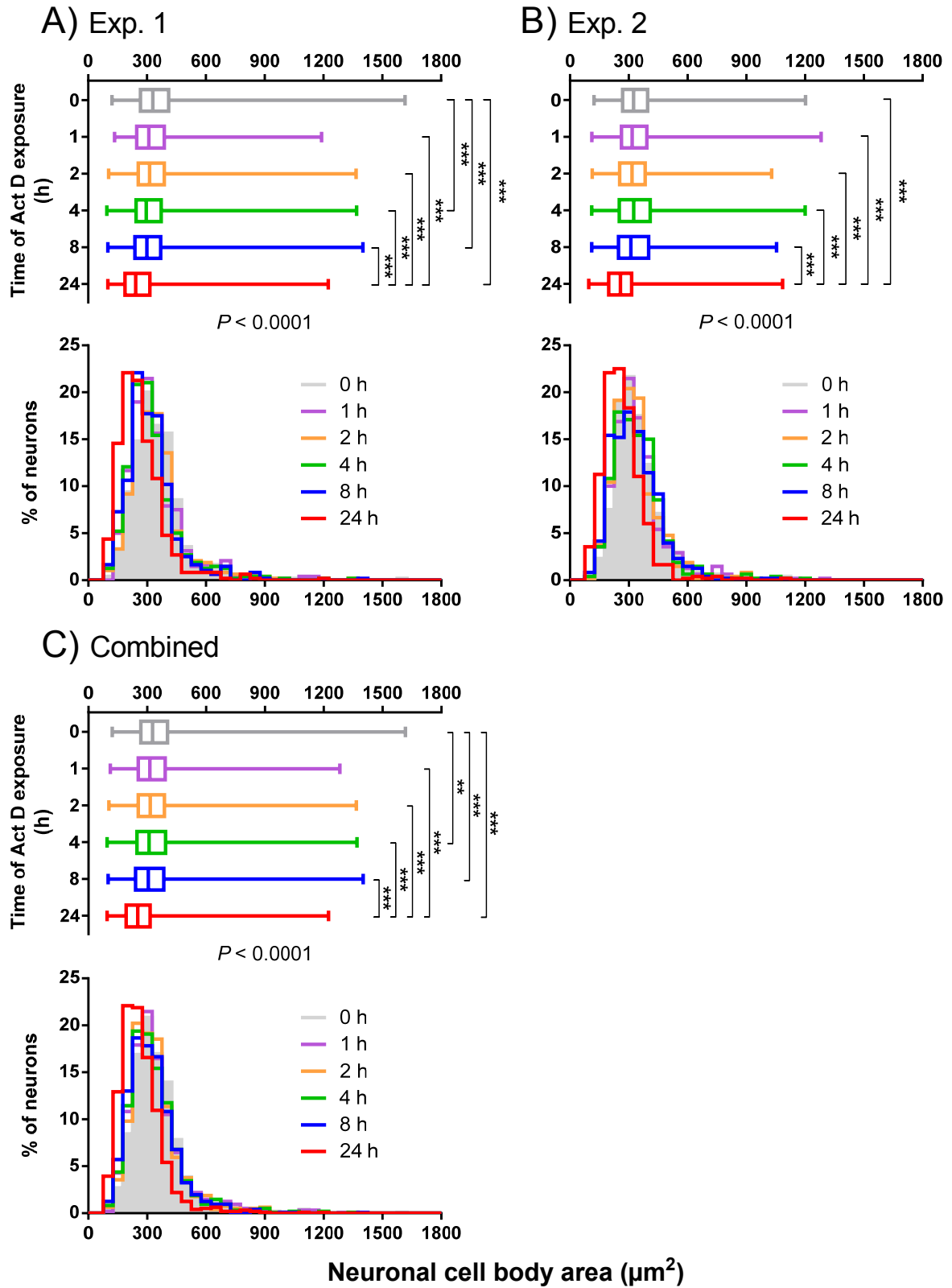


**Figure 4.9. Time-course of actinomycin D-induced cell body atrophy in cultured DRG neurons.**

DRG cells were harvested from three rats for each experiment and cultured for three days before experiments. Then they were continuously exposed to 3  $\mu\text{M}$  actinomycin D (Act D) for up to one day. Two independent experiments were conducted (A and B). In each experiment, a total of 480 neurons from three culture wells for each time-point were measured for cell body areas. Then the data from individual experiments were combined to achieve a group size of  $n=960$  (C).

Data show that the cell body size of cultured DRG neurons was decreased over time by actinomycin D treatment.

Data are presented as frequency histograms with bin width of  $50 \mu\text{m}^2$  and box-and-whiskers plots indicating the median value (vertical line across the box), interquartile range (box) and range (whiskers). *P* values in the figure are for overall difference between groups by Kruskal-Wallis test. \*\*  $P<0.01$ , \*\*\*  $P<0.001$  indicate the statistical significance of differences between indicated groups assessed by Dunn's multiple comparison post-test.



### 4.3. Discussion

The findings described in this chapter have suggested that mechanisms of oxaliplatin-induced peripheral neurotoxicity may involve interrelationships between platinum-DNA damage, transcriptional inhibition and neuronal cell body atrophy in DRG cells. In this study, the time-courses of platinum-DNA damage, transcriptional inhibition and neuronal cell body atrophy induced by oxaliplatin in cultured rat DRG cells were defined and compared. Platinum-DNA damage, as indicated by levels of platinum binding to DNA, was first detected at one hour, and reached its peak level at between four and eight hours, after the start of oxaliplatin treatment. Later, transcriptional inhibition, as indicated by decreases in levels of RNA-incorporated [<sup>3</sup>H]uridine and total RNA content, was first detected at four hours, and reached its maximal level at between one and two days, after the start of oxaliplatin treatment. Finally, neuronal cell body atrophy, as indicated by decreased neuronal cell body areas, was first detected at eight hours, and reached its maximal level at between one and two days, after the start of oxaliplatin treatment. Therefore, oxaliplatin-induced platinum-DNA damage appeared to have occurred before the induction of transcriptional inhibition, while neuronal cell body shrinkage appeared delayed until after the occurrence of platinum-DNA damage and inhibition of transcription. The temporal interrelationships found between these three events have suggested that oxaliplatin-induced platinum-DNA damage may contribute to transcriptional inhibition in DRG cells, which in turn may lead to neuronal cell body atrophy and peripheral neurotoxicity.

Further strengthening possible interrelationships found between transcriptional inhibition and DRG neuronal cell body atrophy was the finding of actinomycin D treatment having caused neuronal cell body atrophy following its inhibition of nascent RNA synthesis in cultured

DRG cells. Actinomycin D is a well-known model transcriptional inhibitor, which binds to DNA within the transcriptional complex thereby preventing elongation of RNA chains by RNA polymerase (Sobell, 1985, Casafont et al., 2006, Bensaude, 2011). To further explore possible linkages between transcriptional inhibition and neuronal cell body atrophy, actinomycin D was studied in regard to whether it could reduce neuronal cell body areas in cultured DRG cells. The data showed that actinomycin D treatment first reduced levels of RNA-incorporated [<sup>3</sup>H]uridine at one hour, and its effect persisted throughout the rest of the experiment until twenty-four hours. Later, actinomycin D treatment reduced neuronal cell body areas first at four hours and reached its maximal levels of effect at twenty-four hours. Taken together, these findings provide further evidence suggesting that DRG neuronal cell body atrophy may be due to transcriptional inhibition.

An alternative explanation for the observed decreases in levels of RNA-incorporated [<sup>3</sup>H]uridine, total RNA content and neuronal cell body areas induced by oxaliplatin in cultured DRG cells could have been the loss of neurons under the conditions used for the experiments in which these measurements were made. Loss of neurons, especially large neurons with high levels of nascent RNA synthesis, could be expected to lead to measurable decreases in levels of RNA-incorporated [<sup>3</sup>H]uridine, total RNA content and neuronal cell body areas as these measurements were uncorrected for cell number. In keeping with the possibility of loss of cells occurring under the experimental conditions was the finding that the DNA content in cultured DRG cells became reduced over time by oxaliplatin treatment, especially at one and two days after treatment. To test whether loss of neurons was induced by oxaliplatin treatment under these experimental conditions, the number of DRG neurons was counted over time after oxaliplatin treatment. These data showed no effect of oxaliplatin on the number of DRG neurons. This finding suggests that loss of neurons did not contribute

to the decreased levels of RNA-incorporated [<sup>3</sup>H]uridine, total RNA content and neuronal cell body areas observed in cultured DRG cells after oxaliplatin treatment. However, effects on non-neuronal DRG cells under the experimental conditions may have contributed to the oxaliplatin treatment-related changes in DNA content of DRG cultures. Findings described in this chapter showed that oxaliplatin treatment caused apoptosis in non-neuronal cells but not in DRG neurons under these similar treatment conditions. In addition, like other platinum-based anticancer drugs, oxaliplatin is known for inhibiting DNA replication (Mani et al., 2002, Graham et al., 2004, Wang and Lippard, 2005), which may have led to measurable reductions in the DNA content of DRG cultures after treatment. Taken together, these considerations suggest that the effects of oxaliplatin treatment on nascent RNA synthesis, total RNA content and neuronal cell body size in cultured DRG cells were not attributable simply to the loss of neurons.

In the current study, two different endpoints of transcriptional activity, levels of RNA-incorporated [<sup>3</sup>H]uridine and total RNA content, were used to study the effects of oxaliplatin treatment on cultured DRG cells. Both levels of RNA-incorporated [<sup>3</sup>H]uridine and total RNA content were first reduced at four hours, and reached their maximal levels of reduction at between one and two days, after the start of oxaliplatin treatment. These findings were in keeping with those obtained using RNA-incorporation of 5-ethynyl uridine (EU) described in Chapter 3, thereby providing further evidence of the transcriptional inhibition induced by oxaliplatin in DRG neurons. However, unlike RNA-incorporated EU which indicated individual neuron levels of transcriptional activity, these two endpoints measured transcriptional activity of whole cultures. Although these two endpoints provided simple and efficient way to measure transcriptional activity in cultured DRG cells, loss of non-neuronal cells could potentially affect their results to some extent. However, as discussed in Chapter 3,

DRG neurons had strong fluorescence labelling of RNA-incorporated EU, whereas little or no labelling was observed in non-neuronal cells, which implied that DRG neurons may have much higher levels of nascent RNA synthesis than non-neuronal cells. Therefore, it may be reasonable to conclude that loss of non-neuronal cells contributed less than transcriptional inhibition in neurons to the observed changes in levels of RNA-incorporated [<sup>3</sup>H]uridine and total RNA content induced by oxaliplatin in cultured DRG cells.

This study demonstrated a specific pattern of binding of oxaliplatin-derived platinum to the DNA of cultured DRG cells, whereby platinum-DNA levels increased during and shortly after oxaliplatin treatment, and then decreased but persisted after drug removal. DNA-bound platinum was first detected at one hour, and then peaked at between four and eight hours, after the start of oxaliplatin treatment of cultured DRG cells. Thereafter, DNA-bound platinum decreased but still remained at about half of its peak level two days after drug removal. For oxaliplatin-derived platinum to become bound to DNA, oxaliplatin (or its active metabolites) must first enter the target cell, convert to its aquated forms and transit to the nucleus, and then undergo ligand substitution reactions with components of DNA (Kweekel et al., 2005, Jung and Lippard, 2007, Alcindor and Beauger, 2011). Thereafter, DNA-bound platinum may be removed by nucleotide excision repair and/or other DNA repair mechanisms (Di Francesco et al., 2002, Chaney et al., 2005). These different processes involved in the formation and removal of platinum-DNA adducts may explain the specific pattern, levels and persistence of DNA binding of oxaliplatin-derived platinum observed in this study.

In conclusion, the findings presented in this chapter suggest that platinum-DNA damage-induced transcriptional inhibition may contribute to the induction of DRG neuronal cell body atrophy and peripheral neurotoxicity by oxaliplatin.

# **Chapter 5. Effects of inhibitors on oxaliplatin toxicity in cultured rat DRG cells**

## **5.1. Introduction**

In the previous chapter, studies of interrelationships between platinum-DNA damage, transcriptional inhibition and neuronal cell body atrophy in DRG cells suggested that these processes were involved in mechanisms of oxaliplatin-induced peripheral neurotoxicity. Oxaliplatin-induced platinum-DNA damage appeared to have occurred before the induction of transcriptional inhibition, while neuronal cell body atrophy appeared delayed until after the occurrence of platinum-DNA damage and inhibition of transcription. Therefore, the temporal interrelationship found between these three events have suggested that oxaliplatin-induced platinum-DNA damage may contribute to transcriptional inhibition in DRG cells, which in turn may lead to neuronal cell body atrophy and peripheral neurotoxicity.

To further investigate this potential mechanism, the studies described in this chapter used sodium thiosulfate and cimetidine because of their potential of preventing platinum-DNA damage in DRG cells, which was hypothesised to thereby prevent oxaliplatin-induced transcriptional inhibition and neuronal cell body atrophy in these cells. Sodium thiosulfate is a reactive thiol compound used clinically as an antidote against cyanide poisoning (Harned et al., 2008). It has been previously shown to inactivate the electrophilic platinum-based anticancer drugs by forming biologically inactive platinum-sodium thiosulfate complex (Iwamoto et al., 1985, Nagai et al., 1995, Sooriyaarachchi et al., 2012). Previous studies have demonstrated that co-incubation with sodium thiosulfate reduced the extent of DNA binding

of cisplatin-derived platinum (Viale et al., 1999, Brouwers et al., 2008b). It has also been demonstrated that concurrent sodium thiosulfate treatment reduced cellular uptake and cytotoxicity of cisplatin (Catino et al., 1986, Viale et al., 1999, Kovacs and Cinatl, 2002). Furthermore, sodium thiosulfate has shown protective effects against platinum drug-associated side effects. A clinical trial has revealed that sodium thiosulfate co-administration with intra-arterial cisplatin administration led to a significant reduction of persistent neurotoxicity induced by cisplatin, as measured by vibration threshold values in hands and feet (Brouwers et al., 2009). It is noteworthy that long-term plasma platinum levels were also significantly reduced by sodium thiosulfate co-administration in these patients (Brouwers et al., 2008a). In addition, sodium thiosulfate has been previously suggested to prevent cisplatin-induced ototoxicity and nephrotoxicity (Dickey et al., 2005) and carboplatin-induced ototoxicity (Neuwelt et al., 1996, Doolittle et al., 2001, Neuwelt et al., 2006).

Cimetidine is a histamine H<sub>2</sub>-receptor antagonist widely used for the treatment of dyspepsia and peptic ulcers. It has been identified as organic cation transporter 2 (OCT2) substrate and inhibitor (Burger et al., 2011, Ciarimboli, 2012). Therefore, cimetidine could theoretically affect both the efficacy of treatment and the severity of side effects of platinum-based anticancer drugs that have also been demonstrated as OCT2 substrates (Burger et al., 2011, Ciarimboli, 2012). Indeed, contemporaneous incubation with cimetidine markedly reduced the binding of oxaliplatin-derived platinum to the DNA of OCT2-transfected cells (Zhang et al., 2006). There are also evidence showing that cimetidine significantly decreased cellular platinum accumulation following cisplatin and oxaliplatin treatment and attenuated their cytotoxicity *in vitro* (Ludwig et al., 2004, Ciarimboli et al., 2005, Yonezawa et al., 2005, Zhang et al., 2006, Buss et al., 2009, Pabla et al., 2009). In addition, protective effects of concurrent cimetidine treatment against platinum drug-associated adverse effects have been

demonstrated in animal models (Ciarimboli et al., 2010, Franke et al., 2010, Katsuda et al., 2010, Sprowl et al., 2013) and patients (Sleijfer et al., 1987, Zhang and Zhou, 2012). In particular, concurrent administration of cimetidine protected mice from acute oxaliplatin-induced peripheral neurotoxicity, as indicated by cold hypersensitivity and mechanical allodynia (Sprowl et al., 2013). However, relatively little is known about the effects of sodium thiosulfate and cimetidine on oxaliplatin-induced platinum-DNA damage, transcriptional inhibition or neuronal cell body atrophy in DRG cells, especially in context of the interrelationships between these three events.

Apoptotic volume decrease (AVD) leading to cell shrinkage, under normotonic conditions, is an early-phase hallmark of apoptosis, which precedes cytochrome *c* release, caspase-3 activation, DNA fragmentation, ultrastructural alterations and eventual cell death (Maeno et al., 2000, Okada et al., 2001, Pasantes-Morales and Tuz, 2006, Nunez et al., 2010). AVD has been associated with efflux of  $K^+$  and/or  $Cl^-$  ions through their corresponding ion channels and osmotically obligated loss of water (Bortner and Cidlowski, 2002, Okada et al., 2006, Pasantes-Morales and Tuz, 2006, Bortner and Cidlowski, 2007, Nunez et al., 2010). Platinum-based anticancer drugs have been demonstrated to activate  $Cl^-$  channels and induce AVD and apoptosis in cancer cells (Ise et al., 2005, He et al., 2010, Poulsen et al., 2010, Min et al., 2011). Impaired activity of  $Cl^-$  channels and dysfunction of AVD are associated with cisplatin resistance (Lee et al., 2007, Poulsen et al., 2010, Min et al., 2011). In neurons, AVD has also been observed after exposure to apoptosis stimuli, and  $K^+$  and/or  $Cl^-$  channel blockers protected neurons from AVD and cell death (Wei et al., 2004, Hernandez-Enriquez et al., 2010, Hernandez-Enriquez et al., 2011).

DNA-dependent protein kinase (DNA-PK) and poly(ADP-ribose) polymerase 1 (PARP-1) are proteins that both play key roles in DNA damage repair (Meek et al., 2008, Luo and

Kraus, 2012). DNA-PK has been shown to repress the RNA polymerase I machinery of rRNA synthesis (Kuhn et al., 1995, Michaelidis and Grummt, 2002). The role of PARP-1 in rRNA transcription has also been suggested (Desnoyers et al., 1996, Boamah et al., 2012). Most recently, Calkins and colleagues have proposed that a sequential activation of DNA-PK and PARP-1 is critically involved in cisplatin-induced inhibition of rRNA synthesis (Calkins et al., 2013). Inhibition of either DNA-PK or PARP-1 prevented cisplatin-induced block of rRNA synthesis, and loss of DNA-PK function impeded activation of PARP-1 in damaged cells (Calkins et al., 2013). Nevertheless, the role of AVD or DNA-PK/PARP-1 in oxaliplatin toxicity in DRG cells is still not well investigated.

With this background, the aim of this study was to investigate the effects of different pharmacological inhibitors on oxaliplatin toxicity in cultured DRG cells, in an attempt to further explore potential mechanisms of oxaliplatin-induced neuronal cell body atrophy and peripheral neurotoxicity.

## **5.2. Results**

### **5.2.1. Sodium thiosulfate**

To investigate protective effects of sodium thiosulfate against oxaliplatin toxicity in cultured rat DRG cells, amounts of platinum binding to DNA were measured at four hours, and levels of RNA-incorporated [<sup>3</sup>H]uridine and neuronal cell body areas were measured at two days, after continuous exposure to oxaliplatin (10 or 30  $\mu$ M) with or without sodium thiosulfate (8 mM).



Data showed that levels of platinum-DNA damage in oxaliplatin-treated cultured DRG cells were reduced by concurrent sodium thiosulfate treatment (Figure 5.1). Following a 4-h continuous exposure to 30  $\mu$ M oxaliplatin without sodium thiosulfate, the level of platinum binding to DNA was  $0.0154 \pm 0.0007$  ng/ $\mu$ g DNA. In contrast, co-incubation of sodium thiosulfate (8 mM) with oxaliplatin significantly reduced DNA-bound platinum to undetectable levels ( $P < 0.001$ ).

Co-incubation with sodium thiosulfate also protected cultured DRG cells against oxaliplatin-induced inhibition of nascent RNA synthesis (Figure 5.2). Compared with untreated controls ( $100 \pm 31.4\%$ ), levels of RNA-incorporated [ $^3$ H]uridine were reduced following a two-day continuous exposure to 10 and 30  $\mu$ M oxaliplatin without sodium thiosulfate to  $49.0 \pm 23.8\%$  ( $P < 0.01$ ) and  $39.2 \pm 6.4\%$  ( $P < 0.001$ ) of control, respectively. In contrast, when oxaliplatin was co-incubated with sodium thiosulfate (8 mM), the levels of RNA-incorporated [ $^3$ H]uridine were similar to the untreated control values and significantly higher ( $P < 0.05$ ) compared to those achieved with oxaliplatin alone. Compared to oxaliplatin treatment alone, levels of RNA-incorporated [ $^3$ H]uridine following a two-day continuous exposure to 10 and 30  $\mu$ M oxaliplatin concurrently with sodium thiosulfate were  $96.5 \pm 17.4\%$  ( $P < 0.05$ ) and  $94.9 \pm 34.5\%$  ( $P < 0.01$ ) of control, respectively.

Concurrent sodium thiosulfate treatment also prevented the induction of cell body atrophy in cultured DRG neurons by oxaliplatin (Figure 5.3). Following a two-day continuous exposure to oxaliplatin (10 or 30  $\mu$ M), DRG neuronal cell body area distribution profiles were shifted to lower values, but this effect was prevented by the addition of sodium thiosulfate (8 mM). Compared with untreated controls (median: 353  $\mu$ m<sup>2</sup>, interquartile range: 280-453  $\mu$ m<sup>2</sup>), median neuronal cell body areas were significantly decreased by 10 and 30  $\mu$ M oxaliplatin alone to 84.8% (median: 299  $\mu$ m<sup>2</sup>, interquartile range: 249-371  $\mu$ m<sup>2</sup>,  $P < 0.001$ ) and 72.9%

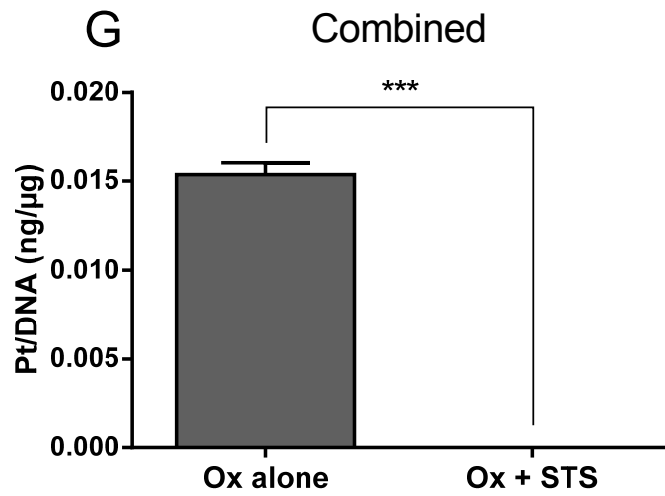
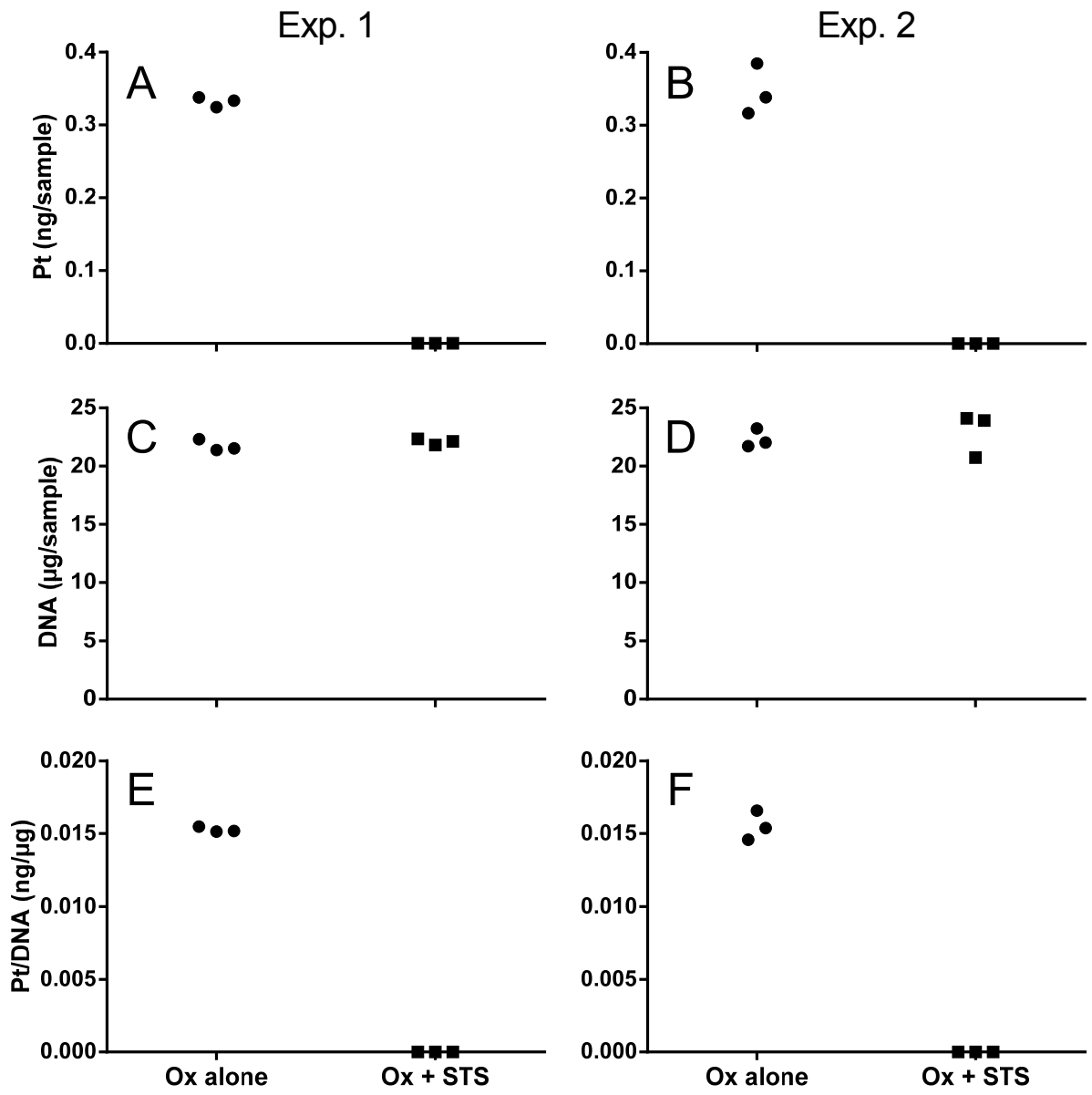


**Figure 5.1. Sodium thiosulfate reduced platinum binding to the DNA of cultured DRG cells after exposure to oxaliplatin.**

DRG cells were harvested from 10 rats for each experiment and cultured for three days before experiments. Then they were continuously exposed to 30  $\mu\text{M}$  oxaliplatin (Ox) with or without 8 mM sodium thiosulfate (STS) for 4 h. Two independent experiments were conducted (experiment 1: A, C and E; experiment 2: B, D and F). In each experiment, three culture wells for each treatment condition were independently assayed for platinum (A and B) and DNA content (C and D), followed by calculation of platinum content per DNA content (E and F). Then the data from individual experiments for platinum content per DNA content (E and F) were combined (G).

Data show that sodium thiosulfate reduced platinum binding to the DNA of cultured DRG cells after exposure to oxaliplatin, without any apparent effect on the DNA content.

(A-F) (●) Ox alone, (■) Ox with STS.

(G) Combined data are presented as mean  $\pm$  standard deviation (n=6). \*\*\*  $P < 0.001$  indicates the statistical significance of difference compared to oxaliplatin alone assessed by unpaired t-test.

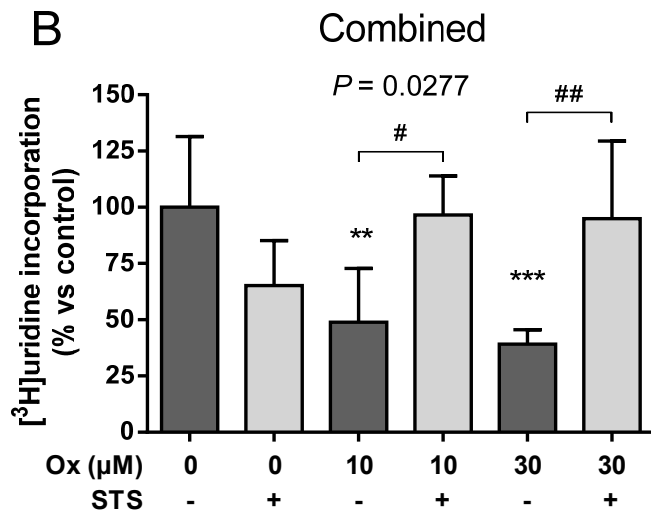
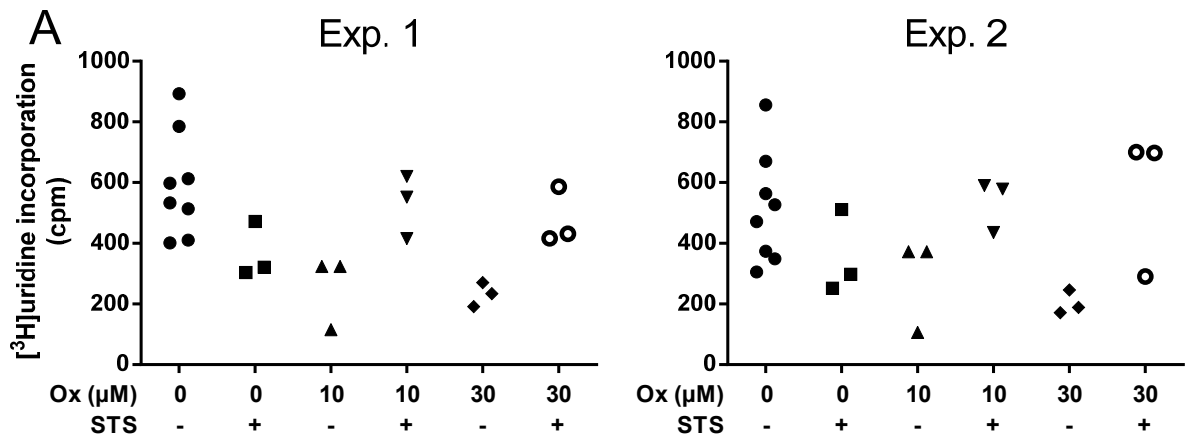


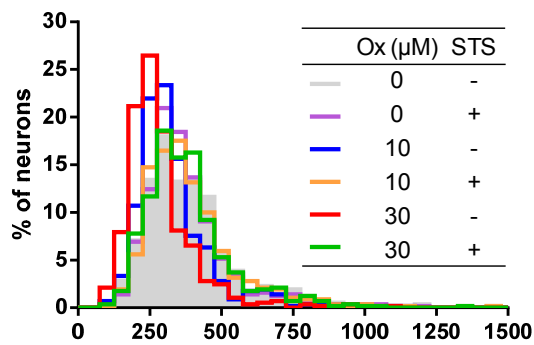
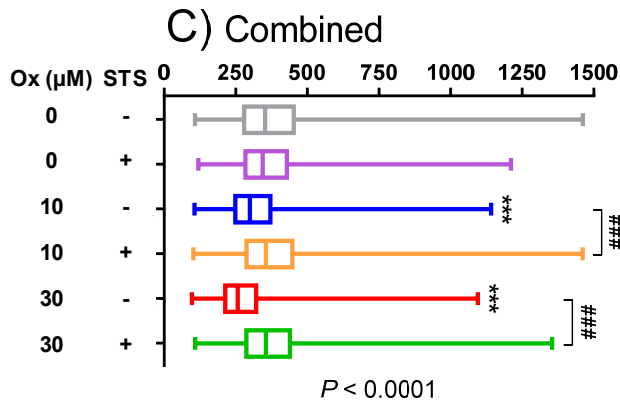
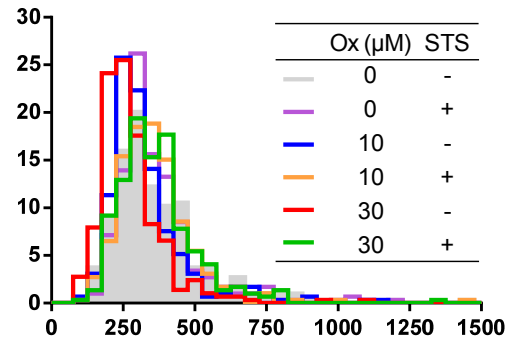
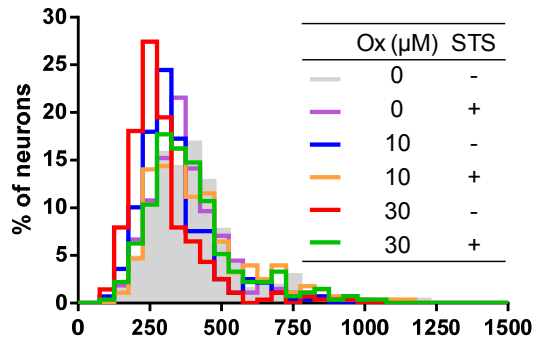
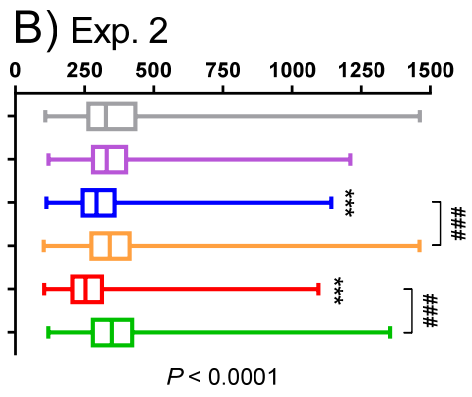
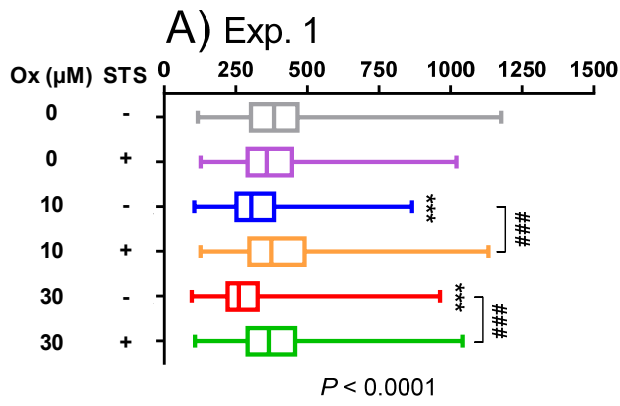
**Figure 5.2. Sodium thiosulfate protected cultured DRG cells from inhibition of nascent RNA synthesis induced by oxaliplatin.**

DRG cells were harvested from two rats for each experiment and cultured for three days before experiments. Then they were continuously exposed to 10 or 30  $\mu\text{M}$  oxaliplatin (Ox) with or without 8 mM sodium thiosulfate (STS) for two days. Two independent experiments were conducted (A). In each experiment, between three to eight culture wells for each treatment condition were independently studied for levels of RNA-incorporated [ $^3\text{H}$ ]uridine. Then the data from individual experiments were combined after normalization to the mean value of their respective untreated controls (B).

Data show that sodium thiosulfate protected cultured DRG cells from inhibition of nascent RNA synthesis induced by oxaliplatin.

(A) (●) Untreated control, (■) STS alone, (▲) 10  $\mu\text{M}$  Ox, (▼) 10  $\mu\text{M}$  Ox with STS, (◆) 30  $\mu\text{M}$  Ox, (○) 30  $\mu\text{M}$  Ox with STS.

(B) Combined data are presented as mean  $\pm$  standard deviation (n=6-16). The *P* value in the figure is for overall difference between groups by one-way ANOVA test. \*\*  $P < 0.01$ , \*\*\*  $P < 0.001$  compared to untreated control; #  $P < 0.05$ , ##  $P < 0.01$  compared to oxaliplatin alone (Tukey's multiple comparison post-tests following one-way ANOVA).



Neuronal cell body area ( $\mu\text{m}^2$ )

**Figure 5.3. Sodium thiosulfate protected cultured DRG neurons from cell body atrophy induced by oxaliplatin.**

DRG cells were harvested from two rats for each experiment and cultured for three days before experiments. Then they were continuously exposed to 10 or 30  $\mu\text{M}$  oxaliplatin (Ox) with or without 8 mM sodium thiosulfate (STS) for two days. Two independent experiments were conducted (A and B). In each experiment, a total of 269-294 neurons from two culture wells for each treatment condition were measured for cell body areas. Then the data from individual experiments were combined to achieve a group size of  $n=563-570$  (C).

Data show that sodium thiosulfate protected cultured DRG neurons from cell body atrophy induced by oxaliplatin.

Data are presented as frequency histograms with bin width of  $50 \mu\text{m}^2$  and box-and-whiskers plots indicating the median value (vertical line across the box), interquartile range (box) and range (whiskers). *P* values in the figure are for overall difference between groups by Kruskal-Wallis test. \*\*\*  $P < 0.001$  compared to untreated control; ###  $P < 0.001$  compared to oxaliplatin alone (Dunn's multiple comparison post-tests following Kruskal-Wallis test).

(median: 257  $\mu\text{m}^2$ , interquartile range: 214-321  $\mu\text{m}^2$ ,  $P<0.001$ ) of control, respectively. In contrast, with co-incubation with sodium thiosulfate (8 mM), median neuronal cell body areas were similar to those from untreated controls and higher than those achieved by oxaliplatin alone. With concurrent sodium thiosulfate treatment, median neuronal cell body areas were 100.8% (median: 355  $\mu\text{m}^2$ , interquartile range: 288-448  $\mu\text{m}^2$ ,  $P<0.001$ ) and 100.9% (median: 356  $\mu\text{m}^2$ , interquartile range: 287-440  $\mu\text{m}^2$ ,  $P<0.001$ ) of control at oxaliplatin concentrations of 10 and 30  $\mu\text{M}$ , respectively.

Taken together, the results showed that sodium thiosulfate reduced platinum binding to DNA, and protected cultured rat DRG cells from both inhibition of nascent RNA synthesis and neuronal cell body shrinkage induced by oxaliplatin.

### **5.2.2. Cimetidine**

To investigate protective effects of cimetidine against oxaliplatin toxicity in cultured rat DRG cells, amounts of platinum binding to DNA were measured at four hours, and levels of RNA-incorporated [ $^3\text{H}$ ]uridine and neuronal cell body areas were measured at one day, after the start of a 3-h exposure to oxaliplatin (30 or 100  $\mu\text{M}$ ) with or without cimetidine (1 mM).

Data showed that levels of platinum-DNA damage in oxaliplatin-treated cultured DRG cells were reduced by concurrent cimetidine treatment (Figure 5.4). Four hours after the start of a 3-h exposure to 100  $\mu\text{M}$  oxaliplatin alone, the level of platinum binding to DNA was  $0.0379 \pm 0.0066$  ng/ $\mu\text{g}$  DNA. In contrast, co-incubation of cimetidine (1 mM) with oxaliplatin significantly reduced the level of DNA-bound platinum to 54.3% ( $0.0206 \pm 0.0027$  ng/ $\mu\text{g}$  DNA,  $P<0.001$ ) of the level achieved with oxaliplatin alone.



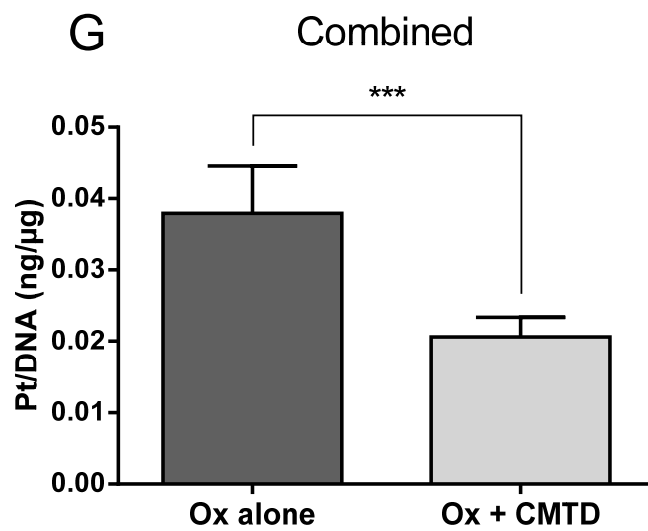
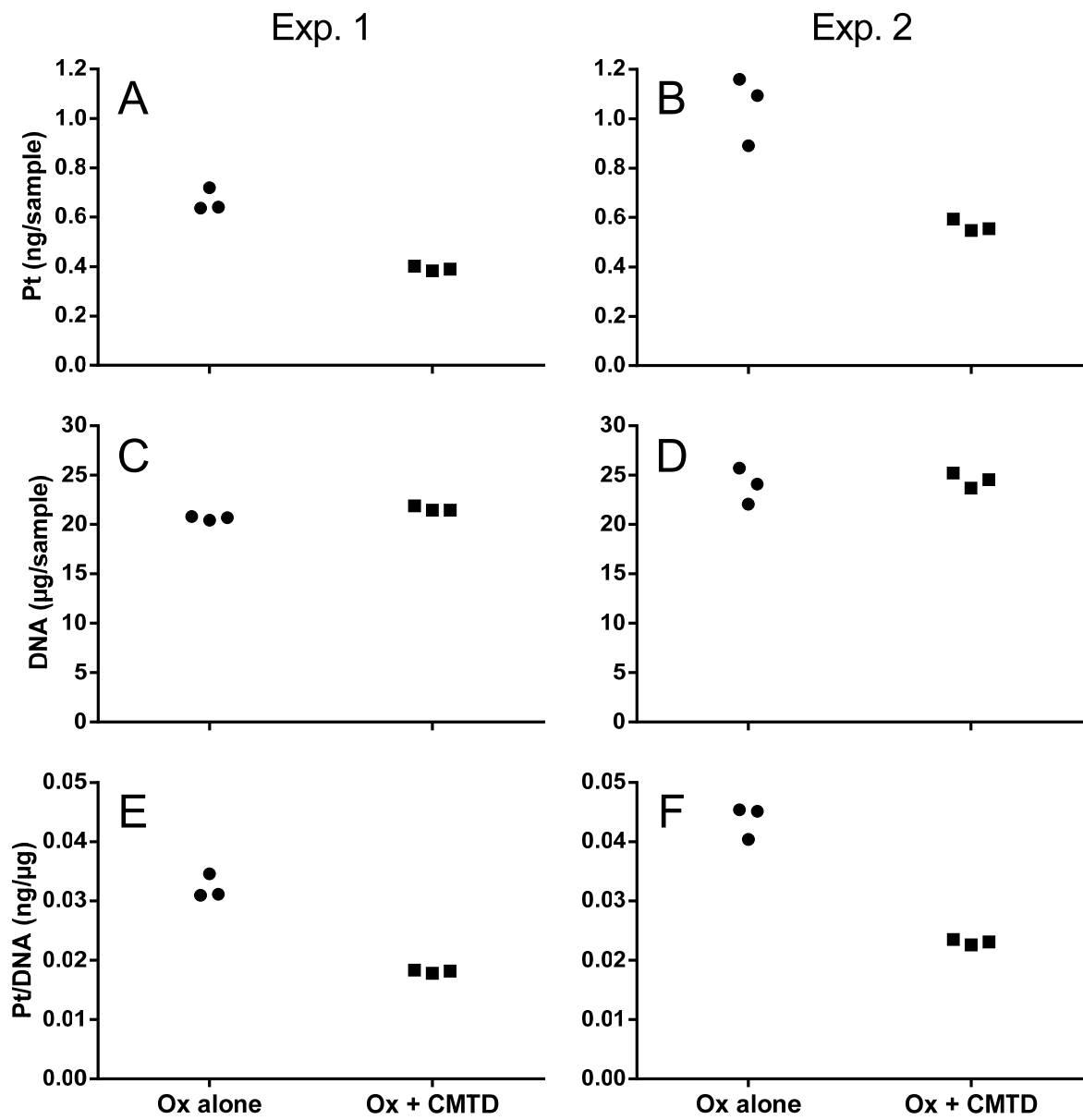


**Figure 5.4. Cimetidine reduced platinum binding to the DNA of cultured DRG cells after exposure to oxaliplatin.**

DRG cells were harvested from 10 rats for each experiment and cultured for three days before experiments. Then they were exposed to 100  $\mu$ M oxaliplatin (Ox) with or without 1 mM cimetidine (CMTD) for 3 h, followed by culture in drug-free medium until 4 h after the start of treatment. Two independent experiments were conducted (experiment 1: A, C and E; experiment 2: B, D and F). In each experiment, three culture wells for each treatment condition were independently assayed for platinum (A and B) and DNA content (C and D), followed by calculation of platinum content per DNA content (E and F). Then the data from individual experiments for platinum content per DNA content (E and F) were combined (G).

Data show that cimetidine reduced platinum binding to the DNA of cultured DRG cells after exposure to oxaliplatin, without any apparent effect on the DNA content.

(A-F) (●) Ox alone, (■) Ox with CMTD.

(G) Combined data are presented as mean  $\pm$  standard deviation (n=6). \*\*\*  $P < 0.001$  indicates the statistical significance of difference compared to oxaliplatin alone assessed by unpaired t-test.

Co-incubation with cimetidine also partially protected cultured DRG cells against oxaliplatin-induced inhibition of nascent RNA synthesis (Figure 5.5). Compared to untreated controls ( $100 \pm 37.9\%$ ), levels of RNA-incorporated [ $^3\text{H}$ ]uridine were reduced one day after a 3-h exposure to 30 and 100  $\mu\text{M}$  oxaliplatin without cimetidine to  $42.5 \pm 12.5\%$  ( $P < 0.001$ ) and  $23.2 \pm 3.4\%$  ( $P < 0.001$ ) of control, respectively. In contrast, when oxaliplatin was co-incubated with cimetidine (1 mM), the levels of RNA-incorporated [ $^3\text{H}$ ]uridine appeared higher compared to those achieved with oxaliplatin alone. Compared to oxaliplatin treatment alone, levels of RNA-incorporated [ $^3\text{H}$ ]uridine one day after a 3-h exposure to 30 and 100  $\mu\text{M}$  oxaliplatin concurrently with cimetidine were  $49.6 \pm 11.5\%$  ( $P > 0.05$ ) and  $46.0 \pm 15.6\%$  ( $P < 0.001$ ) of control, respectively.

Concurrent cimetidine treatment also partially prevented the induction of cell body atrophy in cultured DRG neurons by oxaliplatin (Figure 5.6). One day after a 3-h exposure to oxaliplatin (30 or 100  $\mu\text{M}$ ), DRG neuronal cell body area distribution profiles were shifted to lower values, but this effect was partially prevented by the addition of cimetidine (1 mM). Compared with untreated controls (median:  $324 \mu\text{m}^2$ , interquartile range:  $261\text{-}398 \mu\text{m}^2$ ), median neuronal cell body areas were significantly reduced by 30 and 100  $\mu\text{M}$  oxaliplatin alone to 89.7% (median:  $291 \mu\text{m}^2$ , interquartile range:  $237\text{-}354 \mu\text{m}^2$ ,  $P < 0.001$ ) and 79.4% (median:  $258 \mu\text{m}^2$ , interquartile range:  $211\text{-}312 \mu\text{m}^2$ ,  $P < 0.001$ ) of control, respectively. In contrast, with co-incubation with cimetidine (1 mM), median neuronal cell body areas were higher than those achieved by oxaliplatin alone. With concurrent cimetidine treatment, median neuronal cell body areas were 92.9% (median:  $301 \mu\text{m}^2$ , interquartile range:  $241\text{-}371 \mu\text{m}^2$ ,  $P < 0.05$ ) and 86.3% (median:  $280 \mu\text{m}^2$ , interquartile range:  $229\text{-}344 \mu\text{m}^2$ ,  $P < 0.001$ ) of control at oxaliplatin concentrations of 30 and 100  $\mu\text{M}$ , respectively.

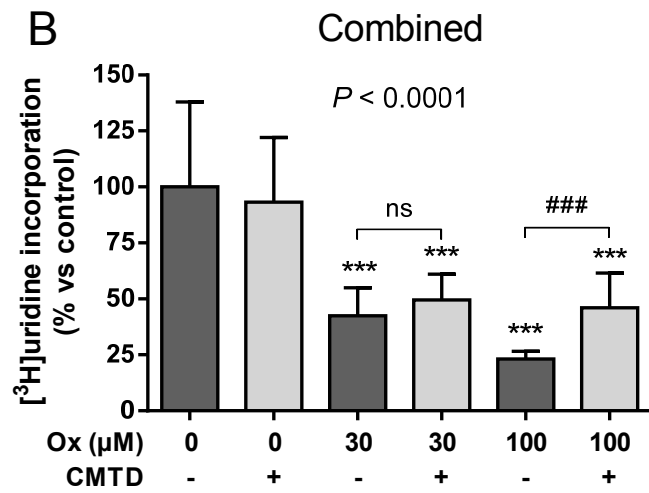
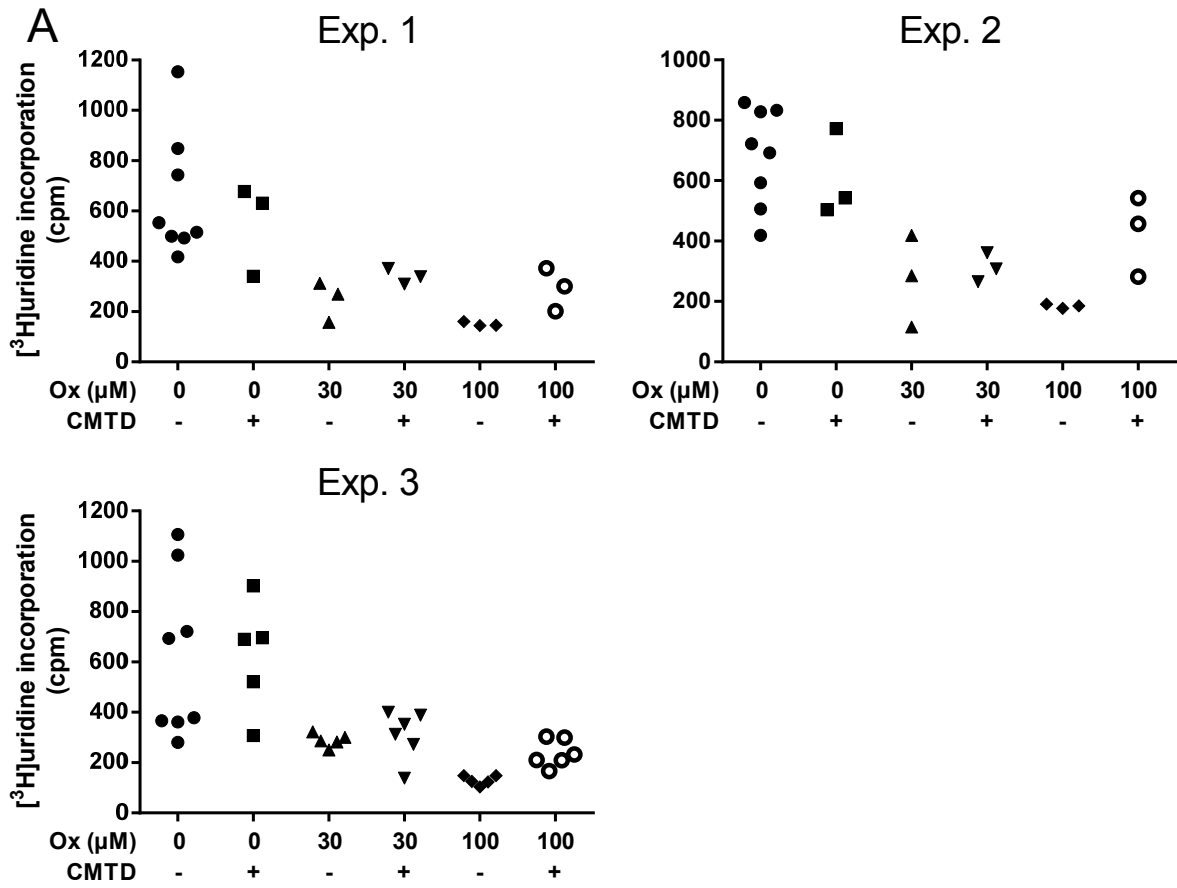


**Figure 5.5. Cimetidine partially protected cultured DRG cells from inhibition of nascent RNA synthesis induced by oxaliplatin.**

DRG cells were harvested from two to three rats for each experiment and cultured for three days before experiments. Then they were exposed to 30 or 100  $\mu\text{M}$  oxaliplatin (Ox) with or without 1 mM cimetidine (CMTD) for 3 h, followed by culture in drug-free medium for a further one day. Three independent experiments were conducted (A). In each experiment, between three to eight culture wells for each treatment condition were independently studied for levels of RNA-incorporated [ $^3\text{H}$ ]uridine. Then the data from individual experiments were combined after normalization to the mean value of their respective untreated controls (B).

Data show that cimetidine partially protected cultured DRG cells from inhibition of nascent RNA synthesis induced by oxaliplatin.

(A) (●) Untreated control, (■) CMTD alone, (▲) 30  $\mu\text{M}$  Ox, (▼) 30  $\mu\text{M}$  Ox with CMTD, (◆) 100  $\mu\text{M}$  Ox, (○) 100  $\mu\text{M}$  Ox with CMTD.

(B) Combined data are presented as mean  $\pm$  standard deviation (n=11-24). The *P* value in the figure is for overall difference between groups by one-way ANOVA test. \*\*\* *P*<0.001 compared to untreated control (Tukey's multiple comparison post-tests following one-way ANOVA). ### *P*<0.001 compared to oxaliplatin alone; ns, not significant (unpaired t-test).

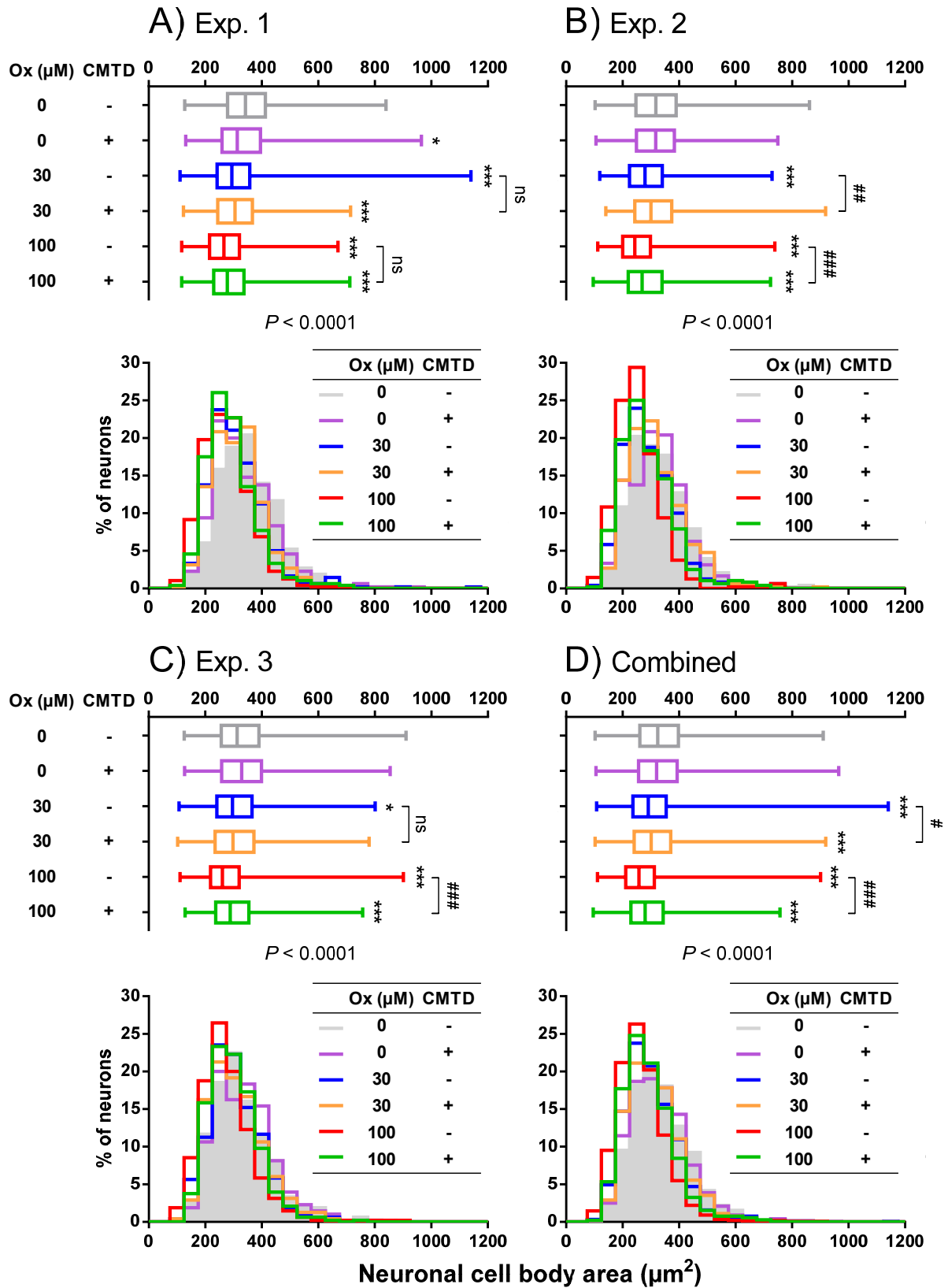


**Figure 5.6. Cimetidine partially protected cultured DRG neurons from cell body atrophy induced by oxaliplatin.**

DRG cells were harvested from two to three rats for each experiment and cultured for three days before experiments. Then they were exposed to 30 or 100  $\mu\text{M}$  oxaliplatin (Ox) with or without 1 mM cimetidine (CMTD) for 3 h, followed by culture in drug-free medium for a further one day. Three independent experiments were conducted (A-C). In each experiment, a total of 480 neurons from three culture wells for each treatment condition were measured for cell body areas. Then the data from individual experiments were combined to achieve a group size of  $n=1440$  (D).

Data show that cimetidine partially protected cultured DRG neurons from cell body atrophy induced by oxaliplatin.

Data are presented as frequency histograms with bin width of  $50 \mu\text{m}^2$  and box-and-whiskers plots indicating the median value (vertical line across the box), interquartile range (box) and range (whiskers).  $P$  values in the figure are for overall difference between groups by Kruskal-Wallis test. \*  $P<0.05$ , \*\*\*  $P<0.001$  compared to untreated control; #  $P<0.05$ , ##  $P<0.01$ , ###  $P<0.001$  compared to oxaliplatin alone; ns, not significant (Dunn's multiple comparison post-tests following Kruskal-Wallis test).

Taken together, the results showed that cimetidine reduced platinum binding to DNA, and partially protected cultured rat DRG cells from both inhibition of nascent RNA synthesis and neuronal cell body shrinkage induced by oxaliplatin.

### **5.2.3. DNA-dependent protein kinase (DNA-PK) inhibition**

The effects of DNA-PK inhibitors, wortmannin and NU 7026, on oxaliplatin-induced inhibition of nascent RNA synthesis in cultured DRG cells were studied. Levels of RNA-incorporated [<sup>3</sup>H]uridine were measured one day after a 3-h exposure to oxaliplatin (30 or 100 μM) with or without a 1-h pre-treatment of wortmannin (100 nM) or NU 7026 (10 μM). Data showed no effects of wortmannin or NU 7026 on oxaliplatin-induced inhibition of nascent RNA synthesis (Figure 5.7). Compared with untreated controls (582.5 ± 150.2 cpm), levels of RNA-incorporated [<sup>3</sup>H]uridine were decreased similarly by wortmannin pre-treatment before oxaliplatin versus oxaliplatin alone (30 μM oxaliplatin: 144.3 ± 25.7 cpm versus 171.7 ± 29.2 cpm, *P*>0.05; 100 μM oxaliplatin: 61.3 ± 23.2 cpm versus 95.7 ± 23.4 cpm, *P*>0.05). Compared with untreated controls (284.1 ± 50.8 cpm), levels of RNA-incorporated [<sup>3</sup>H]uridine were decreased similarly by NU 7026 pre-treatment before oxaliplatin versus oxaliplatin alone (30 μM oxaliplatin: 236.7 ± 25.0 cpm versus 171.3 ± 34.3 cpm, *P*>0.05; 100 μM oxaliplatin: 112.3 ± 34.0 cpm versus 119.3 ± 10.7 cpm, *P*>0.05).

### **5.2.4. Poly(ADP-ribose) polymerase 1 (PARP-1) inhibition**

The effects of PARP-1 inhibitors, benzamide and olaparib, on oxaliplatin-induced inhibition of nascent RNA synthesis in cultured DRG cells were studied. Levels of RNA-incorporated [<sup>3</sup>H]uridine were measured one day after a 3-h exposure to oxaliplatin (30 or 100 μM) with or without a 1-h pre-treatment of benzamide (200 μM) or olaparib (1 μM). Data showed no



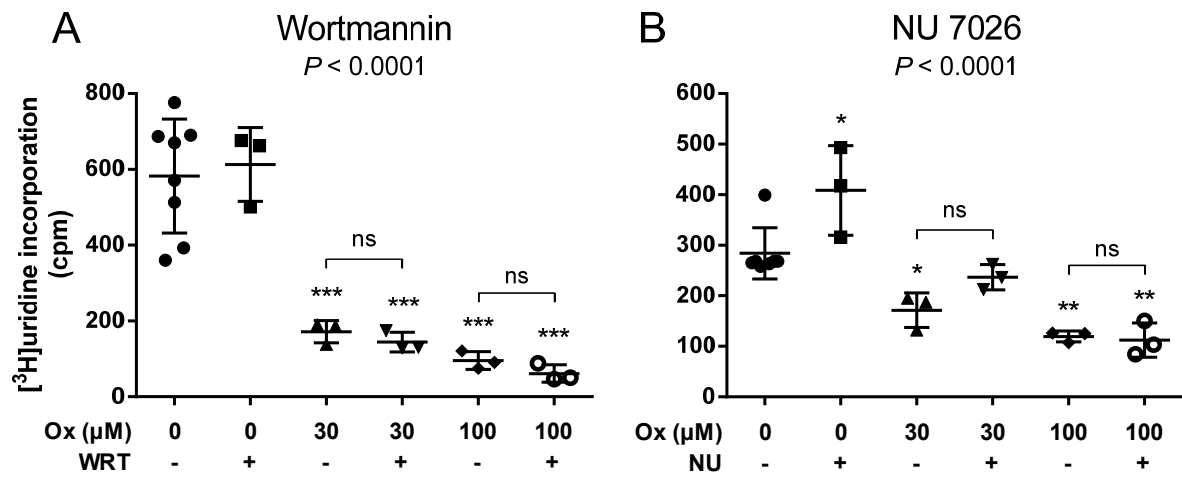


**Figure 5.7. Lack of effect of DNA-PK inhibitors on oxaliplatin-induced inhibition of nascent RNA synthesis in cultured DRG cells.**

DRG cells were harvested from two to three rats for each experiment and cultured for three days before experiments. Then they were pre-treated with or without wortmannin (WRT, 100 nM) (A) or NU 7026 (NU, 10  $\mu$ M) (B) for 1 h before exposure to oxaliplatin (Ox, 30 or 100  $\mu$ M) for 3 h, followed by culture in drug-free medium for a further one day. In each experiment, between three to eight culture wells for each treatment condition were independently studied for levels of RNA-incorporated [ $^3$ H]uridine.

Data show that DNA-PK inhibitors had no effect on oxaliplatin-induced inhibition of nascent RNA synthesis in cultured DRG cells.

(A) (●) Untreated control, (■) WRT alone, (▲) 30  $\mu$ M Ox, (▼) 30  $\mu$ M Ox with WRT, (◆) 100  $\mu$ M Ox, (○) 100  $\mu$ M Ox with WRT.

(B) (●) Untreated control, (■) NU alone, (▲) 30  $\mu$ M Ox, (▼) 30  $\mu$ M Ox with NU, (◆) 100  $\mu$ M Ox, (○) 100  $\mu$ M Ox with NU.

The horizontal lines represent mean  $\pm$  standard deviation. *P* values in the figures are for overall difference between groups by one-way ANOVA test. \* *P*<0.05, \*\* *P*<0.01, \*\*\* *P*<0.001 compared to untreated control; ns, no significant difference compared to oxaliplatin alone (Tukey's multiple comparison post-tests following one-way ANOVA).

effects of benzamide or olaparib on oxaliplatin-induced inhibition of nascent RNA synthesis (Figure 5.8). Compared with untreated controls ( $582.5 \pm 150.2$  cpm), levels of RNA-incorporated [ $^3\text{H}$ ]uridine were decreased similarly by benzamide pre-treatment before oxaliplatin versus oxaliplatin alone (30  $\mu\text{M}$  oxaliplatin:  $158.0 \pm 10.6$  cpm versus  $171.7 \pm 29.2$  cpm,  $P>0.05$ ; 100  $\mu\text{M}$  oxaliplatin:  $87.3 \pm 9.7$  cpm versus  $95.7 \pm 23.4$  cpm,  $P>0.05$ ). Compared with untreated controls ( $474.7 \pm 94.4$  cpm), levels of RNA-incorporated [ $^3\text{H}$ ]uridine were decreased similarly by olaparib pre-treatment before oxaliplatin versus oxaliplatin alone (30  $\mu\text{M}$  oxaliplatin:  $270.0 \pm 19.0$  cpm versus  $296.7 \pm 22.8$  cpm,  $P>0.05$ ; 100  $\mu\text{M}$  oxaliplatin:  $127.0 \pm 14.4$  cpm versus  $178.0 \pm 30.2$  cpm,  $P>0.05$ ).

#### **5.2.5. $\text{K}^+$ channel blockade**

The effects of  $\text{K}^+$  channel blockers, tetraethylammonium chloride (TEA) and elevated extracellular  $\text{K}^+$ , on oxaliplatin-induced cell body atrophy in cultured DRG neurons were studied. Neuronal cell body areas were measured after one day of continuous exposure to oxaliplatin (10 or 30  $\mu\text{M}$ ) with or without TEA (10 mM) or elevated extracellular  $\text{K}^+$  (25 mM). Data showed no effects of TEA or elevated extracellular  $\text{K}^+$  on oxaliplatin-induced neuronal cell body atrophy (Figure 5.9). Compared with untreated controls (median:  $388 \mu\text{m}^2$ , interquartile range:  $320\text{-}477 \mu\text{m}^2$ ), neuronal cell body areas were reduced similarly by treatment with TEA plus oxaliplatin versus oxaliplatin alone (10  $\mu\text{M}$  oxaliplatin: 330 versus  $331 \mu\text{m}^2$ ,  $P>0.05$ ; 30  $\mu\text{M}$  oxaliplatin: 311 versus  $300 \mu\text{m}^2$ ,  $P>0.05$ ). Compared with untreated controls (median:  $381 \mu\text{m}^2$ , interquartile range:  $317\text{-}467 \mu\text{m}^2$ ), neuronal cell body areas were reduced similarly by treatment with elevated extracellular  $\text{K}^+$  plus oxaliplatin versus oxaliplatin alone (296 versus  $311 \mu\text{m}^2$ ,  $P>0.05$ ).

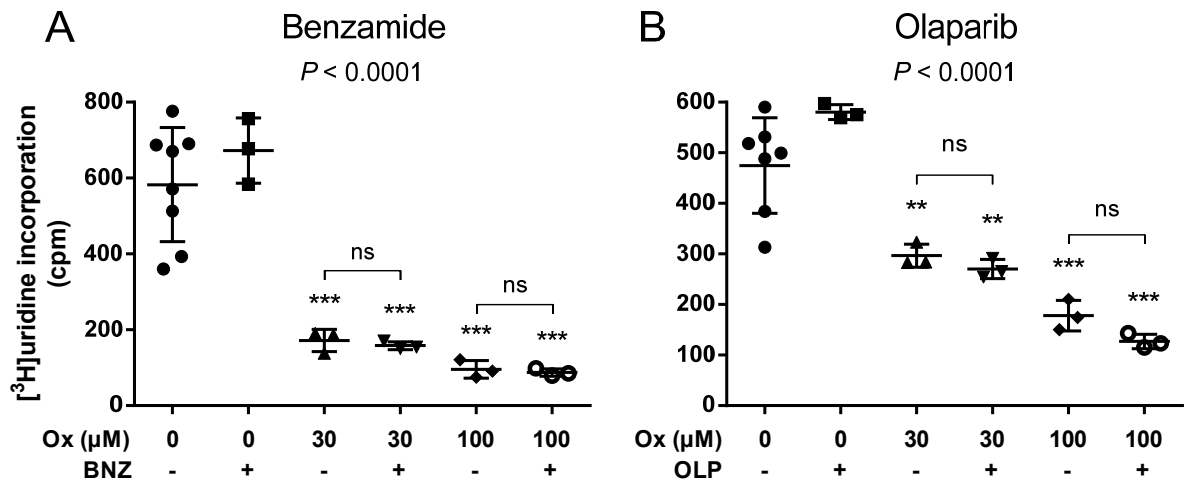


**Figure 5.8. Lack of effect of PARP-1 inhibitors on oxaliplatin-induced inhibition of nascent RNA synthesis in cultured DRG cells.**

DRG cells were harvested from two to three rats for each experiment and cultured for three days before experiments. Then they were pre-treated with or without benzamide (BNZ, 200  $\mu$ M) (A) or olaparib (OLP, 1  $\mu$ M) (B) for 1 h before exposure to oxaliplatin (Ox, 30 or 100  $\mu$ M) for 3 h, followed by culture in drug-free medium for a further one day. In each experiment, between three to eight culture wells for each treatment condition were independently studied for levels of RNA-incorporated [ $^3$ H]uridine.

Data show that PARP-1 inhibitors had no effect on oxaliplatin-induced inhibition of nascent RNA synthesis in cultured DRG cells.

(A) (●) Untreated control, (■) BNZ alone, (▲) 30  $\mu$ M Ox, (▼) 30  $\mu$ M Ox with BNZ, (◆) 100  $\mu$ M Ox, (○) 100  $\mu$ M Ox with BNZ.

(B) (●) Untreated control, (■) OLP alone, (▲) 30  $\mu$ M Ox, (▼) 30  $\mu$ M Ox with OLP, (◆) 100  $\mu$ M Ox, (○) 100  $\mu$ M Ox with OLP.

The horizontal lines represent mean  $\pm$  standard deviation. *P* values in the figures are for overall difference between groups by one-way ANOVA test. \*\* *P*<0.01, \*\*\* *P*<0.001 compared to untreated control; ns, no significant difference compared to oxaliplatin alone (Tukey's multiple comparison post-tests following one-way ANOVA).

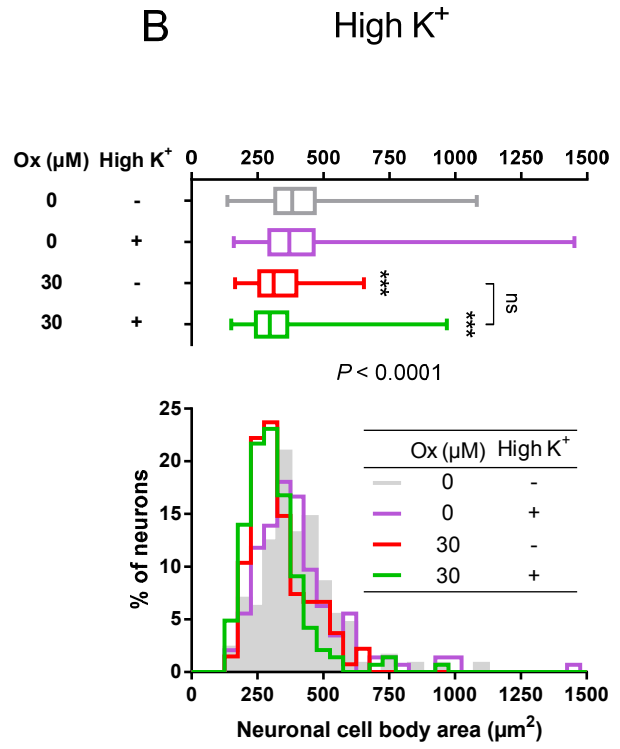
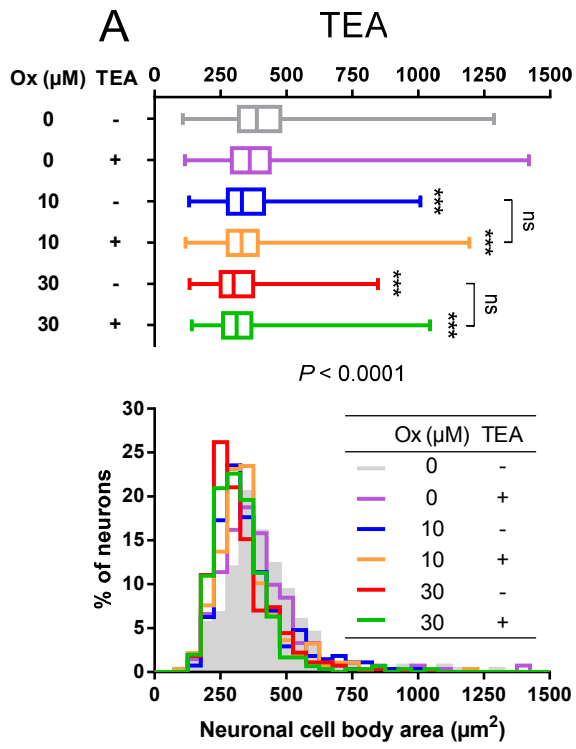


**Figure 5.9. Lack of effect of K<sup>+</sup> channel blockers on oxaliplatin-induced cell body atrophy in cultured DRG neurons.**

DRG cells were harvested from two rats for each experiment and cultured for three days before experiments. Then they were continuously exposed to oxaliplatin (Ox, 10 or 30  $\mu\text{M}$ ) with or without tetraethylammonium chloride (TEA, 10 mM) (A) or elevated extracellular K<sup>+</sup> (High K<sup>+</sup>, 25 mM) (B) for one day. A total of 268-301 neurons from two culture wells (A) or 129-144 neurons from one culture well (B) for each treatment condition were measured for cell body areas.

Data show that K<sup>+</sup> channel blockers had no effect on oxaliplatin-induced cell body atrophy in cultured DRG neurons.

Data are presented as frequency histograms with bin width of 50  $\mu\text{m}^2$  and box-and-whiskers plots indicating the median value (vertical line across the box), interquartile range (box) and range (whiskers). *P* values in the figure are for overall difference between groups by Kruskal-Wallis test. \*\*\* *P*<0.001 compared to untreated control; ns, no significant difference compared to oxaliplatin alone (Dunn's multiple comparison post-tests following Kruskal-Wallis test).

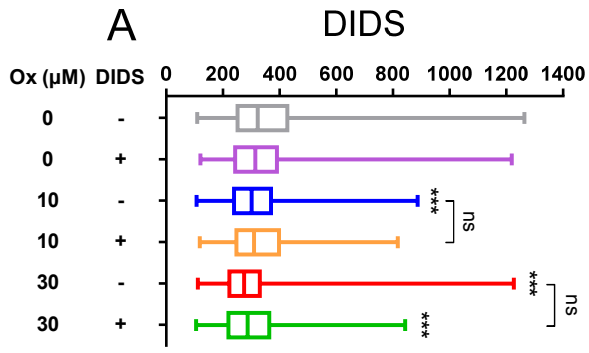
### 5.2.6. Cl<sup>-</sup> channel blockade

The effects of Cl<sup>-</sup> channel blockers, 4,4'-diisothiocyanatostilbene-2,2'-disulfonic acid (DIDS) and 5-nitro-2-(3-phenylpropylamino)benzoic acid (NPPB), on oxaliplatin-induced cell body atrophy in cultured DRG neurons were studied. Neuronal cell body areas were measured after one day of continuous exposure to oxaliplatin (10 or 30  $\mu\text{M}$ ) with or without DIDS (500  $\mu\text{M}$ ) or NPPB (100  $\mu\text{M}$ ). Data showed no effects of DIDS or NPPB on oxaliplatin-induced neuronal cell body atrophy (Figure 5.10). Compared with untreated controls (median: 323  $\mu\text{m}^2$ , interquartile range: 252-427  $\mu\text{m}^2$ ), neuronal cell body areas were reduced similarly by treatment with DIDS plus oxaliplatin versus oxaliplatin alone (10  $\mu\text{M}$  oxaliplatin: 310 versus 302  $\mu\text{m}^2$ ,  $P>0.05$ ; 30  $\mu\text{M}$  oxaliplatin: 288 versus 275  $\mu\text{m}^2$ ,  $P>0.05$ ). Compared with untreated controls (median: 305  $\mu\text{m}^2$ , interquartile range: 248-389  $\mu\text{m}^2$ ), neuronal cell body areas were reduced similarly by treatment with NPPB plus oxaliplatin versus oxaliplatin alone (10  $\mu\text{M}$  oxaliplatin: 264 versus 278  $\mu\text{m}^2$ ,  $P<0.05$ ; 30  $\mu\text{M}$  oxaliplatin: 220 versus 234  $\mu\text{m}^2$ ,  $P>0.05$ ).

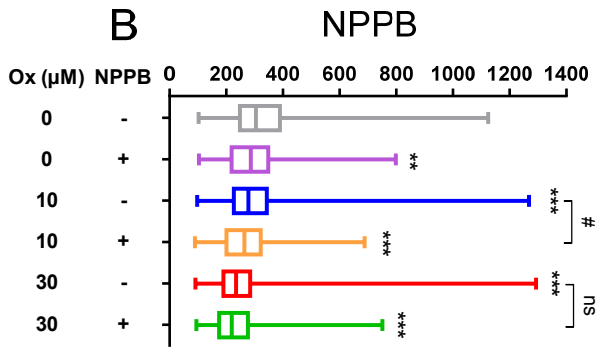
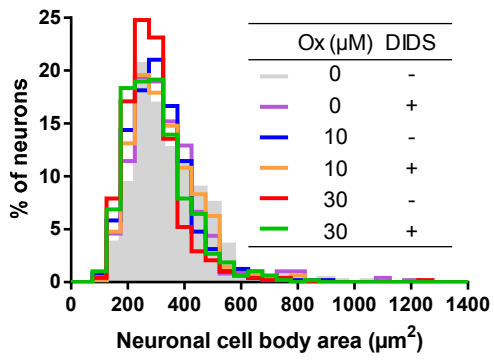
## 5.3. Discussion

The current study has suggested that platinum-DNA damage may be critically involved in mechanisms of oxaliplatin-induced DRG neuronal cell body atrophy and peripheral neurotoxicity by inducing transcriptional inhibition. Furthermore, this study showed that limiting platinum-DNA damage may reduce oxaliplatin-induced neuronal atrophy and peripheral neurotoxicity. Both sodium thiosulfate and cimetidine reduced the amount of platinum binding to DNA in cultured DRG cells, and protected them from both the inhibition of nascent RNA synthesis and neuronal cell body shrinkage, induced by oxaliplatin. Moreover, as shown in the previous chapter, binding of oxaliplatin-derived platinum to the





$P < 0.0001$



$P < 0.0001$

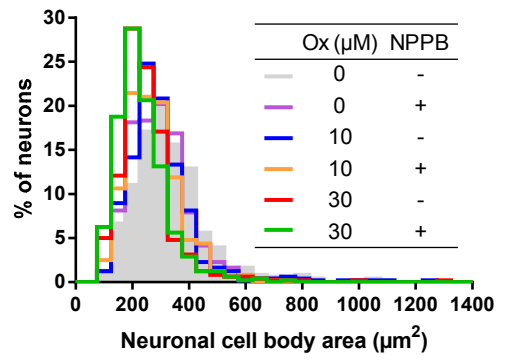


**Figure 5.10. Lack of effect of Cl<sup>-</sup> channel blockers on oxaliplatin-induced cell body atrophy in cultured DRG neurons.**

DRG cells were harvested from two rats for each experiment and cultured for three days before experiments. Then they were continuously exposed to oxaliplatin (Ox, 10 or 30  $\mu\text{M}$ ) with or without 4,4'-diisothiocyanatostilbene-2,2'-disulfonic acid (DIDS, 500  $\mu\text{M}$ ) (A) or 5-nitro-2-(3-phenylpropylamino)benzoic acid (NPPB, 100  $\mu\text{M}$ ) (B) for one day. In each experiment, a total of 480 neurons from three culture wells for each treatment condition were measured for cell body areas.

Data show that Cl<sup>-</sup> channel blockers had no effect on oxaliplatin-induced cell body atrophy in cultured DRG neurons.

Data are presented as frequency histograms with bin width of 50  $\mu\text{m}^2$  and box-and-whiskers plots indicating the median value (vertical line across the box), interquartile range (box) and range (whiskers). *P* values in the figure are for overall difference between groups by Kruskal-Wallis test. \*\* *P*<0.01, \*\*\* *P*<0.001 compared to untreated control; # *P*<0.05 compared to oxaliplatin alone; ns, not significant (Dunn's multiple comparison post-tests following Kruskal-Wallis test).

DNA of cultured DRG cells appeared to have occurred before the induction of inhibition of nascent RNA synthesis and depletion of total RNA content. Oxaliplatin-induced neuronal cell body shrinkage appeared delayed until after the occurrence of binding of platinum to DNA and inhibition of transcription. Taken together, these findings suggested that mechanisms of oxaliplatin-induced neuronal cell body atrophy and peripheral neurotoxicity may critically involve platinum-DNA damage and its induction of transcriptional inhibition. Minimizing platinum-DNA damage in DRG neurons occurring during exposure to chemotherapy drugs may therefore be a useful strategy for protecting against chemotherapy-induced peripheral neurotoxicity.

The findings described in this chapter have suggested that sodium thiosulfate prevented oxaliplatin neurotoxicity by lessening platinum-DNA damage in DRG neurons. Concurrent sodium thiosulfate treatment reduced DNA-bound platinum to undetectable levels in oxaliplatin-treated cultured DRG cells, and protected them from both inhibition of nascent RNA synthesis and neuronal cell body atrophy. As a reactive thiol compound, sodium thiosulfate has been previously shown to bind to and inactivate the electrophilic platinum-based anticancer drugs, at high molar excess (Iwamoto et al., 1985, Nagai et al., 1995, Sooriyaarachchi et al., 2012). Therefore, the decreased levels of platinum-DNA damage and oxaliplatin neurotoxicity caused by concurrent sodium thiosulfate treatment observed in this study may be due to decreased active platinum compounds being available for binding to the DNA of DRG neurons. A major concern with regards to the clinical use of sodium thiosulfate as a protective agent against oxaliplatin-induced neurotoxicity is the potential attenuation of antitumor efficacy of oxaliplatin, which is also thought to critically involve binding of oxaliplatin-derived platinum to DNA (Di Francesco et al., 2002). Some studies have reported a neutralizing effect of sodium thiosulfate on antitumor efficacy of platinum drugs (Catino et

al., 1986). However, separating oxaliplatin and sodium thiosulfate by time and/or route of administration could minimize the unwanted interactions between them and therefore provide neuroprotection against oxaliplatin without compromising the antitumor efficacy. Post-treatment of sodium thiosulfate after cisplatin has been shown to protect cisplatin-induced ototoxicity without interfering with antitumor activity (Harned et al., 2008). The efficacy of carboplatin chemotherapy was also maintained with sodium thiosulfate protection by temporal and spatial separation of the thiol from platinum (Muldoon et al., 2000, Neuwelt et al., 2004, Neuwelt et al., 2006). However, the use of sodium thiosulfate after oxaliplatin treatment was not investigated in the current study or elsewhere as far as we are aware, but could be a topic of future work.

The findings described in this chapter have also suggested that cimetidine protected against oxaliplatin neurotoxicity by reducing platinum-DNA damage in DRG neurons. Concurrent cimetidine treatment almost halved the level of DNA-bound platinum in oxaliplatin-treated cultured DRG cells, and partially protected them from both inhibition of nascent RNA synthesis and neuronal cell body atrophy. Cimetidine is a known substrate and inhibitor of organic cation transporter 2 (OCT2), which competes with platinum drugs for OCT2-mediated cellular uptake (Burger et al., 2011, Ciarimboli, 2012, 2014). Therefore, the decreased levels of platinum-DNA damage and oxaliplatin neurotoxicity caused by concurrent cimetidine treatment observed in this study may be due to decreased cellular platinum accumulation induced by OCT2 inhibition. As for sodium thiosulfate, a major concern with regards to the clinical use of cimetidine as a protective agent against oxaliplatin neurotoxicity is the potential reduction of the antitumor efficacy. However, the differential expression of OCT2 between tumour and DRG tissues provides the possibility of selective treatment for oxaliplatin neurotoxicity without affecting antitumor potency. One study has

demonstrated OCT2 protein and mRNA expression in DRG tissues (Sprowl et al., 2013). On the other hand, OCT2 expression in colorectal tumour samples and cell lines were undetectable (Filipski et al., 2009, Burger et al., 2010a, Franke et al., 2010, Sprowl et al., 2013). Importantly, cimetidine has been shown to protect against cisplatin-induced nephrotoxicity without any influence on the antitumor activity of cisplatin (Katsuda et al., 2010). Collectively, these findings suggested that cimetidine may prevent oxaliplatin neurotoxicity by lessening platinum-DNA damage in DRG neurons, probably without interfering with antitumor efficacy.

This study has suggested that DNA-dependent protein kinase (DNA-PK) and poly(ADP-ribose) polymerase 1 (PARP-1) may not be critically involved in the mechanism of oxaliplatin toxicity in cultured DRG cells, at least under the experimental conditions used in this study. Two DNA-PK inhibitors, wortmannin and NU 7026, and two PARP-1 inhibitors, benzamide and olaparib, were studied for their effects on oxaliplatin-induced inhibition of nascent RNA synthesis in cultured DRG cells, but none of them showed any alteration of effects of oxaliplatin. This study has also suggested that apoptotic volume decrease may not be involved in oxaliplatin toxicity in cultured DRG cells, at least under the experimental conditions used in this study. Two K<sup>+</sup> channel blockers, tetraethylammonium chloride (TEA) and elevated extracellular K<sup>+</sup>, and two Cl<sup>-</sup> channel blockers, 4,4'-diisothiocyanatostilbene-2,2'-disulfonic acid (DIDS) and 5-nitro-2-(3-phenylpropylamino)benzoic acid (NPPB), were studied for their effects on oxaliplatin-induced DRG neuronal cell body atrophy, but none of them showed any alteration of effects of oxaliplatin. In addition, as shown in Chapter 4, no evident apoptosis was shown in oxaliplatin-treated DRG neurons by using TUNEL staining.

In conclusion, the findings presented in this chapter have suggested that platinum-DNA damage may be critically involved in mechanisms of oxaliplatin-induced DRG neuronal cell

body atrophy and peripheral neurotoxicity by inducing transcriptional inhibition. Limiting platinum-DNA damage in DRG neurons may be a potential therapeutic strategy for protecting against oxaliplatin-induced neuronal cell body atrophy and peripheral neurotoxicity.

# Chapter 6. Comparative effects of different platinum drugs on cultured rat DRG cells

## 6.1. Introduction

Platinum-based anticancer drugs have been widely used for the treatment of a variety of cancers. Cisplatin is currently used to treat testicular, head and neck, ovarian, cervical, bladder, non-small cell lung and small cell lung cancer, and melanomas, lymphomas and myelomas (Windebank and Grisold, 2008, Wheate et al., 2010). Particularly, since the introduction of cisplatin treatment, mortality of testicular cancer has been dramatically reduced from 90% at 5 years to a cure rate of more than 80% (Windebank and Grisold, 2008, Wheate et al., 2010). Carboplatin has a similar anticancer spectrum as cisplatin, and is now the drug of choice for the treatment of ovarian cancer, in preference to cisplatin (Wheate et al., 2010). Oxaliplatin has been regarded as one of the most important chemotherapeutic drugs used for the clinical treatment of colorectal cancer (Stein and Arnold, 2012). Ormaplatin was selected for clinical development due to its antitumor activity against leukaemia, ovarian cancer, melanoma, myeloma and mammary cancers *in vitro* and *in vivo* (Luo et al., 1999, Wheate et al., 2010). However, the clinical application of platinum-based anticancer drugs can be limited by peripheral neurotoxicity. Interestingly, some platinum-based anticancer drugs cause frequent or severe peripheral neurotoxicity in cancer patients, while others are associated with infrequent or mild symptoms (Screnci et al., 2000). Peripheral neurotoxicity is a major dose-limiting side effect of cisplatin (Mollman, 1990, Siegal and Haim, 1990, Cavaletti et al., 1992a), and affects approximately 50% of patients treated with cisplatin (van der Hoop et al., 1990). Peripheral neurotoxicity is also a common dose-limiting side effect of

oxaliplatin (Grothey, 2003, Cersosimo, 2005, Pasetto et al., 2006), and develops in almost all the patients receiving oxaliplatin treatment (Machover et al., 1996). As with cisplatin and oxaliplatin, the dose-limiting side effect associated with ormaplatin is peripheral neurotoxicity. However, because the neurotoxicity of ormaplatin is severe and poorly reversible, the clinical development of ormaplatin was abandoned during phase I clinical trials (O'Rourke et al., 1994, Schilder et al., 1994). In contrast, carboplatin administration is less likely to cause peripheral neurotoxicity than cisplatin, oxaliplatin and ormaplatin (Canetta et al., 1985, McKeage, 1995).

Oxaliplatin and ormaplatin are both diaminocyclohexane (DACH) platinum-based compounds which contain DACH group as their carrier ligand. Because DACH group has two chiral centres, it can exist as three possible isomeric forms, *trans-R,R*-DACH, *trans-S,S*-DACH and *cis-R,S*-DACH. Oxaliplatin is the pure *R,R*-enantiomer of Pt(DACH)oxalato. Ormaplatin was used clinically as a racemic mixture of *R,R*- and *S,S*-enantiomers of Pt(DACH)Cl<sub>4</sub>. The antitumor activity of the DACH platinum-based compounds has been reported to depend on the enantiomeric configuration of the DACH group. The *R,R*-enantiomers of DACH platinum compounds demonstrated higher antitumor potency than their corresponding *S,S*-enantiomers (Pendyala et al., 1995, Di Francesco et al., 2002). Furthermore, DACH platinum-based compounds exhibit stereoselective peripheral neurotoxicity. The *R,R*-enantiomers of oxaliplatin, ormaplatin and their common biotransformation product Pt(DACH)Cl<sub>2</sub> induced peripheral neurotoxicity at lower cumulative doses and at earlier times than their corresponding *S,S*-enantiomers during repeated dosing in rats (Screnci et al., 1997). Recently, several studies have demonstrated different interactions with DNA between *R,R*- and *S,S*-enantiomers of DACH platinum-based compounds (Kasparkova et al., 2008, Zhang et al., 2013). Zhang and colleagues showed that



the diadduct formation rate of oxaliplatin is higher than that of its corresponding *S,S*-enantiomer, although the proportions of micro-loops and long-range cross-links for *S,S*-enantiomer are higher than those for oxaliplatin (Zhang et al., 2013).

The results from the previous two chapters have suggested a pivotal role of platinum-DNA damage-induced transcriptional inhibition in oxaliplatin-induced dorsal root ganglion (DRG) neuronal cell body atrophy and peripheral neurotoxicity. Binding of oxaliplatin-derived platinum to the DNA of cultured DRG cells appeared to have occurred before the induction of inhibition of nascent RNA synthesis and depletion of total RNA content. Oxaliplatin-induced neuronal cell body shrinkage appeared delayed until after the occurrence of binding of platinum to DNA and inhibition of transcription (see Chapter 4). Both sodium thiosulfate and cimetidine reduced the amount of platinum binding to DNA in cultured DRG cells, and protected them from both the inhibition of nascent RNA synthesis and neuronal cell body shrinkage, induced by oxaliplatin (see Chapter 5). In addition, treatment of cultured DRG cells with a model transcriptional inhibitor, actinomycin D, caused neuronal cell body atrophy following its inhibition of nascent RNA synthesis (see Chapter 4). Collectively, these findings suggested that platinum-DNA damage-induced transcriptional inhibition may contribute to the induction of DRG neuronal cell body atrophy and peripheral neurotoxicity by oxaliplatin. However, the role of platinum-DNA damage-induced transcriptional inhibition in DRG neuronal cell body atrophy and peripheral neurotoxicity induced by other platinum-based anticancer drugs has not been previously investigated, especially in a comparative study.

Given this background, the aim of the study presented in this chapter was to compare the effects of different platinum drugs and compounds on cultured DRG cells, in an attempt to further explore the potential role of platinum-DNA damage-induced transcriptional inhibition

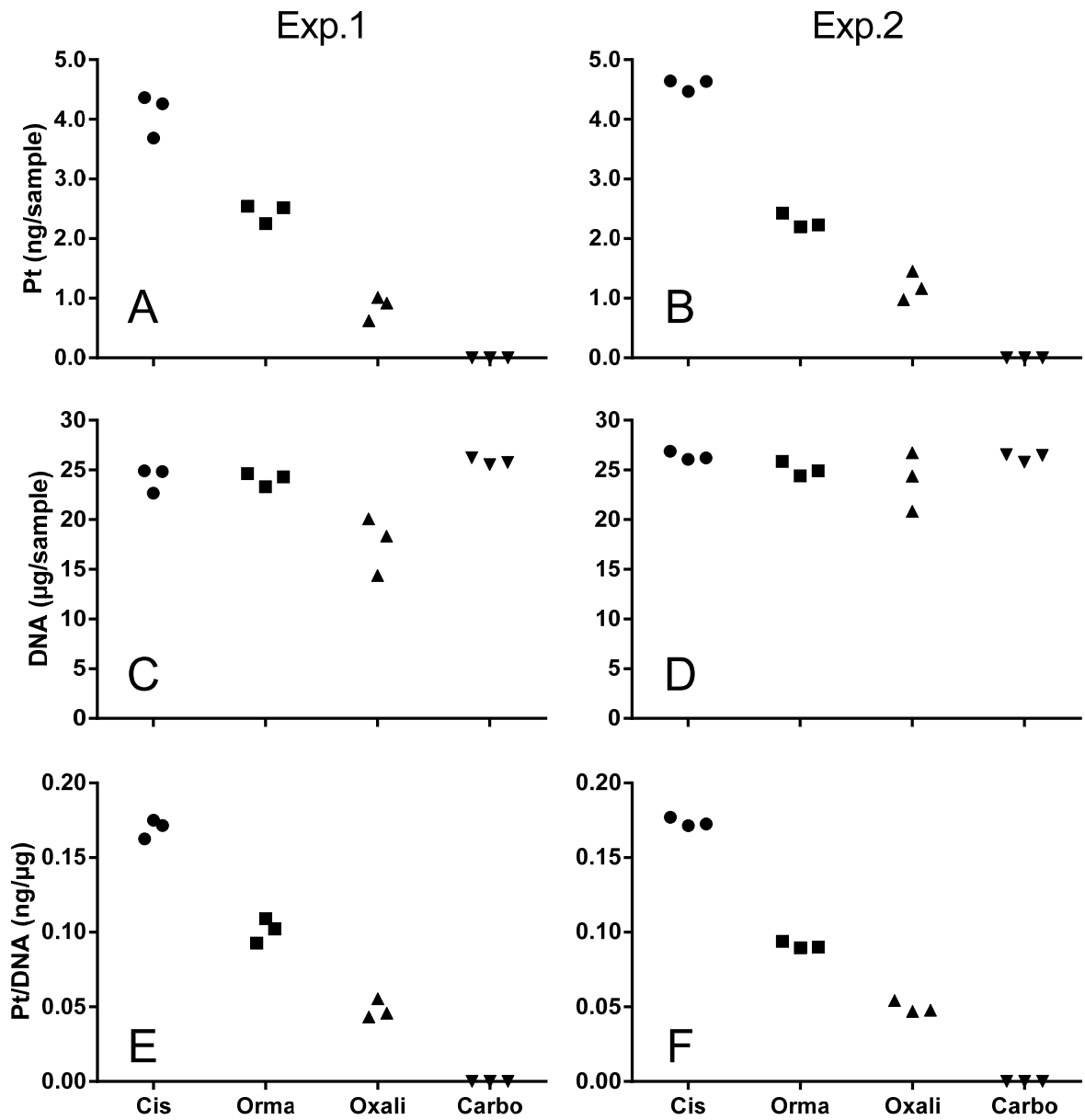
in DRG neuronal cell body atrophy and peripheral neurotoxicity induced by platinum-based anticancer drugs.

## **6.2. Results**

### **6.2.1. Platinum-based anticancer drugs**

To compare the effects of four clinical platinum-based anticancer drugs, cultured DRG cells were treated with cisplatin, carboplatin, oxaliplatin or ormaplatin and the resulting amount of platinum binding to DNA, inhibition of RNA-incorporation of [<sup>3</sup>H]uridine and alteration of neuronal cell body areas were measured after a 3-h exposure at 100 μM.

Treatment with cisplatin, ormaplatin and oxaliplatin resulted in detectable levels of platinum binding to the DNA of cultured DRG cells, whereas DNA-bound platinum was undetectable after carboplatin treatment. When cisplatin, ormaplatin and oxaliplatin were ranked according to the level of platinum binding to the DNA of cultured DRG cells, treatment with cisplatin resulted in the highest level, followed by ormaplatin and then oxaliplatin (Figure 6.1). Four hours after the start of a 3-h exposure to 100 μM cisplatin, ormaplatin and oxaliplatin, levels of platinum binding to DNA were  $0.1717 \pm 0.0050$ ,  $0.0963 \pm 0.0078$  and  $0.0489 \pm 0.0049$  ng/μg DNA, respectively. In contrast, 3-h treatment with 100 μM carboplatin resulted in levels of DNA-bound platinum that were below the detection limit of the ICP-MS platinum assay (0.1 ng/sample). In addition, levels of platinum binding to DNA were significantly different between any two platinum drugs ( $P < 0.001$ ; Tukey's post-test following one-way ANOVA), without any apparent change in the DNA content.



**G Combined**

$P < 0.0001$

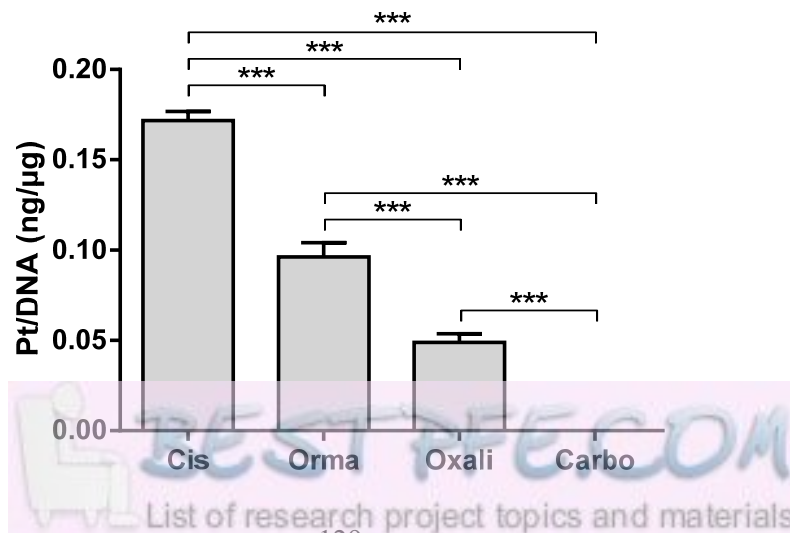


**Figure 6.1. Platinum binding to the DNA of cultured DRG cells after exposure to different platinum-based anticancer drugs.**

DRG cells were harvested from 8 to 12 rats for each experiment and cultured for three days before experiments. Then they were exposed to 100  $\mu$ M cisplatin (Cis), ormaplatin (Orma), oxaliplatin (Oxali) or carboplatin (Carbo) for 3 h, followed by culture in drug-free medium until 4 h after the start of treatment. Two independent experiments were conducted (experiment 1: A, C and E; experiment 2: B, D and F). In each experiment, three culture wells for each treatment condition were independently assayed for platinum (A and B) and DNA content (C and D), followed by calculation of platinum content per DNA content (E and F). Then the data from individual experiments for platinum content per DNA content (E and F) were combined (G).

Data show that when the platinum-based anticancer drugs were ranked according to the level of platinum binding to the DNA of cultured DRG cells, treatment with cisplatin resulted in the highest level, followed by ormaplatin and then oxaliplatin, whereas carboplatin treatment resulted in undetectable levels of DNA-bound platinum.

(A-F) (●) Cisplatin, (■) Ormaplatin, (▲) Oxaliplatin, (▼) Carboplatin.

(G) Combined data are presented as mean  $\pm$  standard deviation (n=6). The *P* value in the figure is for overall difference between groups by one-way ANOVA test. \*\*\* *P*<0.001 indicate the statistical significance of differences between indicated groups assessed by Tukey's multiple comparison post-test.

Treatment with cisplatin, ormaplatin and oxaliplatin significantly inhibited nascent RNA synthesis in cultured DRG cells, but carboplatin treatment appeared not to alter their levels of nascent RNA synthesis (Figure 6.2). Compared to their respective vehicle controls of 0.9% NaCl ( $100 \pm 34.4\%$ ) or 5% glucose ( $100 \pm 25.9\%$ ), levels of RNA-incorporated [ $^3\text{H}$ ]uridine were significantly reduced one day after a 3-h exposure to 100  $\mu\text{M}$  cisplatin, ormaplatin and oxaliplatin to  $4.0 \pm 1.5\%$  ( $P < 0.001$ ),  $13.7 \pm 6.3\%$  ( $P < 0.001$ ) and  $26.2 \pm 12.1\%$  ( $P < 0.001$ ) of control, respectively. In contrast, a 3-h treatment with 100  $\mu\text{M}$  carboplatin showed no effect on levels of RNA-incorporated [ $^3\text{H}$ ]uridine ( $100.4 \pm 38.6\%$  of control,  $P > 0.05$ ). In addition, when cisplatin, ormaplatin and oxaliplatin were ranked according to their effects of treatment on levels of RNA-incorporated [ $^3\text{H}$ ]uridine, treatment with cisplatin numerically resulted in the greatest effect, followed by ormaplatin and then oxaliplatin, although these differences between cisplatin, ormaplatin and oxaliplatin did not reach statistical significance ( $P > 0.05$ ).

Treatment with cisplatin, ormaplatin and oxaliplatin significantly reduced the cell body size of cultured DRG neurons, but carboplatin treatment appeared not to alter DRG neuronal cell body size (Figure 6.3). DRG neuronal cell body area distribution profiles were shifted to lower values one day after a 3-h exposure to 100  $\mu\text{M}$  cisplatin, ormaplatin and oxaliplatin, but were unaffected by carboplatin treatment. Compared to their respective vehicle controls of 0.9% NaCl (median: 321  $\mu\text{m}^2$ , interquartile range: 256-389  $\mu\text{m}^2$ ) or 5% glucose (median: 329  $\mu\text{m}^2$ , interquartile range: 267-409  $\mu\text{m}^2$ ), median neuronal cell body areas were significantly reduced by cisplatin, ormaplatin and oxaliplatin to 82.3% (median: 264  $\mu\text{m}^2$ , interquartile range: 216-319  $\mu\text{m}^2$ ,  $P < 0.001$ ), 81.3% (median: 260  $\mu\text{m}^2$ , interquartile range: 215-319  $\mu\text{m}^2$ ,  $P < 0.001$ ) and 77.8% (median: 255  $\mu\text{m}^2$ , interquartile range: 210-306  $\mu\text{m}^2$ ,  $P < 0.001$ ) of control, respectively. In contrast, a 3-h treatment with 100  $\mu\text{M}$  carboplatin showed no effect on neuronal cell body areas (median: 322  $\mu\text{m}^2$ , interquartile range: 259-392

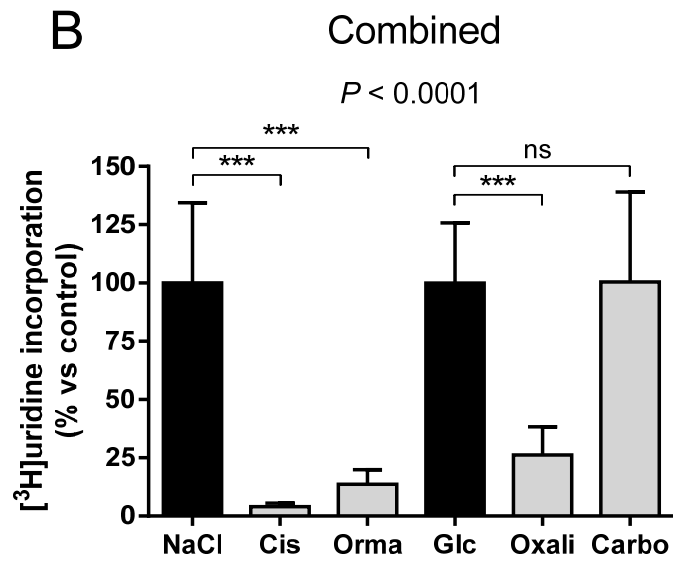
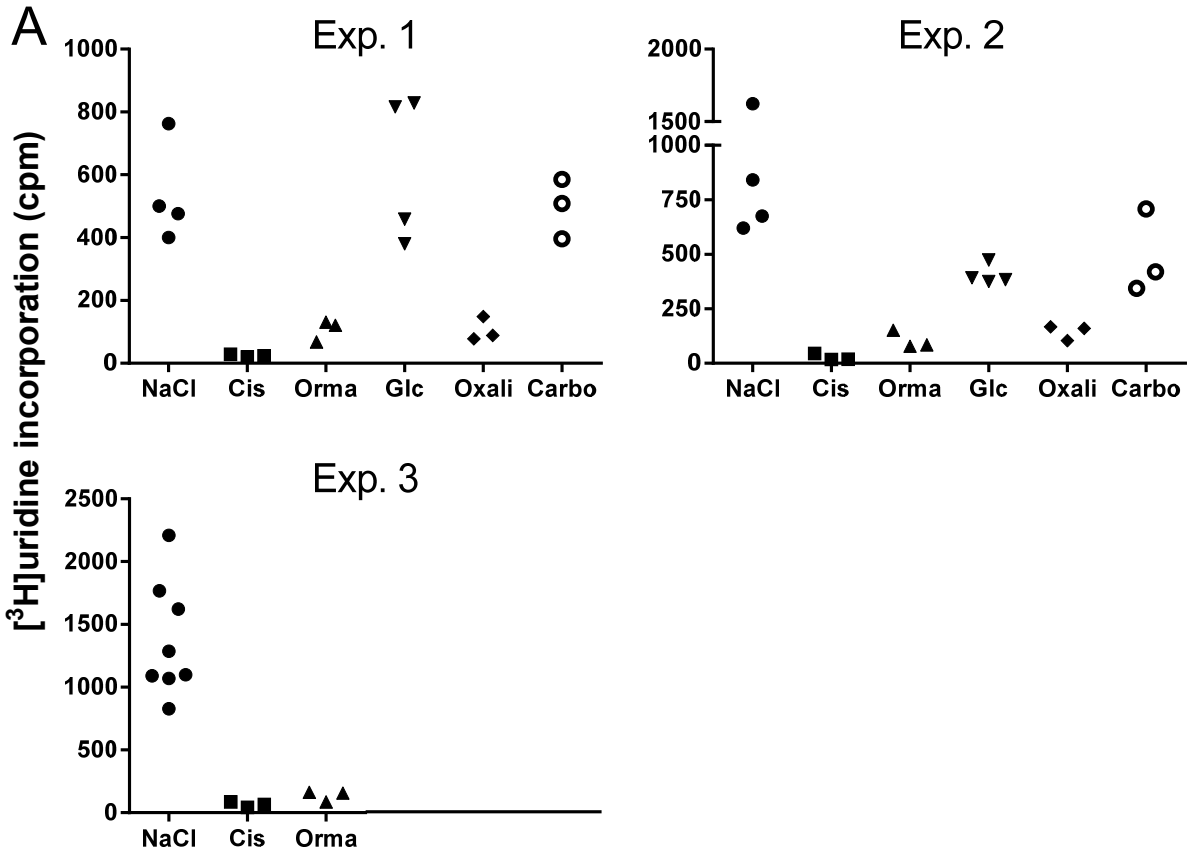


**Figure 6.2. Effects of different platinum-based anticancer drugs on nascent RNA synthesis in cultured DRG cells.**

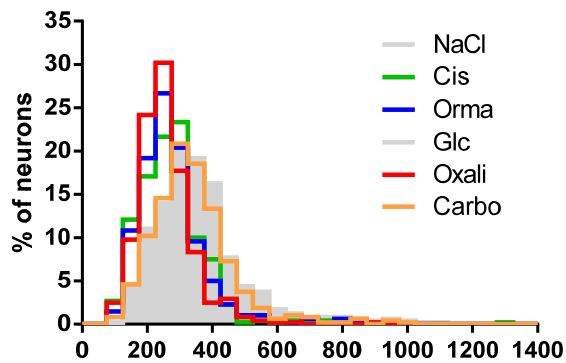
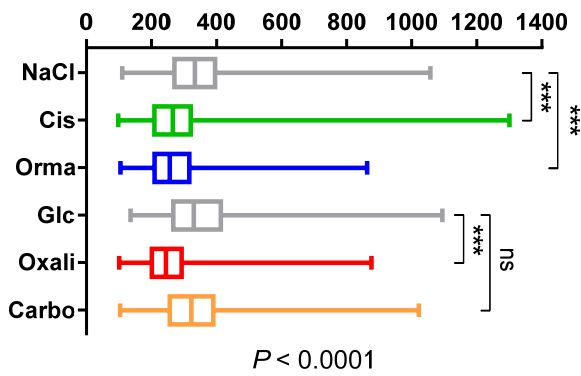
DRG cells were harvested from two to three rats for each experiment and cultured for three days before experiments. Then they were exposed to different platinum-based anticancer drugs (cisplatin: Cis, ormaplatin: Orma, oxaliplatin: Oxali, carboplatin: Carbo) at 100  $\mu$ M or respective drug vehicles (0.9% NaCl: NaCl, 5% glucose: Glc) for 3 h, followed by culture in drug-free medium for a further one day. Three independent experiments were conducted (A). In each experiment, between three to eight culture wells for each treatment condition were independently studied for levels of RNA-incorporated [<sup>3</sup>H]uridine. Then the data from individual experiments were combined after normalization to the mean value of their respective vehicle controls (0.9% NaCl for cisplatin and ormaplatin; 5% glucose for oxaliplatin and carboplatin) (B).

Data show that treatment with cisplatin, ormaplatin and oxaliplatin significantly inhibited nascent RNA synthesis in cultured DRG cells, but carboplatin treatment appeared not to alter their levels of nascent RNA synthesis.

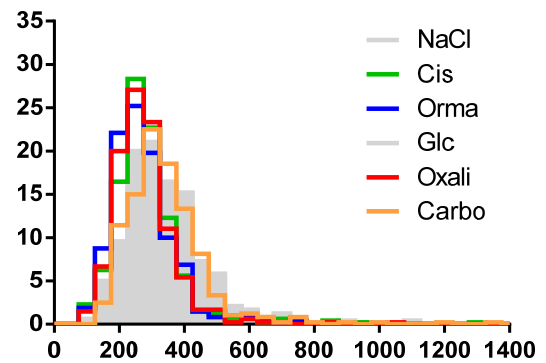
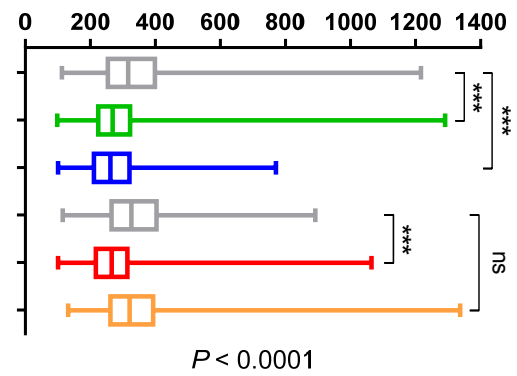
(A) (●) 0.9% NaCl, (■) cisplatin, (▲) ormaplatin, (▼) 5% glucose, (◆) oxaliplatin, (○) carboplatin.

(B) Combined data are presented as mean  $\pm$  standard deviation (n=6-16). The *P* value in the figure is for overall difference between groups by one-way ANOVA test. \*\*\* *P*<0.001 indicate the statistical significance of differences between indicated groups assessed by Tukey's multiple comparison post-test. ns, not significant.

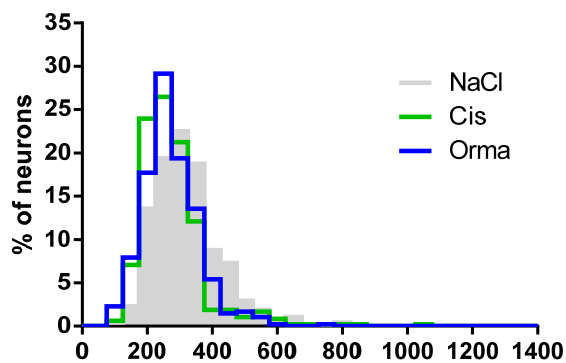
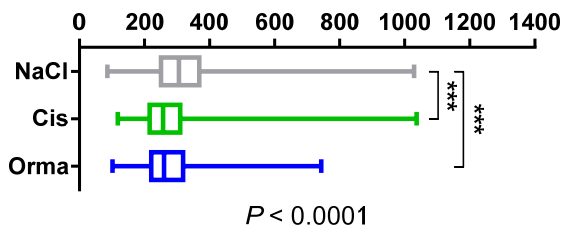
A) Exp. 1



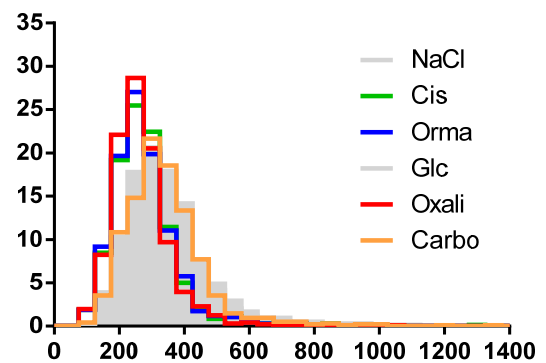
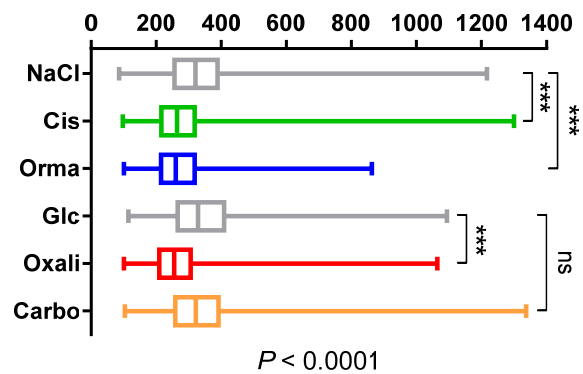
B) Exp. 2



C) Exp. 3



D) Combined



Neuronal cell body area ( $\mu\text{m}^2$ )



**Figure 6.3. Effects of different platinum-based anticancer drugs on cell body size of cultured DRG neurons.**

DRG cells were harvested from two to three rats for each experiment and cultured for three days before experiments. Then they were exposed to different platinum-based anticancer drugs (cisplatin: Cis, ormaplatin: Orma, oxaliplatin: Oxali, carboplatin: Carbo) at 100  $\mu$ M or respective drug vehicles (0.9% NaCl: NaCl, 5% glucose: Glc) for 3 h, followed by culture in drug-free medium for a further one day. Three independent experiments were conducted (A-C). In each experiment, a total of 480 neurons from three culture wells for each treatment condition were measured for cell body areas. Then the data from individual experiments were combined to achieve a group size of n=960-1440 (D).

Data show that treatment with cisplatin, ormaplatin and oxaliplatin significantly reduced the cell body size of cultured DRG neurons, but carboplatin treatment appeared not to alter DRG neuronal cell body size.

Data are presented as frequency histograms with bin width of 50  $\mu$ m<sup>2</sup> and box-and-whiskers plots indicating the median value (vertical line across the box), interquartile range (box) and range (whiskers). *P* values in the figure are for overall difference between groups by Kruskal-Wallis test. \*\*\* *P*<0.001 indicate the statistical significance of differences between indicated groups assessed by Dunn's multiple comparison post-test. ns, not significant.

$\mu\text{m}^2$ ,  $P>0.05$ ). No statistically significant differences in the effects on neuronal cell body areas were shown between cisplatin, ormaplatin and oxaliplatin treatment ( $P>0.05$ ).

Taken together, the results showed that treatment of cultured DRG cells with four different platinum-based anticancer drugs resulted in different amounts of platinum binding to DNA, which corresponded to their effects of treatment on nascent RNA synthesis and neuronal cell body size.

### 6.2.2. Enantiomers of diaminocyclohexane platinum-based compounds

To compare the effects of *R,R*- and *S,S*-enantiomers of two diaminocyclohexane (DACH) platinum-based compounds, cultured DRG cells were treated with enantiomers of ormaplatin and Pt(DACH)Cl<sub>2</sub> and the resulting amount of platinum binding to DNA, inhibition of RNA-incorporation of [<sup>3</sup>H]uridine and alteration of neuronal cell body areas were measured after a 3-h exposure at 100  $\mu\text{M}$ .

Treatment with *R,R*- and *S,S*-enantiomers of ormaplatin and Pt(DACH)Cl<sub>2</sub> resulted in detectable levels of platinum binding to the DNA of cultured DRG cells. However, treatment with *R,R*-enantiomers of ormaplatin and Pt(DACH)Cl<sub>2</sub> resulted in higher levels of DNA-bound platinum, compared to their corresponding *S,S*-enantiomers (Figure 6.4). Four hours after the start of a 3-h exposure to 100  $\mu\text{M}$  *R,R*-ormaplatin, *S,S*-ormaplatin, *R,R*-Pt(DACH)Cl<sub>2</sub> and *S,S*-Pt(DACH)Cl<sub>2</sub>, levels of platinum binding to DNA were  $0.1221 \pm 0.0101$ ,  $0.0480 \pm 0.0032$ ,  $0.1613 \pm 0.0106$  and  $0.0455 \pm 0.0052$  ng/ $\mu\text{g}$  DNA, respectively. Treatment with *R,R*-ormaplatin and *R,R*-Pt(DACH)Cl<sub>2</sub> resulted in significantly higher levels of DNA-bound platinum compared to their corresponding *S,S*-enantiomers ( $P<0.001$ ), without any apparent change in the DNA content.

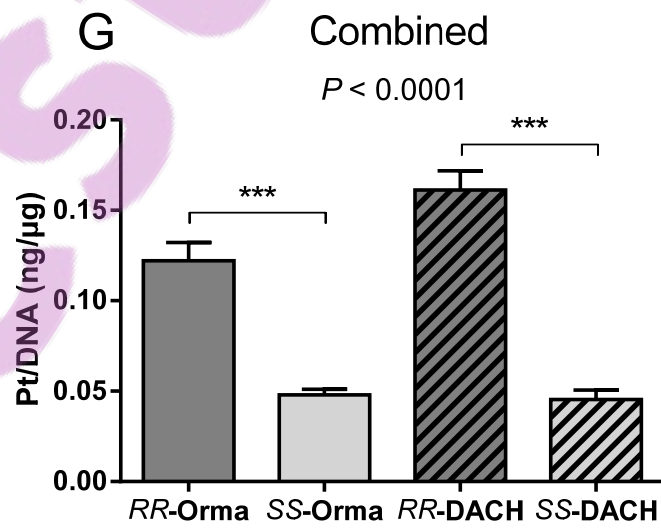
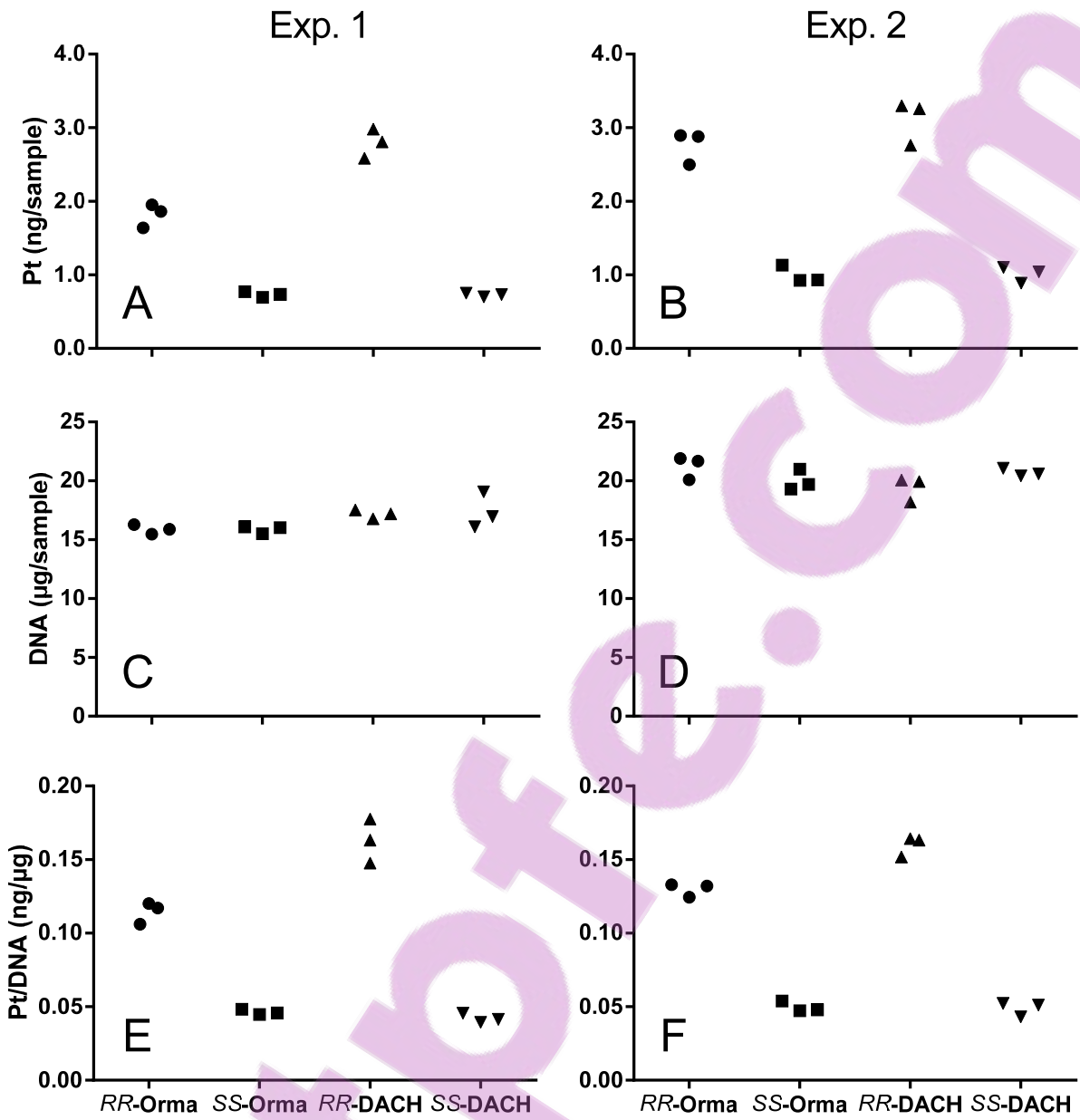


**Figure 6.4. Platinum binding to the DNA of cultured DRG cells after exposure to different enantiomers of diaminocyclohexane platinum-based compounds.**

DRG cells were harvested from five rats for each experiment and cultured for three days before experiments. Then they were exposed to 100  $\mu$ M *R,R*-ormaplatin (*RR*-Orma), *S,S*-ormaplatin (*SS*-Orma), *R,R*-Pt(DACH)Cl<sub>2</sub> (*RR*-DACH) or *S,S*-Pt(DACH)Cl<sub>2</sub> (*SS*-DACH) for 3 h, followed by culture in drug-free medium until 4 h after the start of treatment. Two independent experiments were conducted (experiment 1: A, C and E; experiment 2: B, D and F). In each experiment, three culture wells of each treatment condition were independently assayed for platinum (A and B) and DNA content (C and D), followed by calculation of platinum content per DNA content (E and F). Then the data from individual experiments for platinum content per DNA content (E and F) were combined (G).

Data show that treatment with *R,R*-enantiomers of ormaplatin and Pt(DACH)Cl<sub>2</sub> resulted in higher levels of platinum binding to the DNA of cultured DRG cells, compared to their corresponding *S,S*-enantiomers.

(A-F) (●) *R,R*-ormaplatin, (■) *S,S*-ormaplatin, (▲) *R,R*-Pt(DACH)Cl<sub>2</sub>, (▼) *S,S*-Pt(DACH)Cl<sub>2</sub>.

(G) Combined data are presented as mean  $\pm$  standard deviation (n=6). The *P* value in the figure is for overall difference between groups by one-way ANOVA test. \*\*\* *P*<0.001 indicate the statistical significance of differences between each pair of enantiomers assessed by Tukey's multiple comparison post-test.

Treatment with *R,R*- and *S,S*-enantiomers of ormaplatin and Pt(DACH)Cl<sub>2</sub> inhibited nascent RNA synthesis in cultured DRG cells. However, treatment with *R,R*-enantiomers of ormaplatin and Pt(DACH)Cl<sub>2</sub> resulted in greater inhibition of nascent RNA synthesis, compared to their corresponding *S,S*-enantiomers (Figure 6.5). Compared to vehicle controls of 0.9% NaCl (100 ± 28.7%), levels of RNA-incorporated [<sup>3</sup>H]uridine were significantly reduced one day after a 3-h exposure to 100 μM *R,R*-ormaplatin, *S,S*-ormaplatin, *R,R*-Pt(DACH)Cl<sub>2</sub> and *S,S*-Pt(DACH)Cl<sub>2</sub> to 5.1 ± 0.8% (*P*<0.001), 20.7 ± 6.6% (*P*<0.001), 14.2 ± 10.0% (*P*<0.001) and 26.7 ± 8.1 % (*P*<0.001) of control, respectively. Treatment with *R,R*-ormaplatin (*P*<0.001) and *R,R*-Pt(DACH)Cl<sub>2</sub> (*P*<0.05) resulted in significantly lower levels of RNA-incorporated [<sup>3</sup>H]uridine, compared to their corresponding *S,S*-enantiomers.

Treatment with *R,R*- and *S,S*-enantiomers of ormaplatin and Pt(DACH)Cl<sub>2</sub> reduced cell body size of cultured DRG neurons. However, treatment with *R,R*-enantiomers of ormaplatin and Pt(DACH)Cl<sub>2</sub> caused greater reduction of neuronal cell body size, compared to their corresponding *S,S*-enantiomers (Figure 6.6). DRG neuronal cell body area distribution profiles were shifted to lower values one day after a 3-h exposure to 100 μM *R,R*-ormaplatin and *R,R*-Pt(DACH)Cl<sub>2</sub>, more so than by treatment with the corresponding *S,S*-enantiomers. Compared to vehicle controls of 0.9% NaCl (median: 328 μm<sup>2</sup>, interquartile range: 264-397 μm<sup>2</sup>), median neuronal cell body areas were significantly reduced by *R,R*-ormaplatin, *S,S*-ormaplatin, *R,R*-Pt(DACH)Cl<sub>2</sub> and *S,S*-Pt(DACH)Cl<sub>2</sub> to 79.4% (median: 261 μm<sup>2</sup>, interquartile range: 216-308 μm<sup>2</sup>, *P*<0.001), 84.1% (median: 276 μm<sup>2</sup>, interquartile range: 223-336 μm<sup>2</sup>, *P*<0.001), 76.6% (median: 252 μm<sup>2</sup>, interquartile range: 207-306 μm<sup>2</sup>, *P*<0.001) and 86.6% (median: 284 μm<sup>2</sup>, interquartile range: 232-348 μm<sup>2</sup>, *P*<0.001) of control, respectively. Treatment with *R,R*-ormaplatin and *R,R*-Pt(DACH)Cl<sub>2</sub> resulted in lower median neuronal cell body areas, compared to their corresponding *S,S*-enantiomers (*P*<0.001).

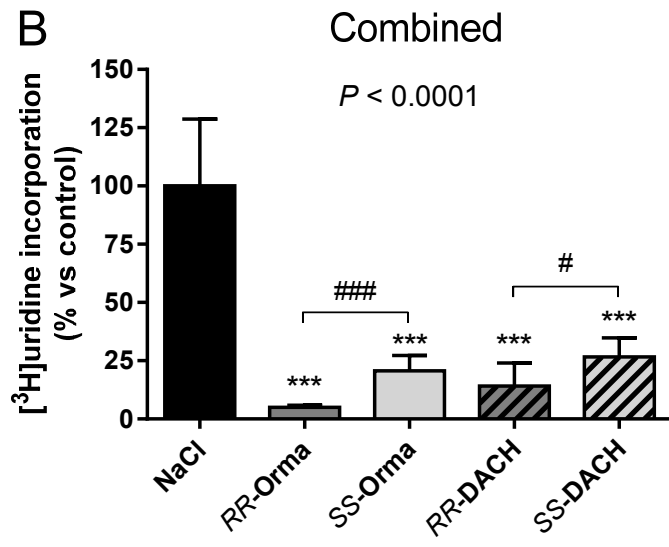
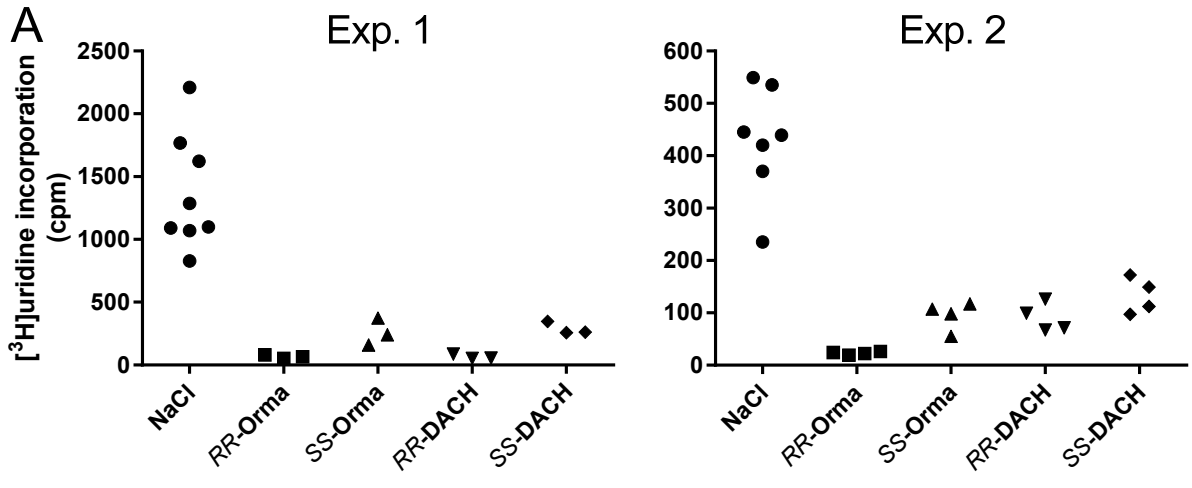


**Figure 6.5. Effects of different enantiomers of diaminocyclohexane platinum-based compounds on nascent RNA synthesis in cultured DRG cells.**

DRG cells were harvested from two to three rats for each experiment and cultured for three days before experiments. Then they were exposed to different enantiomers of DACH platinum-based compounds (*R,R*-ormaplatin: *RR*-Orma, *S,S*-ormaplatin: *SS*-Orma, *R,R*-Pt(DACH)Cl<sub>2</sub>: *RR*-DACH, *S,S*-Pt(DACH)Cl<sub>2</sub>: *SS*-DACH) at 100 μM or drug vehicle (0.9% NaCl: NaCl) for 3 h, followed by culture in drug-free medium for a further one day. Two independent experiments were conducted (A). In each experiment, between three to eight culture wells for each treatment condition were independently studied for levels of RNA-incorporated [<sup>3</sup>H]uridine. Then the data from individual experiments were combined after normalization to the mean value of their respective controls (0.9% NaCl) (B).

Data show that treatment with *R,R*-enantiomers of ormaplatin and Pt(DACH)Cl<sub>2</sub> resulted in greater inhibition of nascent RNA synthesis in cultured DRG cells, compared to their corresponding *S,S*-enantiomers.

(A) (●) 0.9% NaCl, (■) *R,R*-ormaplatin, (▲) *S,S*-ormaplatin, (▼) *R,R*-Pt(DACH)Cl<sub>2</sub>, (◆) *S,S*-Pt(DACH)Cl<sub>2</sub>.

(B) Combined data are presented as mean ± standard deviation (n=7-15). The *P* value in the figure is for overall difference between groups by one-way ANOVA test. \*\*\* *P*<0.001 compared to vehicle control (Tukey's multiple comparison post-tests following one-way ANOVA). # *P*<0.05, ### *P*<0.001 compared between each pair of enantiomers (unpaired *t*-test).





**Figure 6.6. Effects of different enantiomers of diaminocyclohexane platinum-based compounds on cell body size of cultured DRG neurons.**

DRG cells were harvested from two to three rats for each experiment and cultured for three days before experiments. Then they were exposed to different enantiomers of DACH platinum-based compounds (*R,R*-ormaplatin: *RR*-Orma, *S,S*-ormaplatin: *SS*-Orma, *R,R*-Pt(DACH)Cl<sub>2</sub>: *RR*-DACH, *S,S*-Pt(DACH)Cl<sub>2</sub>: *SS*-DACH) at 100 μM or drug vehicle (0.9% NaCl: NaCl) for 3 h, followed by culture in drug-free medium for a further one day. Two independent experiments were conducted (A and B). In each experiment, a total of 480 neurons from three culture wells for each treatment condition were measured for cell body areas. Then the data from individual experiments were combined to achieve a group size of n=960 (C).

Data show that treatment with *R,R*-enantiomers of ormaplatin and Pt(DACH)Cl<sub>2</sub> caused greater reduction of cell body size of cultured DRG neurons, compared to their corresponding *S,S*-enantiomers.

Data are presented as frequency histograms with bin width of 50 μm<sup>2</sup> and box-and-whiskers plots indicating the median value (vertical line across the box), interquartile range (box) and range (whiskers). *P* values in the figure are for overall difference between groups by Kruskal-Wallis test. \*\*\* *P*<0.001 compared to vehicle control; ### *P*<0.001 compared between each pair of enantiomers; ns, not significant (Dunn's multiple comparison post-tests following Kruskal-Wallis test).

Taken together, the results showed that treatment of cultured DRG cells with *R,R*-enantiomers of ormaplatin and Pt(DACH)Cl<sub>2</sub> resulted in higher levels of platinum binding to DNA compared to their corresponding *S,S*-enantiomers, which corresponded to their effects of treatment on nascent RNA synthesis and neuronal cell body size.

### 6.3. Discussion

The findings described in this chapter have suggested that platinum-DNA damage-induced transcriptional inhibition may play an important role in DRG neuronal cell body atrophy and peripheral neurotoxicity induced by platinum drugs and compounds. Treatment of cultured DRG cells with cisplatin, carboplatin, oxaliplatin or ormaplatin resulted in different amounts of platinum binding to DNA, which corresponded to the effects of the different treatments on nascent RNA synthesis and neuronal cell body size. Treatment with cisplatin, ormaplatin and oxaliplatin resulted in detectable levels of platinum binding to DNA, and significantly reduced nascent RNA synthesis and neuronal cell body size. In contrast, carboplatin treatment resulted in undetectable levels of DNA-bound platinum, and appeared not to alter nascent RNA synthesis and neuronal cell body size. Given that the detection limit of the ICP-MS platinum assay was 0.1 ng per sample and the average DNA content used for sample preparation was ~13 µg, the level of DNA-bound platinum after carboplatin treatment should be less than 0.0077 ng/µg DNA. Therefore, the level of platinum binding to the DNA of cultured DRG cells resulted from carboplatin treatment was at least six-fold less than those achieved with cisplatin (0.1717 ng/µg DNA), ormaplatin (0.0963 ng/µg DNA) and oxaliplatin treatment (0.0489 ng/µg DNA) at equimolar concentration. In addition, treatment of cultured DRG cells with *R,R*- and *S,S*-enantiomers of ormaplatin and Pt(DACH)Cl<sub>2</sub>, an active metabolite of oxaliplatin and ormaplatin (Luo et al., 1999), resulted in different levels

of platinum binding to DNA, which corresponded to their effects of treatment on nascent RNA synthesis and neuronal cell body size. Treatment with *R,R*-ormaplatin and *R,R*-Pt(DACH)Cl<sub>2</sub> resulted in higher levels of DNA-bound platinum, and caused greater reduction of nascent RNA synthesis and neuronal cell body size, compared to their corresponding *S,S*-enantiomers. Furthermore, previous chapters have shown that, in cultured DRG cells, oxaliplatin-induced platinum-DNA damage appeared to have occurred before the induction of transcriptional inhibition, while neuronal cell body shrinkage appeared delayed until after the occurrence of platinum-DNA damage and inhibition of transcription (see Chapter 4). Limiting platinum-DNA damage in cultured DRG cells reduced oxaliplatin-induced transcriptional inhibition and neuronal cell body shrinkage (see Chapter 5). Taken together, these findings suggested that platinum-DNA damage-induced transcriptional inhibition may play a key role in DRG neuronal cell body atrophy and peripheral neurotoxicity induced by platinum drugs and compounds.

Further strengthening the possible role of platinum-DNA damage-induced transcriptional inhibition in peripheral neurotoxicity induced by different platinum-based anticancer drugs was the finding that the amount of platinum binding to DNA and extent of inhibition of nascent RNA synthesis in cultured DRG cells measured after treatment with cisplatin, carboplatin, oxaliplatin or ormaplatin broadly corresponded to their relative peripheral neurotoxicity observed in patients and experimental animals. Treatment of cultured DRG cells with cisplatin, ormaplatin and oxaliplatin resulted in detectable levels of platinum binding to DNA and significantly inhibited nascent RNA synthesis. Correspondingly, peripheral neurotoxicity is a common dose-limiting side effect of cisplatin and oxaliplatin, and clinical development of ormaplatin has been abandoned because of severe neurotoxicity in patients (Pasetto et al., 2006, Wheate et al., 2010, Amptoulach and Tsavaris, 2011). The

prevalence of peripheral neurotoxicity in clinical trials of cisplatin, ormaplatin or oxaliplatin has been reported to be 47% (95% CI: 41-53%), 87% (95% CI: 47-100%) and 97% (95% CI: 92-99%), respectively (Screnci and McKeage, 1999). The cumulative doses of cisplatin, ormaplatin and oxaliplatin required for inducing peripheral neurotoxicity in a rat model have been reported to be 46.7, 26.0 and 15.0  $\mu\text{mol/kg}$ , respectively (Screnci et al., 2000). In contrast, carboplatin treatment resulted in undetectable levels of platinum binding to DNA and appeared not to alter the level of nascent RNA synthesis in cultured DRG cells. Correspondingly, the peripheral neurotoxicity resulting from carboplatin administration has been reported to be less frequent in cancer patients [5.8% (95% CI: 3.8-8.5%)] (Screnci and McKeage, 1999) and to require higher cumulative doses in a rat model (302  $\mu\text{mol/kg}$ ) (Screnci et al., 2000) than observed with other platinum-based anticancer drugs. Taken together, these findings provided further evidence suggesting that platinum-DNA damage-induced transcriptional inhibition may play an important role in peripheral neurotoxicity induced by platinum-based anticancer drugs. The differences in platinum-DNA damage in DRG cells could at least partially explain the different peripheral neurotoxicity profile of platinum-based anticancer drugs.

This study has also suggested that differences in the amount of platinum-DNA damage and extent of its induction of transcriptional inhibition in DRG cells may play an important role in the stereoselective induction of DRG neuronal cell body atrophy and peripheral neurotoxicity by diaminocyclohexane (DACH) platinum enantiomers. The amount of platinum binding to DNA and extent of inhibition of nascent RNA synthesis in cultured DRG cells measured after treatment with *R,R*- and *S,S*-enantiomers of ormaplatin and  $\text{Pt}(\text{DACH})\text{Cl}_2$  corresponded to their effects of treatment on neuronal cell body size of cultured DRG cells and to their relative peripheral neurotoxicity observed *in vivo*. Treatment of cultured DRG cells with *R,R*-

ormaplatin and *R,R*-Pt(DACH)Cl<sub>2</sub> resulted in higher levels of DNA-bound platinum and greater inhibition of nascent RNA synthesis, compared to their corresponding *S,S*-enantiomers at equimolar concentration. Correspondingly, treatment with *R,R*-ormaplatin and *R,R*-Pt(DACH)Cl<sub>2</sub> led to greater reduction of neuronal cell body size of cultured DRG cells, compared to their corresponding *S,S*-enantiomers. Furthermore, treatment with *R,R*-ormaplatin and *R,R*-Pt(DACH)Cl<sub>2</sub> has been shown to induce peripheral neurotoxicity at lower cumulative doses and at earlier times than their corresponding *S,S*-enantiomers in a rat model (Screnci et al., 1997). It is noteworthy that no apparent difference in platinum accumulation within DRG was observed between *R,R*- and *S,S*-enantiomers of ormaplatin and Pt(DACH)Cl<sub>2</sub> (Screnci et al., 1997), which suggested that the stereoselective peripheral neurotoxicity of ormaplatin and Pt(DACH)Cl<sub>2</sub> enantiomers may not be due to differences in the total amount of platinum accumulating in DRG tissue. Taken together, these findings suggested that differences in the amount of platinum-DNA damage and extent of its induction of transcriptional inhibition in DRG cells may play a pivotal role in the stereoselective induction of DRG neuronal cell body atrophy and peripheral neurotoxicity by DACH platinum enantiomers.

In conclusion, the findings presented in this chapter have suggested that platinum-DNA damage-induced transcriptional inhibition may play an important role in DRG neuronal cell body atrophy and peripheral neurotoxicity induced by platinum-based anticancer drugs.

## Chapter 7. General Discussion

The findings described in this thesis have suggested that mechanisms of platinum drug-induced peripheral neurotoxicity may involve interrelationships between platinum-DNA damage, transcriptional inhibition and neuronal cell body atrophy in dorsal root ganglion (DRG) cells. In the work presented in this thesis, primary cultured rat DRG cells were used as experimental model. Platinum-DNA damage was determined by measuring the amount of platinum binding to DNA. Transcriptional activity was indicated by the levels of RNA-incorporated 5-ethynyl uridine (EU) or [<sup>3</sup>H]uridine or total RNA content. Neuronal cell body size was represented by the cross-sectional areas of neuronal cell bodies. The level of RNA-incorporated EU in individual DRG neurons correlated with their cell body area, but both were reduced by oxaliplatin treatment in a concentration-dependent manner. Binding of oxaliplatin-derived platinum to the DNA of cultured DRG cells appeared to have occurred before the induction of inhibition of RNA-incorporation of [<sup>3</sup>H]uridine and depletion of total RNA content. Oxaliplatin-induced decrease in neuronal cell body areas appeared delayed until after the occurrence of binding of platinum to DNA, inhibition of RNA-incorporation of [<sup>3</sup>H]uridine and depletion of total RNA content. Both sodium thiosulfate and cimetidine reduced platinum binding to DNA, and protected cultured DRG cells from both the inhibition of RNA-incorporation of [<sup>3</sup>H]uridine and decrease in neuronal cell body areas induced by oxaliplatin. Treatment of cultured DRG cells with four different platinum-based anticancer drugs, cisplatin, carboplatin, oxaliplatin and ormaplatin, and two pairs of enantiomers of diaminocyclohexane (DACH) platinum-based compounds, ormaplatin and Pt(DACH)Cl<sub>2</sub>, resulted in different amounts of platinum binding to DNA, which corresponded to the effects of the different treatments on RNA-incorporation of [<sup>3</sup>H]uridine and neuronal cell body areas. A model transcriptional inhibitor, actinomycin D, also reduced neuronal cell body areas

following its inhibition of RNA-incorporation of [<sup>3</sup>H]uridine in cultured DRG cells. Taken together, these findings suggested that platinum-DNA damage formed by oxaliplatin and other platinum-based anticancer drugs may induce transcriptional inhibition in DRG cells, which in turn may lead to neuronal cell body atrophy and peripheral neurotoxicity.

In this chapter, the results presented in this thesis are divided into three categories, platinum-DNA damage, transcriptional inhibition and neuronal cell body atrophy, and are discussed in the context of the interrelationships between these three events. Potential mechanisms linking platinum-DNA damage, transcriptional inhibition, neuronal cell body atrophy and peripheral neurotoxicity are also discussed, based on the findings described in this thesis and other reports.

## **7.1. Platinum-DNA damage**

Platinum-based anticancer drugs have been widely used for treatment of a variety of cancers (Windebank and Grisold, 2008, Wheate et al., 2010, Stein and Arnold, 2012). The anticancer activity of platinum drugs is mainly based on the formation of various platinum-DNA adducts, which inhibits DNA replication and transcription and in turn triggers cancer cell death (Jung and Lippard, 2007, Todd and Lippard, 2009). Recently, an increasing number of studies have suggested that platinum-DNA damage within DRG neurons may be critically involved in platinum drug-induced peripheral neurotoxicity. Compared to a cancer cell line, cultured DRG neurons accumulated higher levels of platinum-DNA adducts after cisplatin treatment *in vitro* (McDonald et al., 2005). DRG tissue was also shown to accumulate more platinum-DNA adducts than other tissues exposed to equivalent blood levels in cisplatin-treated rats (McDonald et al., 2005). Oxaliplatin and cisplatin treatment resulted in different

amounts of platinum-DNA adducts in cultured DRG neurons, which correlated with their neurotoxicity *in vitro* (Ta et al., 2006). Mice with dysfunctional nucleotide excision repair (NER) showed greater amounts of platinum-DNA adducts in DRG cells and more severe peripheral neuropathy after cisplatin treatment compared to those proficient for NER functions. In addition, independently from the specific NER phenotype, the amount of platinum-DNA adducts in DRG neurons was significantly correlated with the severity of peripheral neuropathy (Dzagnidze et al., 2007).

The findings described in this thesis provided further evidence that platinum-based anticancer drugs produce platinum-DNA damage in DRG cells. The time-course data demonstrated a specific pattern of binding of oxaliplatin-derived platinum to the DNA of cultured DRG cells, whereby platinum-DNA levels increased during and shortly after oxaliplatin treatment, and then decreased but persisted after drug removal. Co-incubation with either sodium thiosulfate or cimetidine reduced amounts of platinum binding to the DNA of cultured DRG cells after oxaliplatin treatment. Treatment with cisplatin, ormaplatin and oxaliplatin resulted in detectable levels of platinum binding to the DNA of cultured DRG cells, whereas DNA-bound platinum was undetectable after carboplatin treatment. When cisplatin, ormaplatin and oxaliplatin were ranked according to the level of platinum binding to the DNA of cultured DRG cells, treatment with cisplatin resulted in the highest level, followed by ormaplatin and then oxaliplatin. Treatment with *R,R*- and *S,S*-enantiomers of ormaplatin and Pt(DACH)Cl<sub>2</sub> resulted in detectable levels of platinum binding to the DNA of cultured DRG cells. However, treatment with *R,R*-enantiomers of ormaplatin and Pt(DACH)Cl<sub>2</sub> resulted in higher levels of DNA-bound platinum, compared to their corresponding *S,S*-enantiomers. Taken together, these findings showed that treatment with platinum-based anticancer drugs resulted in platinum-DNA damage in DRG cells, but to a different extent.



The accumulation of platinum-DNA damage in target cells after treatment with platinum-based anticancer drugs involves multiple processes, including drug cellular uptake, activation of the platinum compound, binding to DNA, and repair of DNA lesions (Wang and Lippard, 2005, Jung and Lippard, 2007). First, platinum drugs and/or their active metabolites enter target cells through carrier-facilitated and active transport as well as passive diffusion. Several membrane transporters have been found to contribute to cellular uptake of platinum drugs, such as copper transporters (CTR) and organic cation transporters (OCT) (Liu et al., 2012). However, these transporters showed differential activity towards structurally diverse platinum compounds. For instance, OCT2 was shown to have higher activity to oxaliplatin, ormaplatin and Pt(DACH)Cl<sub>2</sub>, in comparison to cisplatin and carboplatin (Burger et al., 2010a). Then, platinum compounds are converted to their active forms through aquation reactions replacing their leaving ligands with water molecules. However, the aquation reactions for platinum compounds containing bidentate bis-carboxylate leaving groups, such as oxaliplatin and carboplatin, are slower than that for platinum compounds containing chloride leaving groups, such as ormaplatin, Pt(DACH)Cl<sub>2</sub> and cisplatin (Alberts and Dorr, 1998, Go and Adjei, 1999, Di Francesco et al., 2002, Mani et al., 2002). Next, the active forms of platinum compounds bind to DNA at the N-7 position of guanine (G) or adenine (A) to form approximately 60-65% GG, 25-30% AG and 5-10% GNG intrastrand cross-links as well as a small portion of interstrand cross-links (Chaney et al., 2005, Kweekel et al., 2005, Todd and Lippard, 2009). Although similar in their type and site, the platinum-DNA adducts formed by different platinum compounds contain different carrier ligands. Cisplatin and carboplatin form the same platinum-DNA adducts containing the *cis*-diammine carrier ligand. Oxaliplatin and ormaplatin produce platinum-DNA adducts containing the diaminocyclohexane (DACH) ligand, with the difference being that the DACH carrier ligand of oxaliplatin is *R,R*-form whereas that of ormaplatin is a racemic mixture of *R,R*- and *S,S*-

enantiomers. Several conformational differences between *cis*-diammine and DACH platinum adducts were observed, which may be responsible for the differences in their protein recognition and cellular processing (Chaney et al., 2005, Sharma et al., 2007, Wu et al., 2007). Thereafter, platinum-DNA adducts can be removed by nucleotide excision repair (NER) and/or other DNA repair mechanisms (Reardon et al., 1999, Di Francesco et al., 2002, Wang and Lippard, 2005). NER appeared not to discriminate between *cis*-diammine and DACH platinum adducts, whereas mismatch repair was shown to discriminate between these structurally different platinum-DNA adducts (Chaney et al., 2005). Collectively, these different processes involved in the formation and removal of platinum-DNA adducts may explain the specific pattern and levels of DNA binding of platinum drugs observed in the studies of this thesis.

## **7.2. Transcriptional inhibition**

Transcriptional inhibition has been demonstrated to be induced by platinum-based anticancer drugs, and has been suggested to directly correlate with platinum drug cytotoxicity (Todd and Lippard, 2009). Treatment of human fibrosarcoma cells with cisplatin and oxaliplatin inhibited rRNA synthesis at the level of transcription of 47S/45S rRNA, and caused nucleolar disintegration (Burger et al., 2010b). In addition, cisplatin treatment caused a redistribution of the major components of the rRNA transcription machinery, including upstream binding factor and RNA polymerase I, in the nucleolus of HeLa cells (Jordan and Carmo-Fonseca, 1998). Inhibition of mRNA synthesis was also observed in human fibroblasts treated with cisplatin, which correlated with the induction of p53, p21 and apoptosis (Ljungman et al., 1999).

The studies presented in this thesis for the first time directly demonstrated that treatment with oxaliplatin and some other platinum-based anticancer drugs inhibited transcription of post-mitotic DRG neurons *in vitro*. RNA-incorporation of 5-ethynyl uridine (EU) in cultured DRG neurons was significantly suppressed by oxaliplatin treatment in a concentration-dependent manner. Time-dependence of effects of oxaliplatin treatment on RNA-incorporation of [<sup>3</sup>H]uridine in cultured DRG cells was also observed. The finding that total RNA content was reduced by oxaliplatin treatment in a time-dependent manner provided further evidence for oxaliplatin-induced transcriptional inhibition in cultured DRG cells. In addition, treatment of cultured DRG cells with cisplatin, ormaplatin and Pt(DACH)Cl<sub>2</sub> significantly reduced the levels of RNA-incorporated [<sup>3</sup>H]uridine, whereas carboplatin treatment appeared not to affect the RNA-incorporation of [<sup>3</sup>H]uridine. These new findings could explain the nucleolar dysfunction and disorganization observed in DRG neurons after treatment with platinum-based anticancer drugs (Tomiwa et al., 1986, Turecek et al., 1996, McKeage et al., 2001, Ip et al., 2013). Similar results were also demonstrated by another study showing cisplatin treatment induced transcriptional inhibition in cultured cortical neurons (Gozdz et al., 2008). Taken together, these findings showed that treatment with platinum drugs inhibited transcription of cultured DRG cells.

In the work presented in this thesis, three different methods were used to study the effects of oxaliplatin treatment on transcriptional activity of cultured DRG cells. The first method was based on the biosynthetic incorporation of EU into newly synthesized RNA and the use of a subsequent click chemistry reaction to attach a fluorophore label to the RNA-incorporated EU. The fluorescently-labelled RNA-incorporated EU was visualized and quantitated by fluorescence microscopy and image analysis. With this method, transcriptional activity was visualized and quantitated at the level of individual DRG neurons, which made it possible to

distinguish transcriptional activity of neurons from that of non-neuronal cells in mixed cultures of DRG cells. Moreover, it was possible to relate the level of transcription to other characteristics of the particular neuron, such as its size and DNA content. However, microscopy imaging and image analysis was laborious, requiring days to weeks of time. The second method relied on labelling newly synthesized RNA with [<sup>3</sup>H]uridine, which can be quantitated by scintillation counting. This method was relatively simple and efficient compared to the first one, although a high level of caution was required when working with radioactive materials. Unlike RNA-incorporation of EU that indicated individual neuron levels of transcription, this method measured transcriptional activity of whole cultures consisting of DRG neurons and non-neuronal cells. However, DRG neurons may have had much higher levels of transcription than non-neuronal cells, which was suggested by the finding that DRG neurons showed strong fluorescence labelling of RNA-incorporated EU, whereas little or no labelling was observed in non-neuronal cells. Therefore, it may be reasonable to conclude that the measurement of RNA-incorporation of [<sup>3</sup>H]uridine in whole cultures reflects mainly the transcriptional activity of DRG neurons. The third method measured total RNA content of the whole culture. Since total RNA content is determined by both transcriptional activity and degradation rate, this method was indirect. However, without the need of labelling, this method provided a simple and efficient way to obtain supporting information about transcriptional activity of cultured DRG cells. It should be noted that separate experiments using these three different methods demonstrated similar trends of effects of oxaliplatin treatment on transcriptional activity of cultured DRG cells.

The findings presented in this thesis suggested that transcriptional inhibition in cultured DRG cells after treatment with platinum-based anticancer drugs may be induced by platinum-DNA damage. Time-course data showed that binding of oxaliplatin-derived platinum to the DNA

of cultured DRG cells appeared to have occurred before the induction of inhibition of RNA-incorporation of [<sup>3</sup>H]uridine and depletion of total RNA content. In addition, reduction of the amount of platinum binding to DNA by sodium thiosulfate and cimetidine protected cultured DRG cells from oxaliplatin-induced inhibition of RNA-incorporation of [<sup>3</sup>H]uridine. Furthermore, treatment of cultured DRG cells with different platinum drugs or compounds resulted in different amounts of platinum binding to DNA, which corresponded to the effects of the different treatments on RNA-incorporation of [<sup>3</sup>H]uridine. Specifically, treatment with cisplatin, ormaplatin and oxaliplatin resulted in detectable levels of platinum binding to DNA and significantly reduced levels of RNA-incorporated [<sup>3</sup>H]uridine. In contrast, carboplatin treatment resulted in undetectable levels of DNA-bound platinum and appeared not to alter RNA-incorporation of [<sup>3</sup>H]uridine. Treatment with *R,R*-ormaplatin and *R,R*-Pt(DACH)Cl<sub>2</sub> resulted in higher levels of DNA-bound platinum and caused greater inhibition of RNA-incorporation of [<sup>3</sup>H]uridine, compared to their corresponding *S,S*-enantiomers. Taken together, these findings suggested that transcription inhibition in cultured DRG cells treated with platinum drugs may be due to platinum-DNA damage.

The mechanism by which platinum-DNA damage inhibits transcription has not been fully elucidated, although several hypotheses have been proposed. Some findings suggested that platinum-DNA damage may induce transcriptional inhibition through DNA damage signalling pathways, such as DNA-dependent protein kinase (DNA-PK)/poly(ADP-ribose) polymerase 1 (PARP-1) pathway. DNA-PK and PARP-1 are proteins that both play key roles in DNA damage repair (Meek et al., 2008, Luo and Kraus, 2012). DNA-PK was shown to repress the RNA polymerase I machinery of rRNA synthesis (Kuhn et al., 1995, Michaelidis and Grummt, 2002). The role of PARP-1 in rRNA transcription was also suggested (Desnoyers et al., 1996, Boamah et al., 2012). Most recently, a study using EU incorporation

assay to monitor RNA synthesis showed that inhibition of either DNA-PK or PARP-1 prevented cisplatin-induced block of rRNA synthesis, and that loss of DNA-PK function impeded activation of PARP-1 in damaged cells (Calkins et al., 2013). Therefore, the authors of this study proposed that a sequential activation of DNA-PK and PARP-1 by DNA damage may contribute to cisplatin-induced inhibition of rRNA synthesis. However, the findings presented in this thesis suggested that DNA-PK and PARP-1 may not be critically involved in the mechanism of platinum-DNA damage-induced transcriptional inhibition in cultured DRG cells, at least under the experimental conditions used in the study. Two DNA-PK inhibitors, wortmannin and NU 7026, and two PARP-1 inhibitors, benzamide and olaparib, were studied for their effects on oxaliplatin-induced inhibition of RNA-incorporation of [<sup>3</sup>H]uridine in cultured DRG cells, but none of them showed any alteration of effects of oxaliplatin. Other potential mechanisms underlying platinum-DNA damage-induced transcriptional inhibition were also hypothesized, including physical blockade of RNA polymerase, disruption of nucleosome dynamics and hijacking of transcription factors (Todd and Lippard, 2009). However, these mechanisms have not been studied in DRG neurons as far as we are aware, but could be a topic of future work.

### **7.3. Neuronal cell body atrophy and peripheral neurotoxicity**

Peripheral sensory neurotoxicity is a dose-limiting side effect of some platinum-based anticancer drugs, such as oxaliplatin, cisplatin and ormaplatin (Screnci and McKeage, 1999, McKeage et al., 2001, Amptoulach and Tsavaris, 2011). The mechanisms of platinum drug-induced peripheral neurotoxicity have not been fully understood so far. However, it has been generally accepted that the primary damage happens at the level of the cell bodies of sensory neurons within DRGs (Tomiwa et al., 1986, Cavaletti et al., 1992b, Holmes et al., 1998,

Krarp-Hansen et al., 1999, Cavaletti et al., 2001, McKeage et al., 2001, Jamieson et al., 2005, Liu et al., 2009, Renn et al., 2011, Ip et al., 2013). Histopathological studies demonstrated that the decrease in cell body size of DRG neurons was one of the morphological hallmarks of platinum drug-induced peripheral neuropathy in patients (Krarp-Hansen et al., 1999) and animal models (Tomiwa et al., 1986, Cavaletti et al., 1992b, Holmes et al., 1998, Cavaletti et al., 2001, Jamieson et al., 2005, Renn et al., 2011). The decrease in DRG neuronal cell body size appeared to indicate cell body atrophy given the lack of evidence of cell loss or death (Tomiwa et al., 1986, Barajon et al., 1996, Jamieson et al., 2005). Therefore, cell body atrophy of DRG neurons provides a strong indicator of platinum drug-induced peripheral neurotoxicity *in vivo* and has been employed by many researchers (Holmes et al., 1998, Renn et al., 2011, Ip et al., 2013).

The studies presented in this thesis demonstrated that treatment with platinum-based anticancer drugs caused cell body atrophy of DRG neurons *in vitro*. To our best knowledge, this was the first time an *in vitro* culture system was used to investigate DRG neuronal cell body atrophy. Oxaliplatin treatment reduced cell body areas of DRG neurons in a time- and concentration-dependent manner. However, the number of DRG neurons appeared not to be affected by oxaliplatin treatment under the experimental conditions used in these studies, which suggested that the decrease in DRG neuronal cell body areas observed after oxaliplatin treatment may not be due to selective loss of larger neurons. Since apoptotic volume decrease, an early-phase hallmark of apoptosis, is able to cause cell shrinkage under normotonic conditions (Maeno et al., 2000, Nunez et al., 2010), studies were performed to investigate whether the decrease in cell body areas of DRG neurons after oxaliplatin treatment was due to apoptosis. The results of these studies argued against oxaliplatin-induced decrease in DRG neuronal cell body size as an apoptotic event. No apparent TUNEL staining was observed in

cultured DRG neurons after oxaliplatin treatment. Inhibition of apoptotic volume decrease by  $K^+$  and  $Cl^-$  channel blockers did not alter the effects of oxaliplatin treatment on DRG neuronal cell body areas. Given the lack of cell loss or apoptotic cell death, the decrease in cell body areas of DRG neurons after oxaliplatin treatment appeared to indicate cell body atrophy. Furthermore, treatment with cisplatin, ormaplatin,  $Pt(DACH)Cl_2$  reduced cell body areas of cultured DRG neurons, whereas carboplatin treatment appeared not to affect neuronal cell body areas. Taken together, these findings showed that platinum drug-induced DRG neuronal cell body atrophy observed *in vivo* was successfully reproduced in an *in vitro* model.

The findings described in this thesis suggested that platinum drug-induced DRG neuronal cell body atrophy and peripheral neurotoxicity may result from transcriptional inhibition. The level of RNA-incorporated EU in individual DRG neurons correlated with their cell body area, but both were reduced by oxaliplatin treatment in a concentration-dependent manner. Oxaliplatin-induced reductions of levels of RNA-incorporated [ $^3H$ ]uridine and neuronal cell body areas were both reversed by co-incubation with either sodium thiosulfate or cimetidine. In addition, time-course data showed that oxaliplatin-induced decrease in DRG neuronal cell body areas appeared to occur after the induction of inhibition of RNA-incorporation of [ $^3H$ ]uridine and depletion of total RNA content. Moreover, the extent of inhibition of RNA-incorporation of [ $^3H$ ]uridine by different platinum drugs or compounds in cultured DRG cells corresponded to the effects of the different treatments on neuronal cell body areas. Specifically, treatment with cisplatin, ormaplatin and oxaliplatin significantly reduced levels of RNA-incorporated [ $^3H$ ]uridine and neuronal cell body areas of cultured DRG cells. In contrast, carboplatin treatment appeared not to alter RNA-incorporation of [ $^3H$ ]uridine and neuronal cell body areas. Treatment of cultured DRG cells with *R,R*-ormaplatin and *R,R*-



Pt(DACH)Cl<sub>2</sub> caused greater reductions of levels of RNA-incorporated [<sup>3</sup>H]uridine and neuronal cell body areas, compared to their corresponding *S,S*-enantiomers. Further strengthening the possible linkage between transcriptional inhibition and DRG neuronal cell body atrophy was the finding that treatment with a model transcriptional inhibitor, actinomycin D, reduced cell body areas of cultured DRG neurons following its inhibition of RNA-incorporation of [<sup>3</sup>H]uridine. Taken together, these findings suggested that platinum drug-induced DRG neuronal cell body atrophy and peripheral neurotoxicity may be due to transcriptional inhibition.

The mechanism by which transcriptional inhibition leads to cell atrophy remains unclear. However, the findings described in this thesis and other reports have suggested a close correlation between transcriptional activity and cell size. The results presented in this thesis showed that the cell body size of DRG neurons correlated positively with the level of transcription, with highly statistically significant Spearman's rank correlations. A similar relationship between transcriptional activity and neuronal cell body size was also observed in frog spinal motoneurons (Sato et al., 1994). In addition, comparison of different cell types from rodents demonstrated that cell types with large cell size, such as hepatocytes, had higher overall transcriptional activity than cell types with small cell size, such as splenocytes and thymocytes (Schmidt and Schibler, 1995). Moreover, the size-related difference in total transcriptional activity reflected global changes of gene expression, rather than the regulation of a few selected genes (Zhurinsky et al., 2010). According to these findings, it may be reasonable to assume that cells require specific levels of transcription to meet their structural and functional demands. Large cells may need higher levels of transcription than small cells to maintain their large size, increased protein mass and greater metabolic activity (Berciano et al., 2007, Marguerat and Bahler, 2012). When transcription is inhibited by drug treatments,

such as platinum-based anticancer drugs and actinomycin D, or other factors, cells could not produce enough cellular components, such as ribosomes and certain proteins, for maintenance of their normal size (Franklin and Johnson, 1998). Therefore, these cells may have to reduce their size to adapt to the decreased transcriptional activity and protein mass (Franklin and Johnson, 1998).

#### **7.4. Future directions**

Further studies are warranted to determine whether platinum-DNA damage-induced transcriptional inhibition contributes to DRG neuronal cell body atrophy and peripheral neurotoxicity *in vivo*. The Wistar rat is a well-validated animal model to study platinum drug-induced peripheral neurotoxicity (McKeage et al., 2001, Jamieson et al., 2005, Jamieson et al., 2009, Liu et al., 2009). After treatment with platinum-based anticancer drugs, conduction velocity and time of sensory nerve and neuronal cell body areas of DRG tissues could be used as endpoints of peripheral neurotoxicity (Jamieson et al., 2005). Platinum-DNA damage could be determined by measuring levels of platinum binding to the DNA of DRG tissues. Transcriptional activity could be measured by RNA-incorporation of EU or [<sup>3</sup>H]uridine in DRG tissues. Animals treated with platinum-based anticancer drugs may be anticipated to show higher levels of platinum-DNA damage, lower levels of transcription, decreased neuronal cell body size and more severe neurotoxicity compared to untreated controls, should platinum-DNA damage-induced transcriptional inhibition contributes to DRG neuronal cell body atrophy and peripheral neurotoxicity in this species. In addition, further studies on the protective effects of sodium thiosulfate or cimetidine against platinum drug-induced neurotoxicity *in vivo* may be beneficial for developing a therapeutic strategy for platinum drug-induced peripheral neurotoxicity.

## **7.5. Conclusions**

In conclusion, the findings described in this thesis suggested a stepwise mechanism for platinum drug-induced peripheral neurotoxicity. Platinum-DNA damage formed in DRG neurons after treatment with platinum-based anticancer drugs may induce transcriptional inhibition, which in turn may lead to DRG neuronal cell body atrophy and peripheral neurotoxicity. DRG neurons may be particularly vulnerable to platinum drugs through this mechanism due to their requirement for high transcriptional activity to maintain their large cell body size and distant axonal connections. Limiting platinum-DNA damage in DRG neurons may be a potential therapeutic strategy for protecting against platinum drug-induced peripheral neurotoxicity.

## List of references

- Alberts DS, Dorr RT (1998) New Perspectives on an Old Friend: Optimizing Carboplatin for the Treatment of Solid Tumors. *The oncologist* 3:15-34.
- Alcindor T, Beauger N (2011) Oxaliplatin: a review in the era of molecularly targeted therapy. *Current oncology* 18:18-25.
- Amptoulach S, Tsavaris N (2011) Neurotoxicity caused by the treatment with platinum analogues. *Chemotherapy research and practice* 2011:843019.
- Ang WH, Myint M, Lippard SJ (2010) Transcription inhibition by platinum-DNA cross-links in live mammalian cells. *Journal of the American Chemical Society* 132:7429-7435.
- Barajon I, Bersani M, Quartu M, Del Fiacco M, Cavaletti G, Holst JJ, Tredici G (1996) Neuropeptides and morphological changes in cisplatin-induced dorsal root ganglion neuronopathy. *Experimental neurology* 138:93-104.
- Bensaude O (2011) Inhibiting eukaryotic transcription: Which compound to choose? How to evaluate its activity? *Transcription* 2:103-108.
- Berciano MT, Novell M, Villagra NT, Casafont I, Bengoechea R, Val-Bernal JF, Lafarga M (2007) Cajal body number and nucleolar size correlate with the cell body mass in human sensory ganglia neurons. *Journal of structural biology* 158:410-420.
- Boamah EK, Kotova E, Garabedian M, Jarnik M, Tulin AV (2012) Poly(ADP-Ribose) polymerase 1 (PARP-1) regulates ribosomal biogenesis in *Drosophila* nucleoli. *PLoS genetics* 8:e1002442.
- Boisvert FM, Hendzel MJ, Bazett-Jones DP (2000) Promyelocytic leukemia (PML) nuclear bodies are protein structures that do not accumulate RNA. *The Journal of cell biology* 148:283-292.
- Bortner CD, Cidlowski JA (2002) Apoptotic volume decrease and the incredible shrinking cell. *Cell death and differentiation* 9:1307-1310.
- Bortner CD, Cidlowski JA (2007) Cell shrinkage and monovalent cation fluxes: role in apoptosis. *Archives of biochemistry and biophysics* 462:176-188.
- Boulikas T, Vougiouka M (2003) Cisplatin and platinum drugs at the molecular level. (Review). *Oncology reports* 10:1663-1682.

- Breinbauer R, Kohn M (2003) Azide-alkyne coupling: a powerful reaction for bioconjugate chemistry. *Chembiochem : a European journal of chemical biology* 4:1147-1149.
- Brouwers EE, Huitema AD, Beijnen JH, Schellens JH (2008a) Long-term platinum retention after treatment with cisplatin and oxaliplatin. *BMC clinical pharmacology* 8:7.
- Brouwers EE, Huitema AD, Boogerd W, Beijnen JH, Schellens JH (2009) Persistent neuropathy after treatment with cisplatin and oxaliplatin. *Acta oncologica* 48:832-841.
- Brouwers EE, Huitema AD, Schellens JH, Beijnen JH (2008b) The effects of sulfur-containing compounds and gemcitabine on the binding of cisplatin to plasma proteins and DNA determined by inductively coupled plasma mass spectrometry and high performance liquid chromatography-inductively coupled plasma mass spectrometry. *Anti-cancer drugs* 19:621-630.
- Burger H, Loos WJ, Eechoute K, Verweij J, Mathijssen RH, Wiemer EA (2011) Drug transporters of platinum-based anticancer agents and their clinical significance. *Drug resistance updates : reviews and commentaries in antimicrobial and anticancer chemotherapy* 14:22-34.
- Burger H, Zoumaro-Djayoon A, Boersma AW, Helleman J, Berns EM, Mathijssen RH, Loos WJ, Wiemer EA (2010a) Differential transport of platinum compounds by the human organic cation transporter hOCT2 (hSLC22A2). *British journal of pharmacology* 159:898-908.
- Burger K, Muhl B, Harasim T, Rohrmoser M, Malamoussi A, Orban M, Kellner M, Gruber-Eber A, Kremmer E, Holzner M, Eick D (2010b) Chemotherapeutic drugs inhibit ribosome biogenesis at various levels. *The Journal of biological chemistry* 285:12416-12425.
- Buss I, Kalayda GV, Marques-Gallego P, Reedijk J, Jaehde U (2009) Influence of the hOCT2 inhibitor cimetidine on the cellular accumulation and cytotoxicity of oxaliplatin. *International journal of clinical pharmacology and therapeutics* 47:51-54.
- Calkins AS, Iglehart JD, Lazaro JB (2013) DNA damage-induced inhibition of rRNA synthesis by DNA-PK and PARP-1. *Nucleic acids research* 41:7378-7386.
- Canetta R, Rozencweig M, Carter SK (1985) Carboplatin: the clinical spectrum to date. *Cancer treatment reviews* 12 Suppl A:125-136.
- Carmichael N, Cavanagh JB (1976) Autoradiographic localisation of 3H-uridine in spinal ganglion neurones of the rat and the effects of methyl mercury poisoning. *Acta neuropathologica* 34:137-148.
- Casafont I, Berciano MT, Lafarga M (2010) Bortezomib induces the formation of nuclear poly(A) RNA granules enriched in Sam68 and PABPN1 in sensory ganglia neurons. *Neurotoxicity research* 17:167-178.

- Casafont I, Navascues J, Pena E, Lafarga M, Berciano MT (2006) Nuclear organization and dynamics of transcription sites in rat sensory ganglia neurons detected by incorporation of 5'-fluorouridine into nascent RNA. *Neuroscience* 140:453-462.
- Catino JJ, Francher DM, Schurig JE (1986) Evaluation of cis-diamminedichloroplatinum(II) combined with metoclopramide or sodium thiosulfate on L1210 leukemia in vitro and in vivo. *Cancer chemotherapy and pharmacology* 18:1-4.
- Cavaletti G, Bogliun G, Zincone A, Marzorati L, Melzi P, Frattola L, Marzola M, Bonazzi C, Cantu MG, Chiari S, Galli A, Bregni M, Gianni MA (1998) Neuro- and ototoxicity of high-dose carboplatin treatment in poor prognosis ovarian cancer patients. *Anticancer research* 18:3797-3802.
- Cavaletti G, Marzorati L, Bogliun G, Colombo N, Marzola M, Pittelli MR, Tredici G (1992a) Cisplatin-induced peripheral neurotoxicity is dependent on total-dose intensity and single-dose intensity. *Cancer* 69:203-207.
- Cavaletti G, Tredici G, Marmioli P, Petruccioli MG, Barajon I, Fabbrica D (1992b) Morphometric study of the sensory neuron and peripheral nerve changes induced by chronic cisplatin (DDP) administration in rats. *Acta neuropathologica* 84:364-371.
- Cavaletti G, Tredici G, Petruccioli MG, Donde E, Tredici P, Marmioli P, Minoia C, Ronchi A, Bayssas M, Etienne GG (2001) Effects of different schedules of oxaliplatin treatment on the peripheral nervous system of the rat. *European journal of cancer* 37:2457-2463.
- Cavaletti G, Tredici G, Pizzini G, Minoia A (1990) Tissue platinum concentrations and cisplatin schedules. *Lancet* 336:1003.
- Cersosimo RJ (2005) Oxaliplatin-associated neuropathy: a review. *The Annals of pharmacotherapy* 39:128-135.
- Chaney SG, Campbell SL, Bassett E, Wu Y (2005) Recognition and processing of cisplatin- and oxaliplatin-DNA adducts. *Critical reviews in oncology/hematology* 53:3-11.
- Chaney SG, Wyrick S, Till GK (1990) In vitro biotransformations of tetrachloro(d,l-trans)-1,2-diaminocyclohexaneplatinum(IV) (tetraplatin) in rat plasma. *Cancer research* 50:4539-4545.
- Chang LW, Martin AH, Hartmann HA (1972) Quantitative autoradiographic study on the RNA synthesis in the neurons after mercury intoxication. *Experimental neurology* 37:62-67.
- Ciarimboli G (2012) Membrane transporters as mediators of Cisplatin effects and side effects. *Scientifica* 2012:473829.

- Ciarimboli G (2014) Membrane transporters as mediators of cisplatin side-effects. *Anticancer research* 34:547-550.
- Ciarimboli G, Deuster D, Knief A, Sperling M, Holtkamp M, Edemir B, Pavenstadt H, Lanvers-Kaminsky C, am Zehnhoff-Dinnesen A, Schinkel AH, Koepsell H, Jurgens H, Schlatter E (2010) Organic cation transporter 2 mediates cisplatin-induced oto- and nephrotoxicity and is a target for protective interventions. *The American journal of pathology* 176:1169-1180.
- Ciarimboli G, Ludwig T, Lang D, Pavenstadt H, Koepsell H, Piechota HJ, Haier J, Jaehde U, Zisowsky J, Schlatter E (2005) Cisplatin nephrotoxicity is critically mediated via the human organic cation transporter 2. *The American journal of pathology* 167:1477-1484.
- Cmarko D, Verschure PJ, Martin TE, Dahmus ME, Krause S, Fu XD, van Driel R, Fakan S (1999) Ultrastructural analysis of transcription and splicing in the cell nucleus after bromo-UTP microinjection. *Molecular biology of the cell* 10:211-223.
- Cullinane C, Mazur SJ, Essigmann JM, Phillips DR, Bohr VA (1999) Inhibition of RNA polymerase II transcription in human cell extracts by cisplatin DNA damage. *Biochemistry* 38:6204-6212.
- Damsma GE, Alt A, Brueckner F, Carell T, Cramer P (2007) Mechanism of transcriptional stalling at cisplatin-damaged DNA. *Nature structural & molecular biology* 14:1127-1133.
- Danford AJ, Wang D, Wang Q, Tullius TD, Lippard SJ (2005) Platinum anticancer drug damage enforces a particular rotational setting of DNA in nucleosomes. *Proceedings of the National Academy of Sciences of the United States of America* 102:12311-12316.
- Desnoyers S, Kaufmann SH, Poirier GG (1996) Alteration of the nucleolar localization of poly(ADP-ribose) polymerase upon treatment with transcription inhibitors. *Experimental cell research* 227:146-153.
- Desoize B, Madoulet C (2002) Particular aspects of platinum compounds used at present in cancer treatment. *Critical reviews in oncology/hematology* 42:317-325.
- Di Francesco AM, Ruggiero A, Riccardi R (2002) Cellular and molecular aspects of drugs of the future: oxaliplatin. *Cellular and molecular life sciences : CMLS* 59:1914-1927.
- Dickey DT, Wu YJ, Muldoon LL, Neuwelt EA (2005) Protection against cisplatin-induced toxicities by N-acetylcysteine and sodium thiosulfate as assessed at the molecular, cellular, and in vivo levels. *The Journal of pharmacology and experimental therapeutics* 314:1052-1058.

- Doolittle ND, Muldoon LL, Brummett RE, Tyson RM, Lacy C, Bubalo JS, Kraemer DF, Heinrich MC, Henry JA, Neuwelt EA (2001) Delayed sodium thiosulfate as an otoprotectant against carboplatin-induced hearing loss in patients with malignant brain tumors. *Clinical cancer research : an official journal of the American Association for Cancer Research* 7:493-500.
- Dzagnidze A, Katsarava Z, Makhalova J, Liedert B, Yoon MS, Kaube H, Limmroth V, Thomale J (2007) Repair capacity for platinum-DNA adducts determines the severity of cisplatin-induced peripheral neuropathy. *The Journal of neuroscience : the official journal of the Society for Neuroscience* 27:9451-9457.
- Extra JM, Marty M, Brienza S, Misset JL (1998) Pharmacokinetics and safety profile of oxaliplatin. *Seminars in oncology* 25:13-22.
- Filipski KK, Mathijssen RH, Mikkelsen TS, Schinkel AH, Sparreboom A (2009) Contribution of organic cation transporter 2 (OCT2) to cisplatin-induced nephrotoxicity. *Clinical pharmacology and therapeutics* 86:396-402.
- Franke RM, Kosloske AM, Lancaster CS, Filipski KK, Hu C, Zolk O, Mathijssen RH, Sparreboom A (2010) Influence of Oct1/Oct2-deficiency on cisplatin-induced changes in urinary N-acetyl-beta-D-glucosaminidase. *Clinical cancer research : an official journal of the American Association for Cancer Research* 16:4198-4206.
- Franklin JL, Johnson EM (1998) Control of neuronal size homeostasis by trophic factor-mediated coupling of protein degradation to protein synthesis. *The Journal of cell biology* 142:1313-1324.
- Gamelin E, Gamelin L, Bossi L, Quasthoff S (2002) Clinical aspects and molecular basis of oxaliplatin neurotoxicity: current management and development of preventive measures. *Seminars in oncology* 29:21-33.
- Gibbons GR, Wyrick S, Chaney SG (1989) Rapid reduction of tetrachloro(D,L-trans)1,2-diaminocyclohexaneplatinum(IV) (tetraplatin) in RPMI 1640 tissue culture medium. *Cancer research* 49:1402-1407.
- Go RS, Adjei AA (1999) Review of the comparative pharmacology and clinical activity of cisplatin and carboplatin. *Journal of clinical oncology : official journal of the American Society of Clinical Oncology* 17:409-422.
- Goldschmidt RB, Steward O (1992) Retrograde regulation of neuronal size in the entorhinal cortex: consequences of the destruction of dentate gyrus granule cells with colchicine. *Restorative neurology and neuroscience* 3:335-343.
- Gomes C, Smith SC, Youssef MN, Zheng JJ, Hagg T, Hetman M (2011) RNA polymerase 1-driven transcription as a mediator of BDNF-induced neurite outgrowth. *The Journal of biological chemistry* 286:4357-4363.



- Gozdz A, Vashishta A, Kalita K, Szatmari E, Zheng JJ, Tamiya S, Delamere NA, Hetman M (2008) Cisplatin-mediated activation of extracellular signal-regulated kinases 1/2 (ERK1/2) by inhibition of ERK1/2 phosphatases. *Journal of neurochemistry* 106:2056-2067.
- Graham J, Mushin M, Kirkpatrick P (2004) Oxaliplatin. *Nature reviews Drug discovery* 3:11-12.
- Gregg RW, Molepo JM, Monpetit VJ, Mikael NZ, Redmond D, Gadia M, Stewart DJ (1992) Cisplatin neurotoxicity: the relationship between dosage, time, and platinum concentration in neurologic tissues, and morphologic evidence of toxicity. *Journal of clinical oncology : official journal of the American Society of Clinical Oncology* 10:795-803.
- Grothey A (2003) Oxaliplatin-safety profile: neurotoxicity. *Seminars in oncology* 30:5-13.
- Grunberg SM, Sonka S, Stevenson LL, Muggia FM (1989) Progressive paresthesias after cessation of therapy with very high-dose cisplatin. *Cancer chemotherapy and pharmacology* 25:62-64.
- Halicka HD, Bedner E, Darzynkiewicz Z (2000) Segregation of RNA and separate packaging of DNA and RNA in apoptotic bodies during apoptosis. *Experimental cell research* 260:248-256.
- Haller I, Hausott B, Tomaselli B, Keller C, Klimaschewski L, Gerner P, Lirk P (2006) Neurotoxicity of lidocaine involves specific activation of the p38 mitogen-activated protein kinase, but not extracellular signal-regulated or c-jun N-terminal kinases, and is mediated by arachidonic acid metabolites. *Anesthesiology* 105:1024-1033.
- Harned TM, Kalous O, Neuwelt A, Loera J, Ji L, Iovine P, Sposto R, Neuwelt EA, Reynolds CP (2008) Sodium thiosulfate administered six hours after cisplatin does not compromise antineuroblastoma activity. *Clinical cancer research : an official journal of the American Association for Cancer Research* 14:533-540.
- Harper AA, Lawson SN (1985) Conduction velocity is related to morphological cell type in rat dorsal root ganglion neurones. *The Journal of physiology* 359:31-46.
- He W, Li H, Min X, Liu J, Hu B, Hou S, Wang J (2010) Activation of volume-sensitive Cl(-) channel is involved in carboplatin-induced apoptosis in human lung adenocarcinoma cells. *Cancer biology & therapy* 9:885-891.
- Hernandez-Enriquez B, Arellano RO, Moran J (2010) Role for ionic fluxes on cell death and apoptotic volume decrease in cultured cerebellar granule neurons. *Neuroscience* 167:298-311.

- Hernandez-Enriquez B, Guemez-Gamboa A, Moran J (2011) Reactive oxygen species are related to ionic fluxes and volume decrease in apoptotic cerebellar granule neurons: role of NOX enzymes. *Journal of neurochemistry* 117:654-664.
- Hetman M, Vashishta A, Rempala G (2010) Neurotoxic mechanisms of DNA damage: focus on transcriptional inhibition. *Journal of neurochemistry* 114:1537-1549.
- Higby DJ, Wallace HJ, Jr., Albert DJ, Holland JF (1974) Diaminodichloroplatinum: a phase I study showing responses in testicular and other tumors. *Cancer* 33:1219-1215.
- Holmes J, Stanko J, Varchenko M, Ding H, Madden VJ, Bagnell CR, Wyrick SD, Chaney SG (1998) Comparative neurotoxicity of oxaliplatin, cisplatin, and ormaplatin in a Wistar rat model. *Toxicological sciences : an official journal of the Society of Toxicology* 46:342-351.
- Hovestadt A, van der Burg ME, Verbiest HB, van Putten WL, Vecht CJ (1992) The course of neuropathy after cessation of cisplatin treatment, combined with Org 2766 or placebo. *Journal of neurology* 239:143-146.
- International Collaborative Ovarian Neoplasm G (2002) Paclitaxel plus carboplatin versus standard chemotherapy with either single-agent carboplatin or cyclophosphamide, doxorubicin, and cisplatin in women with ovarian cancer: the ICON3 randomised trial. *Lancet* 360:505-515.
- Ip V, Liu JJ, McKeage MJ (2013) Evaluation of effects of copper histidine on copper transporter 1-mediated accumulation of platinum and oxaliplatin-induced neurotoxicity in vitro and in vivo. *Clinical and experimental pharmacology & physiology* 40:371-378.
- Ise T, Shimizu T, Lee EL, Inoue H, Kohno K, Okada Y (2005) Roles of volume-sensitive Cl<sup>-</sup> channel in cisplatin-induced apoptosis in human epidermoid cancer cells. *The Journal of membrane biology* 205:139-145.
- Iwamoto Y, Kawano T, Ishizawa M, Aoki K, Kuroiwa T, Baba T (1985) Inactivation of cis-diamminedichloroplatinum (II) in blood and protection of its toxicity by sodium thiosulfate in rabbits. *Cancer chemotherapy and pharmacology* 15:228-232.
- Jamieson ER, Lippard SJ (1999) Structure, Recognition, and Processing of Cisplatin-DNA Adducts. *Chemical reviews* 99:2467-2498.
- Jamieson SM, Liu J, Connor B, McKeage MJ (2005) Oxaliplatin causes selective atrophy of a subpopulation of dorsal root ganglion neurons without inducing cell loss. *Cancer chemotherapy and pharmacology* 56:391-399.
- Jamieson SM, Subramaniam J, Liu JJ, Jong NN, Ip V, Connor B, McKeage MJ (2009) Oxaliplatin-induced loss of phosphorylated heavy neurofilament subunit neuronal immunoreactivity in rat DRG tissue. *Molecular pain* 5:66.

- Jao CY, Salic A (2008) Exploring RNA transcription and turnover in vivo by using click chemistry. *Proceedings of the National Academy of Sciences of the United States of America* 105:15779-15784.
- Jennerwein MM, Eastman A, Khokhar A (1989) Characterization of adducts produced in DNA by isomeric 1,2-diaminocyclohexaneplatinum(II) complexes. *Chemico-biological interactions* 70:39-49.
- Jong NN, Nakanishi T, Liu JJ, Tamai I, McKeage MJ (2011) Oxaliplatin transport mediated by organic cation/carnitine transporters OCTN1 and OCTN2 in overexpressing human embryonic kidney 293 cells and rat dorsal root ganglion neurons. *The Journal of pharmacology and experimental therapeutics* 338:537-547.
- Jordan P, Carmo-Fonseca M (1998) Cisplatin inhibits synthesis of ribosomal RNA in vivo. *Nucleic acids research* 26:2831-2836.
- Jordan P, Carmo-Fonseca M (2000) Molecular mechanisms involved in cisplatin cytotoxicity. *Cellular and molecular life sciences : CMLS* 57:1229-1235.
- Jung Y, Lippard SJ (2003) Multiple states of stalled T7 RNA polymerase at DNA lesions generated by platinum anticancer agents. *The Journal of biological chemistry* 278:52084-52092.
- Jung Y, Lippard SJ (2006) RNA polymerase II blockage by cisplatin-damaged DNA. Stability and polyubiquitylation of stalled polymerase. *The Journal of biological chemistry* 281:1361-1370.
- Jung Y, Lippard SJ (2007) Direct cellular responses to platinum-induced DNA damage. *Chemical reviews* 107:1387-1407.
- Kalita K, Makonchuk D, Gomes C, Zheng JJ, Hetman M (2008) Inhibition of nucleolar transcription as a trigger for neuronal apoptosis. *Journal of neurochemistry* 105:2286-2299.
- Kalveram B, Lihoradova O, Indran SV, Head JA, Ikegami T (2013) Using click chemistry to measure the effect of viral infection on host-cell RNA synthesis. *Journal of visualized experiments : JoVE*.
- Kartalou M, Essigmann JM (2001) Mechanisms of resistance to cisplatin. *Mutation research* 478:23-43.
- Kasparkova J, Vojtiskova M, Natile G, Brabec V (2008) Unique properties of DNA interstrand cross-links of antitumor oxaliplatin and the effect of chirality of the carrier ligand. *Chemistry* 14:1330-1341.

- Katsuda H, Yamashita M, Katsura H, Yu J, Waki Y, Nagata N, Sai Y, Miyamoto K (2010) Protecting cisplatin-induced nephrotoxicity with cimetidine does not affect antitumor activity. *Biological & pharmaceutical bulletin* 33:1867-1871.
- Kelland L (2007) The resurgence of platinum-based cancer chemotherapy. *Nature reviews Cancer* 7:573-584.
- Kovacs AF, Cinatl J, Jr. (2002) In vitro cytotoxic dose-relation of cisplatin and sodium thiosulphate in human tongue and oesophageal squamous carcinoma cell lines. *Journal of cranio-maxillo-facial surgery : official publication of the European Association for Cranio-Maxillo-Facial Surgery* 30:54-58.
- Krarpup-Hansen A, Rietz B, Krarpup C, Heydorn K, Rorth M, Schmalbruch H (1999) Histology and platinum content of sensory ganglia and sural nerves in patients treated with cisplatin and carboplatin: an autopsy study. *Neuropathology and applied neurobiology* 25:29-40.
- Krishnan AV, Goldstein D, Friedlander M, Kiernan MC (2005) Oxaliplatin-induced neurotoxicity and the development of neuropathy. *Muscle & nerve* 32:51-60.
- Kuhn A, Gottlieb TM, Jackson SP, Grummt I (1995) DNA-dependent protein kinase: a potent inhibitor of transcription by RNA polymerase I. *Genes & development* 9:193-203.
- Kweekel DM, Gelderblom H, Guchelaar HJ (2005) Pharmacology of oxaliplatin and the use of pharmacogenomics to individualize therapy. *Cancer treatment reviews* 31:90-105.
- Laine JP, Egly JM (2006) Initiation of DNA repair mediated by a stalled RNA polymerase II. *The EMBO journal* 25:387-397.
- Lee EL, Shimizu T, Ise T, Numata T, Kohno K, Okada Y (2007) Impaired activity of volume-sensitive Cl<sup>-</sup> channel is involved in cisplatin resistance of cancer cells. *Journal of cellular physiology* 211:513-521.
- Levi F, Metzger G, Massari C, Milano G (2000) Oxaliplatin: pharmacokinetics and chronopharmacological aspects. *Clinical pharmacokinetics* 38:1-21.
- Liu JJ, Jamieson SM, Subramaniam J, Ip V, Jong NN, Mercer JF, McKeage MJ (2009) Neuronal expression of copper transporter 1 in rat dorsal root ganglia: association with platinum neurotoxicity. *Cancer chemotherapy and pharmacology* 64:847-856.
- Liu JJ, Kim Y, Yan F, Ding Q, Ip V, Jong NN, Mercer JF, McKeage MJ (2013) Contributions of rat Ctr1 to the uptake and toxicity of copper and platinum anticancer drugs in dorsal root ganglion neurons. *Biochemical pharmacology* 85:207-215.
- Liu JJ, Lu J, McKeage MJ (2012) Membrane transporters as determinants of the pharmacology of platinum anticancer drugs. *Current cancer drug targets* 12:962-986.

- Ljungman M, Zhang F, Chen F, Rainbow AJ, McKay BC (1999) Inhibition of RNA polymerase II as a trigger for the p53 response. *Oncogene* 18:583-592.
- Ludwig T, Riethmuller C, Gekle M, Schwerdt G, Oberleithner H (2004) Nephrotoxicity of platinum complexes is related to basolateral organic cation transport. *Kidney international* 66:196-202.
- Luger K (2006) Dynamic nucleosomes. *Chromosome research : an international journal on the molecular, supramolecular and evolutionary aspects of chromosome biology* 14:5-16.
- Luo FR, Wyrick SD, Chaney SG (1999) Comparative neurotoxicity of oxaliplatin, ormaplatin, and their biotransformation products utilizing a rat dorsal root ganglia in vitro explant culture model. *Cancer chemotherapy and pharmacology* 44:29-38.
- Luo X, Kraus WL (2012) On PAR with PARP: cellular stress signaling through poly(ADP-ribose) and PARP-1. *Genes & development* 26:417-432.
- Machover D, Diaz-Rubio E, de Gramont A, Schilf A, Gastiaburu JJ, Brienza S, Itzhaki M, Metzger G, N'Daw D, Vignoud J, Abad A, Francois E, Gamelin E, Marty M, Sastre J, Seitz JF, Ychou M (1996) Two consecutive phase II studies of oxaliplatin (L-OHP) for treatment of patients with advanced colorectal carcinoma who were resistant to previous treatment with fluoropyrimidines. *Annals of oncology : official journal of the European Society for Medical Oncology / ESMO* 7:95-98.
- Maeno E, Ishizaki Y, Kanaseki T, Hazama A, Okada Y (2000) Normotonic cell shrinkage because of disordered volume regulation is an early prerequisite to apoptosis. *Proceedings of the National Academy of Sciences of the United States of America* 97:9487-9492.
- Mani S, Graham MA, Bregman DB, Ivy P, Chaney SG (2002) Oxaliplatin: a review of evolving concepts. *Cancer investigation* 20:246-263.
- Marguerat S, Bahler J (2012) Coordinating genome expression with cell size. *Trends in genetics : TIG* 28:560-565.
- Mauldin SK, Gibbons G, Wyrick SD, Chaney SG (1988) Intracellular biotransformation of platinum compounds with the 1,2-diaminocyclohexane carrier ligand in the L1210 cell line. *Cancer research* 48:5136-5144.
- McDonald ES, Randon KR, Knight A, Windebank AJ (2005) Cisplatin preferentially binds to DNA in dorsal root ganglion neurons in vitro and in vivo: a potential mechanism for neurotoxicity. *Neurobiology of disease* 18:305-313.
- McKeage MJ (1995) Comparative adverse effect profiles of platinum drugs. *Drug safety* 13:228-244.

- McKeage MJ, Hsu T, Screnci D, Haddad G, Baguley BC (2001) Nucleolar damage correlates with neurotoxicity induced by different platinum drugs. *British journal of cancer* 85:1219-1225.
- McWhinney SR, Goldberg RM, McLeod HL (2009) Platinum neurotoxicity pharmacogenetics. *Molecular cancer therapeutics* 8:10-16.
- Meek K, Dang V, Lees-Miller SP (2008) DNA-PK: the means to justify the ends? *Advances in immunology* 99:33-58.
- Meijer C, de Vries EG, Marmiroli P, Tredici G, Frattola L, Cavaletti G (1999) Cisplatin-induced DNA-platination in experimental dorsal root ganglia neuropathy. *Neurotoxicology* 20:883-887.
- Mello JA, Lippard SJ, Essigmann JM (1995) DNA adducts of cis-diamminedichloroplatinum(II) and its trans isomer inhibit RNA polymerase II differentially in vivo. *Biochemistry* 34:14783-14791.
- Micetich KC, Barnes D, Erickson LC (1985) A comparative study of the cytotoxicity and DNA-damaging effects of cis-(diammino)(1,1-cyclobutanedicarboxylato)-platinum(II) and cis-diamminedichloroplatinum(II) on L1210 cells. *Cancer research* 45:4043-4047.
- Michaelidis TM, Grummt I (2002) Mechanism of inhibition of RNA polymerase I transcription by DNA-dependent protein kinase. *Biological chemistry* 383:1683-1690.
- Min XJ, Li H, Hou SC, He W, Liu J, Hu B, Wang J (2011) Dysfunction of volume-sensitive chloride channels contributes to cisplatin resistance in human lung adenocarcinoma cells. *Experimental biology and medicine* 236:483-491.
- Mollman JE (1990) Cisplatin neurotoxicity. *The New England journal of medicine* 322:126-127.
- Muldoon LL, Pagel MA, Kroll RA, Brummett RE, Doolittle ND, Zuhowski EG, Egorin MJ, Neuwelt EA (2000) Delayed administration of sodium thiosulfate in animal models reduces platinum ototoxicity without reduction of antitumor activity. *Clinical cancer research : an official journal of the American Association for Cancer Research* 6:309-315.
- Nagai N, Hotta K, Yamamura H, Ogata H (1995) Effects of sodium thiosulfate on the pharmacokinetics of unchanged cisplatin and on the distribution of platinum species in rat kidney: protective mechanism against cisplatin nephrotoxicity. *Cancer chemotherapy and pharmacology* 36:404-410.
- Neuwelt EA, Brummett RE, Remsen LG, Kroll RA, Pagel MA, McCormick CI, Guitjens S, Muldoon LL (1996) In vitro and animal studies of sodium thiosulfate as a potential chemoprotectant against carboplatin-induced ototoxicity. *Cancer research* 56:706-709.

- Neuwelt EA, Gilmer-Knight K, Lacy C, Nicholson HS, Kraemer DF, Doolittle ND, Hornig GW, Muldoon LL (2006) Toxicity profile of delayed high dose sodium thiosulfate in children treated with carboplatin in conjunction with blood-brain-barrier disruption. *Pediatric blood & cancer* 47:174-182.
- Neuwelt EA, Pagel MA, Kraemer DF, Peterson DR, Muldoon LL (2004) Bone marrow chemoprotection without compromise of chemotherapy efficacy in a rat brain tumor model. *The Journal of pharmacology and experimental therapeutics* 309:594-599.
- Nunez R, Sancho-Martinez SM, Novoa JM, Lopez-Hernandez FJ (2010) Apoptotic volume decrease as a geometric determinant for cell dismantling into apoptotic bodies. *Cell death and differentiation* 17:1665-1671.
- O'Rourke TJ, Weiss GR, New P, Burris HA, 3rd, Rodriguez G, Eckhardt J, Hardy J, Kuhn JG, Fields S, Clark GM, et al. (1994) Phase I clinical trial of ormaplatin (tetraplatin, NSC 363812). *Anti-cancer drugs* 5:520-526.
- Ober M, Lippard SJ (2007) Cisplatin damage overrides the predefined rotational setting of positioned nucleosomes. *Journal of the American Chemical Society* 129:6278-6286.
- Ober M, Lippard SJ (2008) A 1,2-d(GpG) cisplatin intrastrand cross-link influences the rotational and translational setting of DNA in nucleosomes. *Journal of the American Chemical Society* 130:2851-2861.
- Okada Y, Maeno E, Shimizu T, Dezaki K, Wang J, Morishima S (2001) Receptor-mediated control of regulatory volume decrease (RVD) and apoptotic volume decrease (AVD). *The Journal of physiology* 532:3-16.
- Okada Y, Shimizu T, Maeno E, Tanabe S, Wang X, Takahashi N (2006) Volume-sensitive chloride channels involved in apoptotic volume decrease and cell death. *The Journal of membrane biology* 209:21-29.
- Ozols RF, Ostchega Y, Myers CE, Young RC (1985) High-dose cisplatin in hypertonic saline in refractory ovarian cancer. *Journal of clinical oncology : official journal of the American Society of Clinical Oncology* 3:1246-1250.
- Ozols RF, Young RC (1985) High-dose cisplatin therapy in ovarian cancer. *Seminars in oncology* 12:21-30.
- Pabla N, Murphy RF, Liu K, Dong Z (2009) The copper transporter Ctr1 contributes to cisplatin uptake by renal tubular cells during cisplatin nephrotoxicity. *American journal of physiology Renal physiology* 296:F505-511.
- Page JD, Husain I, Sancar A, Chaney SG (1990) Effect of the diamminocyclohexane carrier ligand on platinum adduct formation, repair, and lethality. *Biochemistry* 29:1016-1024.

- Palanca A, Casafont I, Berciano MT, Lafarga M (2014) Proteasome inhibition induces DNA damage and reorganizes nuclear architecture and protein synthesis machinery in sensory ganglion neurons. *Cellular and molecular life sciences : CMLS* 71:1961-1975.
- Pasantes-Morales H, Tuz K (2006) Volume changes in neurons: hyperexcitability and neuronal death. *Contributions to nephrology* 152:221-240.
- Pasetto LM, D'Andrea MR, Rossi E, Monfardini S (2006) Oxaliplatin-related neurotoxicity: how and why? *Critical reviews in oncology/hematology* 59:159-168.
- Pendyala L, Kidani Y, Perez R, Wilkes J, Bernacki RJ, Creaven PJ (1995) Cytotoxicity, cellular accumulation and DNA binding of oxaliplatin isomers. *Cancer letters* 97:177-184.
- Piccart MJ, Lamb H, Vermorken JB (2001) Current and future potential roles of the platinum drugs in the treatment of ovarian cancer. *Annals of oncology : official journal of the European Society for Medical Oncology / ESMO* 12:1195-1203.
- Pope JE, Deer TR, Kramer J (2013) A systematic review: current and future directions of dorsal root ganglion therapeutics to treat chronic pain. *Pain medicine* 14:1477-1496.
- Poulsen KA, Andersen EC, Hansen CF, Klausen TK, Hougaard C, Lambert IH, Hoffmann EK (2010) Deregulation of apoptotic volume decrease and ionic movements in multidrug-resistant tumor cells: role of chloride channels. *American journal of physiology Cell physiology* 298:C14-25.
- Qu D, Zhou L, Wang W, Wang Z, Wang G, Chi W, Zhang B (2013) 5-Ethynylcytidine as a new agent for detecting RNA synthesis in live cells by "click" chemistry. *Analytical biochemistry* 434:128-135.
- Quasthoff S, Hartung HP (2002) Chemotherapy-induced peripheral neuropathy. *Journal of neurology* 249:9-17.
- Raymond E, Chaney SG, Taamma A, Cvitkovic E (1998) Oxaliplatin: a review of preclinical and clinical studies. *Annals of oncology : official journal of the European Society for Medical Oncology / ESMO* 9:1053-1071.
- Reardon JT, Vaisman A, Chaney SG, Sancar A (1999) Efficient nucleotide excision repair of cisplatin, oxaliplatin, and Bis-aceto-amine-dichloro-cyclohexylamine-platinum(IV) (JM216) platinum intrastrand DNA diadducts. *Cancer research* 59:3968-3971.
- Renn CL, Carozzi VA, Rhee P, Gallop D, Dorsey SG, Cavaletti G (2011) Multimodal assessment of painful peripheral neuropathy induced by chronic oxaliplatin-based chemotherapy in mice. *Molecular pain* 7:29.



- Rixe O, Ortuzar W, Alvarez M, Parker R, Reed E, Paull K, Fojo T (1996) Oxaliplatin, tetraplatin, cisplatin, and carboplatin: spectrum of activity in drug-resistant cell lines and in the cell lines of the National Cancer Institute's Anticancer Drug Screen panel. *Biochemical pharmacology* 52:1855-1865.
- Roelofs RI, Hrushesky W, Rogin J, Rosenberg L (1984) Peripheral sensory neuropathy and cisplatin chemotherapy. *Neurology* 34:934-938.
- Rosenberg B, Vancamp L, Krigas T (1965) Inhibition of Cell Division in Escherichia Coli by Electrolysis Products from a Platinum Electrode. *Nature* 205:698-699.
- Rosenberg B, VanCamp L, Trosko JE, Mansour VH (1969) Platinum compounds: a new class of potent antitumour agents. *Nature* 222:385-386.
- Rostovtsev VV, Green LG, Fokin VV, Sharpless KB (2002) A stepwise Huisgen cycloaddition process: copper(I)-catalyzed regioselective "ligation" of azides and terminal alkynes. *Angewandte Chemie* 41:2596-2599.
- Sadoni N, Zink D (2004) Nascent RNA synthesis in the context of chromatin architecture. *Chromosome research : an international journal on the molecular, supramolecular and evolutionary aspects of chromosome biology* 12:439-451.
- Sapunar D, Kostic S, Banozic A, Puljak L (2012) Dorsal root ganglion - a potential new therapeutic target for neuropathic pain. *Journal of pain research* 5:31-38.
- Saris CP, van de Vaart PJ, Rietbroek RC, Blommaert FA (1996) In vitro formation of DNA adducts by cisplatin, lobaplatin and oxaliplatin in calf thymus DNA in solution and in cultured human cells. *Carcinogenesis* 17:2763-2769.
- Sato S, Burgess SB, McIlwain DL (1994) Transcription and motoneuron size. *Journal of neurochemistry* 63:1609-1615.
- Schilder RJ, LaCreta FP, Perez RP, Johnson SW, Brennan JM, Rogatko A, Nash S, McAleer C, Hamilton TC, Roby D, et al. (1994) Phase I and pharmacokinetic study of ormaplatin (tetraplatin, NSC 363812) administered on a day 1 and day 8 schedule. *Cancer research* 54:709-717.
- Schmidt EE, Schibler U (1995) Cell size regulation, a mechanism that controls cellular RNA accumulation: consequences on regulation of the ubiquitous transcription factors Oct1 and NF-Y and the liver-enriched transcription factor DBP. *The Journal of cell biology* 128:467-483.
- Schmidt W, Chaney SG (1993) Role of carrier ligand in platinum resistance of human carcinoma cell lines. *Cancer research* 53:799-805.

- Screnci D, Er HM, Hambley TW, Galettis P, Brouwer W, McKeage MJ (1997) Stereoselective peripheral sensory neurotoxicity of diamminocyclohexane platinum enantiomers related to ormaplatin and oxaliplatin. *British journal of cancer* 76:502-510.
- Screnci D, McKeage MJ (1999) Platinum neurotoxicity: clinical profiles, experimental models and neuroprotective approaches. *Journal of inorganic biochemistry* 77:105-110.
- Screnci D, McKeage MJ, Galettis P, Hambley TW, Palmer BD, Baguley BC (2000) Relationships between hydrophobicity, reactivity, accumulation and peripheral nerve toxicity of a series of platinum drugs. *British journal of cancer* 82:966-972.
- Scroggs RS, Fox AP (1992) Calcium current variation between acutely isolated adult rat dorsal root ganglion neurons of different size. *The Journal of physiology* 445:639-658.
- Sensenbrenner M, Treska-Ciesielski J, Lodin Z, Mandel P (1970) Autoradiographic study of RNA synthesis in isolated cells in culture from chick embryo spinal ganglia. *Zeitschrift fur Zellforschung und mikroskopische Anatomie* 106:615-626.
- Sghirlanzoni A, Pareyson D, Lauria G (2005) Sensory neuron diseases. *The Lancet Neurology* 4:349-361.
- Sharma S, Gong P, Temple B, Bhattacharyya D, Dokholyan NV, Chaney SG (2007) Molecular dynamic simulations of cisplatin- and oxaliplatin-d(GG) intrastand cross-links reveal differences in their conformational dynamics. *Journal of molecular biology* 373:1123-1140.
- Siegal T, Haim N (1990) Cisplatin-induced peripheral neuropathy. Frequent off-therapy deterioration, demyelinating syndromes, and muscle cramps. *Cancer* 66:1117-1123.
- Sleijfer DT, Offerman JJ, Mulder NH, Verweij M, van der Hem GK, Schraffordt Koops HS, Meijer S (1987) The protective potential of the combination of verapamil and cimetidine on cisplatin-induced nephrotoxicity in man. *Cancer* 60:2823-2828.
- Smith DS, Skene JH (1997) A transcription-dependent switch controls competence of adult neurons for distinct modes of axon growth. *The Journal of neuroscience : the official journal of the Society for Neuroscience* 17:646-658.
- Sobell HM (1985) Actinomycin and DNA transcription. *Proceedings of the National Academy of Sciences of the United States of America* 82:5328-5331.
- Sooriyaarachchi M, Narendran A, Gailer J (2012) The effect of sodium thiosulfate on the metabolism of cis-platin in human plasma in vitro. *Metallomics : integrated biometal science* 4:960-967.

- Sorenson CM, Barry MA, Eastman A (1990) Analysis of events associated with cell cycle arrest at G2 phase and cell death induced by cisplatin. *Journal of the National Cancer Institute* 82:749-755.
- Sorenson CM, Eastman A (1988a) Influence of cis-diamminedichloroplatinum(II) on DNA synthesis and cell cycle progression in excision repair proficient and deficient Chinese hamster ovary cells. *Cancer research* 48:6703-6707.
- Sorenson CM, Eastman A (1988b) Mechanism of cis-diamminedichloroplatinum(II)-induced cytotoxicity: role of G2 arrest and DNA double-strand breaks. *Cancer research* 48:4484-4488.
- Sprowl JA, Ciarimboli G, Lancaster CS, Giovinazzo H, Gibson AA, Du G, Janke LJ, Cavaletti G, Shields AF, Sparreboom A (2013) Oxaliplatin-induced neurotoxicity is dependent on the organic cation transporter OCT2. *Proceedings of the National Academy of Sciences of the United States of America* 110:11199-11204.
- Stein A, Arnold D (2012) Oxaliplatin: a review of approved uses. *Expert opinion on pharmacotherapy* 13:125-137.
- Ta LE, Espeset L, Podratz J, Windebank AJ (2006) Neurotoxicity of oxaliplatin and cisplatin for dorsal root ganglion neurons correlates with platinum-DNA binding. *Neurotoxicology* 27:992-1002.
- Thompson SW, Davis LE, Kornfeld M, Hilgers RD, Standefer JC (1984) Cisplatin neuropathy. Clinical, electrophysiologic, morphologic, and toxicologic studies. *Cancer* 54:1269-1275.
- Todd RC, Lippard SJ (2009) Inhibition of transcription by platinum antitumor compounds. *Metallomics : integrated biometal science* 1:280-291.
- Todd RC, Lippard SJ (2010) Consequences of cisplatin binding on nucleosome structure and dynamics. *Chemistry & biology* 17:1334-1343.
- Tomiwa K, Nolan C, Cavanagh JB (1986) The effects of cisplatin on rat spinal ganglia: a study by light and electron microscopy and by morphometry. *Acta neuropathologica* 69:295-308.
- Tornaletti S, Patrick SM, Turchi JJ, Hanawalt PC (2003) Behavior of T7 RNA polymerase and mammalian RNA polymerase II at site-specific cisplatin adducts in the template DNA. *The Journal of biological chemistry* 278:35791-35797.
- Tornøe CW, Christensen C, Meldal M (2002) Peptidotriazoles on solid phase: [1,2,3]-triazoles by regiospecific copper(i)-catalyzed 1,3-dipolar cycloadditions of terminal alkynes to azides. *The Journal of organic chemistry* 67:3057-3064.

- Turecek R, Mandys V, Bar PR, Likovsky Z (1996) Cisplatin-induced changes in the number of argyrophilic nucleolar granules in cultured chick dorsal root ganglion neurons. *Neurosci Res Commun* 18:185-193.
- Tutsch KD, Arzoomanian RZ, Alberti D, Tombes MB, Feierabend C, Robins HI, Spriggs DR, Wilding G (1999) Phase I clinical and pharmacokinetic study of an one-hour infusion of ormaplatin (NSC 363812). *Investigational new drugs* 17:63-72.
- Uddin M, Altmann GG, Leblond CP (1984) Radioautographic visualization of differences in the pattern of [3H]uridine and [3H]orotic acid incorporation into the RNA of migrating columnar cells in the rat small intestine. *The Journal of cell biology* 98:1619-1629.
- van der Hoop RG, van der Burg ME, ten Bokkel Huinink WW, van Houwelingen C, Neijt JP (1990) Incidence of neuropathy in 395 patients with ovarian cancer treated with or without cisplatin. *Cancer* 66:1697-1702.
- van Glabbeke M, Renard J, Pinedo HM, Cavalli F, Vermorcken J, Sessa C, Abele R, Clavel M, Monfardini S (1988) Iproplatin and carboplatin induced toxicities: overview of phase II clinical trial conducted by the EORTC Early Clinical Trials Cooperative Group (ECTG). *European journal of cancer & clinical oncology* 24:255-262.
- Viale M, Zhang JG, Pastrone I, Mariggio MA, Esposito M, Lindup WE (1999) Cisplatin combined with tiopronin or sodium thiosulfate: cytotoxicity in vitro and antitumor activity in vivo. *Anti-cancer drugs* 10:419-428.
- Vichi P, Coin F, Renaud JP, Vermeulen W, Hoeijmakers JH, Moras D, Egly JM (1997) Cisplatin- and UV-damaged DNA lure the basal transcription factor TFIID/TBP. *The EMBO journal* 16:7444-7456.
- Walsh TJ, Clark AW, Parhad IM, Green WR (1982) Neurotoxic effects of cisplatin therapy. *Archives of neurology* 39:719-720.
- Wang D, Lippard SJ (2005) Cellular processing of platinum anticancer drugs. *Nature reviews Drug discovery* 4:307-320.
- Wang Q, Chan TR, Hilgraf R, Fokin VV, Sharpless KB, Finn MG (2003) Bioconjugation by copper(I)-catalyzed azide-alkyne [3 + 2] cycloaddition. *Journal of the American Chemical Society* 125:3192-3193.
- Wassermann K, Newman RA, Davis FM, Mullins TD, Rose KM (1988) Selective inhibition of human ribosomal gene transcription by the morpholinyl anthracyclines cyanomorpholinyl- and morpholinyl-doxorubicin. *Cancer research* 48:4101-4106.
- Wei L, Xiao AY, Jin C, Yang A, Lu ZY, Yu SP (2004) Effects of chloride and potassium channel blockers on apoptotic cell shrinkage and apoptosis in cortical neurons. *Pflugers Archiv : European journal of physiology* 448:325-334.

- Wei X, Somanathan S, Samarabandu J, Berezney R (1999) Three-dimensional visualization of transcription sites and their association with splicing factor-rich nuclear speckles. *The Journal of cell biology* 146:543-558.
- Wells MR, Vaidya U (1994) RNA transcription in axotomized dorsal root ganglion neurons. *Brain research Molecular brain research* 27:163-166.
- Wheate NJ, Walker S, Craig GE, Oun R (2010) The status of platinum anticancer drugs in the clinic and in clinical trials. *Dalton transactions* 39:8113-8127.
- Wilson RH, Lehky T, Thomas RR, Quinn MG, Floeter MK, Grem JL (2002) Acute oxaliplatin-induced peripheral nerve hyperexcitability. *Journal of clinical oncology : official journal of the American Society of Clinical Oncology* 20:1767-1774.
- Windebank AJ, Blexrud MD (1989) Biological activity of a new neuronal growth factor from injured peripheral nerve. *Brain research Developmental brain research* 49:243-251.
- Windebank AJ, Grisold W (2008) Chemotherapy-induced neuropathy. *Journal of the peripheral nervous system : JPNS* 13:27-46.
- Workman JL (2006) Nucleosome displacement in transcription. *Genes & development* 20:2009-2017.
- Woynarowski JM, Chapman WG, Napier C, Herzig MC, Juniewicz P (1998) Sequence- and region-specificity of oxaliplatin adducts in naked and cellular DNA. *Molecular pharmacology* 54:770-777.
- Woynarowski JM, Faivre S, Herzig MC, Arnett B, Chapman WG, Trevino AV, Raymond E, Chaney SG, Vaisman A, Varchenko M, Juniewicz PE (2000) Oxaliplatin-induced damage of cellular DNA. *Molecular pharmacology* 58:920-927.
- Wu B, Davey CA (2008) Platinum drug adduct formation in the nucleosome core alters nucleosome mobility but not positioning. *Chemistry & biology* 15:1023-1028.
- Wu B, Droge P, Davey CA (2008) Site selectivity of platinum anticancer therapeutics. *Nature chemical biology* 4:110-112.
- Wu Y, Bhattacharyya D, King CL, Baskerville-Abraham I, Huh SH, Boysen G, Swenberg JA, Temple B, Campbell SL, Chaney SG (2007) Solution structures of a DNA dodecamer duplex with and without a cisplatin 1,2-d(GG) intrastrand cross-link: comparison with the same DNA duplex containing an oxaliplatin 1,2-d(GG) intrastrand cross-link. *Biochemistry* 46:6477-6487.
- Yonezawa A, Masuda S, Nishihara K, Yano I, Katsura T, Inui K (2005) Association between tubular toxicity of cisplatin and expression of organic cation transporter rOCT2 (Slc22a2) in the rat. *Biochemical pharmacology* 70:1823-1831.

- Zhai X, Beckmann H, Jantzen HM, Essigmann JM (1998) Cisplatin-DNA adducts inhibit ribosomal RNA synthesis by hijacking the transcription factor human upstream binding factor. *Biochemistry* 37:16307-16315.
- Zhang HY, Liu YR, Ji C, Li W, Dou SX, Xie P, Wang WC, Zhang LY, Wang PY (2013) Oxaliplatin and its enantiomer induce different condensation dynamics of single DNA molecules. *PLoS one* 8:e71556.
- Zhang J, Zhou W (2012) Ameliorative effects of SLC22A2 gene polymorphism 808 G/T and cimetidine on cisplatin-induced nephrotoxicity in Chinese cancer patients. *Food and chemical toxicology : an international journal published for the British Industrial Biological Research Association* 50:2289-2293.
- Zhang S, Lovejoy KS, Shima JE, Lagpacan LL, Shu Y, Lapuk A, Chen Y, Komori T, Gray JW, Chen X, Lippard SJ, Giacomini KM (2006) Organic cation transporters are determinants of oxaliplatin cytotoxicity. *Cancer research* 66:8847-8857.
- Zhu G, Song L, Lippard SJ (2013) Visualizing inhibition of nucleosome mobility and transcription by cisplatin-DNA interstrand crosslinks in live mammalian cells. *Cancer research* 73:4451-4460.
- Zhurinsky J, Leonhard K, Watt S, Marguerat S, Bahler J, Nurse P (2010) A coordinated global control over cellular transcription. *Current biology : CB* 20:2010-2015.

# Appendix

## Publications Resulting in Part or in Full from this Thesis

### Journal Article:

Yan F, Liu JJ, Ip V, Jamieson SM, McKeage MJ (2015) Role of platinum DNA damage-induced transcriptional inhibition in chemotherapy-induced neuronal atrophy and peripheral neurotoxicity. *Journal of neurochemistry* doi:10.1111/jnc.13355 (in press).

### Abstracts:

Yan F, Ip V, Jamieson SM, McKeage MJ (2014) Platinum-DNA damage-induced transcriptional inhibition in cultured rat DRG cells contributes to neuronal cell body atrophy and neurotoxicity induced by oxaliplatin. 19th North American International Society for the Study of Xenobiotics (ISSX) meeting and 29th Japanese Society for the Study of Xenobiotics (JSSX) annual meeting. San Francisco, California, USA.

Yan F, Ip V, Jamieson SM, McKeage MJ (2014) Platinum-DNA damage-induced transcriptional inhibition contributes to neuronal cell body atrophy induced by oxaliplatin in cultured rat DRG cells. Australasian Society of Clinical and Experimental Pharmacologists and Toxicologists New Zealand section (ASCEPT NZ) scientific meeting. Queenstown, New Zealand.

Yan F, McKeage MJ (2013) Transcriptional inhibition is a mechanism of platinum drug-induced cell body atrophy in cultured rat dorsal root ganglion neurons. Australasian Society of Clinical and Experimental Pharmacologists and Toxicologists New Zealand section (ASCEPT NZ) scientific meeting. Queenstown, New Zealand.

Yan F, Liu JJ, McKeage MJ (2012) A cell body size-based method for determining platinum anticancer drug-induced peripheral neurotoxicity in cultured rat dorsal root ganglion neurons. Australasian Society of Clinical and Experimental Pharmacologists and Toxicologists New Zealand section (ASCEPT NZ) scientific meeting. Queenstown, New Zealand.

ORIGINAL  
ARTICLE

## Role of platinum DNA damage-induced transcriptional inhibition in chemotherapy-induced neuronal atrophy and peripheral neurotoxicity

Fang Yan,\* Johnson J Liu,\*† Virginia Ip,\* Stephen M F Jamieson\*‡ and Mark J McKeage\*‡

\*Department of Pharmacology and Clinical Pharmacology, School of Medical Sciences, Faculty of Medical and Health Sciences, University of Auckland, Auckland, New Zealand

†School of Medicine, Faculty of Health, University of Tasmania, Hobart, Tasmania, Australia

‡Auckland Cancer Society Research Centre, School of Medical Sciences, Faculty of Medical and Health Sciences, University of Auckland, Auckland, New Zealand

## Abstract

Platinum-based anticancer drugs cause peripheral neurotoxicity by damaging sensory neurons within the dorsal root ganglia (DRG), but the mechanisms are incompletely understood. The roles of platinum DNA binding, transcription inhibition and altered cell size were investigated in primary cultures of rat DRG cells. Click chemistry quantitative fluorescence imaging of RNA-incorporated 5-ethynyluridine showed high, but wide ranging, global levels of transcription in individual neurons that correlated with their cell body size. Treatment with platinum drugs reduced neuronal transcription and cell body size to an extent that corresponded to the amount of preceding platinum DNA binding, but without any loss of neuronal cells. The effects of platinum drugs on neuronal transcription and cell body size were

inhibited by blocking platinum DNA binding with sodium thiosulfate, and mimicked by treatment with a model transcriptional inhibitor, actinomycin D. *In vivo* oxaliplatin treatment depleted the total RNA content of DRG tissue concurrently with altering DRG neuronal size. These findings point to a mechanism of chemotherapy-induced peripheral neurotoxicity, whereby platinum DNA damage induces global transcriptional arrest leading in turn to neuronal atrophy. DRG neurons may be particularly vulnerable to this mechanism of toxicity because of their requirements for high basal levels of global transcriptional activity.

**Keywords:** anticancer drug toxicity, DNA damage, DRG neurons, global transcription, neuronal atrophy, neurotoxicity. *J. Neurochem.* (2015) 10.1111/jnc.13355

The platinum-based anticancer drugs, cisplatin, carboplatin and oxaliplatin, are used clinically for the routine treatment of a wide range of human cancers. Their mechanism of action involves platinum binding to DNA at the N7 position of purine bases to form bifunctional 1,2- and 1,3-intrastrand crosslinks on the DNA template, which inhibit DNA replication and transcription, leading to tumour cell cycle arrest and apoptosis (Wang and Lippard 2005). Platinum drugs also cause peripheral neurotoxicity by damaging post-mitotic dorsal root ganglia (DRG) sensory neurons (Avan *et al.* 2015). In the clinic, the resulting neurological symptoms and functional deficits can interfere with the delivery of cancer chemotherapy or persist long after completion of treatment, thereby compromising patient quality of life and the chance of cancer control or cure.

Platinum drug-induced DNA damage is known for inhibiting transcription in some cell types (Todd and Lippard 2009). Platinum DNA crosslinks inhibit transcription via multiple mechanisms, including (i) physical blockade of

Received June 14, 2015; revised manuscript received August 19, 2015; accepted September 9, 2015.

Address correspondence and reprint requests to Mark J McKeage, Department of Pharmacology and Clinical Pharmacology, School of Medical Sciences, Faculty of Medical and Health Sciences, University of Auckland, Auckland, New Zealand. E-mail: m.mckeage@auckland.ac.nz

*Abbreviations used:* AUC, area under the concentration–time curve; DACH, diamincyclohexane; DNA-PK, DNA-dependent protein kinase; DRG, dorsal root ganglia; EU, 5-ethynyluridine; IQR, interquartile range; PARP-1, poly(ADP-ribose) polymerase 1; TUNEL, terminal deoxynucleotidyl transferase-mediated dUTP nick end labelling.



progression of RNA polymerases along the DNA template (Ang *et al.* 2010); (ii) binding of transcription factors preventing their interaction with gene promoters and initiation of transcription (Treiber *et al.* 1994; Vichi *et al.* 1997; Jordan and Carmo-Fonseca 1998); (iii) disruption of nucleosomal structure and mobility interfering with the access of transcription proteins to DNA (Zhu *et al.* 2013) and (iv) activation of signal transduction proteins, such as DNA-dependent protein kinase (DNA-PK), poly(ADP-ribose) polymerase 1 (PARP-1) or coilin, which repress RNA synthesis (Gilder *et al.* 2011; Calkins *et al.* 2013). Increasing evidence has pointed to a possible role for platinum DNA damage in the peripheral neurotoxicity induced by platinum drugs. Previous studies have shown platinum DNA adducts forming in DRG neuronal cells after treatment with cisplatin and oxaliplatin (Meijer *et al.* 1999; McDonald *et al.* 2005; Ta *et al.* 2006), and that neuronal DNA repair capacity may be a factor influencing the severity of the resulting peripheral neurotoxicity (Dzagnidze *et al.* 2007). Exactly how platinum DNA damage leads to chemotherapy-induced peripheral neurotoxicity is still unclear, however. Possible mechanisms include DNA damage-induced neuronal apoptosis (Gill and Windebank 1998; Fischer *et al.* 2001; McDonald and Windebank 2002; Gozdz *et al.* 2003), inhibition of mitochondrial DNA replication (Podratz *et al.* 2011) and transcription inhibition (Gozdz *et al.* 2008; Hetman *et al.* 2010).

DRG neurons have large cell bodies, prominent nucleoli and distant axonal connections (Scott 1992; Sghirlanzoni *et al.* 2005; Berciano *et al.* 2007). Studies of other cell types suggest that cell size is dependent on their global transcriptional activity as a generalizable biological relationship (Marguerat and Bähler 2012), but there have been few studies of the global transcriptional activity of DRG neurons since early autoradiography studies (Sensenbrenner *et al.* 1970; Chang *et al.* 1972; Carmichael and Cavanagh 1976; Wells and Vaidya 1994). Reduced DRG neuronal cell body size is a morphological hallmark of platinum-induced peripheral neurotoxicity, demonstrated in many previous *in vivo* studies of human and animal DRG tissue (Tomiwa *et al.* 1986; Cavaletti *et al.* 1992, 2001; Holmes *et al.* 1998; Krarup-Hansen *et al.* 1999; Jamieson *et al.* 2005; Renn *et al.* 2011), but exactly how platinum drugs alter neuronal size is unclear. Previous morphological studies revealed nucleolar disruption in DRG neurons after treatment with platinum drugs suggesting inhibited transcription (Tomiwa *et al.* 1986; Cavaletti *et al.* 1992; Holmes *et al.* 1998; McKeage *et al.* 2001).

These considerations led us to hypothesize that DRG neurons may require high levels of global transcriptional activity, for maintaining their significant size and distant axonal connections, making them vulnerable to neuronal dysfunction and altered size from platinum DNA damage-induced transcription inhibition (Hetman *et al.* 2010). To investigate this hypothesis, we established a click chemistry

5-ethynyluridine (EU) RNA incorporation fluorescence labelling assay to visualize and measure global transcriptional activity (Jao and Salic 2008) in individual DRG neurons *in vitro*, and related these measurements to those of neuronal cell body size. Cultured DRG cells were treated with oxaliplatin and other platinum drugs using *in vitro* experimental conditions mimicking clinically achievable chemotherapy drug systemic exposures (Han *et al.* 2013). Effects of *in vitro* treatment with platinum drugs on DRG neuronal size and global transcriptional activity were related to levels of platinum DNA binding, measured by inductively coupled plasma mass spectrometry (Brouwers *et al.* 2008). The role of platinum DNA damage-induced transcription inhibition in chemotherapy-induced peripheral neurotoxicity was further examined in experiments using a series of clinical platinum-based drugs and diaminocyclohexane (DACH) platinum enantiomers (Screnci *et al.* 1997, 2000) with differing peripheral neurotoxicity clinical and experimental profiles, as well as model inhibitors of platinum DNA binding (Viale *et al.* 1999), apoptosis volume decrease (Wei *et al.* 2004; Hernandez-Enriquez *et al.* 2010, 2011), global transcription (Bensaude 2011) and PARP-1 and DNA-PK signalling (Calkins *et al.* 2013).

## Methods

### Chemicals and reagents

Oxaliplatin was obtained from Sanofi (Paris, France) and Sigma-Aldrich (St Louis, MO, USA). Cisplatin and carboplatin were obtained from Sigma-Aldrich. The racemic mixture of ormaplatin was kindly provided by the National Cancer Institute (Bethesda, MD, USA). *R,R*-ormaplatin, *S,S*-ormaplatin, *R,R*-Pt(DACH)Cl<sub>2</sub> and *S,S*-Pt(DACH)Cl<sub>2</sub> were synthesized as outlined previously (Screnci *et al.* 1997). Sodium thiosulfate pentahydrate was purchased from Scharlau (Barcelona, Spain). Actinomycin D, tetraethylammonium chloride, potassium chloride, 4,4'-diisothiocyanatostilbene-2,2'-disulfonic acid disodium salt hydrate, 5-nitro-2-(3-phenylpropylamino)benzoic acid and benzamide were purchased from Sigma-Aldrich. Wortmannin, NU 7026 and olaparib were purchased from Cayman Chemical (Ann Arbor, MI, USA). Both 5% glucose and 0.9% sodium chloride were obtained from Baxter (Deerfield, IL, USA).

### Cell culture

Primary cultures of rat DRG cells were established as described previously with slight modifications (Jong *et al.* 2011; Liu *et al.* 2013). In brief, DRG from all spinal levels were dissected from 20-day-old Wistar rats killed with pentobarbitone (Chemstock Animal Health, Christchurch, New Zealand). DRG were pooled during processing before culture, from one up to 12 animals, depending on the requirements of each experiment. DRG were then digested with 2.5 mg/mL collagenase and 1 mg/mL dispase (Life

Technologies, Carlsbad, CA, USA) for 50 min at 37°C, followed by trypsinization using 0.25% trypsin (Life Technologies) for 40 min at 37°C. Subsequently, DRG were mechanically triturated using fine-bore glass Pasteur pipettes to dissociate and release cells, and the resulting cell suspension was filtered through a 100- $\mu$ m cell strainer (Becton-Dickinson, Franklin Lakes, NJ, USA) to remove tissue debris. DRG cells were isolated by centrifugation at 800 *g* in Percoll solution (density: 1.040 g/mL) (Sigma-Aldrich) for 20 min at room temperature. DRG cells were then re-suspended and cultured in Neurobasal-A medium supplemented with 5% horse serum, 100 U/mL penicillin, 0.1 mg/mL streptomycin, 2 mM glutamine and 1% N-2 supplement (Life Technologies) at 37°C in a humid atmosphere of 5% CO<sub>2</sub>-95% air. For the first 2 days of culture, 40  $\mu$ M 5-fluoro-2'-deoxyuridine and 120  $\mu$ M uridine (Sigma-Aldrich) were added to suppress growth of non-neuronal cells. DRG cells were then cultured in the normal culture medium for 1 day before any experimental manipulation.

Cultured DRG cells consisted of sensory neurons and non-neuronal cells that were easily distinguishable by their morphology under phase-contrast microscopy. Typically, DRG neurons were characterized by their large and round cell bodies with a sharp halo, whereas non-neuronal cells showed small and spindle-shaped morphology.

#### Experimental incubation

Unless stated otherwise, cultured rat DRG cells grown on plates or chamber slides were exposed to experimental conditions either for 3 h followed by culture in drug-free medium until up to 48 h after the start of treatment, or continuously for up to 48 h, as indicated in figure legends.

#### Assessment of new RNA synthesis by EU incorporation

A Click-iT RNA Imaging Kit (Life Technologies) was used according to the manufacturer's instructions with slight modifications. In brief, 20 h before the end of the experiment, 1 mM EU was added to the cells grown on chamber slides. At the end of the experiment, cells were washed with pre-warmed phosphate-buffered saline (PBS), fixed with 4% paraformaldehyde for 15 min at room temperature, and then permeabilized using 0.2% Triton X-100 in PBS for 15 min at room temperature. To detect RNA-incorporated EU using a click chemistry reaction with Alexa594-labelled azide, cells were then incubated with Click-iT reaction cocktail for 30 min at room temperature, protected from light. After incubation, cells were washed with Click-iT reaction rinse buffer and PBS, and then counterstained and coverslipped with VECTASHIELD mounting medium containing 4',6-diamidino-2-phenylindole (DAPI) (Vector Laboratories, Burlingame, CA, USA).

Fluorescence images were acquired using a Nikon Eclipse Ti-U inverted microscope equipped with a Nikon DS-Fi1c

digital camera (Nikon, Tokyo, Japan), at 540–580 nm excitation and 600–660 nm emission for Alexa594 labelling of RNA-incorporated EU and at 330–380 nm excitation and > 420 nm emission for DAPI staining of nuclear DNA. After background correction, the fluorescence pixel intensities of EU-Alexa594 staining within cell bodies and DAPI staining within nuclei were measured for individual neurons using Nikon NIS-Elements software. The same individual neurons were also measured for cell body areas as described below.

#### Assessment of new RNA synthesis by [<sup>3</sup>H]uridine incorporation

One hour before the end of the experiment, 5  $\mu$ Ci/mL [5-<sup>3</sup>H]uridine (sp. act. > 20 Ci/mmol, PerkinElmer, Waltham, MA, USA) was added to the culture. At the end of the experiment, labelling medium was removed and cells were re-suspended using 0.25% trypsin (Life Technologies). The cell suspension was thoroughly mixed with ice-cold 10% (w/v) trichloroacetic acid (Sigma-Aldrich) and placed on ice for 30 min. The acid-precipitable material was collected on a GF/C glass-fibre filtermat (Filtermat A, PerkinElmer) by a plate harvester (Harvester 96, Tomtec, Hamden, CT, USA). The filtermats were dried at room temperature overnight and their radioactivity was measured in a scintillation cocktail (Betaplate Scint, PerkinElmer) by a liquid scintillation counter (Wallac 1450 MicroBeta JET, PerkinElmer).

#### Assessment of platinum binding to DNA

Following experimental incubations, DRG cells were harvested and their genomic DNA was extracted using a Wizard Genomic DNA Purification Kit (Promega, Madison, WI, USA) according to the manufacturer's instructions, with the modification that isopropanol precipitation was performed at 4°C overnight. The DNA content was determined by measuring the absorbance at 260 nm with a NanoDrop ND-1000 spectrophotometer (Thermo Fisher Scientific, Waltham, MA, USA). Subsequently, DNA samples were digested with an equal volume of 70% nitric acid at room temperature overnight and then at 95°C for 2 h. The resulting digests were diluted in Milli-Q water spiked with 50 ppb thallium (SPEX CertiPrep, Metuchen, NJ, USA) as internal standard. The platinum content was quantitated by inductively coupled plasma mass spectrometry on a Varian 820-MS (Varian, Palo Alto, CA, USA) using a standard calibration method. The final platinum content was normalized to the DNA content.

#### Measurement of total RNA content of cultured DRG cells

Total RNA from cultured DRG cells was extracted using an RNeasy Mini Kit (Qiagen, Venlo, Netherlands) according to the manufacturer's instructions. Total RNA content was determined by measuring the absorbance at 260 nm with a NanoDrop ND-1000 spectrophotometer (Thermo Fisher Scientific).

### Measurement of neuronal cell body size and number

Cultured DRG cells were photographed by phase-contrast microscopy on a Nikon Eclipse Ti-U inverted microscope equipped with a Nikon DS-Fi1c digital camera. Cross-sectional areas of neuronal cell bodies were measured using Nikon NIS-Elements software. The number of neurons in each photomicrograph was determined using ImageJ software (National Institutes of Health).

### Apoptosis assay

Apoptosis assay was performed using an *In Situ* Cell Death Detection Kit (Roche, Basel, Switzerland) based on terminal deoxynucleotidyl transferase-mediated dUTP nick end labelling (TUNEL) technique, according to the manufacturer's instructions with slight modifications. After the experimental manipulations, cultured DRG cells grown on chamber slides were washed, fixed and permeabilized as described above. Cells were then incubated with TUNEL reaction mixture in a humidified atmosphere for 60 min at 37°C in the dark. After incubation, cells were washed with PBS, and then coverslipped as described above. Fluorescence images were acquired using a Nikon Eclipse Ti-U inverted microscope equipped with a Nikon DS-Fi1c digital camera at 465–495 nm excitation and 515–555 nm emission.

### Real-time PCR array analysis

Following experimental incubations, total RNA from cultured rat DRG cells was extracted and quantitated as described above. cDNA was synthesized from 400 ng RNA using an RT<sup>2</sup> First Strand Kit (Qiagen) according to the manufacturer's instructions, and then mixed with RT<sup>2</sup> SYBR Green qPCR Mastermix (Qiagen). The mixtures were loaded into a commercially available pre-validated RT<sup>2</sup> Profiler PCR Array 96-well plate containing optimized primer assays for a set of five reference genes (Gusb, Hprt, Hsp90ab1, Gapdh and Actb) and 86 Abc and Slc drug transporter genes (Qiagen), with diverse mechanisms of transcriptional regulation (Chen *et al.* 2013). Real-time PCR reactions were performed according to the array manufacturer's instructions using Applied Biosystems 7900HT Fast Real-Time PCR System and SDS 2.3 software (Life Technologies). The temperature profile was as follows: 95°C for 10 min and then 40 cycles of 95°C for 15 s and 60°C for 1 min. The threshold cycle (Ct) values were obtained for each sample. The mRNA expression levels were expressed as  $2^{-\Delta Ct}$ , where  $\Delta Ct = Ct$  of target gene – Ct of housekeeping gene, and then corrected for the total RNA yield.

### Animals and drug treatment

Age-matched 10-week-old female Wistar rats weighing approximately 270 g at the commencement of the experiment were used in this study. Animals were housed in a temperature-controlled environment with access to food and

water *ad libitum*, and were acclimatized to handling prior to drug treatment. Oxaliplatin was diluted for injection in 5% glucose. Animals were treated with either oxaliplatin at a dose of 1.85 mg/kg or the vehicle control solution of 5% glucose twice weekly for 8 weeks, by intraperitoneal injection at a volume of 15 mL/kg. All injections were performed on a Wednesday and Friday between 2 and 4 PM to avoid possible time-dependent variation in pharmacokinetics and pharmacodynamics. All animal procedures were approved by and performed in compliance with ethical guidelines of the Animal Ethics Committee of the University of Auckland.

### Measurement of total RNA content of DRG tissue

One week after the conclusion of the 8-week dosing period, animals were killed with pentobarbitone. Blood was exsanguinated from the animals by incision of the left axillary artery, in some cases, followed by rapid perfusion of the heart with PBS for adequate exsanguination. Subsequently, lumbar 3–6 DRG were dissected rapidly from the spinal cord, pooled for each animal prior to homogenization. Total RNA was extracted using an Aurum Total RNA Fatty and Fibrous Tissue Kit (Bio-Rad, Hercules, CA, USA) according to the manufacturer's instructions. Total RNA content was determined by measuring the absorbance at 260 nm with Nanodrop ND-1000 Spectrophotometer. DRG tissue was processed for histo-morphometric analysis of nucleolar and neuronal cell body area as previously described (Jamieson *et al.* 2005; Ip *et al.* 2013).

### Statistical analysis

Data were analysed using GraphPad Prism 6 software (GraphPad Software, La Jolla, CA, USA). The statistical significance of differences between means was assessed by unpaired *t*-test and one-way analysis of variance (ANOVA) with Tukey's post-test. The statistical significance of differences between medians was assessed by Kruskal–Wallis test with Dunn's post-test. The statistical significance of correlations between experimental parameters was assessed by Spearman's rank correlation analysis. In all statistical tests, a  $p < 0.05$  was considered statistically significant.

## Results

### Global transcription in DRG cells

To visualize global transcription *in situ*, cultured rat DRG cells were incubated with EU (1 mM, 20 h) and then fixed before click chemistry fluorescence labelling of newly synthesized RNA. Imaging of cultured DRG cells revealed neuronal cells with large round cell bodies, sharp pericellular halos (Fig. 1a right-hand image) and DAPI-stained nuclei (Fig. 1a middle image), admixed with non-neuronal cells. Fluorescence labelling of newly synthesized RNA was localized to the nuclei of DRG neurons with little or no labelling of the neuronal cytoplasm or non-neuronal cells

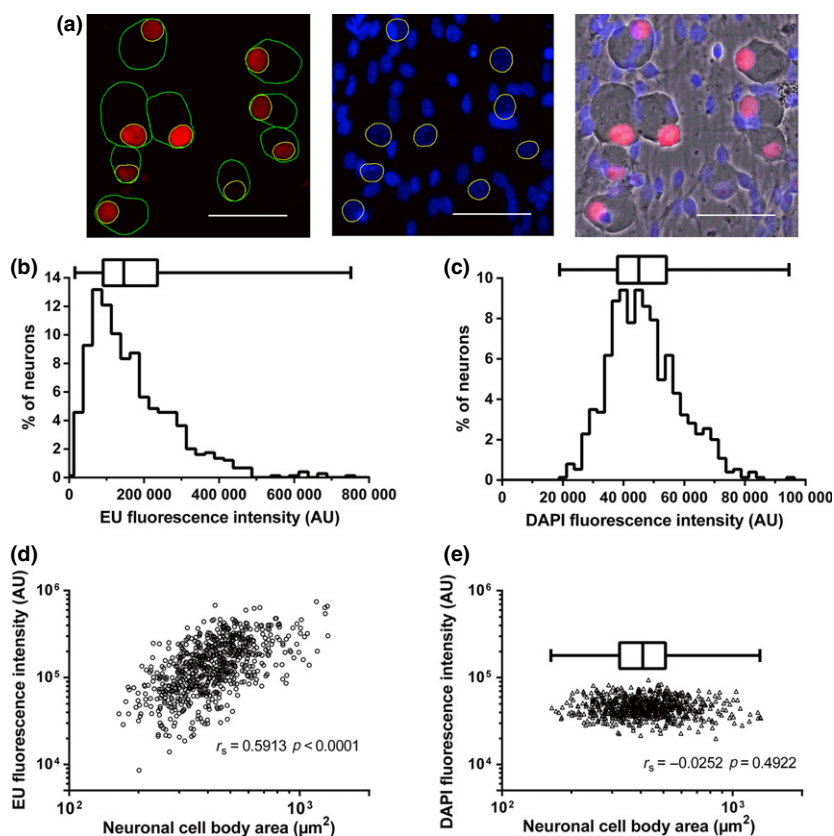


**Fig. 1** Click chemistry quantitative fluorescence imaging of neuronal transcription in cultured dorsal root ganglia (DRG) cells *in situ*. (a) Images show click chemistry fluorescence labelling of newly synthesized RNA (left-hand image) and 4',6-diamidino-2-phenylindole (DAPI) staining of nuclear DNA (middle image) overlaid with a phase-contrast photomicrograph (right-hand image) (scale bar 50  $\mu$ ). Fluorescence labelling of newly synthesized RNA was localized to the nuclei of DRG neurons (yellow circles) with little or no labelling of the neuronal cytoplasm (between the green and yellow circles) or non-neuronal cells. (b–e) Individual neuronal 5-ethynyluridine (EU)

labelling (b and d) and DAPI staining (c and e) fluorescence pixel intensities shown as frequency histograms, box and whisker plots [median, interquartile range (IQR) and range] (b and c) and correlation plots versus neuronal cell body area (d and e) ( $r_s$ , Spearman's rank correlation coefficient). RNA synthesis levels varied widely between individual DRG neurons in correlation with their cell body size. The data shown (Fig. 1b–e) were from measurements of cells ( $n = 744$  neurons) pooled from three culture wells obtained from one harvest from one animal, but were independently replicated in a separate experiment.

(Fig. 1a left- and right-hand images). Individual neuronal fluorescence pixel intensities of EU labelling and DAPI staining were measured. Individual neuronal EU labelling fluorescence pixel intensities showed a > 25-fold range from minimum to maximum values, relative interquartile range (IQR) (IQR/median) of > 100% and a right-skewed frequency histogram (Fig. 1b). In contrast, neuronal DAPI staining intensity and cell body area showed a 5- and 8-fold range from minimum to maximum values, relative IQR of 35% and 45%, respectively, and right-skewed frequency histograms (Fig. 1c and e). Neuronal EU labelling intensity correlated positively with neuronal cell body size (Fig. 1d), with larger neurons having higher levels of transcription ( $p < 0.0001$ ). In contrast, neuronal DAPI staining intensity did not correlate with neuronal cell body size (Fig. 1e).

### Effects of oxaliplatin

To investigate potential effects of oxaliplatin treatment, primary cultures of DRG cells were treated with oxaliplatin then exposed to EU (1 mM for 20 h) before fixation, fluorescence labelling and quantitative imaging. To mimic clinically achievable oxaliplatin exposures *in vitro*, cells were treated for 3 h with 10, 30 and 100  $\mu$ M oxaliplatin. Considering the rate of oxaliplatin degradation in supplemented Neurobasal-A medium ( $t_{1/2} \approx 3$  h; Figure S1), determining by HPLC (Ip *et al.* 2008), these *in vitro* treatments equated to AUCs for oxaliplatin exposure of 21.7, 65 and 217  $\mu$ M.h, respectively, or to those achieved after 1.5, 4.3 and 14 standard clinical doses of oxaliplatin chemotherapy (85–130  $\text{mg}/\text{m}^2$ ) respectively (Han *et al.* 2013). Representative images suggested the presence of

reductions in neuronal EU labelling fluorescence intensity and in cell body size after oxaliplatin treatment (Fig. 2a), which were confirmed by quantitative analysis. Neuronal EU labelling frequency histograms were shifted leftward by oxaliplatin treatment (Fig. 2b). Median EU labelling values were reduced to 64%, 48% and 37% of the untreated control value ( $p < 0.0001$ ) by treatment with 10, 30 and 100  $\mu\text{M}$  of oxaliplatin respectively (Fig. 2b). Neuronal cell body area frequency histograms were shifted leftward by oxaliplatin treatment (Fig. 2c). Median neuronal cell body area values were reduced to 81%, 76% and 73% of the untreated control value ( $p < 0.0001$ ) by treatment with 10, 30 and 100  $\mu\text{M}$  of oxaliplatin respectively (Fig. 2c).

To compare the time-course of effects of oxaliplatin, measurements were made of DNA-bound platinum (Fig. 3a), RNA-incorporated [ $^3\text{H}$ ]uridine (Fig. 3b), total RNA content (Fig. 3c), neuronal cell body area (Fig. 3d) and neuronal numbers (Fig. 3e) at various time points after treatment of cultured DRG cells with oxaliplatin (100  $\mu\text{M}$ ) for 3 h followed by culture in drug-free medium for up to 2 days. Relative to the time of commencing oxaliplatin treatment, platinum binding to DNA was first detected at 1 h, peaked at 4 h and then remained at 50% or more of the peak levels for

the next 2 days (Fig. 3a). Levels of RNA-incorporated [ $^3\text{H}$ ]uridine were reduced to 49%, 26%, 13% and 17% of the pre-treatment level ( $p < 0.0001$ ) at 4, 8, 24 and 48 h, respectively, after the commencement of oxaliplatin treatment (Fig. 3b). The total RNA content of cultured DRG cells was reduced to 87%, 79%, 56% and 37% of the pre-treatment value ( $p < 0.0001$ ) at 4, 8, 24 and 48 h, respectively, after the commencement of oxaliplatin treatment (Fig. 3c). Neuronal cell body areas remained unchanged for at least 4 h after the commencement of oxaliplatin treatment, but thereafter became reduced to 89%, 73% and 74% of the pre-treatment value ( $p < 0.0001$ ) at 8, 24 and 48 h respectively (Fig. 3d). Neuronal cell numbers were not altered by oxaliplatin treatment within the timeframe of the experiment (Fig. 3e). Taken together, the data showed that DNA platinum binding occurred before transcription inhibition and depletion of RNA. Neuronal cell body atrophy occurred after DNA platinum binding, transcription inhibition and RNA depletion, and without the loss of neuronal cells.

To investigate possible contributions of neuronal apoptosis to size changes in DRG cells induced by oxaliplatin, TUNEL staining and blockers of apoptotic volume decrease were studied. Oxaliplatin treatment did not induce TUNEL

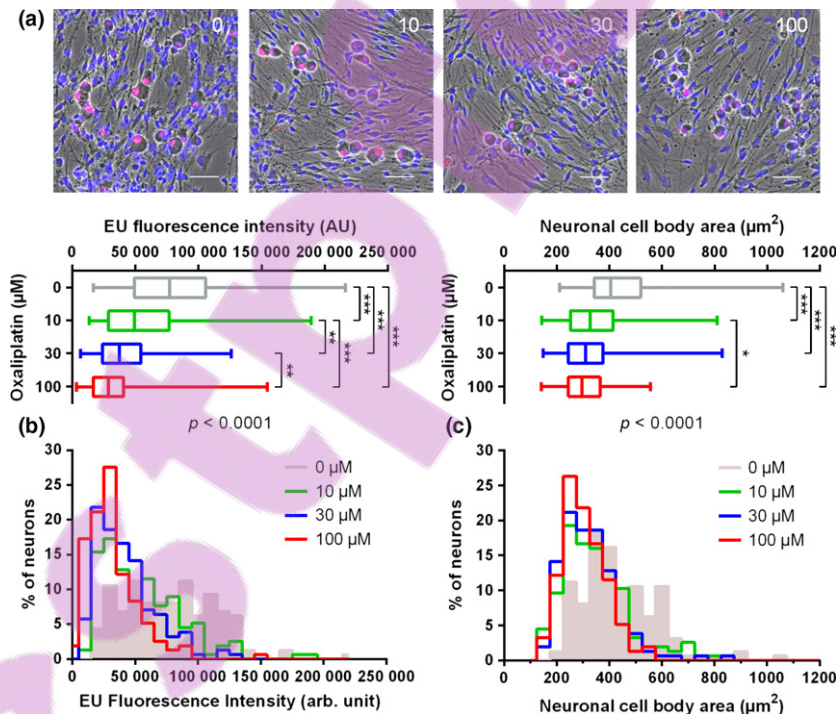


**Fig. 2** Oxaliplatin-induced transcription inhibition and neuronal atrophy *in vitro*. Primary cultures of dorsal root ganglia (DRG) cells were treated with oxaliplatin (10, 30 or 100  $\mu\text{M}$ ; 3 h) then exposed to 5-ethynyluridine (EU) (1 mM for 20 h) before fixation and fluorescence labelling 2 days after oxaliplatin treatment. (a) Representative images of control (0) and treated (10, 30 and 100) cultures (scale bar 50  $\mu\text{m}$ ). (b) and (c) Individual neuronal EU labelling fluorescence pixel intensity (b) and cell

body areas (c) shown as frequency histograms and box and whisker plots [median, interquartile range (IQR) and range] ( $n = 156$ – $161$  neurons from three culture wells obtained from one harvest from one animal). The  $p$  values shown as numbers are from Kruskal–Wallis tests, and those shown as \* ( $p < 0.05$ ), \*\* ( $p < 0.01$ ) and \*\*\* ( $p < 0.001$ ) are from Dunn's multiple comparisons post-tests following a Kruskal–Wallis test. Data were replicated in independent experiments.

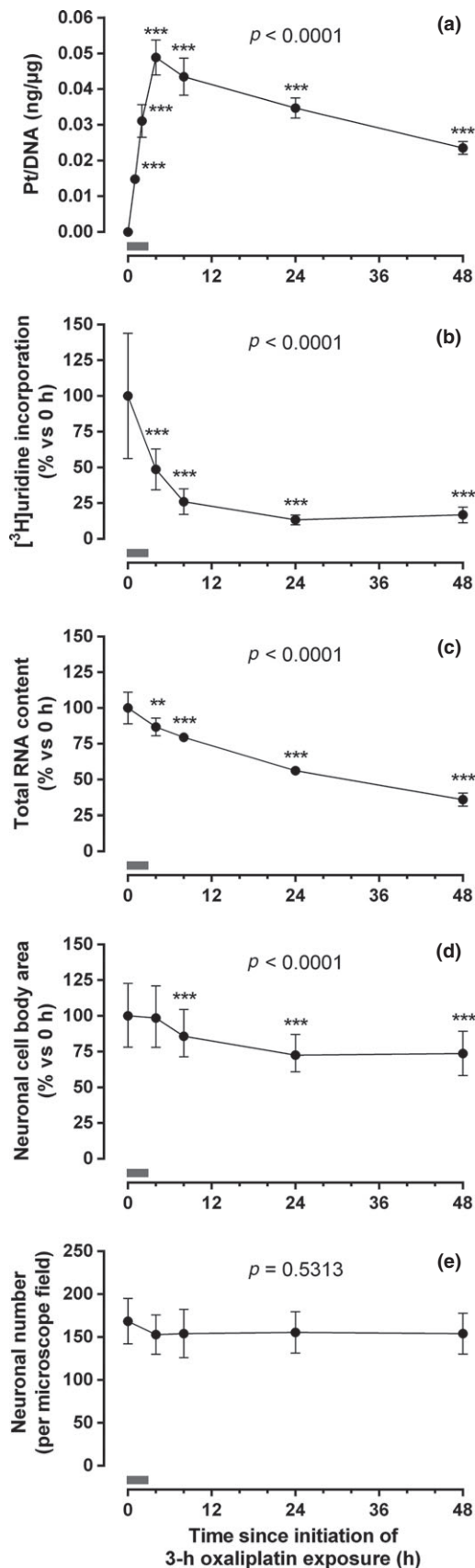


**Fig. 3** Comparative time-courses of oxaliplatin effects on cultured dorsal root ganglia (DRG) cells. Measurements of DNA-bound platinum (a), RNA-incorporated [<sup>3</sup>H]uridine (b), total RNA content (c), neuronal cell body area (d) and neuronal number (e) were made at various time points after treatment of cultured DRG cells with oxaliplatin (100 μM) for 3 h, followed by culture in drug-free medium. DNA platinum binding occurred before transcription inhibition and depletion of RNA. Cell body atrophy followed DNA platinum binding, transcription inhibition and RNA depletion, but occurred without concurrent loss of neuronal cells. Symbols represent the mean [a ( $n = 6$  culture wells), b ( $n = 12$ –33 culture wells), c ( $n = 6$  culture wells), e ( $n = 12$  microscope fields pooled from six culture wells)] or median [d ( $n = 960$  neurons pooled from six culture wells)] and standard deviation (a, b, c and e) or interquartile range (IQR) (d) of replicates from at least two independent experiments. The  $p$  values shown as numbers are from one-way ANOVA (a, b, c and e) or Kruskal–Wallis tests (d). Those shown as \*\* ( $p < 0.01$ ) and \*\*\* ( $p < 0.001$ ) are from Tukey's (a, b, c and e) or Dunn's (d) multiple comparisons post-tests following one-way ANOVA (a, b, c and e) or Kruskal–Wallis tests (d), respectively, in comparison to the 0 h time point. The grey bar symbolizes the duration of oxaliplatin treatment.

staining in DRG neurons concurrently with its induction of changes in their size (Figure S2).  $K^+$  and  $Cl^-$  channel blockers of apoptotic volume decrease (Wei *et al.* 2004; Hernandez-Enriquez *et al.* 2010, 2011) has no effect on oxaliplatin-induced changes in cell body size (Figure S3).

### Transcription inhibition

To further explore associations between transcription inhibition and neuronal atrophy, the effects of a model transcriptional inhibitor, actinomycin D (Bensaude 2011), were studied. Primary cultures of DRG cells were treated with actinomycin D (3 μM) for up to 24 h before the measurement of RNA-incorporated [<sup>3</sup>H]uridine and neuronal cell body areas at various time points. Actinomycin D treatment reduced levels of RNA-incorporated [<sup>3</sup>H]uridine to < 10% of pre-treatment values ( $p < 0.0001$ ) after 1, 2, 4, 8 and 24 h of treatment (Fig. 4a). Neuronal cell body areas remained unchanged for at least 2 h after the commencement of actinomycin D treatment, but thereafter become reduced to 94%, 93% and 77% of the pre-treatment value ( $p < 0.0001$ ) at 4, 8 and 24 h respectively (Fig. 4b).

The effects of oxaliplatin treatment on the expression of individual genes was studied by quantitative real-time PCR gene expression array analysis of RNA extracted from cultured DRG cells after treatment with oxaliplatin (100 μM) for 3 h followed by culture in drug-free medium for 1 day. Use was made of a commercially available pre-validated RT<sup>2</sup> Profiler PCR array 96-well plate containing optimized assays for five reference genes (Gusb, Hpvt, Hsp90ab1, Gapdh and Actb) and 86 Abc and Slc drug transporter genes, with diverse mechanisms of transcriptional regulation (Chen *et al.* 2013). mRNAs of 39 individual reference or target genes were measurable in both control and oxaliplatin-treated

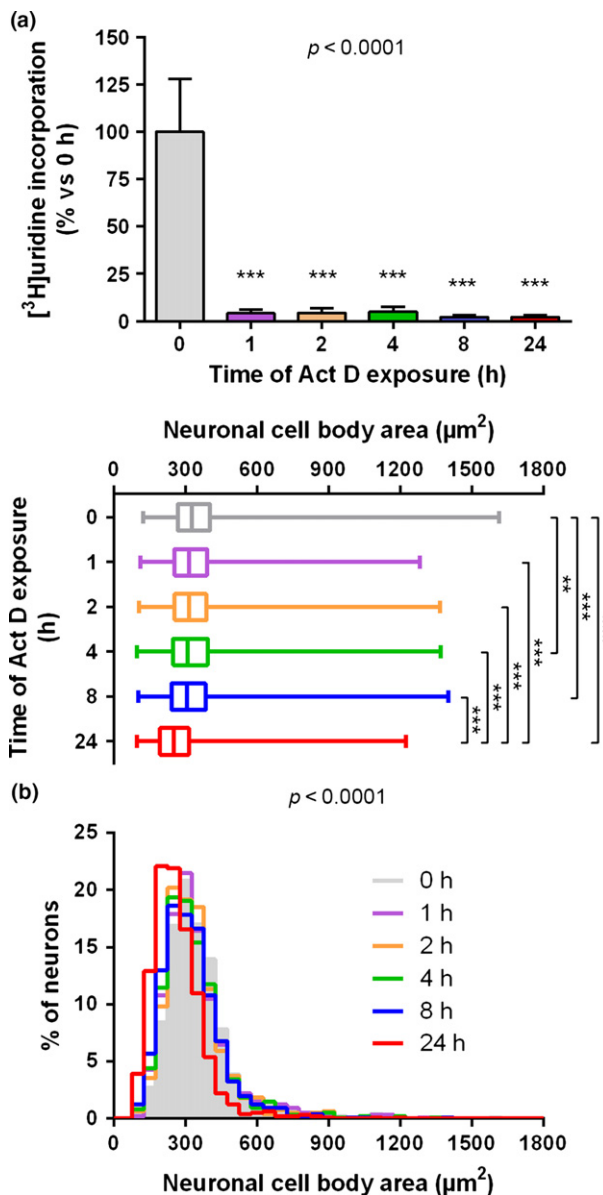


**Fig. 4** Actinomycin D-induced neuronal atrophy following transcriptional inhibition. Primary cultures of dorsal root ganglia (DRG) cells were treated with actinomycin D (3  $\mu\text{M}$ ) for up to 24 h before measurement of RNA-incorporated [ $^3\text{H}$ ]uridine (a) and neuronal cell body size (b). (a) Symbols represent means and standard deviations ( $n = 9\text{--}24$  culture wells from three independent experiments). The  $p$  value shown as a number is from one-way ANOVA and those shown as \*\*\* ( $p < 0.001$ ) are from Tukey's multiple comparisons post-tests following one-way ANOVA, in comparison to the 0 h time point. (b) Individual neuronal cell body areas are shown as frequency histograms and box and whisker plots [median, interquartile range (IQR) and range] ( $n = 960$  neurons pooled from six culture wells from two independent experiments). The  $p$  value shown as a number is from a Kruskal–Wallis test, and those shown as \*\* ( $p < 0.01$ ) and \*\*\* ( $p < 0.001$ ) are from Dunn's multiple comparisons post-tests following a Kruskal–Wallis test.

DRG cells. A linear regression fit ( $r^2 = 0.86$ ) to reference gene- and RNA yield-corrected gene expression values from control and oxaliplatin-treated cells gave a Y-intercept value at  $X = 0.0$  that was significantly  $< 0$  ( $-0.49$ ; 95% CI  $-0.73$  to  $-0.25$ ;  $p < 0.0001$ ) (Figure S4a). The median fold change in gene expression level associated with oxaliplatin treatment was 0.44-fold, with an IQR of 0.27- to 1.07-fold and range from 0.004- to 4.36-fold (Figure S4b). Most individual genes (28 of 39 genes or 72%) with measurable expression by quantitative real-time PCR array analysis showed reduced expression after oxaliplatin treatment.

To investigate possible roles for PARP-1 or DNA-PK in the inhibition of neuronal transcription induced by oxaliplatin, the effects of model inhibitors of PARP-1 and DNA-PK signalling were studied. PARP-1 and DNA-PK inhibitors had no effect on oxaliplatin-induced inhibition of [ $^3\text{H}$ ]uridine incorporation in cultured DRG cells (Figure S5).

#### Comparison of different platinum drugs

To compare the effects of a series of platinum-based anticancer drugs with differing peripheral neurotoxicity clinical profiles (Screnci and McKeage 1999; Screnci *et al.* 2000), primary cultures of DRG cells were treated with cisplatin, ormaplatin, oxaliplatin or carboplatin (100  $\mu\text{M}$ ) for 3 h and then cultured in drug-free medium until measurement of DNA-bound platinum, RNA-incorporated [ $^3\text{H}$ ]uridine and neuronal cell body area. DNA-bound platinum was detected after treatment with cisplatin, ormaplatin and oxaliplatin ( $p < 0.0001$ ), but not after treatment with carboplatin (Fig. 5a). Levels of RNA-incorporated [ $^3\text{H}$ ]uridine were reduced after treatment with cisplatin, ormaplatin and oxaliplatin ( $p < 0.0001$ ), but not after treatment with carboplatin (Fig. 5b). Neuronal cell body areas were reduced after treatment with cisplatin, ormaplatin and oxaliplatin ( $p < 0.0001$ ), but not after treatment with carboplatin (Fig. 5c).

The effects of *R,R*- and *S,S*-DACH platinum enantiomers, which were previously shown to have differing *in vivo* peripheral neurotoxicity experimental profiles (Screnci *et al.* 1997), were compared. Primary cultures of DRG cells were treated with *R,R*-ormaplatin, *S,S*-ormaplatin, *R,R*-Pt(DACH)Cl<sub>2</sub> or *S,S*-Pt(DACH)Cl<sub>2</sub> (100  $\mu\text{M}$ ) for 3 h and then cultured in drug-free medium until measurement of DNA-bound platinum, RNA-incorporated [ $^3\text{H}$ ]uridine and neuronal cell body areas. Levels of DNA-bound platinum were higher after treatment with *R,R*-DACH platinum enantiomers than after treatment with their respective *S,S*-DACH platinum enantiomers ( $p < 0.0001$ ) (Fig. 6a). RNA-incorporated [ $^3\text{H}$ ]uridine was reduced more after treatment with *R,R*-DACH platinum enantiomers than after treatment with their respective *S,S*-DACH platinum enantiomers ( $p < 0.0001$ ) (Fig. 6b). Neuronal cell body areas were reduced more after treatment with *R,R*-DACH platinum enantiomers than after

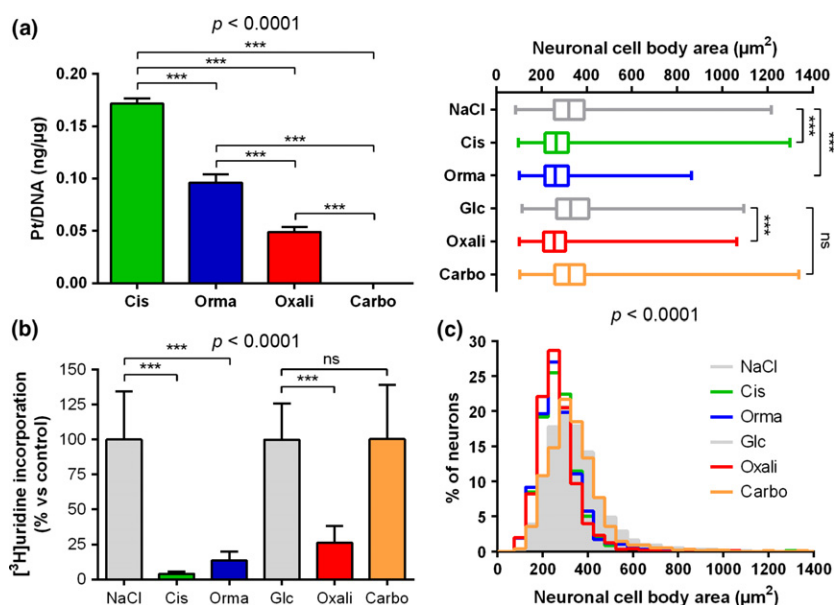


**Fig. 5** Comparison of effects of different clinical platinum drugs on cultured dorsal root ganglia (DRG) cells. Measurements of DNA-bound platinum (a, 4 h), RNA-incorporated [<sup>3</sup>H]uridine (b, 1 d) and neuronal cell body areas (c, 1 d) were made following treatment of cultured DRG cells with drug vehicle alone (NaCl, 0.9% sodium chloride; glc, 5% glucose), cisplatin (cis), ormaplatin (orma), oxaliplatin (oxali) or carboplatin (carbo) (100 μM) for 3 h, then cultured in drug-free medium. (a and b) Symbols represent the means and standard deviations ( $n = 6$ –16 culture wells from two or three independent experiments).  $p$  values shown as numbers are from one-way ANOVA and

those shown as \*\*\* ( $p < 0.001$ ) are from Tukey's multiple comparisons post-tests following one-way ANOVA. (c) Individual neuronal cell body areas are shown as frequency histograms and box and whisker plots [median, interquartile range (IQR) and range] ( $n = 960$ –1440 neurons pooled from six to nine culture wells from three independent experiments). The  $p$  value shown as a number is from a Kruskal–Wallis test, and those shown as \*\*\* ( $p < 0.001$ ) are from Dunn's multiple comparisons post-tests following Kruskal–Wallis test. Levels of DNA platinum binding corresponded to the degree of transcription inhibition and cell body atrophy.

treatment with their respective *S,S*-DACH platinum enantiomers ( $p < 0.0001$ ) (Fig. 6c).

Overall, DNA platinum levels corresponded to the degree of transcription inhibition and cell body atrophy induced by these different clinical platinum drugs and DACH platinum enantiomers.

### Inhibitor studies

Potential protective effects of sodium thiosulfate treatment were studied to further investigate contributions of platinum DNA damage to oxaliplatin-induced transcription inhibition and neuronal cell body shrinkage. Primary cultures of DRG cells were treated with oxaliplatin (10 or 30 μM) with or without sodium thiosulfate (8 mM) before measurement of DNA-bound platinum, RNA-incorporated [<sup>3</sup>H]uridine and neuronal cells body areas. Sodium thiosulfate reduced DNA platinum binding to levels below the detection limit of the platinum assay ( $p = 0.0022$ ) (Fig. 7a). Sodium thiosulfate treatment also protected DRG cells against oxaliplatin-induced inhibition of RNA-incorporation of [<sup>3</sup>H]uridine ( $p < 0.028$ ) and neuronal cell body atrophy ( $p < 0.001$ ) (Fig. 7b and c).

### *In vivo* study

To investigate the *in vivo* significance of these *in vitro* findings, measurements of DRG RNA content and cell body size were made in rats treated with oxaliplatin (1.85 mg/kg i.p. twice weekly for 8 weeks) (Fig. 8a). Compared with age-matched control animals treated with drug vehicle alone, oxaliplatin treatment reduced DRG RNA content by approximately 50% ( $p = 0.019$ ) concurrently with the induction of neuronal cell body atrophy *in vivo* ( $p < 0.0001$ ) (Fig. 8b–h).

### Discussion

In this study, we used a click chemistry EU RNA incorporation fluorescence labelling assay (Jao and Salic 2008) to visualize and measure global transcriptional levels in individual DRG neurons *in vitro*. Since early autoradiography studies (Sensenbrenner *et al.* 1970; Chang *et al.* 1972; Carmichael and Cavanagh 1976; Wells and Vaidya 1994), there have been few previous studies of the global transcriptional activity of DRG neurons. We showed high, but wide ranging, global levels of transcription in individual DRG neurons that correlated with their cell body size.



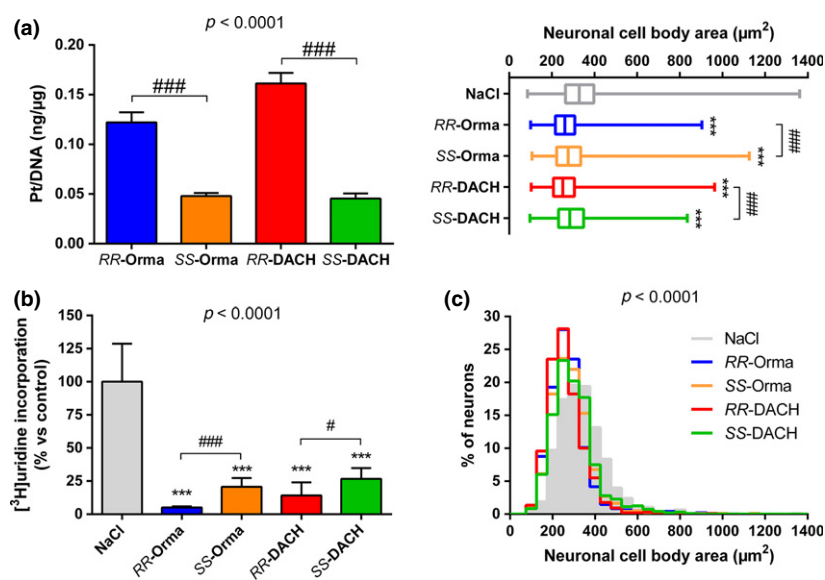


**Fig. 6** Comparison of effects of *R,R*- and *S,S*-diaminocyclohexane (DACH) platinum enantiomers on cultured dorsal root ganglia (DRG) cells. Measurements of DNA-bound platinum (a, 4 h), RNA-incorporated [<sup>3</sup>H]juridine (b, 1 d) and neuronal cell body areas (c, 1 d) were made following treatment of cultured DRG cells with *R,R*-ormaplatin (*RR*-orma), *S,S*-ormaplatin (*SS*-orma), *R,R*-(DACH)Cl<sub>2</sub> (*RR*-DACH) and *S,S*-(DACH)Cl<sub>2</sub> (*SS*-DACH) (100 μM) for 3 h, then cultured in drug-free medium. (a and b) Symbols represent means and standard deviations ( $n = 6$ –15 culture wells from two independent experiments).  $P$  values shown as numbers are from one-way ANOVA. Those shown as # ( $p < 0.05$ ) and ### ( $p < 0.001$ ) are from unpaired T-tests. Those shown as \*\*\* ( $p < 0.001$ ) are from Tukey's multiple comparisons post-

tests following one-way ANOVA for comparison to the no treatment control group. (c) Individual neuronal cell body areas are shown as frequency histograms and box and whisker plots [median, interquartile range (IQR) and range] ( $n = 960$  neurons pooled from six cultured wells from two independent experiments). The  $p$  values shown as a number was from a Kruskal–Wallis test. Those shown as ### ( $p < 0.001$ ) are for comparisons between individual enantiomers and those shown as \*\*\* ( $p < 0.001$ ) are for comparisons to the no treatment control group, both from Dunn's multiple comparisons post-tests following Kruskal–Wallis test. Levels of DNA platinum binding corresponded to the degree of transcription inhibition and cell body atrophy.

Studies of other cell types (Marguerat and Bähler 2012) suggested that global transcriptional output and cell volume are closely correlated as a generalizable biological relationship, but this had not been demonstrated in DRG neurons previously. DRG neurons may require high levels of transcription to maintain their large cell bodies, high metabolism and long axons that project from peripheral targets to the central nervous system (Sghirlanzoni *et al.* 2005). This dependence of DRG neurons upon high levels of transcriptional activity may make them vulnerable to neuronal dysfunction, altered size and loss of distant connections from disrupted transcription arising from DNA damage (Hetman *et al.* 2010).

The findings of this study also demonstrated that platinum drugs induced cell body atrophy in cultured DRG neurons *in vitro*, after platinum binding to DNA and global repression of transcription, but without concomitant loss of neuronal cells. Reduced cell body size is a morphological hallmark of platinum-induced peripheral neurotoxicity *in vivo*, demonstrated in many previous studies of human and animal DRG tissue (Tomiwa *et al.* 1986; Cavaletti *et al.* 1992, 2001; Holmes *et al.* 1998; Krarup-Hansen *et al.* 1999; Jamieson

*et al.* 2005; Renn *et al.* 2011). In the current study, we found altered size profiles in cultured DRG neurons *in vitro* 8–48 h after treatment with platinum drugs, without TUNEL staining or changes in the number of DRG neurons within this time frame. This suggests that platinum drugs may cause DRG neurons to shrink as a consequence to platinum DNA damage-induced inhibition of transcription, which in turn depletes RNA, decreases protein synthesis leading to loss of their protein biomass. Further evidence for this proposed mechanism came from our studies on the effects of actinomycin D, which reduced DRG neuronal cell body size after almost complete inhibition of transcription in these cells. Actinomycin D was previously shown to strongly inhibit protein synthesis secondary to its inhibition of transcription (Cooper and Braverman 1977). Also in support of this proposed mechanism is another published study that reported reductions in the size of cell bodies of cultured peripheral neurons occurring within hours of treatment with protein synthesis inhibitors (Franklin and Johnson 1998).

We further demonstrated significant levels of DNA-bound platinum in cultured DRG neurons following treatment with platinum anticancer drugs that correlated with the degree of

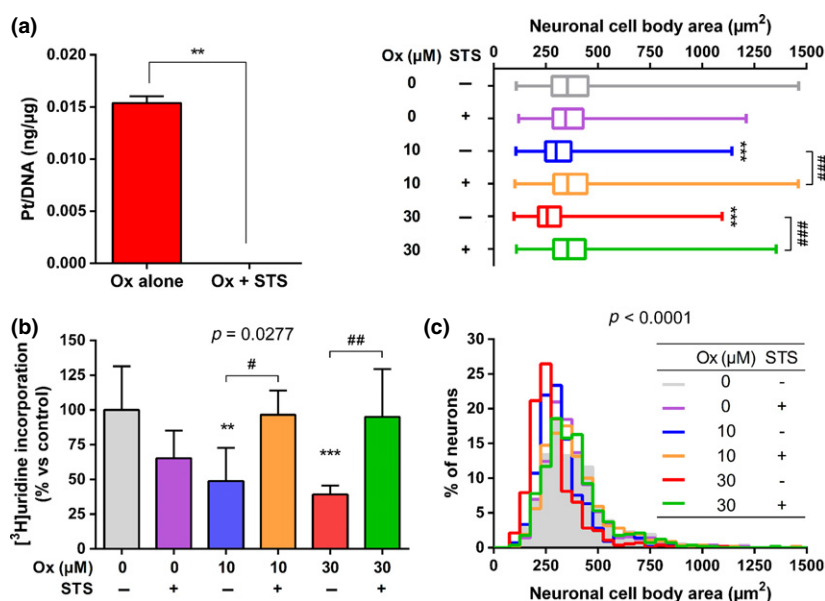


**Fig. 7** Sodium thiosulfate protection of dorsal root ganglia (DRG) cells against oxaliplatin toxicity. Measurements of DNA-bound platinum (a, 4 h), RNA-incorporated [<sup>3</sup>H]thymidine (b, 2 d) and neuronal cell body areas (c, 2 d) were made following treatment of cultured DRG cells with oxaliplatin (10 or 30 μM) with or without sodium thiosulfate (8 mM). (a) DNA-bound platinum 4 h after oxaliplatin treatment (30 μM). Bars represent the mean and standard deviation ( $n = 6$  culture wells from two independent experiments). The  $P$  value shown as \*\*( $p = 0.0022$ ) was from Mann–Whitney test. (b) Symbols represent the mean and standard deviation ( $n = 6$ –16 culture wells from two independent experiments). The  $p$  value shown as a number was from one-way ANOVA. Those shown as \*\*( $p < 0.01$ ) and \*\*\*( $p < 0.001$ ) are for comparisons to no treatment control groups, and those shown as

#( $p < 0.05$ ) and ##( $p < 0.01$ ) are for comparisons to the respective oxaliplatin alone group, both from Tukey's multiple comparisons post-tests following one-way ANOVA. (c) Individual neuronal cell body areas are shown as frequency histograms and box and whisker plots [median, interquartile range (IQR) and range] ( $n = 563$ –570 neurons pooled from four culture wells from two independent experiments). The  $p$  value shown as a number was from a Kruskal–Wallis test. Those shown as \*\*\*( $p < 0.001$ ) are for comparisons to the no treatment control group, and those shown as ###( $p < 0.001$ ) are for comparisons to the respective oxaliplatin alone group, both from Dunn's multiple comparisons post-tests following Kruskal–Wallis test. Sodium thiosulfate protected DRG cells from oxaliplatin-induced DNA platinum binding, transcription inhibition and cell body atrophy.

subsequent transcription inhibition. Platinum damages DNA by binding to the N7 of purine bases to form bifunctional 1,2- and 1,3-intrastrand crosslinks on the DNA template (Jung and Lippard 2007), which inhibit transcription via multiple mechanisms (Todd and Lippard 2009). We showed, first, that the treatment of cultured DRG neurons with cisplatin and oxaliplatin resulted in DNA-bound platinum levels ranging from 0.015 to 0.17 ng Pt/μg DNA, confirming values previously reported by another group (McDonald *et al.* 2005; Ta *et al.* 2006). We then expanded currently available information about neuronal DNA platinum binding to a wider range of platinum compounds, including the *R,R*- and *S,S*-enantiomers of Pt(DACH)Cl<sub>2</sub> and ormaplatin, showing levels of DNA-bound platinum ranging from 0.04 to 0.17 ng Pt/μg DNA, which corresponded to the degree of transcription inhibition. In contrast, treatment of cultured DRG cells with carboplatin or oxaliplatin plus sodium thiosulfate, a known blocker of platinum DNA binding (Viale *et al.* 1999), resulted in no detectable DNA-bound platinum or altered transcription. The levels of DNA-bound

platinum, we and others (McDonald *et al.* 2005; Ta *et al.* 2006) have measured in cultured DRG cells, after treatment with platinum drugs, are significant as they approximately equal up to 20 000 platinum DNA adducts per cell or one adduct per 10<sup>5</sup> base pairs, which exceeds threshold levels expected to induce cytotoxicity (Pera *et al.* 1981). Since N7 purine platinum DNA binding sites are ubiquitously present throughout the genome, and multiple pathways can lead from DNA damage to inhibited transcription (Todd and Lippard 2009), platinum DNA damage-induced transcriptional inhibition might be expected to occur indiscriminately between different genes and globally across the whole genome. In keeping with this, we demonstrated almost complete shut-down (< 5%) of new RNA synthesis, as assessed by uridine incorporation, after the treatment of cultured DRG cells with cisplatin or *R,R*-ormaplatin. In addition, we found significant reductions in steady-state levels of total cellular RNA content and most individual gene mRNAs, whose expression was measurable by quantitative real-time PCR gene expression array analysis.

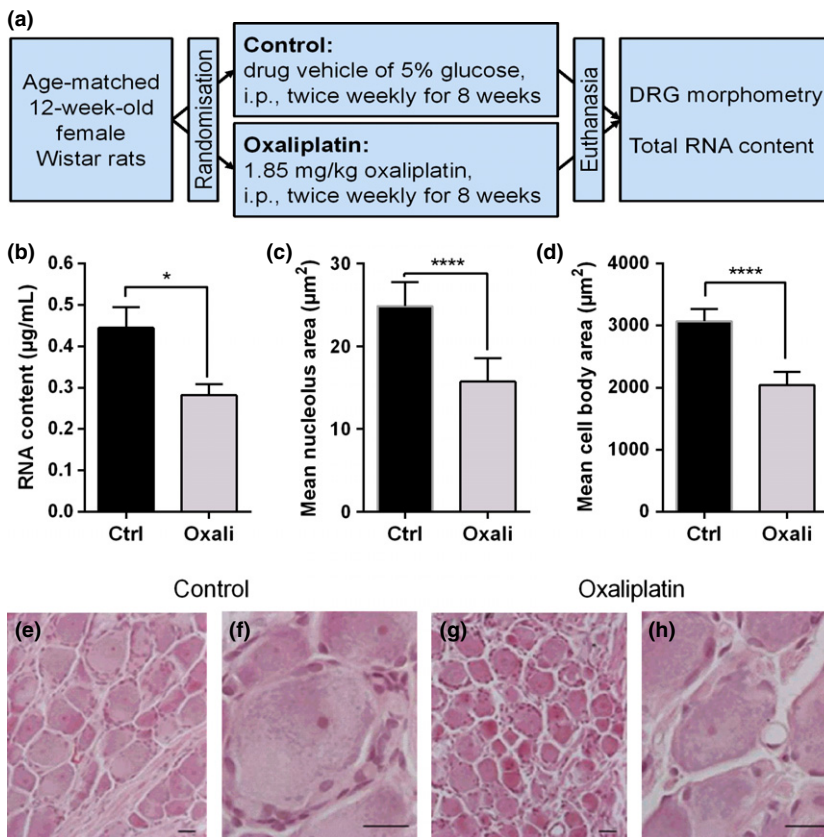


**Fig. 8** *In vivo* oxaliplatin treatment induced RNA depletion and neuronal cell body atrophy in rat dorsal root ganglia (DRG) tissue. (a) Schema of *in vivo* experimental design. (b) DRG RNA content. Bars represent the mean and standard error of the mean of values from six to seven animals. The *p* value shown as \* (*p* = 0.019) was from an unpaired T-test. (c and d) Mean nucleolar and neuronal cell body cross-sectional areas of the ten largest neurons in a L5 DRG from between 10 and 11 animals, as presented previously (Ip *et al.* 2013). Bars represent the mean and standard error of the mean. The *p* values shown as \*\*\*\* (*p* < 0.0001) were from unpaired *T*-tests. (e, f, g and h) Representative images of H&E stained DRG sections from control (e and f) and oxaliplatin-treated (g and h) animals shown at low (e and g) and high (f and h) magnification. Scale bar = 20 µm. The findings shown were verified in an independent experiment.

Together, the findings reported here support a new stepwise mechanism of platinum-induced peripheral neurotoxicity, whereby platinum DNA damage induces global transcriptional arrest leading in turn to neuronal atrophy. However, this new mechanism needs to be reconciled with others proposed to account for neuronal dysfunction developing from platinum-induced DNA damage. Other groups have reported that platinum DNA damage induces apoptosis in DRG and other neuronal cells *in vitro* and *in vivo*, possibly regulated by p53, cyclin D1, Cdk4/6, Rb and bax (Gill and Windebank 1998; Fischer *et al.* 2001; McDonald and Windebank 2002; Gozdz *et al.* 2003). However, some platinum drug-induced peripheral neurotoxicity syndromes may occur without loss of DRG neurons (Jamieson *et al.* 2005), suggesting that mechanisms additional to neuronal apoptosis may contribute to their development. Platinum drugs have been shown to form platinum adducts on mitochondrial DNA, thereby inhibiting mitochondrial DNA replication and transcription, and inducing mitochondrial morphological changes and dysfunction, in DRG cells (Podratz *et al.* 2011). Platinum drugs may also increase production of reactive oxygen species and induce oxidative DNA damage in some cell types including DRG cells (Marullo *et al.* 2013; Kelley *et al.* 2014). These different mechanisms of neuronal dysfunction induced by platinum

DNA damage may not need to be mutually exclusive from each other, but could all collectively contribute to the development of chemotherapy-induced neurotoxicity clinical syndromes. Together, they highlight the central role of platinum binding to neuronal DNA in initiating and controlling the severity of platinum drug-induced peripheral neurotoxicity.

In conclusion, the findings reported here point to a new stepwise mechanism of chemotherapy-induced peripheral neurotoxicity, whereby platinum DNA damage induces global transcriptional arrest leading in turn to neuronal atrophy. DRG neurons may be particularly vulnerable to neurotoxicity from this mechanism because of the high global transcriptional output required for maintaining their large cell bodies and distant axonal connections.

### Acknowledgments and conflict of interest disclosure

Funding for this project was from a China Scholarship Council Scholarship (FY) and grants from the Cancer Society of New Zealand (Project Grant 10/23, MM) and Health Research Council of New Zealand (Project Grant 12/254, MM).

All experiments were conducted in compliance with the ARRIVE guidelines. The authors have no conflict of interest to declare.

## Supporting information

Additional supporting information may be found in the online version of this article at the publisher's web-site:

**Figure S1.** Stability of oxaliplatin in supplemented Neurobasal-A medium.

**Figure S2.** Lack of apoptotic effect of oxaliplatin on cultured DRG neurons.

**Figure S3.** Lack of effect of K<sup>+</sup> and Cl<sup>-</sup> channel blockers on oxaliplatin-induced cell body atrophy in cultured DRG neurons.

**Figure S4.** Effects of oxaliplatin treatment on the expression of individual genes in cultured DRG cells.

**Figure S5.** Lack of effect of DNA-PK and PARP-1 inhibitors on oxaliplatin-induced inhibition of nascent RNA synthesis in cultured DRG cells.

## References

- Ang W. H., Myint M. and Lippard S. J. (2010) Transcription inhibition by platinum-DNA cross-links in live mammalian cells. *J. Am. Chem. Soc.* **132**, 7429–7435.
- Avan A., Postma T. J., Ceresa C., Avan A., Cavaletti G., Giovannetti E. and Peters G. J. (2015) Platinum-induced neurotoxicity and preventive strategies: past, present, and future. *Oncologist* **20**, 411–432.
- Bensaude O. (2011) Inhibiting eukaryotic transcription: which compound to choose? How to evaluate its activity? *Transcription* **2**, 103–108.
- Berciano M. T., Novell M., Villagra N. T., Casafont I., Bengoechea R., Val-Bernal J. F. and Lafarga M. (2007) Cajal body number and nucleolar size correlate with the cell body mass in human sensory ganglia neurons. *J. Struct. Biol.* **158**, 410–420.
- Brouwers E. E. M., Tibben M. M., Pluim D., Rosing H., Boot H., Cats A., Schellens J. H. M. and Beijnen J. H. (2008) Inductively coupled plasma mass spectrometric analysis of the total amount of platinum in DNA extracts from peripheral blood mononuclear cells and tissue from patients treated with cisplatin. *Anal. Bioanal. Chem.* **391**, 577–585.
- Calkins A. S., Iglehart J. D. and Lazaro J. B. (2013) DNA damage-induced inhibition of rRNA synthesis by DNA-PK and PARP-1. *Nucleic Acids Res.* **41**, 7378–7386.
- Carmichael N. and Cavanagh J. B. (1976) Autoradiographic localization of <sup>3</sup>H-uridine in spinal ganglion neurons of the rat and the effects of methyl mercury poisoning. *Acta Neuropathol.* **34**, 137–148.
- Cavaletti G., Tredici G., Marmiroli P., Petruccioli M. G., Barajon I. and Fabbrica D. (1992) Morphometric study of the sensory neuron and peripheral nerve changes induced by chronic cisplatin (DDP) administration in rats. *Acta Neuropathol.* **84**, 364–371.
- Cavaletti G., Tredici G., Petruccioli M. G. et al. (2001) Effects of different schedules of oxaliplatin treatment on the peripheral nervous system of the rat. *Eur. J. Cancer* **37**, 2457–2463.
- Chang L. W., Martin A. H. and Hartmann H. A. (1972) Quantitative autoradiographic study on the RNA synthesis in the neurons after mercury intoxication. *Exp. Neurol.* **37**, 62–67.
- Chen Q. X., Hu H. H., Zhou Q., Yu A. M. and Zeng S. (2013) An overview of ABC and SLC drug transporter gene regulation. *Curr. Drug Metab.* **14**, 253–264.
- Cooper H. L. and Braverman R. (1977) The mechanism by which actinomycin D inhibits protein synthesis in animal cells. *Nature* **269**, 527–529.
- Dzagnidze A., Katsarava Z., Makhalova J., Liedert B., Yoon M. S., Kaube H., Limmroth V. and Thomale J. (2007) Repair capacity for platinum-DNA adducts determines the severity of cisplatin-induced peripheral neuropathy. *J. Neurosci.* **27**, 9451–9457.
- Fischer S. J., McDonald E. S., Gross L. and Windebank A. J. (2001) Alterations in cell cycle regulation underlie cisplatin induced apoptosis of dorsal root ganglion neurons in vivo. *Neurobiol. Dis.* **8**, 1027–1035.
- Franklin J. L. and Johnson E. M. (1998) Control of neuronal size homeostasis by trophic factor-mediated coupling of protein degradation to protein synthesis. *J. Cell Biol.* **142**, 1313–1324.
- Gilder A. S., Do P. M., Carrero Z. I., Cosman A. M., Broome H. J., Velma V., Martinez L. A. and Hebert M. D. (2011) Coilin participates in the suppression of RNA polymerase I in response to cisplatin-induced DNA damage. *Mol. Biol. Cell* **22**, 1070–1079.
- Gill J. S. and Windebank A. J. (1998) Cisplatin-induced apoptosis in rat dorsal root ganglion neurons is associated with attempted entry into the cell cycle. *J. Clin. Invest.* **101**, 2842–2850.
- Gozdz A., Habas A., Jaworski J., Zielinska M., Albrecht J., Chlystun M., Jalili A. and Hetman M. (2003) Role of N-methyl-D-aspartate receptors in the neuroprotective activation of extracellular signal-regulated kinase 1/2 by cisplatin. *J. Biol. Chem.* **278**, 43663–43671.
- Gozdz A., Vashishta A., Kalita K., Szatmari E., Zheng J. J., Tamiya S., Delamere N. A. and Hetman M. (2008) Cisplatin-mediated activation of extracellular signal-regulated kinases 1/2 (ERK1/2) by inhibition of ERK1/2 phosphatases. *J. Neurochem.* **106**, 2056–2067.
- Han C., Khwaounjoo P., Kilfoyle D., Hill A. and McKeage M. (2013) Phase I drug-interaction study of effects of calcium and magnesium infusions on oxaliplatin pharmacokinetics and acute neurotoxicity in colorectal cancer patients. *BMC Cancer* **13**, 495.
- Hernandez-Enriquez B., Arellano R. O. and Moran J. (2010) Role of ionic fluxes on cell death and apoptotic volume decrease in cultured cerebellar granule neurons. *Neuroscience* **167**, 298–311.
- Hernandez-Enriquez B., Guemez-Gamboa A. and Moran J. (2011) Reactive oxygen species are related to ionic fluxes and volume decrease in apoptotic cerebellar granule neurons: role of NOX enzymes. *J. Neurochem.* **117**, 654–664.
- Hetman M., Vashishta A. and Rempala G. (2010) Neurotoxic mechanisms of DNA damage: focus on transcriptional inhibition. *J. Neurochem.* **114**, 1537–1549.
- Holmes J., Stanko J., Varchenko M., Ding H., Madden V. J., Bagnell C. R., Wyrick S. D. and Chaney S. G. (1998) Comparative neurotoxicity of oxaliplatin, cisplatin, and ormaplatin in a Wistar rat model. *Toxicol. Sci.* **46**, 342–351.
- Ip V., McKeage M. J., Thompson P., Damianovich D., Findlay M. and Liu J. J. (2008) Platinum-specific detection and quantification of oxaliplatin and Pt(R, R-diaminocyclohexane)Cl<sub>2</sub> in the blood plasma of colorectal cancer patients. *J. Anal. At. Spectrom.* **23**, 881–884.
- Ip V., Liu J. J. and McKeage M. J. (2013) Evaluation of effects of copper histidine on copper transporter 1-mediated accumulation of platinum and oxaliplatin-induced neurotoxicity in vitro and in vivo. *Clin. Exp. Pharmacol. Physiol.* **40**, 371–378.
- Jamieson S. M., Liu J., Connor B. and McKeage M. J. (2005) Oxaliplatin causes selective atrophy of a subpopulation of dorsal root ganglion neurons without inducing cell loss. *Cancer Chemother. Pharmacol.* **56**, 391–399.
- Jao C. Y. and Salic A. (2008) Exploring RNA transcription and turnover in vivo by using click chemistry. *Proc. Natl Acad. Sci.* **105**, 15779–15784.
- Jong N. N., Nakanishi T., Liu J. J., Tamai I. and McKeage M. J. (2011) Oxaliplatin transport mediated by OCTN1 and OCTN2 in overexpressing HEK293 cells and rat dorsal root ganglion neurons. *J. Pharmacol. Exp. Ther.* **338**, 537–547.

- Jordan P. and Carmo-Fonseca M. (1998) Cisplatin inhibits synthesis of ribosomal RNA in vivo. *Nucleic Acids Res.* **26**, 2831–2836.
- Jung Y. and Lippard S. J. (2007) Direct cellular responses to platinum-induced DNA damage. *Chem. Rev.* **107**, 1387–1407.
- Kelley M. R., Jiang Y., Guo C., Reed A., Meng H. and Vasko M. R. (2014) Role of the DNA base excision repair protein, APE1 in cisplatin, oxaliplatin, or carboplatin induced sensory neuropathy. *PLoS ONE* **9**, e106485.
- Krarup-Hansen A., Rietz B., Krarup C., Heydorn K., Rorth M. and Schmalbruch H. (1999) Histology and platinum content of sensory ganglia and sural nerves in patients treated with cisplatin and carboplatin: an autopsy study. *Neuropathol. Appl. Neurobiol.* **25**, 29–40.
- Liu J. J., Kim Y., Yan F., Ding Q., Ip V., Jong N. N., Mercer J. F. B. and McKeage M. J. (2013) Contributions of rat Ctr1 to the uptake and toxicity of copper and platinum anticancer drugs in dorsal root ganglion neurons. *Biochem. Pharmacol.* **85**, 207–215.
- Marguerat S. and Bähler J. (2012) Coordinating genome expression with cell size. *Trends Genet.* **28**, 560–565.
- Marullo R., Werner E., Degtyareva N., Moore B., Altavilla G., Ramalingam S. S. and Doetsch P. W. (2013) Cisplatin induces a mitochondrial-ROS response that contributes to cytotoxicity depending on mitochondrial redox status and bioenergetic functions. *PLoS ONE*, **8**, e81162.
- McDonald E. S. and Windebank A. J. (2002) Cisplatin-induced apoptosis of DRG neurons involves bax redistribution and cytochrome c release but not fas receptor signaling. *Neurobiol. Dis.* **9**, 220–233.
- McDonald E. S., Randon K. R., Knight A. and Windebank A. J. (2005) Cisplatin preferentially binds to DNA in dorsal root ganglion neurons in vitro and in vivo: a potential mechanism for neurotoxicity. *Neurobiol. Dis.* **18**, 305–313.
- McKeage M. J., Hsu T., Screnci D., Haddad G. and Baguley B. C. (2001) Nucleolar damage correlates with neurotoxicity induced by different platinum drugs. *Br. J. Cancer* **85**, 1219–1225.
- Meijer C., de Vries E. G., Marmiroli P., Tredici G., Frattola L. and Cavaletti G. (1999) Cisplatin-induced DNA-platination in experimental dorsal root ganglia neuropathy. *Neurotoxicology* **20**, 883–887.
- Pera M. F., Rawlings C. J. and Roberts J. J. (1981) The role of DNA-repair in the recovery of human-cells from cisplatin toxicity. *Chem. Biol. Interact.* **37**, 245–261.
- Podratz J. L., Knight A. M., Ta L. E., Staff N. P., Gass J. M., Genelin K., Schlattau A., Lathroum L. and Windebank A. J. (2011) Cisplatin induced Mitochondrial DNA damage in dorsal root ganglion neurons. *Neurobiol. Dis.* **41**, 661–668.
- Renn C. L., Carozzi V. A., Rhee P., Gallop D., Dorsey S. G. and Cavaletti G. (2011) Multimodal assessment of painful peripheral neuropathy induced by chronic oxaliplatin-based chemotherapy in mice. *Mol. Pain.* **7**, 29.
- Scott S. A. (1992) *Sensory Neurons: Diversity, Development and Plasticity*. Oxford University Press, New York, Oxford.
- Screnci D. and McKeage M. J. (1999) Platinum neurotoxicity: clinical profiles, experimental models and neuroprotective approaches. *J. Inorg. Biochem.* **77**, 105–110.
- Screnci D., Er H. M., Hambley T. W., Galetti P., Brouwer W. and McKeage M. J. (1997) Stereoselective peripheral sensory neurotoxicity of diaminocyclohexane platinum enantiomers related to ormaplatin and oxaliplatin. *Br. J. Cancer* **76**, 502–510.
- Screnci D., McKeage M. J., Galetti P., Hambley T. W., Palmer B. D. and Baguley B. C. (2000) Relationships between hydrophobicity, reactivity, accumulation and peripheral nerve toxicity of a series of platinum drugs. *Br. J. Cancer* **82**, 966–972.
- Sensenbrenner M., Treska-Ciesielski J., Lodin Z. and Mandel P. (1970) Autoradiographic study of RNA synthesis in isolated cells in culture from chick embryo spinal ganglia. *Zeitschrift Fur Zellforschung Und Mikroskopische Anatomie* **106**, 615–626.
- Sghirlanzoni A., Pareyson D. and Lauria G. (2005) Sensory neuron diseases. *Lancet Neurol.* **4**, 349–361.
- Ta L. E., Espeset L., Podratz J. and Windebank A. J. (2006) Neurotoxicity of oxaliplatin and cisplatin for dorsal root ganglion neurons correlates with platinum-DNA binding. *Neurotoxicology* **27**, 992–1002.
- Todd R. C. and Lippard S. J. (2009) Inhibition of transcription by platinum antitumor compounds. *Metallomics* **1**, 280–291.
- Tomiwa K., Nolan C. and Cavanagh J. B. (1986) The effects of cisplatin on rat spinal ganglia: a study by light and electron microscopy and by morphometry. *Acta Neuropathol.* **69**, 295–308.
- Treiber D. K., Zhai X., Jantzen H. M. and Essigmann J. M. (1994) Cisplatin-DNA adducts are molecular decoys for the ribosomal RNA transcription factor hUBF (human upstream binding factor). *Proc. Natl Acad. Sci. USA* **91**, 5672–5676.
- Viale M., Zhang J. G., Pastrone I., Mariggio M. A., Esposito M. and Lindup W. E. (1999) Cisplatin combined with tiopronin or sodium thiosulfate: cytotoxicity in vitro and antitumor activity in vivo. *Anticancer Drugs* **10**, 419–428.
- Vichi P., Coin F., Renaud J. P., Vermeulen W., Hoeijmakers J. H. J., Moras D. and Egly J. M. (1997) Cisplatin- and UV-damaged DNA lure the basal transcription factor TFIID/TBP. *EMBO J.* **16**, 7444–7456.
- Wang D. and Lippard S. J. (2005) Cellular processing of platinum anticancer drugs. *Nat. Rev. Drug. Discov.* **4**, 307–320.
- Wei L., Xiao A. Y., Jin C., Yang A. Z., Lu Z. Y. and Yu S. P. (2004) Effects of chloride and potassium channel blockers on apoptotic cell shrinkage and apoptosis in cortical neurons. *Pflugers Arch.* **448**, 325–334.
- Wells M. R. and Vaidya U. (1994) RNA transcription in axotomized dorsal root ganglion neurons. *Mol. Brain Res.* **27**, 163–166.
- Zhu G., Song L. and Lippard S. J. (2013) Visualizing inhibition of nucleosome mobility and transcription by cisplatin-DNA interstrand crosslinks in live mammalian cells. *Cancer Res.* **73**, 4451–4460.